University of Genoa

Pharmacy Department
Pharmacology and Toxicology Section

PhD Course in Experimental Medicine

International Curriculum of Pharmacology and Toxicology
(XXXIII cycle)

Metabotropic glutamate receptor 5 as a target for the modulation of the reactive astrocyte phenotype in the SOD1^{G93A} mouse model of amyotrophic lateral sclerosis.

Candidate: Carola Torazza

Promotors: Prof. Dr. G. Bonanno

Prof. Dr. J. Prickaerts

Co-promotor: Dr. T. Vanmierlo

TABLE OF CONTENTS

ABSTRACT

Amyotrophic Lateral Sclerosis (ALS) is a fatal neurodegenerative disorder due to upper and lower motor neurons (MNs) death. Recognized as a non-cell autonomous disease, ALS is also characterized by damage and degeneration of glial cells, such as astrocytes, microglia, and oligodendrocytes. In particular, astrocytes acquire a reactive and toxic phenotype defined by an abnormal proliferation and by the release of neurotoxic factors.

One major cause for MN degeneration in ALS is represented by the glutamate-mediated excitotoxicity, due to the alteration of glutamate transmission mechanisms, including glutamate receptor function. In this context, the Group I metabotropic glutamate receptor 5 (mGluR5) has been proposed to play an important role in ALS, since it is largely overexpressed during disease progression and is involved in the altered neuronal and glial cellular processes. We previously demonstrated that mGluR5 produces abnormal glutamate release in the spinal cord of the $SOD1^{G93A}$ mouse model of ALS and that halving its expression has a positive impact on *in-vivo* disease progression, including motor neuron survival, astrogliosis and microgliosis.

We here investigated the consequences of reducing the mGluR5 expression in $SOD1^{G93A}$ mice on the reactive phenotype of spinal cord astrocytes cultured from late symptomatic (120 days old) $SOD1^{G93A}$, age matched WT and $SOD1^{G93A}Grm5^{-/+}$ mice. $SOD1^{G93A}$ astrocytes displayed a higher cytoplasmic calcium concentration respect to WT cells and knocking down of mGluR5 reduced calcium level, both under basal and 3,5-DHPG-stimulated conditions. GFAP and S100β, two markers of astrogliosis, were increased in $SOD1^{G93A}$ astrocytes, whereas their overexpression was reduced in $SOD1^{G93A}Grm5^{-/+}$ cells. The same positive effect was obtained in the case of NLRP3, a marker strictly related to inflammation, which was upregulated in $SOD1^{G93A}$ astrocytes and less expressed in double mutant astrocytes. The partial ablation of mGluR5 also resulted in a lower cellular presence of misfolded SOD1. Both the expression and secretion of pro-inflammatory cytokines were strongly reduced in $SOD1^{G93A}Grm5^{-/+}$ respect to $SOD1^{G93A}$ astrocytes. The uncoupling between oxygen consumption and ATP synthesis and the impairment of mitochondria function, present in $SOD1^{G93A}$ astrocytes, were recovered in double mutant astrocytes. Notably, the viability of spinal MNs co-cultured with $SOD1^{G93A}Grm5^{-/+}$ astrocytes was significantly increased respect to MNs co-cultured with $SOD1^{G93A}$ astrocytes. The acute *in-vitro* treatment of $SOD1^{G93A}$ astrocytes with an antisense nucleotide (ASO) specific for mGluR5 decreased the mRNA and protein expression of mGluR5 in these cells and led to

the reduction of GFAP and S100β. The *in-vitro* pharmacological treatment with the negative allosteric modulator of mGluR5, CTEP, also reduced the expression of GFAP and S100β in SOD1^{G93A} astrocytes.

Altogether, these results indicate that mGluR5 ablation has a positive impact on astrocytes in SOD1^{G93A} mice, supporting the idea that the *in-vivo* amelioration of the disease progression, registered after mGluR5 genetical or pharmacological silencing, involve astrocyte phenotype improvement. As a whole, it may be outlined that mGluR5 may represent a potential therapeutic target able to preserve MNs from death, also by modulating the reactive astroglia phenotype in ALS.

Due to the active contribution of microglia to ALS pathogenesis, the effect of mGluR5 partial ablation in SOD1^{G93A} mice on the balance between the pro- and anti-inflammatory profile of microglia acutely purified from the brain and spinal cord of WT, Grm5$^{-/+}$, SOD1^{G93A} and SOD1^{G93A}Grm5$^{-/+}$ mice has been investigated at the early (90 days) and late symptomatic (120 days) stages of ALS by detecting the mRNA and protein levels of some relevant markers involved in neuroinflammation, such as IL-1β, CD86, iNOS, TNF-α (pro-inflammatory), Arginase 1, IL-10, CD206 and IL-4 (anti-inflammatory). Experiments are in progress to complete this part of the project.

Graphical abstract

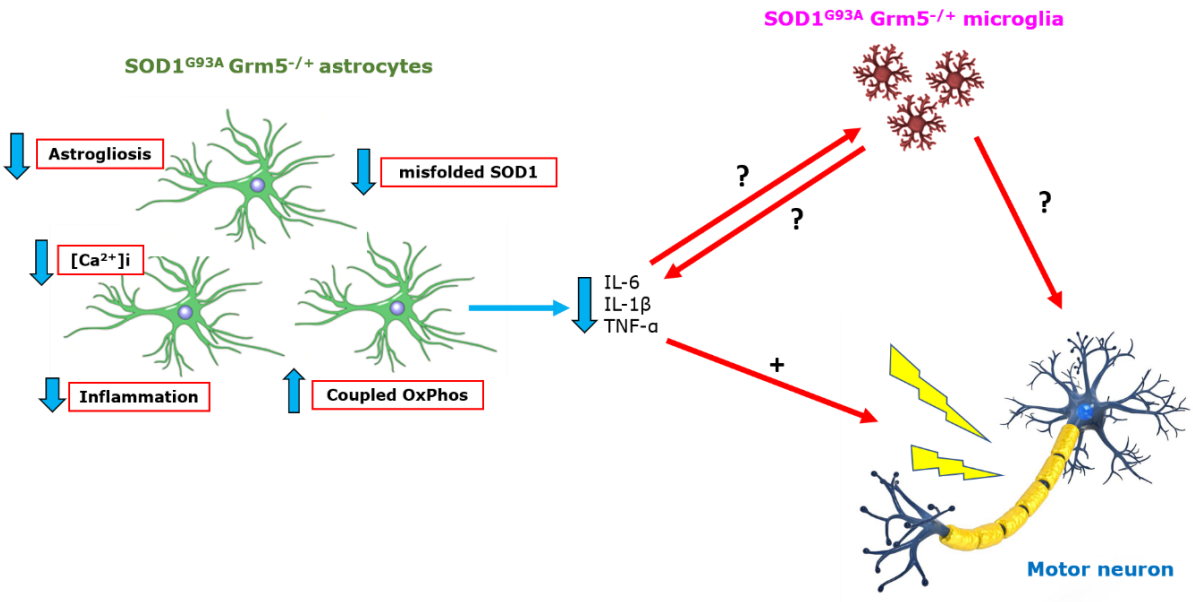

Future perspectives

The lower expression of misfolded SOD1 observed in $SOD1^{G93A}Grm5^{-/+}$ respect to $SOD1^{G93A}$ astrocytes support the hypothesis of an amelioration of the autophagy or of the protein quality control system in these cells. It was investigated the total protein expression of the autophagic marker LC3 and of the specific isoform LC3-II. According to the literature, this protein was more expressed in $SOD1^{G93A}$ respect to WT astrocytes. Double mutant astrocytes, instead, showed a lower level of the marker respect to $SOD1^{G93A}$ cells. However, the results obtained analysing LC3-II were not in line with these observations and deserve further investigation, also measuring more autophagic markers.

The preliminary experiments with microglia acutely isolated from WT, $Grm5^{-/+}$, $SOD1^{G93A}$ and $SOD1^{G93A}Grm5^{-/+}$ mice performed in Hasselt showed a very high instability of the reference genes and of the expressed repetitive elements (EREs) used to normalize data. The results also showed a very low RNA integrity number (RIN) of the samples, possibly indicating their degradation. All the steps of the experimental protocol were revised and optimized trying to solve this issue. However, it was not possible to find an effective solution and, due to the quantity of the available samples produced in Genoa, the analyses were interrupted. Currently, the microglia isolation protocol is being optimized to obtain a better quality of RNA. Moreover, flow cytometry analyses are being performed to substantiate future results.

1. INTRODUCTION

1.1 Amyotrophic Lateral Sclerosis

Amyotrophic Lateral Sclerosis (ALS) is the most common form of the adult nonhereditary motor neuron (MN) diseases. However, much less common forms also exist, such as progressive muscular atrophy (PMA), characterized by degeneration of lower motor neurons (MNs) only; progressive lateral sclerosis (PLS), characterized only by upper MN contribution; progressive bulbar palsy (PBP), with bulbar MN involvement only; spinal muscular atrophy (SMA), a paediatric motor neuron disease; the X-linked spinobulbar muscular atrophy, also called Kennedy's disease; poliomyelitis, the only one to be caused by a virus (Krivickas, 2003).

ALS was described for the first time by Charcot and Joffroy in 1869 (Charcot and Joffroy, 1869) and defined as a condition in which motor neurons degenerate causing a progressive loss of motor skills. They named it Lou Gherig's disease in honour of a baseball hall of fame affected by the pathology.

ALS is a late-onset disease characterized by a progressive degeneration of upper MNs of the motor cortex and corticospinal tract, and lower MNs of the brain stem and spinal cord (Eisen, 2009). ALS can occur in two different forms depending on the origin of lower MN degeneration: bulbar and spinal ALS. Bulbar ALS is characterized by muscle loss caused by degeneration of MNs in the medulla oblongata of the brain, which determines increased salivation, speech disorders, tongue atrophy, dysphagia and difficulties swallowing. Bulbar ALS can also include a pseudobulbar form which may also involve neurons of the limbic areas and leads patients to lose the emotional control, such as laugh and cry, beside the neuromuscular failure. Muscle weakness occurs in both two forms in 1-2 years, after the first symptoms and a progressive respiratory failure causes death within 2-3 years from the onset (Lomen-Hoerth, 2008; Pratt, 2012).

In the *spinal* form of ALS, the disease arises in limb weakness that can affect both inferior and superior limbs. This form is also characterized by symmetric arms weakness and muscles atrophy which cause cramps, difficulties in movement and ambulation. Moreover, spinal ALS patients can even develop bulbar symptoms during the disease progression, but the respiratory failure occurs within 3-5 years, later than the bulbar form, thus leading to an improved prognosis (Lomen-Hoerth, 2008; Pratt, 2012).

Although the most recurrent symptoms are associated to motor neuron degeneration, most of the ALS patients also show cognitive and behavioural impairments (up to 75% and up to

50%, respectively, Huynh *et al*., 2020). This is the reason why a correlation between ALS and Frontal Temporal Dementia (FTD) was postulated in 1932 (Von Braunmuhl, 1932).
In Europe, the incidence of ALS ranges from 2.1 to 3.8 per 100,000 person/year (Longinetti and Fang, 2019). Longinetti and Fang reported a slightly increasing prevalence (the number of people affected by the disease at that time) of ALS ranging values between 4.1 and 8.4 per 100,000 persons. While the incidence is constant, the prevalence tends to increase. This phenomenon can be explained by an amelioration of patient life expectance due to the better palliative care, such as assisted ventilation and re-education of swallowing and speech (Macpherson and Bassile, 2016; Valadi, 2015).
The aetiology of ALS is still poorly understood. However, it is known that the disease can occur in two different forms: the sporadic form (sALS), representing more than 90% of cases, and the familiar form (fALS), which is genetically transmissible and accounts for about 10% of cases. sALS manifests itself at about 65 years of life with a higher incidence in males than females. Conversely, fALS is genetically transmitted in a dominant or recessive autosomal manner. The dominant form usually manifests itself at about 50 years and cannot be distinguished pathologically and symptomatically from sALS. The recessive form is very rare and occurs more frequently in the elderly but has a longer life expectation (Hamida *et al*., 1990).
Even if the pathogenesis of ALS is still unknown, clinical symptoms and disease progression are similar in both sALS and fALS, indicating that common mechanisms may be involved.

1.2 Amyotrophic Lateral Sclerosis and genetic mutations

The familiar form of ALS represents the 5-10% of the cases and is mostly inherited in an autosomal dominant manner. Next generation sequencing has contributed to search better for ALS-linked genes. In fact, more than 30 genes and loci have been identified till now (Renton *et al*., 2014; Cirulli *et al*., 2015) and four of them are responsible for more than 70% of cases (Chiò *et al*., 2014).
The first mutated gene correlated to fALS codes for the superoxide dismutase type 1 (SOD1) (Rosen *et al*., 1993) and it is mutated in 25% of fALS (Saccon *et al*., 2013; Kiernan *et al*., 2011). Subsequently, mutations of the Transactive Response DNA-Binding Protein 43 (TARDBP) (Arai *et al*., 2006; Mackenzie *et al*., 2007), of Fused Sarcoma Protein (FUS) (Vance *et al*., 2009), and more recently of chromosome 9 open reading frame 72 (C9orf72) (DeJesus-Hernandez *et al*., 2011; O'Rourke *et al*., 2015) were discovered. The other fALS

cases are due to other mutated proteins which lead to several forms of the pathology, among which: Alsin (ALS2) that causes a group of overlapping autosomal recessive neurodegenerative disorders characterized by the absence of bulbar and respiratory symptoms and with a typical juvenile onset; Senataxin (SEXT), a putative DNA/RNA helicase which causes ALS4 disease, a rare juvenile autosomal-dominant atypical for of ALS; Vesicle-associated membrane protein-associated protein B/C (VAPB), probably involved in the vesicular trafficking, which generates ASL8 disease; Angiogenin (ANG), a nuclear RNase which induces ALS9 disease and is involved in motor neurons death; factor induced gene 4 (FIG4), phosphatidylinositol 3,5-bisphosphate 5-phosphatase, which induces ALS11 disease; optineurin (OPTN), supposed be involved in signal transduction, gene expression and in vesicular trafficking, which leads to ALS12 disease; tumor necrosis factor (TNF) receptor-associated factor NF-kB activator (TANK)-binding kinase 1 (TBK1) which participates in a variety of cell signal pathways by phosphorylating of various substrates, among which OPTN and p62 (two autophagic adaptors involved in the pathology of FTD and ALS) (Table 1, Mathis *et al*., 2019).

ALS Type	Inheritance	Locus	Gene	Protein
ALS1	AD/AR	21q22.11	SOD1	Cu/Zn superoxide dismutase
ALS2	AR	2q33.1	KIAA1563	Alsin
ALS3	AD	18q21	Unknown	Unknown
ALS4	AD	9q34.13	SETX	Senataxin
ALS5	AR	15q15-21.1	KIAA1840/SPG 11	Spastacin
ALS6	AD/AR	16p11.2	FUS/TLS	Fused in sarcoma/translated in liposarcoma
ALS7	AD	20p13	Unknown	Unknown
ALS8	AD	20q13.32	VAPB	Vesicle-associated membrane protein B angiogenin
ALS9	AD	14q11.2	ANG	Angiogenin
ALS10	AD	1q36.22	TARDBP	TAR DNA-binding protein 43
ALS11	AD	6q21	FIG.4	phosphoinositide 5-phosphatase
ALS12	AD/AR	10p13	OPTN	Optineurin
ALS13	AD	12q24.12	ATXN2	Ataxin-2
ALS14	AD	9p13.3	VCP	Vasolin-containing protein
ALS15	XL	Xp11.21	UBQLN2	Ubiquilin-2
ALS16	AR	9p13.3	SIGMAR1	Sigma nonopioid intracellular receptor 1
ALS17	AD	3p11.2	CHMP2B	Charged multivesicular body protein 2B
ALS18	AD	17p13.2	PFN1	Profilin-1
ALS19	AD	2q34	ERBB4	Chorion protein gene Erb.4
ALS20	AD	12q13	HNRNPA1	Heterogeneous nuclear ribonucleoprotein A1
ALS21	AD	5q31.2	MATR3	Matrin-3
ALS22	AD	2q35	TUBA4A	Tubulin alpha-4A
ALS23	AD	10q22.3	ANXA11	Annexin A11
FTD-ALS1	AD	9p21.2	C9ORF72	Chromosome open reading frame 72
FTD-ALS2	AD	22q11.23	CHCHD10	Coiled-coil-helix-coiled-coil-helix domain containing protein 10
FTD-ALS3	AD	5q35.3	SQSTM1/p62	Sequestome-1
FTD-ALS4	AD	12q14.2	TBK1	TANK-binding kinase 1
LAHCDA	AR	9q34.11	GLE1	GLE1, RNA export mediator

Table 1. fALS and the genetic determinants. The table classifies the different inherited forms of ALS, the type of inheritance (AD=autosomal dominant, AR=autosomal recessive, XL=X-linked), the chromosome location, the gene, and the protein associated to each subtype (adapted and reproduced from Mathis *et al*., 2019).

1.2.1 Superoxide Dismutase 1 (SOD1)

Eukaryotic cells contain two distinct forms of superoxide dismutase (SOD): a mitochondrial manganese-containing enzyme (SOD2) and a cytoplasmic copper/zinc-containing enzyme (SOD1) (see review of Levanon *et al*., 1985). SOD1 is a 154 aminoacidic length protein (UniProt P00441). The human form is encoded by SOD1 gene located in the position 21q22.11 (Ensembl ENSG00000142168). The human protein is a homodimer of 32 kDa composed of two identical non-covalently linked subunits with known amino acid sequences and has an enzymatic function. It catalyses the disproportionation of superoxide anion to produce dioxygen and hydrogen peroxide ($O_2^{\bullet-} + O_2^{\bullet-} + 2H^+ \rightarrow H_2O_2 + O_2$) which can be subsequently cleared by catalase and glutathione peroxidase (Fridovich, 1986; Sea *et al*., 2015). Copper is required for SOD1 activity, whereas zinc is thought to stabilize the protein structure (Kunst, 2004).

1.2.1.1 SOD1 mutations in ALS

Approximately 2% of all ALS cases and 20-25% of fALS cases are associated with SOD1 mutations (Al-Chalabi and Leigh, 2000) and most of them are inherited in an autosomal dominantly fashion. In the *ALSod* database are reported more than 180 SOD1 polymorphisms associated with ALS (Wright *et al.*, 2019). Although most of the mutations reduce dismutation activity, others retain full catalytic function. Moreover, there are no clear correlation between the enzyme activity, clinical progression, and disease phenotype, even if the duration of the disease is similar (Pasinelli and Brown, 2006).

The majority of genetic polymorphisms are missense mutations. The most worldwide common of which is the D90A variant (aspartic acid at codon 90 changed to alanine) and is predominantly represented in North America. The A4V variant (alanine at codon 4 changed to valine) is linked to approximately 50% of fALS cases in the U.S.A. population and the G93A variant (glycine at codon 93 changed to alanine) represent about 25% of fALS cases. The latter is rarer than the other two forms but is one of the most studied in transgenic animal models of the disease, because it was the first that has been discovered (Gurney at al**.**, 1994) and, most importantly, causes degeneration of MNs and ALS symptoms very close to human disease (Pansarasa *et al*., 2018; Andersen, 2006). In general, glycine is the most common amino acid within the SOD1 sequence (16.2%) and 60% of its sites can harbour ALS

mutations (Wright *et al*., 2019). Despite much progress in genetic and molecular studies, the mechanisms by which SOD1 mutations can cause ALS remains mostly unclear.

Phenotype, disease progression and severity can differ significantly depending on the variants involved (Mejzini *et al*., 2019). Patients with A4V, G93A, H43R (histidine at codon 43 changed to arginine), L84V (leucine at codon 84 changed to valine), G85R (glycine at codon 85 changed to arginine) or N86S (asparagine at codon 86 changed to serine) variants showed rapid disease progression and shorter survival; while patients carrying D90A, G93C (glycine at codon 93 changed to cysteine) or H46R (histidine at codon 46 changed to arginine) mutations generally have longer life expectancies (Yamashita and Ando, 2015).

Moreover, ALS patients harbouring particular variants manifest distinct clinical features, suggesting a genotype-phenotype correlation. The AV4 mutation, for example, is associated with the limb-onset form of ALS (Juneja *et al*., 1997). Patients homozygous for the D90A variant generally show a slowly progressive paresis, starting at legs and gradually spreading upstream, together with atypical features such as bladder disturbance (Andersen *et al*., 1996). In contrast, ALS individuals heterozygous for the same mutation manifest bulbar, upper, and lower limb onset with a faster progression (Hong-Fu and Zhi-Ying, 2016).

1.2.1.2 Mutated SOD1 toxicity and ALS

The first findings about SOD1 gene mutations in fALS led to the hypothesis that the disease was caused by a loss of function of the protein which leads to an altered free oxygen radical species (ROS) scavenging (Deng HX *et al*., 1993) and to the subsequently motor neurons death. However, it was demonstrated, some years later, that SOD1 null mice do not develop the motor neuron disease (Reaume *et al*., 1996). Conversely, transgenic mice expressing the mutated SOD1 showed motor neuron damage. Interestingly, the wild-type human SOD1 expressed at similar protein levels of the mutated forms did not cause the disease and showed to be neuroprotective for the oxidative stress. This finding supported the idea of a toxic gain of function of the mutated protein (Gurney, 2000). This phenomenon is linked with alterations of several other proteins involved in regulation of mRNA processing, oxide nitric (NO) metabolism, antioxidant defence and protein degradation, leading to the hypothesis that altered radical handling and abnormal protein aggregation are likely to contribute to motor neuron injury (Allen *et al*., 2003).

More recently, Soo and collaborators demonstrated that mutant SOD1 inhibits the protein transport between endoplasmic reticulum (ER) and Golgi in neuronal cells, an essential mechanism for cell survival (Soo *et al*., 2015). This phenomenon is also correlated with two others ALS-associated mutant proteins: TDP-43 and FUS. Even if the three proteins act trough different processes, each mechanism is dependent on Rab1 function. Rab1 is a member of Rab GTPase protein family which has a master role in regulating all intracellular vesicle trafficking events. Interestingly, Rab1 was found to be misfolded and not functional in sALS (Soo *et al*., 2015). Moreover, Rab1 overexpression restores ER-Golgi transport and reduces ER stress, mutant SOD1 inclusion formation and apoptosis in cells expressing SOD1, TDP-43 and FUS mutant proteins. This finding links the inhibition of ER-Golgi transport to neurodegeneration and leads to the belief that Rab1 restoration can be a therapeutic target in ALS (Soo *et al*., 2015).

SOD1 has been also demonstrated to be involved in sALS pathogenesis. Accordingly, a modified 32 kDa SOD1 polypeptide was detected, together with the well-known 16 kDa SOD1, in spinal cord extracts of fALS and sALS patients but not in the control group (Gruzman *et al*., 2007). This discovery led to further investigate the role of SOD1 in sALS patients. The studies revealed that the 32 kDa protein can acquire toxic properties typical of mutant SOD1, thus determining the development of aggregates, in particular in the nuclei of astrocytes of spinal cords of ALS patients (Ezzi *et al*., 2007; Forsberg *et al*., 2011).

A loss of function of SOD1 in sALS was also observed. Accordingly, SOD1 level was strongly reduced inside the nuclei of MNs and leukocytes of sALS patients and this led to an increase of DNA damage and, consequently, to a more severe disease progression (Cereda *et al*., 2013; Sau *et al*., 2007).

Starting from these considerations, several transgenic mice carrying mutations at different position in human SOD1 have been generated. Although the pathology differently proceeds during the disease progression of the different models, all mutated SOD1 rodents develop progressive muscle weakness and paralysis until death. The transgene copy number would determine the differences of disease onset, whereas the type of the mutation would cause the severity of the disease (Bendotti and Carrì, 2004).

1.2.2 TAR-DNA-binding protein 43 (TDP-43)

Most of the ALS cases are characterized by neuronal cytoplasmic inclusions caused by the aggregation of ubiquitinated or misfolded proteins, as reported also for other neurodegenerative pathologies, such as Alzheimer's (AD) and Parkinson's diseases (PD, Leigh *et al*., 1991). In 2006 the TAR-DNA-binding protein 43 (TDP-43) was discovered as one of the main components of these protein aggregates both in fALS and sALS patients (Arai *et al*., 2006; Neumann *et al*., 2006). Indeed, TDP-43 was also identified in the cytoplasmic aggregates of sporadic cases of the disease which did not have any pathogenic variants in the TARDPB gene, and in those with the C9orf72 hexanucleotide repeat expansion (see review of Mejzini *et al*., 2019). For this reason, the cytoplasmic neuronal inclusions of TDP-43 in the brain and spinal cord are now considered as a pathological hallmark of ALS.

The TARDPB gene encodes for TDP-43 which is a DNA/RNA binding protein composed by 414 amino acids and located in chromosome 1 (UniProt PRO_0000081972). TDP-43 is predominantly a nuclear protein, but in the case of neurodegenerative proteinopathies can be also present in the cytoplasm, presumably next to post-transcriptional modifications (Ayala *et al*., 2008). In fact, the protein was found to be phosphorylated and excised at C-terminals) in the cortex of individuals affected by ALS or by FTD. These fragments aggregate and become not functional (Neumann *et al*., 2006). TDP-43 is a regulator of gene expression and is involved in pre-mRNA splicing, in the regulation of mRNA and non-coding RNAs stability, and in the mRNA transport and translation (Buratti and Baralle, 2010; Tollervey *et al*., 2011; Ratti and Buratti, 2016). Several TDP-43 animal models (*Caenorhabditis elegans*, Zebrafish, Drosophila, mice, and rats) have been created to better understand the role of mutated TDP-43, as in the case of SOD1 (see review of Picher-Martel *et al*., 2016).

1.2.3 Fused in Sarcoma/Translocated in liposarcoma (FUS/TLS)

Soon after the discovery of TDP-43 mutations in ALS, another RNA/DNA binding protein, called *Fused in Sarcoma/Translocated in liposarcoma* (FUS/TLS), was found to be mutated in 4% of fALS and in some rare sALS cases (Kwiatkowski *et al*., 2009; Vance *et al*., 2009). FUS/TLS is a 526 amino acids protein localized in the nucleus and characterized by multiple domains. The C-terminal region is the most likely mutated motif and is responsible for protein-protein interactions, the alternative splicing, and the nuclear localization (Lagier-

Tourenne *et al*., 2010). Abnormal cytoplasmic FUS/TLS inclusions were found in neurons and glia cells in the brain and spinal cord of patients bearing mutations of this protein. Whether TDP-43 and FUS/TLS act in parallel or separately to cause motor neuron degeneration is not still clear. Nevertheless, it has been demonstrated that FUS/TLS binds several microRNAs, some of which are shared with TDP-43, both in mice and in humans (Lagier-Tourenne *et al*., 2010).

1.2.4 Chromosome 9 open reading frame 72 (C9orf72)

In 2011, DeJesus-Hernandez (DeJesus-Hernandez *et al*., 2011), Renton (Renton *et al*., 2011) and their collaborators discovered ALS-linked mutations in a non-coding region of the chromosome 9 open reading frame 72 (C9orf72). These mutations resulted in expansion of the GGGGCC repeat hexanucleotide. C9orf72 codes for a protein with unknown domains and function but highly conserved across species (Bigio, 2011). It is a full-length homologue of Differentially Expressed in Normal and Neoplastic Cells (DENN) proteins which are regulators of cytoplasmic and membrane protein traffic (Levine *et al*., 2013). According to the authors, the GGGGCC hexanucleotide repetition at the first intron of C9orf72, represents 20-40% of fALS and 5% of sALS cases, a feature shared with individuals affected by familial (10-30%) and sporadic (2-10%) forms of FTD (DeJesus-Hernandez *et al*., 2011; Renton *et al*., 2011). In healthy individuals the GGGGCC repeat length ranged from 2-23 hexanucleotide units (DeJesus-Hernandez *et al*., 2011). Conversely, ALS and FTD patients show hundreds or even thousands hexanucleotide repetitions (DeJesus-Hernandez *et al*., 2011; Renton *et al*., 2011). However, the minimal repeat size needed to cause ALS/FTD has not still clarified.

Two main mechanisms were initially proposed through which hexanucleotide expansion repeats might cause the ALS/FTD (Taylor *et al*., 2016): loss of function of the protein, caused by a decreased expression level of C9orf72; gain of function of the protein due to an accumulation of RNA foci in the brains and spinal cord.

The loss of function mechanism was confirmed in cell cultures and in Zebrafish, in which the depletion of C9orf72 exacerbates the toxicity of aggregation-prone proteins such as polyglutamine-expanded ataxin 2 (Sellier *et al*., 2016). However, the reduction of the C9orf72 mRNA by antisense oligonucleotides did not cause any impairments in behaviour

and motor function in mice (Lagier-Tourenne *et al*., 2013). Moreover, the conditional knock out of C9orf72 in the mouse brain did not result in neurodegenerative phenotypes characteristic of ALS and FTD (Koppers *et al*., 2015). The complete ablation of C9orf72 did not cause any motor neuron diseases, but mice revealed abnormal macrophages and microglia activation as well as neuroinflammation and autoimmunity traits (see review of Taylor *et al*., 2016). These observations raise the possibility of a non-cell autonomous contribution to ALS, even if the loss of function of C9orf72 cannot be the sole driver of the disease (see review of Taylor *et al*., 2016).

The second hypothesis involves a toxic gain of function due to accumulated repeat-containing RNA sequestration of RNA-binding proteins that are involved in splicing (La Spada and Taylor, 2010). In addition to this observation, the toxicity of dipeptide repeated proteins (DPRs: poly-GA, -GP, -GR, -PA, -PR) that are produced by repeat associated non-AUG (RAN) translation, an unconventional type of translation which occurs without the involvement of initiating AUG codon, was suggested as a second gain of function mechanism (Zu *et al*., 2011). These dipeptides accumulate in the cytoplasm and nucleus of brain and spinal cord neurons causing the formation of protein inclusions which are positive for ubiquitin and sequestome-1 but negative for TDP-43 (Gendron *et al*., 2013; Zu *et al*., 2013; Mackenzie *et al*., 2013; Ash *et al*., 2013; Mori *et al*., 2013). Notably, intranuclear inclusions of DPRs that co-localize with nucleoli have been identified in the frontal cortex of C9orf72 patients (see review of Zongbing *et al*., 2020). The total amount of inclusions varied remarkably, based on each DPR protein: DPRs are expressed predominantly in the form of poly-GA (Glycine-Alanine) and to a lesser extent in the form of poly-GP (Glycine-Proline) and poly-GR (Glycine-Arginine), compared to poly-PR (Proline-Arginine) and poly-PA (Proline-Alanine; poly-GA > poly-GP > poly-GR > poly-PR/PA). However, only slight pathological correlations of poly-GA, but not of other DPRs, have been reported in C9orf72-associated ALS (C9ALS). In fact, the contribution of other DPRs to the pathogenesis is still unclear (see review of Zongbing *et al*., 2020).

1.3 Amyotrophic Lateral Sclerosis as a multifactorial disease

Nowadays, it is well recognized that ALS is a multifactorial disease, characterized by interactive pathogenic mechanisms and by the involvement of different cell types that concur to the MNs death. Considering the wide spectrum of genetic mutations responsible for or associated to the disease, the common clinical features found in the ALS patients are likely to descend from the concurrence of both genetic and yet unidentified environmental factors which, by acting at different pathogenic levels, converge in a final common pathway (Eisen, 1995; Cozzolino *et al*., 2012).

Some of the mechanisms which take place in this complex scenario are described in the following chapters and schematized in Figure 1.

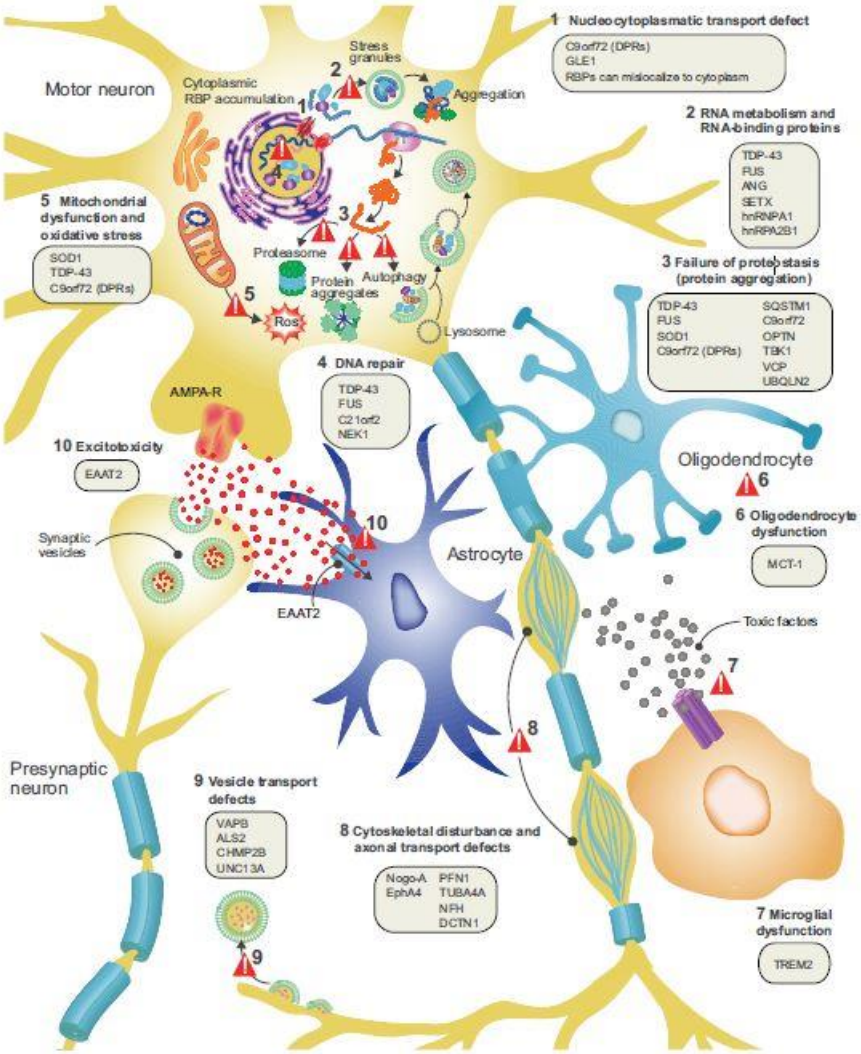

Fig.1 Proposed ALS mechanisms. ALS can be characterized by one (or more than one) of the defective pathways represented in the figure: 1) Nucleocytoplasmatic transport defect; 2) Altered RNA metabolism; 3) Impaired proteostasis with protein aggregation; 4) Impaired DNA repair; 5) Mitochondrial dysfunction and oxidative stress; 6) Oligodendrocytes dysfunction; 7) Neuroinflammation (microglia and astrocytes dysfunction); 8) Axonal transport defects; 9) Vesicle transport defects and 10) Excitotoxicity (see review of Van Damme *et al*., 2017).

1.3.1 Glutamate excitotoxicity

Glutamate is the major excitatory transmitter of the mammalian centrale nervous system, where more than 40% of synapses are glutamatergic, and is essential for neuronal communication as well as for higher-level functions, such as memory and learning. In the physiological processes of excitatory synaptic transmission, glutamate is released from the depolarized presynaptic glutamatergic nerve terminals into the synaptic cleft. Then,

glutamate activates ionotropic (iGluRs) receptors which, in turn, mediate ions influxes in postsynaptic neurons and metabotropic glutamate receptors (mGluRs), which modulate cellular activation state and metabolism (see review of Armada-Moreira *et al*., 2020).

The iGluRs are ligand-gated ion channels permeable to various ions such as sodium (Na^+) and calcium (Ca^{2+}). These receptors can be further subdivided into three classes: N-Methyl-D-Aspartate receptor (NMDAR), α-amino-3-hydroxy-5-methyl-4-isoxazolepropionic acid receptor (AMPAR) and kainate receptor (KAR), and their activation causes neuronal membrane depolarization and/or cytoplasmic Ca^{2+} raise due to cation entrance through the cell membrane (Doble, 1999; Hollmann and Heinemann, 1994; Monaghan *et al*., 1989).

Conversely, mGluRs are C family G-protein-coupled receptors (GPCRs), probably constituting the most diverse receptor family of the CNS and are subdivided into three groups: Group I (mGluR1, mGluR5), Group II (mGluR2, mGluR3) and Group III (mGluR4, mGluR6, mGluR7, mGluR8, see for details chapter 1.5).

Due to the important role of glutamate in the CNS, it is easy to predict that a dysregulation of the glutamatergic system could be implicated in the pathophysiology of neuronal death and can cause the so-called *excitotoxicity* (Bano *et al*., 2005). This term appears for the first time in 1969 in an Onley's study in which exposure to glutamate or aspartate caused the cell death (Olney, 1969).

In excitotoxicity, glutamate dynamics can be affected in several manners, among which: i) defective glutamate uptake; ii) excessive glutamate release; iii) abnormal activation or overexpression of glutamate receptors; iv) neuronal hyperexcitability. These impairments can lead to excessive neuronal Ca^{2+} intake, aberrant Ca^{2+} homeostasis, downstream mitochondrial dysfunction, and increased ROS production (see review of Le Gall *et al*., 2020) and have been all identified in ALS (Leigh and Meldrum, 1996; Cluskey and Ramsden, 2001; Van Den Bosch *et al*., 2006; King *et al*., 2016).

i) In excitotoxicity, glutamate concentration peak can rise well above than the usual levels (>1 mM). Alternatively, the decay of the glutamate concentrations in the synaptic cleft results uncreased (Armada-Moreira *et al*., 2020). Also, the baseline concentration of the neurotransmitter may increase, independently from the depolarization-induced release, and can reach 2-5 µM [Glu] causing neuronal injury (Mark *et al*., 2001). The first proposed mechanism responsible for synaptic elevated glutamate levels in ALS was the loss of glial glutamate transporters. Under normal conditions glutamate homeostasis in the synaptic cleft is guaranteed by the excitatory amino acid transporters (EAATs) which prevent excessive

postsynaptic glutamate receptor activation and ensure fast neuronal synaptic transmission by maintaining low levels of extracellular glutamate (Danbolt *et al*., 1992; Danbolt, 1994; Danbolt *et al*., 1994; Danbolt, 2001). Five glutamate transporters exist in human, termed EAAT1-5. Four homologues of human transporters have been described in rats and mice: GLAST, corresponding to EAAT1; GLT-1, corresponding to EAAT2; EAAC1, also known as EAAT3 and EAAT4. They can be expressed by neurons, particularly at the pre-synaptic terminals (EAAT3 or EAAC1, see review of Pajarillo *et al*., 2019) or by astrocytes (EAAT1/GLAST and EAAT2/GLT-1, Rothstein *et al*., 1994; Danbolt, 2001; Minelli *et al*., 2001). EAAT4 and EAAT5 are mostly expressed in cerebellum and retina, respectively (Fairman *et al*., 1995, Arriza *et al*., 1997). The loss of GLT-1 has been reported to induce increased extracellular levels glutamate and cause MN toxicity and paralysis in animal models (Rothstein *et al*., 1996), whereas the pharmacological stimulation of the transporter has been found to rescue MN degeneration and delay paralysis in $SOD1^{G93A}$ mice (Rothstein *et al*., 2005; Kong *et al*., 2014). These results were confirmed in ALS patients. Accordingly, Rothstein and colleagues showed high glutamate levels in the plasma and in the cerebrospinal fluid (CSF) of ALS patients and a selective loss of EAAT2 in post-mortem motor cortex brain tissue of ALS individuals when compared with healthy control individuals (Rothstein *et al*., 1990; Rothstein *et al*., 1995). A further study revealed that EAAT2 function alteration can be caused by the aberrant truncated transcripts of EAAT2 gene (Lin *et al*., 1998). The EAAT2 transcription, translation and activity can be also alter by other factors, such as oxidative stress, growth factors, fatty acids, and cytokines (Rao *et al*., 2003; Gegelashvili *et al*., 1997; Trotti *et al*., 1995).

ii) As a second mechanisms able to produce high levels of glutamate in the synaptic cleft, my group of research demonstrated that in spinal cord axon terminals (synaptosomes) isolated from the $SOD1^{G93A}$ mouse models of ALS, the glutamate exocytosis is already increased both at the pre-symptomatic and the symptomatic phase of the disease, both in basal conditions and after the application of depolarizing stimuli (Milanese *et al*., 2011; Bonifacino *et al*., 2016). The main causes for the augmented neurotransmitter release were addicted to changes in cytosolic Ca^{2+} concentrations ($[Ca^{2+}]_c$), auto-activation of Ca^{2+}/calmodulin dependent protein kinase II (CaMKII, a crucial protein for plasticity of glutamate neurotransmission) and phosphorylation of Synapsin I (Syn I), an event that contributes to fill up the readily releasable pool (RRP) of vesicles and to boost vesicles fusion. Accordingly, the increase of the number of soluble NSF attachment protein receptor

(SNARE) complexes, of the expression of synaptotagmin-1 (Syt-1), a presynaptic proteins incrreasing release probability, together with inhibition of glycogen synthase kinase 3 (GSK-3, an event that favours SNARE protein assembly) were detected in spinal cord synaptosomes of $SOD1^{G93A}$ mice (Milanese *et al*., 2011; Bonifacino *et al*., 2016).

iii) Glutamate excitotoxicity can be also explained by the impairment or overactivation of glutamate receptors; in particular, AMPARs and mGluRs. Numerous studies reported the involvement of AMPAR in ALS, even if autoradiography binding did not show differences between AMPAR in ALS patients and in healthy controls (Allaoua *et al*., 1992). AMPAR permeability strictly depends on the occurrence of post-transcriptional editing of the mRNA for different receptor subunits (Lorenzini *et al*., 2018). The most validated hypothesis refers to changes of GluR2 subunit. In healthy conditions, GluR2 mRNA is subjected to a post-transcriptional modification by which an arginine substitutes a glutamine in position 607, in the re-entrant M2 membrane loop region, making the receptor impermeable to Ca^{2+} (Sommer *et al*., 1991). Conversely, in ALS the GluR2 mRNA editing resulted incomplete and AMPA receptor becomes permeable to Ca^{2+}, a phenomenon very commonly detected in the spinal cord of ALS patients (Takuma *et al*., 1999). The importance of this phenomenon is supported by the discovery that ALS-linked mutations in proteins regulating RNA processing affects the GluR2 mRNA editing. Interestingly, C9orf72, TDP-43 and FUS have been demonstrated to sequestrate RNA transcript variants of adenosine deaminase 2 (ADAR2) which catalyses GluR2 mRNA editing, determining a reduced receptor activity and an increased permeability to Ca^{2+} in ALS MNs (Donnelly *et al*., 2013; Aizawa *et al*., 2010).
A very recent study underlined some mutation-specific differences in AMPAR responses which may explain the diverse responses to the pharmacological treatment of ALS (Bursh *et al*., 2019). Bursh and colleagues reported differences in AMPAR expression and function in induced-pluripotent stem cells (iPSC)-derived MNs carrying the C9orf72, TDP-43, SOD1 or FUS mutation. C9orf72 MNs showed higher Ca^{2+} peaks following receptor activation compared to controls, even if AMPAR mRNA levels were not change. Also, TDP-43 MNs showed unchanged AMPAR expression and higher intracellular basal level of Ca^{2+} and increased Ca^{2+} peaks respect to control MNs after AMPAR activation. Conversely, in SOD1 and FUS MNs, the Ca^{2+} peak decreased when compared to healthy controls.

As briefly described above mGluRs can be divided into three different groups depending on their amino acids sequence identity. While Group II and III activate intracellular metabolic

pathways that are inhibitory for the cell, Group I receptors are the only excitatory metabotropic glutamate receptors (Pin and Duvoisin, 1995). My research group demonstrated that mGluR1 and mGluR5 abnormally increase the release of glutamate in $SOD1^{G93A}$ mouse model (Giribaldi *et al*., 2013; Milanese *et al*., 2015). Indeed, these receptors are overexpressed in the spinal cord of the $SOD1^{G93A}$ mice at pre-symptomatic stages and during the progression of the disease. Moreover, their function is altered early in the disease progression, suggesting that it can represent a cause rather than a consequence of disease progression (Bonifacino *et al*., 2019b). In support of the importance of these receptors in the disease, we showed that knocking down or knocking out mGluR1 or mGluR5 in $SOD1^{G93A}$ mice improves survival and disease progression, ameliorates motor skills, reduces astrogliosis and microgliosis and improves MNs survival (Milanese *et al*., 2014; Bonifacino *et al*., 2017; Bonifacino *et al*., 2019a), suggesting again the big role of excitotoxicity in this ALS mouse model.

Another interesting finding linked to glutamate excitotoxicity and glutamate release has been identified again by my group of research which demonstrated that glutamate release can be enhanced in the spinal cord of ($SOD1^{G93A}$ mice by the activation of glycine and γ-aminobutyric acid (GABA) heterotransporters (transporters that recognize and take up in the nerve terminal foreign neurotransmitters coming from neighbouring structures, Bonanno and Raiteri, 1994, Raiteri *et al*., 2002). Comparing the activation of these transporters on glutamatergic terminals of the transgenic and control mice, they found a more elevated release in $SOD1^{G93A}$ mice (Raiteri *et al*., 2003; 2004). Activation of glycine and GABA heterotransporters elicit glutamate release partly by homotransporter reversal and largely through anion channel opening; both the mechanisms probably boosted by ion co-transport during glycine and GABA uptake (Raiteri *et al*., 2005a; 2005b). Recently, in the attempt to reconcile the different altered release mechanisms described in $SOD1^{G93A}$ mice, they demonstrated that the excessive glycine and GABA heterotransporter-mediated glutamate release in the spinal cord of $SOD1^{G93A}$ mice is due to the heterotransporter overexpression at the nerve terminal membrane, promoted by increased transporter trafficking consequent to the excessive glutamate exocytosis (Milanese *et al*., 2015).

iv) Another event that may explain excitotoxicity in ALS is the neuronal hyperexcitability. Several studies demonstrated an alteration of MN excitability already in the early phase of the disease suggesting that lower intensity stimuli can be sufficient to generate a response in ALS-affected MNs (Vucic and Kiernan, 2006). In accordance, a

decrease of the inhibitory function of GABAergic interneurons has been also found in the motor cortex of ALS animal models (Moser *et al*., 2013; McGown *et al*., 2013). Of note, post-mortem tissue of ALS patients revealed a reduction of the mRNA of the $GABA_A$ receptor subunit α; an occurrence that can directly affect the GABAergic transmission, by reducing GABA binding to $GABA_A$ receptors (Petri *et al*., 2003). Therefore, this phenomenon could determine the MN response even if the cells receive a sub-threshold stimulus (Wagle-Shukla *et al*., 2009). Another important finding sustaining the hyperexcitability hypothesis has been described in $SOD1^{G93A}$ mice that showed unchanged fast transient and increased persistent Na^+ currents in cortical neurons being in particular the amplitude higher when compared to WT neurons (Pieri *et al*., 2009).

Persistent Na^+ currents allow to sustain and generate prolonged depolarization. Therefore, an impairment of Na^+ currents amplitude may cause hyperexcitability. However, the treatment of these transgenic neurons with Riluzole only reduced the persistent Na^+ current and the firing frequency, without modifying the resting membrane potential. This suggests that other mechanisms can sustain hyperexcitability, such as alteration of K^+ currents; indeed, the decreased expression of Kv1.1, Kv1.2 and Kv7.1 K^+ channels in ALS patients confirmed this hypothesis: K^+ outward currents lead to higher level of extracellular K^+, causing an increase of resting membrane potential and the firing frequency of MNs (Kanai *et al*., 2006; Shibuya *et al*., 2011).

Altogether, points i) - iv) demonstrate the alteration of the glutamate machinery at the neurons and peri-synaptic astrocyte level. The importance of the glutamate excitotoxicity in the etiopathology of ALS is also underlined by clinical evidence. To date the only available drug to treat the pathology is Riluzole, which blocks the glutamatergic neurotransmission (Doble, 1996). However, the mechanism of action bases on the inhibition of the voltage dependent Na^{2+} channels, leading to the non-specific reduction of neurotransmitter release, both excitatory, supported by glutamate, and inhibitory, supported by glycine and GABA. For this reason, a selective inhibition of glutamate release would be required to obtain more valuable effects.

1.3.2 Oxidative stress

Cell metabolisms (such as signal transduction, gene transcription, oxidative phosphorylation, and ATP production) produce the so-called ROS and reactive nitrogen species (RNS), through enzymatic and nonenzymatic reactions. ROS can have radical or

nonradical forms and derive from the partial reduction of oxygen, such as superoxide anion ($O_2^{\bullet-}$), hydrogen peroxide (H_2O_2), and hydroxyl radical ($HO^{\bullet}$) (Halliwell, 2006; Uday *et al*., 1990).

Under physiological conditions, the production and clearance of ROS are balanced and regulated by enzymatic [SOD, catalase (CAT), glutathione peroxidase (GPx), glutathione reductase (GR), thioredoxin (Trx)] and nonenzymatic [glutathione (GSH), vitamins A, C and E, flavonoids, albumin, ceruplasmin, and metallothioein] antioxidants (Niedzielska *et al*., 2016). However, abnormal production of ROS or defective antioxidant defence could lead to a loss of this equilibrium and, subsequently, to cell damage or death. Indeed, cell structure can be damaged by oxidation of different biomolecules, such as lipids, proteins, and DNA/RNA (Yu *et al*., 2009). Lipids are highly susceptible to oxidation and their damage can cause a perturbation of plasma membrane fluidity and permeability, promoting the entrance of substances, in particular ions, inside the cell (Brown and Murphy, 2009). Lipid peroxidation promotes the propagation of oxidative damage that ultimately affects proteins and RNA/DNA, determining structural and functional modifications, with increased protein aggregation and proteolysis (Halliwell and Gutteridge, 1984).

The most important sites of intracellular ROS and RNS production are mitochondria, due to their major role in ATP production mechanisms in which molecular oxygen is reduced to water in the electron transport chain (Brand MD, 2010; Kausar *et al*., 2018). Therefore, mitochondria dysfunction can lead to apoptosis or cell senescence causing catastrophic events, especially in non-proliferative cells, as neurons (Wang *et al*., 2013; Redza-Dutordoir and Averill-Bates, 2016).

Several studies have reported increased levels of oxidative damage in proteins, lipids, and DNA of post-mortem neuronal tissues, as well as in CSF, plasma and urine collected from ALS patients (Kikuchi *et al*., 2002; Mendez *et al*., 2015). In these individuals, there is also evidence of a dampened response to oxidative stress demonstrated by lower level of GSH in motor cortex compared to healthy volunteers (Weiduschat *et al*., 2014; Cohen *et al*., 2012).

Although ROS are not believed to cause ALS, they are likely to exacerbate the disease progression (Liu J and Wang, 2017) also contributing to the degeneration of the neuromuscular junction (Pollari *et al*., 2014). However, the impossibility to evaluate the markers of oxidative stress in humans at the early stage of the pathology constitutes an obstacle to understand if oxidative damage represents a primary cause or a consequence of the pathology (Oliveira *et al*., 2020). Animal models can bring some insights about this issue.

For example, the activation of the nuclear factor erythroid-2-related factor 2 (Nrf2)-antioxidant response element (ARE) of the oxidative stress responsive system has been described in distal muscle of $SOD1^{G93A}$ mice before the disease onset (Kraft *et al*., 2007), supporting the hypothesis that Nrf2-ARE activation progresses in a retrograde fashion along the motor pathway culminating in MNs loss.

In normal condition Nrf2 is bound to the endogenous inhibitor Kelch-like ECH associated protein 1 (Keap1). Endogenous or exogenous stressors can induce translocation of Nrf2 from the cytoplasm to the nucleus, where it binds to ARE, a regulatory enhancer region of DNA. The Nrf2-ARE interaction promotes the transcription of several genes involved in the cellular antioxidant and anti-inflammatory defence, such as phase 2 detoxification enzymes [NAD(P)H, quinone oxyreductase (NQO1) and glutathione-disulfide reductase (GSR) that are necessary for glutathione biosynthesis], extracellular SOD, glutamate-6-phosphate-dehydrogenase, heat shock proteins and ferritin. Furthermore, Nrf2 promotes the synthesis of pro- and anti-inflammatory enzymes, such as cyclooxygenase-2, nitric oxide synthase (iNOS), and heme oxygenase-1 (HO-1) (Petri *et al*., 2012). Because of the important role of Nrf2 in regulating antioxidant response many studies focused on the administration of Nrf2 activators to slow down ALS progression. The treatment of $SOD1^{G93A}$ mice with some of these molecules resulted in an amelioration of motor performance, reduction of body weight loss and prolonged survival of the mice (Neymotin *et al*., 2011).

SOD1 mutations represent a direct link with oxidative stress in ALS because of the main role of the protein in converting of $O_2^{\bullet-}$ into O_2 and H_2O_2. The influence of SOD1 mutations is numerous and can be associated with a decrease, maintenance or increase in the protein dismutase activity, compared to the WT SOD1 (Oliveira *et al*., 2020). Even if it has been suggested that mutated SOD1 exerts its deleterious effects by a toxic gain of function (Menzies *et al*., 2002), none of the mechanisms linked to this toxic gain is currently known (Oliveira *et al*., 2020).

Oxidative reductase (redox) alterations have been also found in fALS caused by C9orf72, TDP-43 and FUS mutations, suggesting a correlation between RNA metabolism dysregulation and oxidative stress. For example, it has been demonstrated that the oxidative stress causes TDP-43 delocalization from the nucleus to the cytoplasm and increases the tendency of the protein to aggregate (Cohen *et al*., 2015). Moreover, both TDP-43 and FUS can co-localize with stress granules, that represent one of the responses of cells to oxidative stress insults modulating gene expression by prioritizing translation of stress response-linked

genes (Li *et al*., 2013; Bentmann, 2012). If stress granules persist, they will play a pivotal role in aggregate formation (Parker *et al*., 2012).

TDP-43, FUS or C9orf72 co-localization with mitochondria can also occurs, causing oxidative stress. Three hypotheses have been proposed to explain this mechanism: a direct damage may occur due to sequestration of mitochondrial proteins by RNA-binding proteins (Magranè *et al*., 2014; Deng *et al*., 2015) and an interaction with non-mitochondrial proteins that are involved in mitochondrial protein synthesis; among these, Forkhead box O3 (FOXO3) acts by down-regulating many nuclear-encoded genes that control mitochondrial function. TDP-43 inhibits FOXO3; therefore, when TDP-43 compartmentalize in the cytoplasm respect to the nucleus, due to TDP-43 mutations linked to ALS, it exerts an increased inhibitory activity leading to a reduction of the mitochondrial functions (Ferber *et al*., 2012; Zhang *et al*., 2014). Finally, TDP-43 and FUS have been also shown to regulate specific mRNAs coding for proteins which preserve mitochondria physiology. Accordingly, mutant TDP-43 has been shown to alter the splicing pattern of nuclear-transcribed mRNA, coding for mitochondrial fission regulator-1 (Mtfr-1) and complex I subunits ND3 and ND6, causing complex I disassembly (Finelli *et al*., 2015; Wang *et al*., 2013).

1.3.3 Mitochondria alterations

Mitochondria are essential organelles of the cells: they provide for cell survival and metabolism. Moreover, they produce ATP, the energy supply of the cells, via oxidative phosphorylation and contribute to phospholipid biogenesis, calcium homeostasis and apoptosis (see the review Smith *et al*., 2019). Mitochondria play a central role in CNS cells, especially in neurons. In fact, these cells consume 20% of the produced ATP and need calcium buffering to modulate several mechanisms, including neurotransmitter release (Smith *et al*., 2019). These findings underline the important role of mitochondria in neurodegenerative diseases.

Several studies demonstrated the presence of abnormal mitochondria both in mouse model of ALS (Dal Canto and Gurney, 1995; Kong and Xu, 1998; Jaarsma *et al*., 2001) and in patients affected by the sporadic form of the disease (Vielhaber *et al*., 2000). Mitochondria of motor neuron are vacuolated and show disorganized cristae and broken outer membrane even at the early stages of the disease. Moreover, they show an impairment in the enzymatic activity and several mutations in the mitochondrial DNA (mtDNA), both in spinal cord and skeletal muscle of sALS patients (Vielhaber *et al*., 2000; Sasaki *et al*., 2007).

The ATP synthesis and the mitochondria respiration rates are impaired in both spinal cord and brain of $SOD1^{G93A}$ transgenic mice before the onset and persist throughout the course of the disease. Accordingly, complex I+II, II+III and IV activities are reduced in spinal cord of symptomatic mice and complex IV activity is decreased in mouse forebrain at pre-symptomatic, symptomatic, and late symptomatic stage of the disease (Kirkinezos *et al*., 2005; Mattiazzi *et al.*, 2002). The reduced activity of complex II and IV, followed by a decreased activity of mitochondrial membrane potential (MMP), was also confirmed by *invitro* experiments using NSC-34 motor neuron-like cell line expressing $SOD1^{G93A}$ or $SOD1^{G37R}$ mutations (Menzies *et al*., 2002; Coussee *et al*., 2010). Similar results were obtained in skeletal muscle, lymphocytes, and fibroblasts of sALS patients (Parisa *et al*., 2012; Kirk *et al*., 2014).

The mitochondrial damage results in deficiency of energy production but also in oxidative stress. ROS produced by cells may act as signalling molecules, but they can damage DNA, proteins, and lipids when generated in excess. They can induce inflammatory pathways activation, ER stress, protein aggregation, excitotoxicity and can lead to cell death (see the review of Smith *et al*., 2019).

Another mechanism by which mitochondria can damage the cell is the calcium mishandling. An early loss of calcium buffering was observed in $SOD1^{G93A}$ mice before the disease onset (Damiano *et al*., 2006). Accordingly, in NSC34 cells expressing the $SOD1^{G37R}$ or the $SOD1^{G93A}$ mutations, loss of MMP can alter the cell calcium buffering capacity, a typical mark of motor neurons of ALS patients (Damiano *et al*., 2006; Carrì *et al*., 1997).

Recently, our research group characterized the mitochondria aerobic metabolism in an *in-vitro* model of pre-synaptic axon terminals and peri-synaptic astrocyte processes in $SOD1^{G93A}$ mice (Ravera *et al*., 2018). We observed that synaptosomes of $SOD1^{G93A}$ mice show impaired bioenergetics already before the clinical onset of the disease. Conversely, gliosomes of the same mouse genotype display a decrement of mitochondrial energy production at the late phase of the disease only. Taken together these results show that the two neuronal and astrocyte models may differently contribute to the synaptic damage in ALS.

Based on this work, we proceeded analysing the activity of some enzymes in glycolysis, Krebs cycle and lactate fermentation in synaptosomes and gliosomes isolated from the spinal cord and motor cortex of $SOD1^{G93A}$ mice. The aim of this study was to investigate if an impairment of the upstream glucose catabolism could cause the mitochondrial dysfunction at the presynaptic site and the involvement of peri-synaptic astrocyte zones in the

metabolism alteration (Ravera *et al*., 2019). Spinal cord $SOD1^{G93A}$ synaptosomes from early stage and motor cortex $SOD1^{G93A}$ synaptosomes from symptomatic stages displayed high activity of the key glycolysis and of Krebs cycle enzymes, but did not display modification of lactate dehydrogenase, the key enzyme of lactate fermentation. Conversely, glycolysis and lactate fermentation, but not Krebs cycle activity, was increased in gliosomes from the spinal cord and motor cortex of $SOD1^{G93A}$ mice at the symptomatic stages of the disease only. The observed metabolic modifications might be considered an attempt to restore the altered energetic balance and indicate that mitochondria represent the ultimate site of the bioenergetic impairment in ALS.

1.3.4 Calcium homeostasis alterations

Most of the pathological causes of ALS, e.g., genetic mutations, excitotoxicity, oxidative stress, mitochondrial disfunction, and deregulated inflammatory processes, can interfere with calcium homeostasis (see review of Tedeschi *et al*., 2019). Indeed, loss of Ca^{2+} homeostasis has been detected in several ALS animal models and in patients, already at the early symptomatic stage of the disease (Bonifacino *et al*., 2016; Stoica *et al*., 2016; Damiano *et al*., 2006; Mórotz *et al*., 2012).

One of the causes of the Ca^{2+} impairment, as already described in chapter 1.3.1, is due to specific alterations of AMPA receptors, which, depending on their subunit combinations, acquire different cation selectivity (see review of Greger *et al*., 2017). AMPAR Ca^{2+} permeability depends on the GluR2 subunit which undergoes physiological post transcriptional mRNA editing that results incomplete in ALS, making the receptor permeable to Ca^{2+} (Van der Bosh *et al*., 2000). Interestingly, it has been demonstrated that human spinal motor neurons, unlike most of the neuronal groups in the human CNS, express atypical calcium permeable AMPA receptors, lacking the GluR2 subunit. This characteristic may render this cell group selectively vulnerable to excessive glutamate-mediated intracellular calcium flux (Williams *et al*., 1997).

Beside the massive Ca^{2+} influx during excitatory transmission, this high sensibility of MNs to Ca^{2+} homeostasis determines low expression levels of parvalbumin and calbindin, two essential Ca^{2+} buffering proteins (Van den Bosh *et al*., 2000). Accordingly, $SOD1^{G93A}$ MNs showed a higher intracellular Ca^{2+} concentration, even if they did not display any differences in the Ca^{2+} permeability respect to controls, neither through AMPAR nor through voltage-

activated calcium channels (Guatteo *et al*., 2007). This impairment in the ability of Ca^{2+} buffering renders MNs highly dependent from mitochondria and ER. Accordingly, an impairment of the ER function, that, together which mitochondria, regulates the dynamics of Ca^{2+} by sequestering the cytoplasmic ion when its concentration is increased, can exacerbate MN death.

Indeed, nanomolar concentration of Ca^{2+} produces a pro-survival signal to MNs in an experimental model of ALS, while increasing cytoplasmic Ca^{2+} concentration can impair the buffering capacity of ER, causing Ca^{2+} leakage from the ER stores (Petrozziello *et al*., 2017). Ca^{2+} dysregulation can be also caused by the loss of communication between ER and mitochondria, which physiologically allows the exchange of the cation between the two organelles. Mitochondria and ER communicate through several protein complexes, such as mitochondria nucleoid factor 1 (Mnf1), Mnf2, inositol 1,4,5-triphosphate receptor (IP3R) and Voltage Dependent Anion Channel 1 (VDCA1, Manfredi *et al*., 2016). This interaction mechanism has been found to be impaired in mutant SOD1-, TDP-43-, and FUS-related ALS (Stoica *et al*., 2014; Stoica *et al*., 2016; Bernard-Marissal *et al*., 2015).

Among the several variables in regulating neuronal calcium homeostasis in neurons, the calcium binding proteins, such as calbindin-D28K, parvalbumin and calmodulin, play an important role. Indeed, they are differently expressed in CNS neuronal populations, therefore their presence or absence may contribute to selective vulnerability in ALS. Accordingly, Alexianu and colleagues demonstrated that the MNs which degenerated early in ALS, unlike the MNs which dye later, do not show immunoreactivity for calbindin-D28K and parvalbumin (Alexianu *et al*., 1994). Another calcium binding protein which plays an important role in ALS is S100β. It consists in an acidic protein expressed primarily by glial cells, which can act as a mitogen or neurotrophic factor stimulating proliferation of glial cells or differentiation of immature neuron and which can also increase of $[Ca^{2+}]_i$ in both glial and neuronal cells (Barger and Van Eldik, 1992). These results are consistent with the connection of S100β to neurological disorders, among which Down's syndrome, AD, and ALS (Barger and Van Eldik, 1992; Migheli *et al*., 1999). Accordingly, S100β protein has been found to be overexpressed in cortical and spinal cord astrocytes and MNs of ALS patients (Migheli *et al.,* 1999). Its levels were also increased in the cerebrospinal fluid (CSF) of ALS individuals, positively correlating with a worse prognosis (Sussmuth *et al*., 2010). S100β overexpression was also confirmed in rodent models of ALS and its direct influence on the expression of reactivity-linked/proinflammatory molecules in astrocytes from $SOD1^{G93A}$ mice has been recently demonstrated (Serrano *et al*., 2017).

The uncontrolled calcium influx into the cell can also activate calcium dependent proteases, such as calpain, which can induce tissue damage. Indeed, the calpastatin-mediated inhibition of calpain, which has been found to be more activated in $SOD1^{G93A}$ mice, prevents the toxicity in motor neuron cell culture isolated from spinal cord of $SOD1^{G93A}$ mice (Tradewell and Durham, 2010). In addition to this protein, several other enzymes can be activated by the abnormal intracellular calcium concentration, among which nitric oxide (NO) synthases, endonucleases, protein kinases C (PKC) and phospholipases and their mis-activation can lead to cell death (Bar, 2000).

Lastly, dysfunctional Ca^{2+} level may also induce abnormal misfolding of proteins in ALS, thus facilitating their aggregation, another main cause of ALS (see below; Leal *et al*., 2013).

1.3.5 Protein Aggregation

Protein aggregation is a process characterized by proteins aberrant folding that may lead to self-association into oligomers and eventually in fibrils via polymerization. This mechanism, typical of misfolded or unfolded proteins, can lead to non-specific interactions of oligomers with other cellular proteins or with cellular membranes harming membrane integrity, leakage of cellular material, and cell death (see review of Malik and Wiedau, 2020).

Protein aggregation is a hallmark of ALS and of many other neurodegenerative diseases like FTD, AD, Spinocerebellar Ataxia (SCA), Huntington disease (HD) and Inclusion Body Myositis (IBM). In ALS cytoplasmic inclusions can be found in degenerating motor neurons of spinal cord but also in frontal and temporal cortices of the brain, hippocampus and cerebellum (Al Chalabi *et al*., 2012). The first protein found to be aggregated in fALS cases was SOD1 because of a mutation in the corresponding gene, coding for the $SOD1^{G93A}$ protein (Rosen *et al*., 1993). Later, several other proteins, such as TDP-43, FUS, Ataxin 2 (ATXN2), OPTN, Ubiquilin 2 (UBQLN2), and C9orf72 were found to be involved in this mechanism. Despite the central role of protein aggregation in ALS pathology, the causes that drive protein deposition, the cellular mechanisms involved or affected, the role of proteins carrying ALS-associated mutations in the aggregate formation is still unclear (see for a review of Blockhuis *et al*., 2013).

In 2011 it has been hypothesized that in ALS protein aggregation may propagate from one cell to the other in a prion like fashion (Polymenidou and Cleveland, 2011, King *et al*., 2012). Moreover, some ALS proteins, such as FUS and TDP-43, share some features with yeast prion proteins and once aggregated, can sequester native proteins. Another phenomenon

linked to protein aggregation is the stress granules (SG) formation. Accordingly, FUS, TDP-43 and ATXN2 have been shown to be all implicated in SG formation (Blockhuis *et al*., 2013). These findings were confirmed in post-mortem sALS patients' spinal cords, in which colocalization of TDP-43 positive inclusions with SG markers was found in MNs (Bentmann *et al*., 2012; Liu-Yesucevitz *et al*., 2010; Volkening *et al*., 2009).

The aggregation of ALS proteins in ectopic sites of the cell can also prevent these proteins from executing their correct and physiological function. However, knocking out or knocking down the corresponding genes leads often to motor dysfunction or to death (Blockhuis *et al*., 2013). The aggregation of some proteins may also cause a toxic effect via sequestration of other proteins essential for neuronal functions.

In eukaryotic cells two mechanisms are mainly involved in protein degradation: the ubiquitin-proteasome system (UPS), which is highly selective for short-lived proteins, and autophagy, which acts on long-lived cytosolic proteins and organelles (Ciechanover, 2006). The second mechanism represents the most prominent pathway to promote motor neuron survival in ALS and in other neurodegenerative diseases (Ferrucci *et al*., 2011; Tan *et al*., 2008). Three forms of autophagy have been described: macro autophagy, micro autophagy, and chaperon-mediated autophagy (CMA). The first form is the most studied autophagy type: membranes separate from original sources (e.g., ER, mitochondria, Golgi apparatus or plasma membrane) and form an isolated vesicle, also called phagophore. Phagophore continues expanding to form the autophagosome, a ball-like double member structure. Microtubule-associated light chain 3-II (LC3-II) is one of the major protein markers of this type of autophagy in eukaryotes (see review of Song *et al*., 2012). Several studies showed an increase of autophagic markers in SOD1 mutant mice and ALS patients, even if autophagy seems insufficient or impaired. Indeed, LC3-II level was increased in spinal cord of $SOD1^{G93A}$ mice (Li *et al*., 2008; Morimoto *et al*., 2007; Zhang *et al.*, 2011). Moreover, Zhang and co-workers showed that LC3-II levels were increased in 90 days-old $SOD1^{G93A}$ mice, at the beginning of clinical symptoms, and reached the peak at the end stage of the disease (Zhang *et al*., 2011).

As briefly described above, one of the most mutated gene in fALS is the SOD1 coding gene. Interestingly, it was reported that the mutated protein can interact with dynein to alter its location and inhibit the normal fusion of autophagosome-lysosome in $SOD1^{G93A}$ mice (Hang *et al*., 2007). Moreover, the motor neurons loss can be delayed by the autophagic clearance of mutant SOD1 suggesting a positive impact of autophagy in ALS (Hetz *et al*., 2009; Crippa *et al*., 2010).

1.3.6 Axonal transport impairment

Motor neurons are highly polarized cells, often characterized by a very long axon. To maintain the correct homeostasis, functionality, and survival they need an efficient and bidirectional communication among the cellular body, dendrites, and distant cellular sites (e.g., synapses). Two main classes of axonal transport are distinguished: slow and fast. Both are mediated by the same molecular machinery and differ with respect to the speed by which the cargo is moved. The motor proteins, such as kinesins and dynein, can move the cargo along the microtubule polymers in antero- and retrograde directions (see review of Burk and Pasterkamp, 2019).

Several defects in axonal transport and mutations in different proteins involved in the process have been reported in both sALS and fALS patients. Accordingly, changes in axonal transport are one of the first pathological hallmarks of the disease and may be an early and a key event of the pathology. In 1996, damage at the retrograde axonal transport in ALS patients was primarily found (Sasaki and Iwata, 1996). Subsequently, the result was confirmed in the $SOD1^{G93A}$ mice both at the pre- and symptomatic phase of the disease (Sasaki *et al*., 2005; Lalli and Schiavo, 2002; Bilsland *et al*., 2010). Other studies investigated the anterograde transport responsible for RNA, mitochondria and neurofilaments transport toward the synapses. An impairment was found in spinal cord of $SOD1^{G93A}$ mice and ALS patients (Zhang *et al*., 1997; Delisle and Carpenter, 1984; Mendonça *et al*., 2005).

Besides the motor proteins which allow the cargo to move along the axon, other important proteins are involved in the impairment of axonal transport, such as mRNA-binding proteins (mRBPs) which regulate the RNA processing, mRNA trafficking and local protein synthesis within dendrites and axons. In ALS, an impairment of ribonucleoproteins assembly can, in fact, cause defects in axonal mRNA localization and in local translation (see review of Khalil *et al*., 2018).

The reduction of microtubules stability, mitochondrial damage and pathogenic signalling that alters the phosphorylation of molecular motors and the regulation of their function, as well as that of cargoes, such as neurofilaments, thus disrupting their association with motors, and of protein aggregation can also cause axonal transport impairment (see review of De Vos and Hafezparast, 2017).

1.3.7 Neuroinflammation

After having been considered only a consequence of MNs death, neuroinflammation is now established as an important player in ALS and in many other neurodegenerative diseases, such as PD, AD, multiple sclerosis, cerebrovascular disease, and HIV-associated encephalopathy (Hooten *et al*., 2015). Both in human patients and in animal models of ALS two main neuroinflammatory cell states can be identified: the neuroprotective and the neurotoxic one. They are associated with the different phenotypes acquired by the main cell actors involved in neuroinflammation, among which microglia.

In the mutant $SOD1^{G93A}$ mice two clinical phases have been identified after the onset of the disease: an initial slow phase during while mice do not appear to clinically worsen and a subsequent rapid phase where mice clinically decline until death.

During the slow phase ALS is characterized by a predominance of M2 factors, among which interleukin-10 (IL-10), interleukin-4 (IL-4), insulin-like growth factor-1 (IGF-1) and brain-derived neurotrophic factor (BDNF), released by astrocytes, microglia, T helper 2 (Th2) cells and T regulatory cells (Tregs) (Figure 2A, Beers *et al*., 2011b).

Conversely, during the fast phase of the disease pro-inflammatory and cytotoxic T cells predominate, together with T helper 1 cells (Th1) and start producing pro-inflammatory cytokines, among which interleukin-6 (IL-6), interleukin-1 (IL-1), tumor necrosis factor- α (TNF-α), and interferon-ɣ (IFN-ɣ). This event, together with the Treg function suppression, promotes the proliferation of Th1 and Th17 cells and M1 microglia polarization which in turn activate astrocytes and exacerbate MNs degeneration (Figure 2B, Beers *et al*., 2011b).

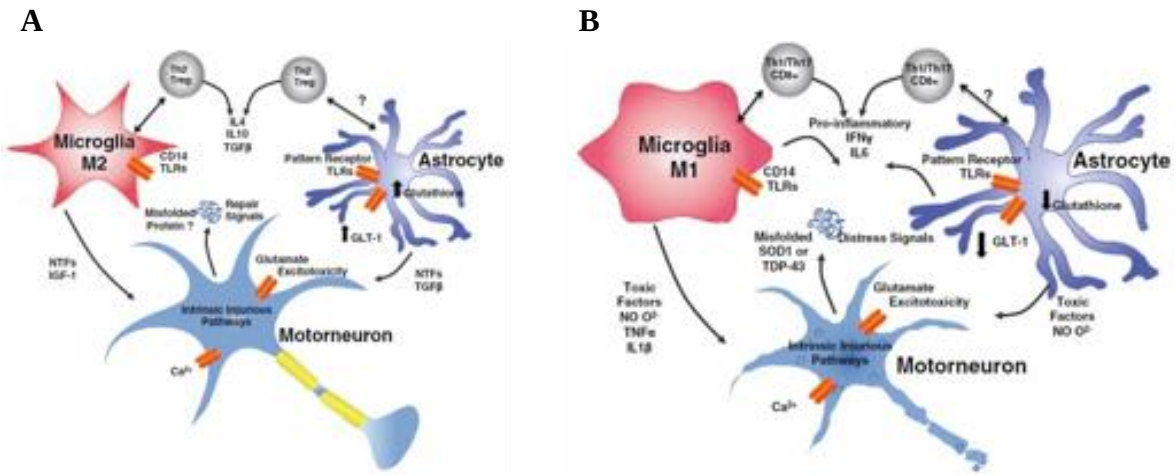

Fig.2 Schematic representation of neuroprotective and neurotoxic phases of neuroinflammation in ALS. (**A**) The first and slow phase of ALS is characterized by an anti-inflammatory/neuroprotective response of surrounding glia and immune cells. This phase is governed by Th2, Treg cells, M2 polarized microglia and supportive astrocytes secreting neurotrophic factors and decreasing neuronal stress. (**B**) The second and fast phase of ALS is characterized by a transition to an injurious response exerted by the surrounding glial and immune cells. This is assumed to be a vicious cycle that starts when MNs start dying inciting further inflammation and release of toxic factors (B) (Hooten *et al*., 2015).

These data have been also confirmed in ALS patients. Accordingly, peripheral blood monocytes involved in the innate immune system, showed to be more active in fast progressive forms of ALS (Zhao *et al*., 2017). In the same patients T-lymphocytes were found to be dysregulated and the number of Treg reduced. Moreover, *in-vitroin-vitro* experiments with Treg cells demonstrated their inability to suppress responder T lymphocytes, suggesting Tregs dysfunction (Beers *et al*., 2017).

Among the several molecules involved in immune system response, the major histocompatibility complex I (MHCI) represents a key player in the presentation of antigens. Recently, it has been also found in the CNS where it regulates long-term plasticity of excitatory synaptic transmission (Chiarotto *et al*., 2017) and exerts an important role in axon regeneration (Oliveira *et al*., 2004). The important function of this molecule in CNS has been confirmed by transgenic mice overexpressing MHCI, which recovered more efficiently the locomotor function after spinal cord injury, compared to WT mice (Joseph *et al*., 2011). In $SOD1^{G93A}$ mice, an altered distribution of MHCI has been reported already at the early phases of the disease, before the onset of motor symptoms. While in control animals MHCI is localized in lumbar spinal cord MN perikarya, in $SOD1^{G93A}$ mice, during disease progression, it distributes in efferent motor axons and in synaptic terminals (Nardo *et al*.,

2016). In the early phase of ALS, MHCI localization was associated with increased levels of two immunoproteasome subunits, β2 microglobulin (β2m) and Low-molecular mass protein-7 (Lmp7) which are involved in antigen peptide production, indicating the ability of MNs to produce and expose MHCI linked with antigens to cytotoxic T cells that infiltrate the peripheral nervous system. Consistently, $SOD1^{G93A}$ mice knock-out for β2m showed an anticipation of motor performance decline, axonal impairment, and denervation of hind limb muscle (Staats *et al*., 2013). On the contrary, in the late stage of the disease, MHCI overexpression exerted a detrimental effect, due to the strongly activation of pro-inflammatory microglia, accelerating denervation and atrophy of forelimbs in $SOD1^{G93A}$ mice. These effects are partially recovered by the β2m deletion which promotes the maintenance of forelimb innervations and prolongs mouse survival (Nardo *et al*., 2018).
In astrocytes, the silencing of MHCI regulates the astrogliosis by reducing the expression of glial fibrillary acidic protein (GFAP) and of some pro-inflammatory cytokines (Bombeiro *et al*., 2016). However, these cells are unable to activate MHCI *in-vivo*. Accordingly, no activation of the MHCI complex was observed in spinal cord of $SOD1^{G93A}$ mice during disease progression (Nardo *et al*., 2013). Conversely, spinal cord microglia of $SOD1^{G93A}$ mice expressed high level of MHCI cause an exacerbation of inflammation by recruiting cytotoxic CD8+ T lymphocytes and promote MN death (Nardo *et al*., 2016). A further confirmation of the important role of MHCI in microglia activation derives from $SOD1^{G93A}$ mice knock-out for β2M in which the inflammatory response was reduce both *in-vitroin-vitro* and *in-vivo* (Nardo *et al*., 2018).

The inflammatory response can be also developed by the nuclear factor kappa-light-chain-enhancer of activated B cells (NFκB). This factor is responsible for the gene expression of cytokines, chemokines, enzymes, adhesion molecules, pro- and anti-apoptotic proteins. NFκB is composed by two of five DNA-binding protein (p50, p52, p65 RelA, c-Rel, RelB) and the different assembly determines specific transcriptional activity. As soon as inflammatory mediators bind their respective receptors, a signalling cascade leads to phosphorylation and activation of I-Kappa-B Kinase (IKKB), which, in turn, phosphorylates the NFκB inhibitory protein IκBα and determines its proteasomal degradation. Finally, NFκB (p65/p50) can translocate to the nucleus where it modulates gene transcription (Ghosh and Karin, 2002).

NFκB has been found up-regulated in glial cells of both fALS and sALS patients, confirming its involvement in neuroinflammation in ALS and the consequent important role of

astrocytes and microglia in the disease progression (Haidet-Phillips *et al.*, 2011; Swarup *et al*., 2011). Frakes and colleagues demonstrated that the NFκB inhibition obtained by the selective partial deletion of IKKB in microglia isolated from $SOD1^{G93A}$ mice significantly increased survival of these mice. Moreover, the knock-down of IKKB in $SOD1^{G93A}$ microglia reduced typical markers of pro-inflammatory microglia (M1), such as CD68, CD86 and iNOS. Unexpectedly, the same deletion in astrocytes did not produce an improvement in disease symptoms, suggesting the existence of different mechanisms for astrocyte-mediated toxicity (Frakes *et al*., 2014).

NFκB can have a neuroprotective or neurotoxic effect, depending on the acetylation state of RelA subunit (Lanzillotta *et al*., 2010). This subunit has been found to be highly expressed in mutant SOD1 MNs *in-vitro* models and in ALS patients (Lanzillotta *et al*., 2013; Jiang *et al*., 2005). A subsequent study carried in spinal cord of $SOD1^{G93A}$ mice demonstrated that RelA presented an aberrant acetylation state, represented by global lysine deacetylation, and enhanced acetylation of a specific residue of lysine in position 310 (K310). This latter promotes the transcription of pro-apoptotic factors inducing neurodegeneration (Schiaffino *et al*., 2018; Lanzillotta *et al*., 2013). The administration of MS-275 (Entinostat), an inhibitor of the histone deacetylases (HDAC), and resveratrol, which mediates the selective deacetylation of K310, reverted the aberrant acetylation state of RelA and increased the expression of B-cell lymphoma-extralarge (Bcl-xL), an anti-apoptotic protein, in lumbar spinal cord of $SOD1^{G93A}$ mice. These biochemical read-outs translated into a delay of disease onset, an amelioration of motor skills and an increase of survival (Schiaffino *et al.*, 2018).

Another relevant mediator of neuroinflammation development in ALS is the cytosolic nucleotide-binding oligomerization domain (NOD)-like receptor (NLR) pyrin domain containing 3 (NLRP3; inflammasome). NLRP3 is formed by three components: a cytosolic pattern recognition receptor (PRR), the pro-caspase 1 and the apoptosis-associated speck-like protein (ASC), containing a caspase recruitment domain. Its assembly is triggered after binding of pathogen-associated molecular patterns (PAMPs) and DAMPs or endogenous cytokines to the toll-like receptors (TLRs). Indeed, TLRs and cytokines promote NLRP3, pro-interleukin-1β (pro-IL-1β) and pro-IL-18 transcription through the NFκB pathway. After this first step, NLRP3 binds ASC and the following activation of caspase 1. The activated caspase 1 leads to the proteolytic cleavage of pro-IL-1β and pro-IL-18 in their respective active forms, mediating the innate immune response (Singhal *et al*., 2014; Davis *et al*., 2011; He *et al*., 2016).

Increased levels of NLRP3 and active caspase 1, together with higher expression of Toll-like receptor 4 (TLR4) and NFκB, have been reported in $SOD1^{G93A}$ rat brain (Gugliandolo *et al*., 2018). NLRP3 activation has been also reported in the early stage of ALS. Accordingly, Johann and colleagues detected higher concentrations of inflammasome and IL-1β in spinal cord of 60 days-old $SOD1^{G93A}$ mice and in post-mortem tissue from ALS patients (Johann *et al*., 2015). A hypothesis supporting the increased expression of NLRP3 is given by the protein nitration. Reactive oxygen and nitrogen species are hallmarks of ALS and cause protein damage, among which protein tyrosine nitration. The treatment of $SOD1^{G93A}$ microglia with iNOS and NOX2 inhibitors reduced nitrotyrosine levels and, consequently, caspase 1 and NLRP3 activation, supporting the involvement of protein nitration in neuroinflammation spread (Belleza *et al*., 2018).

1.4 ALS as a non-cell autonomous disease

The progression of ALS mostly arises from degeneration of motor neurons. Nevertheless, the toxicity to these cells often derives from nonneuronal cell populations, specifically from astrocytes, microglia, and oligodendrocytes. Accordingly, all the mutated genes, which cause the inherited form of the disease, are ubiquitously expressed, or expressed in multiple cells types (Boillée *et al*., 2006a). Several studies carried on $SOD1^{G93A}$ mice demonstrated that the toxicity of mutated SOD1 is not just due exclusively to MN damage (Ilieva *et al*., 2009) since high expression levels of the mutant protein in most (Clement *et al*., 2003) or all (Yamanaka *et al*., 2008a) motor neurons only are not sufficient for early disease onset. Conversely, astrocytes and microglia expressing mutant SOD1 develop autologous damage properties and, in turn, cause an acceleration of the disease by affecting MNs. In line with these observations, a selective reduction of mutant SOD1 in astrocytes has been demonstrated to slow disease progression and delay microglia activation, demonstrating a cross talk between the two types of glia cells (Ilieva H *et al*., 2009).

1.4.1 Astrocytes and ALS

Astrocytes are the most abundant cells in the CNS, display various structures and functions and are ubiquitous in all CNS regions. Their unique morphology and phenotypic features allow them to easily sense and communicate with the surrounding cells and quickly respond

to changes in the microenvironment. In fact, the numerous and greatly ramified astrocytic processes form highly organized domains which overlap with adjacent cells (Allaman *et al*., 2011). Astrocytes are interconnected each other by functional networks via gap junctions. This kind of connection is strictly region, astrocyte, and neuronal activity dependent, suggesting the existence of glial circuits (Houades *et al*., 2006).
As neurons, astrocytes are very heterogenous and can be distinguished by morphology, location, antigenic phenotype and by their functions.

Even if they are electrically non-excitable cells, they express several molecules, such as ion channels (in particular, Ca^{2+} and Na^{+} channels), neurotransmitters, neuromodulators and neurohormones receptors. Ion changes monitor neurotransmitters concentration, pH homeostasis and ROS neutralization (Verkhratsky and Zorec, 2018). The astrocytic expression of receptors for a variety of neurotransmitters allows these cells to be actively responsive to the release of neuronal messengers. Accordingly, as soon as neurons release transmitter molecules, such as glutamate or ATP, the astrocytic ionotropic NMDA or AMPA receptors or G protein coupled receptors (GPCRs) get activated and lead to intracellular Ca^{2+} rise by ligand activated ion channels or by the release from ER (Barres, 2008).

Astrocytes take part in the so-called tripartite synapse, together with post- and presynaptic neurons, helping to remove toxin metabolites and to control ions levels and neurotransmitters from the extracellular space (Barres, 2008). These astrocytes are characterized by a high plastic capacity and by releasing trophic factors, nutrients, and neuroactive substances, sustain the synaptogenesis, lead to synapse maturation, and enhance the pre- and postsynaptic functions (Barres, 2008; Verkhratsky and Zorec, 2018).

Some specialized astrocytic processes, called *endfeet*, closely surround endothelial cells and pericytes, promoting the correct structure of blood vessels and blood-brain barrier (BBB) (Volterra and Maldolesi, 2005; Sykova and Chavatal, 1993). Astrocytes play an important role also in neurovascular and neurometabolic coupling. According to the context they can release either vasoconstrictor or vasodilator agents (Barres, 2008). The involvement of astrocytes in the structure and function of BBB was firstly demonstrated in 1999, when Bush and collaborators showed the critical role of these cells in sealing the BBB after brain injury (Bush *et al*., 1999). Interestingly, it has been demonstrated that during postnatal development, when stem cell, which regulate the formation functions of the BBB, are depleted, the maintenance of the barrier is regulated by astrocytes (Cahoy *et al*., 2008).

At the metabolic level, astrocytes respond to glutamatergic activation by increasing their rate of glucose consumption and releasing lactate in the extracellular space, which sustains the neuronal energy demands (Magistretti, 2006; Tsacopoulus and Magistretti, 1996).

Another important role of astrocytes is represented by their involvement, in concert with microglia, in regulating the immune response of the CNS to infections, neurodegenerative disorders, and injuries (Farina *et al*., 2007; Rivest, 2009) by releasing inflammatory factor, such as cytokines, chemokines, complement proteins and reactive oxygen or nitrogen species availability (Philips *et al*., 2014). Accordingly, they express pattern recognition receptors (PRRs) (Bsibsi *et al*., 2006; Bsibsi *et al*., 2002; Farina *et al*., 2005) which are key sensors of tissue damage signals, facilitators of local neuroinflammation in CNS diseases and are involved in the crosstalk between neurons and glia and between the infiltrating immune cells and resident CNS cells (Li *et al*., 2020). Toll-like receptors represent the best characterized family of PRRs (Akira, 2001; Kawai and Akira, 2011). These glial receptors can exert different roles: i) they defend the host from pathogens during infectious diseases by anti-microbial and pro-inflammatory responses; ii) they can stimulate astrocytes to release neuroprotective agents, depending on the ligands present in the milieu; iii) they can recognize specific pathogenic proteins, typical of neurodegenerative diseases, and promote the pro-inflammatory response of astrocytes by releasing of cytokines and chemokines; iv) they can facilitate the internalization and clearance of aggregated proteins by astrocytes (Li *et al*., 2020).

Astrocytes can be classified in two main groups: reactive A1-type neurotoxic astrocytes, which promote neurodegeneration and neurotoxicity, and neuroprotective A2-type astrocytes, which secrete neurotrophic factors to provide neuronal repair and neuroprotection (Table 2). Considering the key role of astrocytes in the CNS homeostasis and the strong metabolic cooperation with neurons, it is easy to predict that astrocytic dysfunctions may cause or contribute to neurodegenerative processes. Upon injury, stress or neurodegeneration, astrocytes undergo astrogliosis and change their morphology and gene expression profile, becoming activated (Liddelow and Barres, 2015). At this stage, they can respond to stimuli by releasing supporting messengers, such as BDNF, vascular-endothelial growth factor (VEGF), and basic fibroblast growth factor (bFGF), or opposing messengers, such as cytotoxins, Lipocalin-2 (Lcn2) and inflammatory factors (e.g., IL-1β, TNF-α and

NO, Liddelow and Barres, 2015). The signalling pathways which can induce the shift between A1 and A2 astrocytes are still unknown.

Table 2 The molecular expression changes between two A1 and A2 astrocytes (Li *et al*., 2019).

Reactive astrocytes	Molecular Expression	
A1 astrocytes	Up regulation	Inflammatory signalling through NF-kB
		Glutamate and ATP release
		Secretion of inflammatory mediators (prostaglandinD2, IFN-ɣ, and TGF-β)
		Lcn2 secretion
		IL-1α, C1q, TNF
	Down regulation	GPC4, GPC6, SPARCL1 expression
		EAAT2, GLT1
		Trophic factor release
		Lactate transportation
		GABA release through GAT-3
A2 astrocytes	Up regulation	Inflammatory signalling through STAT3
		Thrombospondins (THBS1 and THBS2)
		Aquaporin-4
		HMGB1 and β-2 integrin
		Trophic factors release (BDNF, VEGF and bFGF)
	Down regulation	H2-D1, Gbp2, Fkbp5, Srgn

Several changes in astrocytic phenotype have been found in SOD1-ALS models. Astrocytes carrying the human mutated $SOD1^{G85R}$ were immune positive for ubiquitinated-SOD1, suggesting a defective proteostasis (Bruijn *et al*., 1997). They also express cleaved caspase-3 and are localized near damaged MNs, confirming their pro-degenerative phenotype (Rossi *et al*., 2008). Aberrant astrocytes isolated form $SOD1^{G93A}$ rats showed a similar phenotype and exerted direct and selective toxicity to MNs by secreting soluble factors (Diaz-Amarilla *et al*., 2011). Astrocyte-mediated toxicity to MNs was demonstrated also *in-vivo*: transplantation of mutant SOD1 astrocyte precursors into the spinal cord of wild-type rats lead to motor neuron degeneration (Papadeas *et al*., 2011), whereas the transplantation of wild-type astrocytic precursors into ALS mouse model spinal cord decreased MN death (Lepore *et al*., 2008).
Consistent with these observations, another *in-vivo* study in $SOD1^{G93A}$ mice demonstrated that astrocytes can be defective for glutamate uptake, mainly due to a decreased GLT-1 expression, resulting in extracellular accumulation of the neurotransmitter which causes excitotoxicity (Rothstein *et al*., 2006; Pardo *et al*., 2006; Rothstein, 2009; Lobsiger and Cleveland, 2007).

Another astrocyte-released messenger molecule linked to glutamate excitotoxicity is D-serine that bind the glycine site at NMDA receptor, thus allowing the receptor activation, and that was found increased in mutated-SOD1 mice (Sasabe *et al*., 2012). Intriguingly, a mutation in D-amino acid oxidase, the enzyme which controls D-serine level, was also found to be linked to the familiar form of the pathology (Mitchell *et al*., 2010).
In addition to these abnormalities, astrocytic mitochondria were found to be damaged. The defects of these organelles can lead to an increase of ROS production, both in SOD1-ALS mice (Cassina *et al*., 2008) and in human astrocytes (Marchetto *et al*., 2008).

Another important role of astrocytes in ALS pathogenesis is represented by neuroinflammation. During the slow progression of the disease an anti-inflammatory process governs the cellular and the extracellular environment. Conversely, during the rapid progression of the pathology a proinflammatory state prevails (Hooten *et al*., 2015). Accordingly, high levels of circulating pro-inflammatory cytokines such as TNF-α, IL-1β and IFN-γ have been described both in human patients and in animal models of ALS (Tolosa *et al*., 2011). Interestingly, Liddelow and colleagues recently demonstrated that microglia exposed to a neuroinflammatory insult, such as lipopolysaccharide (LPS), secreted

interleukin-1α (IL-1α), TNF-α and the Complement factor 1q (C1q). This event induced the conversion of quiescent astrocytes into activated ones (called A1 astrocytes, Liddelow *et al*., 2017). Consequently, these reactive astrocytes lost many of their physiological functions and secreted one or more unknown factors potentially toxic for neurons and oligodendrocytes. Moreover, these A1 astrocytes overexpressed the complement component 3 (C3), a reactive astrocyte marker, which is also found to be elevated in mutated SOD1 and C9orf72 fALS and in sALS patients. Soon later the same group of research investigated if the prevention of neuroinflammatory reactive astrocyte phenotype could be beneficial for ALS patients (Guttenplan *et al*., 2020). Therefore, they generated IL-1$\alpha^{-/-}$ TNF-$\alpha^{-/-}$ and C1qa$^{-/-}$ SOD1^{G93A} transgenic mice and compared this mouse model with the SOD1^{G93A}. They found lower levels of C3 expressed by astrocytes and an extension of lifespan of the IL-1$\alpha^{-/-}$ TNF-$\alpha^{-/-}$ and C1qa$^{-/-}$ SOD1^{G93A} mice of over 50%, the longest ever found in all the ALS animal models (Guttenplan *et al*., 2020).

Astrocytes represent a major source of energy for MNs. Another astrocytic pathological trait identified in SOD1^{G93A} mice is linked to the impairment of many proteins involved in lactate shuttle. Neuronal glutamate release induces the activation of the Na^+/K^+-ATPase pump that consumes the ATP produced by phosphoglycerate kinase (Pgk) leading to glucose uptake, its glycolytic processing, and the astrocytic release of lactate, fundamental for neuronal energy demand associated with synaptic transmission (Pellerin *et al*., 2007). In SOD1^{G93A} astrocytes, some of the proteins involved in this mechanism, such as mice glutamate aspartate transporter-1 (GLAST-1), Na^+/K^+-ATPase, Pgk and the lactate efflux transporter Solute carrier 16a4 (Slc16a4) were found to be impaired. This gene expression analysis was confirmed by the reduction of lactate level in the spinal cord of SOD1^{G93A} transgenic mice. The reduced lactate shuttle of SOD1^{G93A} mice has been identified already at the early stage of the disease, followed by a further decrease during ALS progression. (Ferraiuolo *et al*., 2011).

Astrocytes can release several trophic factors, including nerve growth factor (NGF) which has a key role in modulating neuronal differentiation and survival by binding at Tyrosin receptor kinase A (TrKA). Conversely, the precursor of NGF (pro-NGF) preferentially binds to the p75 receptor which determines axonal growth and remodelling during development. The expression of this receptor in adult life in barely detectable, however it increases in pathological conditions where p75 shows to promote apoptosis by boosting NF-kB, p53 and Bax. SOD1^{G93A} astrocytes, indeed, have been shown to express higher pro-NGF levels

respect to WT astrocytes and an up regulation of p75 and its pro-apoptotic associated protein (Ngfrap1). These alterations together with a decrease level of mature NGF, causes MN death in ALS mice (Ferraiuolo *et al*., 2011).

In Figure 3 Yamanaka and Komine resume the main typical feature of activated astrocytes in ALS (Yamanaka and Komine, 2018).

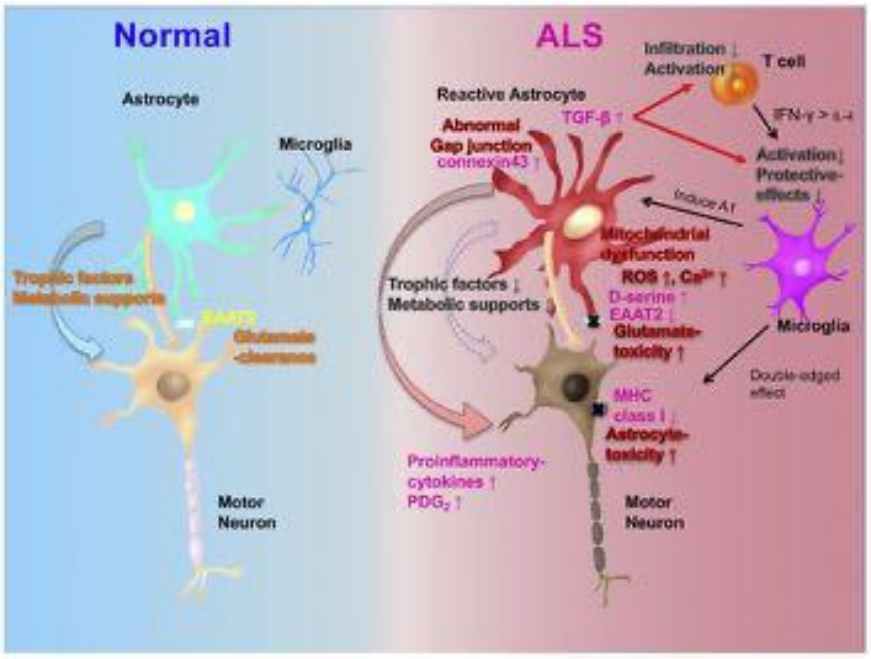

Fig. 3 Multi-dimensional roles of astrocytes in non-cell autonomous neurodegeneration in ALS. In normal condition (on the left), astrocytes support motor neurons releasing trophic factors, giving metabolic support, and controlling the glutamate concentration at synaptic cleft. In ALS (on the right) astrocytes lose these homeostatic functions, fail to support motor neurons, and start secreting toxic factors. Microglia and lymphocytes are also involved in the non-cell autonomous neurodegeneration (Yamanaka and Komine, 2018).

Other typical markers of astrogliosis, not shown in Figure 3, are GFAP, Vimentin and calcium-binding protein S100β (Phatnani and Maniatis, 2015).

Clinical findings confirmed those of $SOD1^{G93A}$ mouse models described above. CNS tissues of patients affected by neurodegenerative diseases, among which ALS, showed a ubiquitous astrogliosis (Hamby and Sofroniew, 2010; Rossi and Volterra, 2009). In particular, the degree of reactive astrocyte presence correlates with the neurodegeneration level of ALS

patients. Induced-astrocytes (i-astrocytes) derived from the adult neural progenitor cells (NPCs), which were isolated from post-mortem lumbar spinal cord tissue of fALS and sALS individuals, showed a toxic effect to healthy motor neurons in culture (Haidet Philips *et al*., 2011; Meyer *et al*., 2014). The same toxicity was demonstrated converting SOD1 and C9orf72 ALS patients' fibroblasts into tripotent induced NPCs and subsequently into i-astrocytes and testing them in co-culture with MNs (Meyer *et al*., 2014).

Moreover, astrocytes of C9orf72 and sALS patients showed an impaired nucleosides metabolism (Allen *et al*., 2019). Accordingly, higher level of adenosine, the last step of ATP metabolism has been shown in ALS. The increased concentration of this nucleoside causes the stimulation of low affinity receptors on astrocytes, promoting astrocyte proliferation and activation, reducing glutamate uptake, and inducing Ca^{2+}-dependent glutamate release (Rothstein *et al*., 1996). In C9orf72 astrocytes the higher level of adenosine was related to lower expression of adenosine deaminase (ADA), an enzyme which converts adenosine in inosine. The detrimental effect of this event was confirmed by the inhibition of ADA in control astrocytes which, accordingly, caused death of MN co-cultured with treated astrocytes. The exposure of these astrocytes to inosine partially rescued MN survival, confirming the important function of both the nucleosides in ALS (Allen *et al*., 2019).

In light with the findings described in this chapter several questions arise: i) which is the relationship between the astrocyte profile (whether A1 or A2) and the different stages of the disease? ii) which elements influence balance between A1 to A2 astrocytes? iii) are A2 reactive astrocytes able transform directly into A1 astrocytes and vice versa?

Answers to these questions may provide molecular astrocytic targets for pharmacological intervention to treat ALS and, possibly, other neurodegenerative diseases.

1.4.2 Microglia and ALS

The concept of microglia was introduced, for the first time, by Del Rio-Hortega in 1923 and all his statements are still valid today. He postulated that: i) microglia enter the brain during early development; ii) microglia have a mesodermal origin and, at that stage, show an amoeboid morphology; iii) once the brain matures, microglia transform into a branched, ramified morphological phenotype (known today as the surveying microglia); iv) microglia are evenly dispersed throughout the CNS and display little variation; v) each cell seems to occupy a defined territory; vi) after a pathological event microglia undergo a transformation

acquiring an amoeboid morphology, like that observed during early development (known today as the activated microglia) (Kettenmann *et al*., 2011).

Microglia have the capability to migrate, proliferate and phagocytize, although the phagocytic function is less efficient than that exhibited by activated macrophages (Kettenmann *et al*., 2011; Barres, 2008). Microglia represent the only innate immune cells of the brain and spinal cord and represent about 10% of CNS glia. In physiological condition they monitor the extracellular environment, rapidly responding to changes or injury and triggering inflammatory responses, similarly to the peripheral macrophages, that affect neural surroundings cells or to non-neural immune cells in the CNS (Barres, 2008). Microglia have been demonstrated to monitor and maintain the synapses in uninjured brains not only diffusing signals in the extracellular space but also making frequent and direct contacts with them (Wake *et al*., 2009). Accordingly, microglia play a key role in synaptic pruning during postnatal development of mice (Paolicelli *et al*., 2011). This function is partly mediated by the fractalkine signalling, a chemokine whose receptor is exclusively expressed by microglia in the CNS, and links microglia surveillance to synaptic maturation (Paolicelli *et al*., 2011).

During development, microglia can also refine neuronal connections, including axonal guidance and synaptogenesis (Verney *et al.*, 2010), and secrete neurotrophic factors, such as BDNF, glial cell line-derived neurotrophic factor (GDNF) and IGF-1 (Ban *et al*., 2019).

The activation state of microglia, similar to macrophages, may be distinguished as two discrete phenotypes, called M1 (toxic) and M2 (protective; Du *et al*., 2017). The M1 polarized microglia, characterized by ameboid shape, high mobility, and strong phagocytic capacity, produce, and release pro-inflammatory cytokines, such as TNF-α, IL-6, interleukin-23 (IL-23), IL-1β, interleukin-12 (IL-12), NO, cytotoxic substances (among which ROS), prostaglandin E2 and chemokines. Conversely, M2 polarized microglia show thin cell body and branched processes and express anti-inflammatory molecules, such as IL-10, TGF-β and extracellular matrix molecules, such as fibronectin (Du *et al*., 2017).

This functional classification was confirmed by studies investigating the role of microglia in ALS. In fact, during the progression of the disease microglia increase in number and shifts its reactive state from the protective M2 to the toxic M1 (Figure 4; Liao *et al*., 2012; Chiu *et al*., 2013).

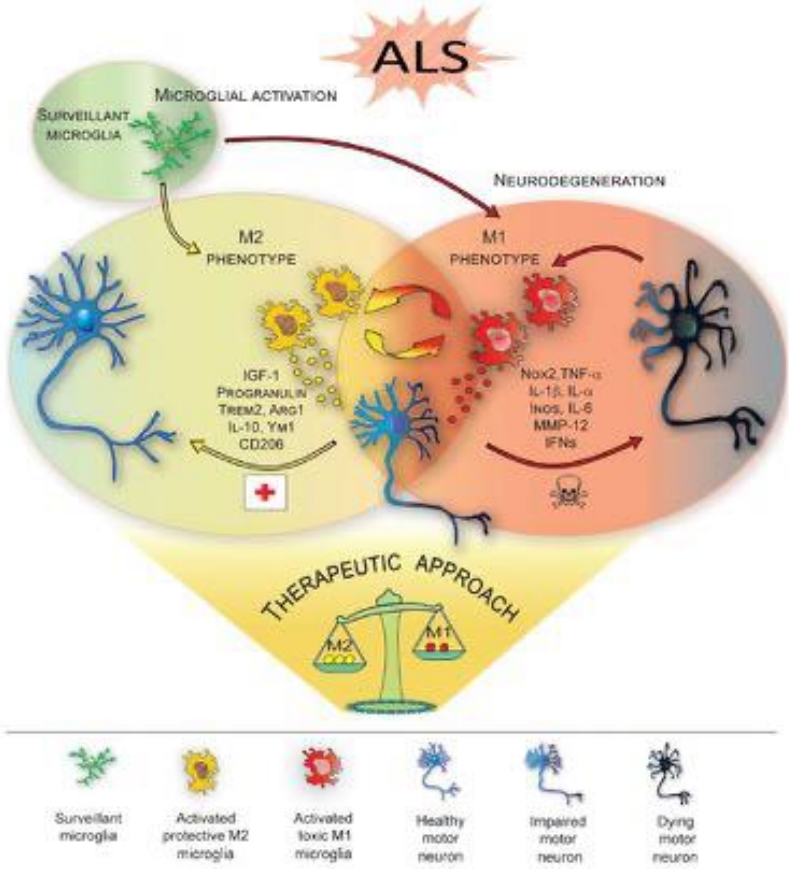

Fig. 4 Microglia polarization during ALS. During the progression of the disease activated microglia shift from the neuroprotective M2 phenotype, which promotes tissue repair and supports neuronal survival by releasing neurotrophic factors, to the toxic M1 phenotype, which produces cytokines increasing inflammation. Targeting microglia polarization to induce M2 phenotype may represent a therapeutic strategy to ameliorate local neurodegeneration (Geloso *et al*., 2017).

Accordingly, $SOD1^{G93A}$ and $SOD1^{G37R}$ murine microglia, isolated at the pre-onset stage of ALS, exhibited an anti-inflammatory profile, characterized by overexpression of IL-10 and downregulation of Toll like receptor 2 (TLR2) response (Gravel *et al.*, 2016). Subsequently, at the disease onset and during the slowly progression phase, microglia prevalently express M2 markers, such as Ym1 and CD206 (Beers *et al*., 2011a). At the end stages of the disease, microglia express high levels of NOX2, the subunit of nicotinamide-adenine-dinucleotide-phosphate (NADPH) oxidase that is considered a M1 prototypic marker (Beers *et al*., 2011b).

Another evidence supporting the important role of microglia in ALS was produced by Boillée and Wang in different SOD1 mouse model of the disease. They showed that reducing mutant SOD1 in microglia slows down the progression of the pathology (Boillée *et al*.,

2006b; Wang *et al*., 2009). Conversely, it has also reported that microglia expressing the mutant $SOD1^{G93A}$ produce higher levels of peroxides, nitrates, and nitrites than microglia expressing $SOD1^{WT}$, both in resting condition and after an activation with LPS. The production of these neurotoxic species can exacerbate the progression of the disease and increase MN death (Beers *et al*., 2006). The same study showed that bone marrow transplant, aimed to completely substitute microglia, slows down the progression of ALS, but not the onset of the disease.

Altogether these data focus to microglia as a therapeutic target to treat ALS. Several drugs have been tested in animal models to modulate the M1/M2 balance of microglia centring on the molecular pathways related to microglia polarization. The results obtained demonstrated an amelioration of the local neurodegeneration (Geloso *et al*., 2017). Accordingly, it was recently demonstrated that the microglial nuclear factor kappa-light-chain-enhancer of activated B cells (NFkB) suppression combined with mutant SOD1 reduction in astrocytes and motor neurons results in attenuated neuroinflammation and neurodegeneration and increases mice mean survival (Frakes *et al*., 2017).

1.4.3 Oligodendrocytes and ALS

Oligodendrocytes are highly specialized glial cells in the CNS which closely interact with axons of neurons. These cells show two main functions: i) generating a compact multi-layered myelin sheath around the axon (see review of Nonneman *et al*., 2014); ii) providing neurons with energy support (Lee *et al*., 2012, Morrison *et al*., 2013).

The first function is essential to propagate axon potentials very fast and efficiently over long distances through saltatory conduction which takes place through the nodes of Ranvier (Poliak and Peles, 2003). The second role of oligodendrocytes is fundamental to maintain the functional integrity of neurons. Lactate, pyruvate, and ketone bodies are essential monocarboxylate substrates for the CNS. They are transported across the membranes by monocarboxylate transporters (MCTs), being the MCT1 specific for lactate and highly expressed by oligodendrocytes (Pierre and Pellerin, 2005; Chiry *et al*., 2011; Pierre *et al*., 2000). The downregulation or inhibition of MCT1 leads to axon degeneration, underlying the importance of lactate for neurons (Lee *et al*., 2012; Morrison *et al*., 2013). This energetic substrate is also important for the development of oligodendrocytes and is an essential nutrient for the synthesis of lipids needed for myelinization (Rinholm *et al*., 2011). Each

alteration of one of these two oligodendrocyte function can contributes to the onset of important neurodegenerative diseases (Nave, 2010a; Nave, 2010b; Lee *et al*., 2012).

Oligodendrocytes are generated from multipotent neural stem cells (NSCs) during CNS development. NSCs, located in the embryonic spinal cord, give rise to glial progenitor cells and subsequently to oligodendroglia precursor cells, also called NG2+ glial cells because of their characteristic expression of proteoglycan NG2 (Nishiyama *et al*., 2009; Trotter *et al*., 2010; Levine *et al*., 2001). NG2+ cells differentiate into oligodendrocytes during the late embryonical and early postnatal stages. Lately, oligodendrocytes further mature into functionally myelinating cells that wrap their membrane several times around axon to form a multi-layered myelin sheath. This mechanism of myelination together with oligodendrocyte generation takes also place during the adulthood (Bartzokis, 2004; Young, 2013). However, with aging myelin slowly gets thinner and its breakdown results into slower propagation of action potentials. This process is typical of every healthy adult, but during neurodegeneration it occurs more rapidly (Bartzokis, 2004).

The role of oligodendrocytes and their precursors in ALS has been ignored for long time. However, pathological inclusions of TDP-43 were found in the cytoplasm of oligodendrocytes from post-mortem tissues of both sALS and fALS patients. The same was observed for the FUS protein, which aggregates in oligodendrocytes of ALS patients affected by the mutation of the protein (Mackenzie *et al*., 2011). The abundance of FUS inclusions correlates with the age of the disease onset: patients with late onset are characterized by abundant FUS inclusions in oligodendrocytes; conversely, patients with early onset show these aggregates predominantly in neurons (Mackenzie *et al*., 2011). In addition to protein inclusions, myelin abnormalities, demyelination and oligodendrocyte degeneration were found in the grey matter of the ventral spinal cord of sALS and fALS patients, as well as changes in NG2+ oligodendrocytes precursor cells (Kang *et al*., 2013). The same oligodendrocyte abnormalities of ALS individuals were confirmed in ALS mouse models (Lee *et al*., 2012; Philips *et al*., 2013; Kang *et al*., 2013; Stieber *et al*., 2000). For example, it was demonstrated that the grey matter oligodendrocytes in the spinal cord of mutant SOD1 mice degenerate before motor neurons degeneration (Philips *et al*., 2013; Kang *et al*., 2013). An important indicator of oligodendrocytes degeneration is the abnormal morphology. Impaired oligodendrocytes show thickened and irregular shaped cell body, enlarged cytoplasm and elongated processes (Philips *et al*., 2013). Oligodendrocytes acquiring these characteristics are defined as dysmorphic and are in an apoptotic state. In $SOD1^{G93A}$ mice the number of dysmorphic oligodendrocytes is significantly high before the onset of disease

and progressively increases, more than fivefold, during disease progression (Philips *et al*., 2013). Notwithstanding this progressive degeneration, the overall number of oligodendrocytes and their density do not change throughout the course of the disease respect to $SOD1^{WT}$ mice (Philips *et al*., 2013; Kang *et al*., 2013). This is due to an actively replacement of the cells operated by NG2+ precursors. Unfortunately, oligodendrocytes newly generated in spinal cord of $SOD1^{G93A}$ mice are often associated with axons characterized by damage and degeneration, probably because the new oligodendrocytes are dysfunctional and less efficient (Nonneman *et al*., 2014). The knowledge about the possible causes of oligodendrocytes damage in ALS has been growing since years. Nonneman and colleagues hypothesized that three phases of damaging insults are responsible for oligodendroglia cell pathology in ALS (Nonneman *et al*., 2014). They are schematized in Figure 5.

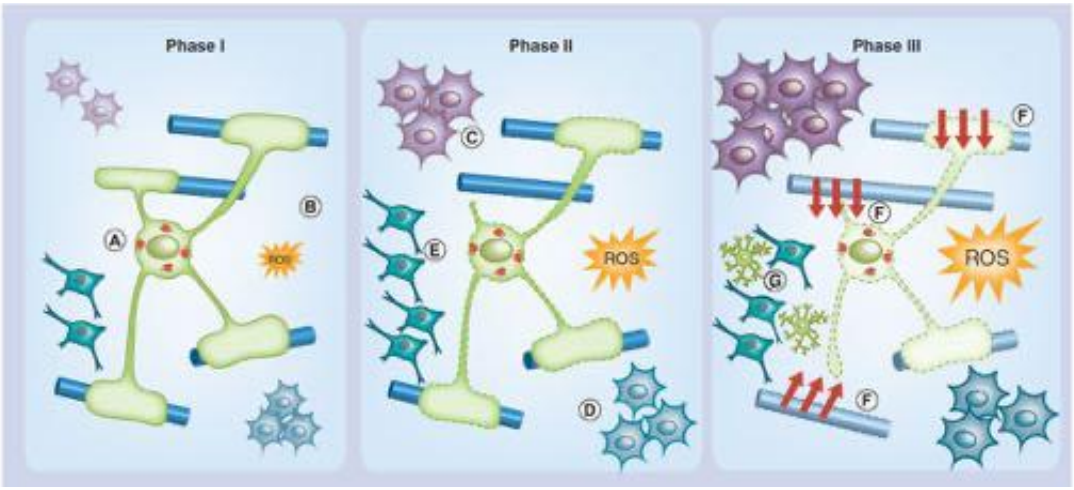

Fig. 5 The involvement of oligodendrocytes in ALS. (**Phase I**) In the first phase of damaging insults to oligodendrocytes the presence of mutated genes (indicated in the panel with letter A) is likely to cause oligodendrocytes to be more vulnerable to other insults, such as ROS (indicated in the panel with letter B). (**Phase II**) This latter event is then amplified by microglia (indicated in the panel with letter C) and astrocytes (indicated in the panel with letter D) that become reactive and release proinflammatory cytokines and ROS. In parallel and in response to oligodendrocytes damage, NG2+ precursor cells become reactive and start proliferating (indicated in the panel with letter E). (**Phase III**) The third phase represents the symptomatic stages of ALS in which motor neuron degeneration concurs to oligodendrocytes damage (indicated in the panel with letter F). Motor neuron degeneration can induce excitotoxicity in the oligodendrocytes, meanwhile microglia and astrocytes become more activated. This toxic environment also impairs the differentiation of NG2+ precursor cells into oligodendrocytes leading to production of immature and dysfunctional oligodendrocytes (indicated in the panel with letter G) (Nonneman *et al*., 2014).

All the above findings demonstrate the important role that oligodendrocytes, similarly to astrocytes and microglia, play in ALS. Therefore, clarification of their role in neurodegeneration and of the mechanisms involved it would be essential in the next future.

1.5 Glutamate metabotropic receptors

Glutamate is the most abundant excitatory neurotransmitter of the brain and exerts its function through ionotropic and metabotropic receptors. As briefly described in chapter 1.3.1, iGluRs are ligand-gated ion channels, permissive to cations (Na^+, K^+ and Ca^{2+}) flux across the cell membrane, they mediate fast excitatory synaptic signalling and have a key role in synaptic plasticity (Wollmuth, 2018). Conversely, mGluRs are GPCRs that participate in the modulation of synaptic transmission and neuronal excitability via second messenger signalling pathways. On the basis of their sequence homology, pharmacology and

transduction mechanism, they are further subdivided into three groups: the predominantly postsynaptic excitatory Group I receptors (mGluR1 and mGluR5), the pre- and postsynaptic Group II receptors (mGluR2 and mGluR3), and the predominantly presynaptic Group III receptors (mGluR4, mGluR6, mGluR7, mGluR8) (Table 3; Kim *et al*., 2020).

Family	Receptors	G-protein coupling	Characteristics	Type
Group I	mGluR1	**G_q coupled**	Primarly postsynaptic. Expressed in neurons.	**Excitatory**
	mGluR5		Pre- and postsynaptic. Expressed in neurons and astrocytes.	
Group II	mGluR2	**G_i coupled**	Primarly presynaptic. Expressed in neurons and astrocytes.	**Inhibitory**
	mGluR3		Primarly postsynaptic. Expressed in neurons and astrocytes.	
Group III	mGluR4		Pre- and postsynaptic. Expressed in neurons and reactive astrocytes.	
	mGluR6		Pre- and postsynaptic. Exclusively in postsynapses of retinal bipolar metabotropic (ON-center) cells.	
	mGluR7		Primarly postsynaptic. Expressed in neurons.	
	mGluR8		Primarly presynaptic. Expressed in neurons and reactive astrocytes	

Table 3. Classification and features of metabotropic glutamate receptors (adapted from Rubio *et al*., 2012).

All known GPCRs share a common structural domain composed of 7 transmembrane helices, an extracellular N-terminal domain, and an intracellular C-terminal domain. In mammals, the sequence comparison of this structure allowed to identify several families of GPCRs (Pin *et al*., 2003). mGluRs defined a new family of GPCRs, the family 3 GPCRs, which was discovered when the mGluRs were cloned (Houamed *et al*., 1991; Masu *et al*., 1991). This finding revealed a protein sequence which differed from the first big identified

GPCR family composed by rhodopsin and related receptors (the so-called rhodopsin-like GPCRs, Pin *et al*., 2003).

As the other GPCRs, mGluRs consist of a large N-terminal extracellular signal sequence that guides insertion into the plasma membrane, a hydrophilic extracellular agonist-binding domain that contains nineteen cysteine residues, the seven transmembrane domains (7TM), and a cytoplasmic carboxyl-terminal (C-terminal) domain variable in length (Figure 6) (Conn and Pin, 1997). The cysteine-rich extracellular domain and the extracellular loops are conserved among all the members of mGluR family, suggesting the important role of these components either in three-dimensional structure of the molecule or in the intracellular signal transduction. Another characteristic shared by these receptor family is the N-terminal binding site, composed by two globular domains with a hinge region which can deeply modifies its conformation depending on the ligand interaction **(**Conn and Pin, 1997).

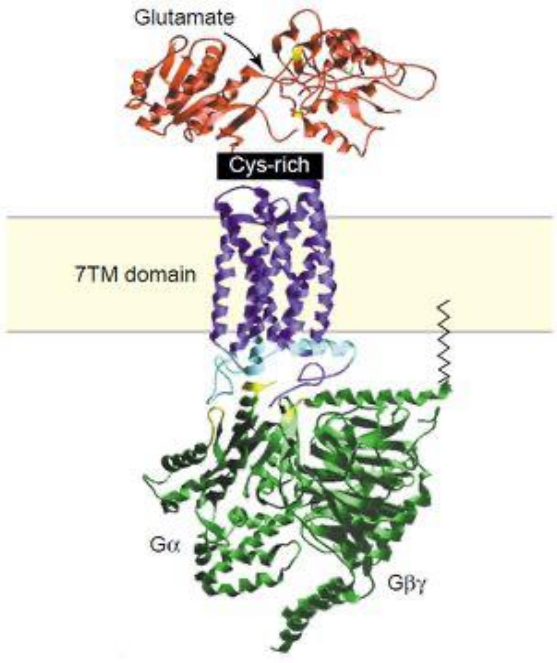

Fig. 6 Metabotropic glutamate receptor associated with a G protein. The ligand binding domain is showed in red. The residues represented in yellow are crucial for glutamate binding. The seven transmembrane regions are shown in purple. The regions involved in G protein coupling are shown in light blue, the heterotrimeric G protein in green and the regions of the α-subunits involved in the coupling to mGluRs in yellow (De Blasi *et al.,* 2001).

1.5.1 Group I metabotropic receptors: structure and signal transduction

Group I mGluRs are broadly distributed throughout the CNS, they are specifically localized at synaptic and extra synaptic sites in both neurons and glia and have several splice variants depending on the different C-terminal domain assembly such as mGluR1a, 1b, 1c, 1d and mGluR5a, 5b. Although Group I mGluRs were thought to be mainly expressed in the postsynaptic terminals, several debates emerged about their presynaptic expression (Pin *et al*., 2003; Raiteri, 2008; Musante *et al*., 2010; Giribaldi *et al*., 2013). Accordingly, many studies functionally demonstrated their presynaptic localization by immunocytochemical and biochemical analyses (Cartmell and Shoepp, 2000; Marino *et al*., 2001; Schoepp, 2001; Muly *et al*., 2003; Musante *et al*., 2008).

Depending on the brain region and the subcellular localization, mGluR1 and mGluR5 can either exert different functions (Moroni *et al*., 1998; Reid *et al*., 1999; Fazal *et al*., 2003; Sistiaga *et al*., 1998; Wang and Sihra, 2004) or work together (Musante *et al*., 2008; Musante *et al*., 2010). Accordingly, while mGluR1 is highly implicated in the regulation of sensory and motor functions in different brain regions (Swanson and Kalivas, 200; Nakao *et al*., 2007; Bennet *et al*., 2012), mGluR5 has not been associated to motor control, but instead it is involved in synaptic plasticity, learning, cognition process and memory (Naie and Manahan-Vaughan, 2004; Simonyi *et al*., 2005). Moreover, notwithstanding the common pathways often shared by the two mGluRs, it has been demonstrated their distinct or even opposite effect in cellular plasticity. Indeed, Gross and colleagues demonstrated that while mGluR5 positive modulation decreased dendritic spine densities in the nucleus accumbens (NAs), the *in-vivo* treatment with an mGluR1 PAM, increased the spine densities. The same result was obtained with the mGluR5 selective agonist *(RS)*-2-chloro-5-hydroxyphenylglycine (CHPG, Gross *et al*., 2016).

The functional interaction between mGluR1 and mGluR5 has been also reported (Benquet *et al*., 2002; Fazal *et al*., 2003; Musante *et al*., 2008; Sevastyanova and Kammermeier, 2014), even if the existence of the mGluR1/mGluR5 heterodymers has been demonstrated only recently (Doumazane *et al*., 2011; Pandya *et al*., 2016). The heterodimer composition has been hypothesized to play a role in case of knocking down mGluR1 or mGluR5 (Milanese *et al*., 2014; Bonifacino *et al*., 2017).

As mentioned before Group I mGluRs are also heterogeneously distributed in neuronal and non-neuronal cells in the mammalian CNS leading to different receptor functions and

activation of different pathways. An example is given by the microglial expression of mGluR1 and mGluR5 which participate in cell migration (Liu *et al*., 2009) and modulate the inflammatory phenotype (Pinteaux-Jones *et al*., 2008). Several evidence exist as to the expression of mGluR5 in astrocytes, where its activation participates in enhancing cell repair after injury, either through the actions of neurotrophins and growth factors, or through the production of cytokines and inflammatory mediators (see review of Planas-Fontanez, 2020). Among the several functions of mGluR1 and mGluR5, a relevant role is exerted in long-term potentiation (LTP) and long-term depression (LTD) (Faas *et al*., 2002; Koga *et al*., 2016; Wilkerson *et al*., 2017), pain sensation (Pin *et al*., 2003; Pereira and Goudet, 2018), anxiety (Pin *et al*., 2003; Nieswender *et al*., 2010), depression (Bruno *et al*., 2017; Shuvaev *et al*., 2017) and positive mediation of glutamate release at the presynaptic level (Herrero *et al*., 1992; Musante *et al*., 2008).

Group I mGluRs are coupled to $G_{q/11}$ protein, which has an activatory function. The activation of the receptors stimulates several downstream pathways (Figure 7) by activation of different targets, most relevant phospholipase Cβ (PLCβ). This enzyme cleaves phosphatidylinositol-4,5-bisphosphate (PIP2) and leads to intracellular generation of the two second messengers IP3 and diacyl-glycerol (DAG). IP3 induces Ca^{2+} release from the ER and DAG activates protein kinase C (PKC) (Nicoletti F *et al*., 2011).

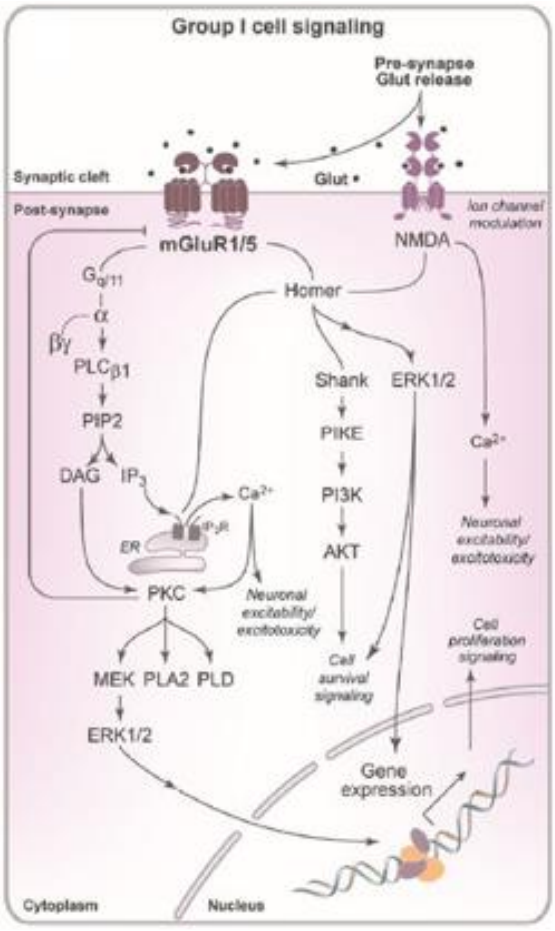

Fig. 7 Schematic representation of some downstream cell-signalling pathways activated by Group I mGluRs expressed by postsynaptic terminals (Ribeiro *et al*., 2017).

Beside the activation of these classical pathways, Group I mGluRs can modulate additional cascades downstream of $G_{q/11}$ protein, as well as signalling pathways regulated by $G_{i/o}$, G_s and by other molecules independent from G proteins (Hermans and Challis 2001). Accordingly, the PLC and PKC activation and the increase of intracellular Ca^{2+} levels are not the unique consequences of the Group I mGluRs activation. An example is represented by a study carried *in-vitro* in rat cerebral cortical astrocytes expressing high level of mGlu5 receptors. The non-selective mGluR1 and mGluR5 agonist, 3,5-dihydroxyphenylglycine (3,5-DHPG), caused an accumulation of cyclic AMP (cAMP) in these cells. The same result was also obtained with G_s protein couple receptors agonists. Even though the direct link between mGluR5 and G_s protein has not been clearly demonstrated, the mechanism is independent from PKC, PLC and intracellular Ca^{2+} level (Balazs *et al*., 1998).

The G proteins coupling is mainly regulated by the intracellular loops 2 and 3, however also the C-terminal domain has a crucial role in influencing this mechanism (De Blasi *et al*., 2001). Accordingly, Prezeau and collaborators demonstrated that the long C-terminal domain of mGluR1a confers a small agonist-independent activity to the receptor and a better coupling efficiency to the G proteins (Prezeau *et al*., 1996). Moreover, the C-terminal domain deletion not only influences the efficiency but also the kind of intracellular modifications activated by the receptor stimulation (Gabellini *et al*., 1993; Joly *et al*., 1995). Another aspect underlying the importance of this domain is the capability to interact with scaffolding proteins, like Homer 1. This protein can interact with mGluR5 and mGluR1a, but not with the splice variants mGluR1b and 1c and regulates the insertion and the clustering of Group I mGluRs in the cellular membrane or in other cellular compartments (Pin *et al*., 2003) and forms postsynaptic density protein 95 (PSD-95), Shank and NMDAR macromolecular complexes at postsynaptic elements (Husi *et al*., 2000). One of the proteins which directly interacts with Homer 1 is phosphatidylinositide 3-kinase enhancer L (PIKE-L), a GTPase that binds and activates phosphatidylinositide 3-kinase (PI3K) (Ahn and Ye, 2005). This interaction is important because links Group I mGluRs with an anti-apoptotic signalling pathway PI3K-dependent that supports neuronal survival and sheds light on the relationship between NMDA and mGluR1a. Accordingly, NMDARs activation results in calpain-mediated truncation of the C-terminal domain of mGluR1a. Consequently, the truncated mGluR1a maintains its ability to increase cytosolic Ca^{2+} and no longer activates the neuroprotective signalling pathway PIK3-dependent (Caraci *et al*., 2012; Xu *et al*., 2006).

Another pathway which connects Group I mGluRs and NMDARs is linked to the proto-oncogene tyrosine-protein kinase Src. In the hippocampus the activation of mGluR5 induces phosphorylation of NR2A and NR2B domains of NMDAR resulting in an increase of Ca^{2+} currents. If this pathway is misregulated the excitotoxicity increases, causing neuronal death (Takagi N *et al*., 2012). Similar results were obtained in cortical neurons after stimulation of mGluR1 and the resulting activation of Src mediated pathway (Heidinger V *et al*., 2002).

Another important pathway linked to Group I mGluRs is the extracellular signal-regulated kinases (ERK) cascade, a subgroup of the mitogen-activated protein kinases (MAPKs) family that are key regulators of gene expression and of cell proliferation, differentiation, and survival (Thandi *et al*., 2002). Group I mGluRs have been showed to activate ERK in cortical glia (Peavy RD and Conn PJ, 1998), primary astrocytes (Schinkmann *et al*., 2000) and in Chinese hamster ovary (CHO) cell lines permanently transfected with mGluR1a,

mGluR2 and mGluR4 (Ferraguti *et al*., 1999). To activate this important signalling cascade, mGluR1 and mGluR5 based on different mechanisms. In particular, mGluR1a, but not mGluR5a, activates ERK pathway via $G_{i/o}$ protein (Thandi *et al*., 2002). These data suggest that mGluR1 and mGluR5 not only exhibit different anatomical and cellular distributions in the CNS (Hubert *et al*., 2001; Valenti *et al*., 2002), but they also differ in the downstream signalling partners and in the resulting activated pathways (Thandi *et al*., 2002).

1.5.2 Group I metabotropic receptors: activation and pharmacology

It is now widely accepted that many GPCRs can exist and work as homodimers. Growing evidence sustains the possibility of these receptors also undergo to heterodimerization, an event that changes the ligand binding, the intracellular signalling transduction mechanisms and that can provide novel therapeutic strategies. Indeed, if GPCR homodimers and heterodimers emerge to interact via different sequence elements, it will be possible to target the protein-protein interaction interfaces. Moreover, the different pharmacology, regulation, and function of the GPCRs homo- and heterodimers suggest that several pharmacological agents might sustain different mechanisms *in-vivo* than the one anticipated from the ligand-screening programmes, that rely on heterologous expression of a single GPCR (Milligan, 2006; Milligan and Smith, 2007). The same emerged as to mGluRs (Doumazane *et al*., 2011). Starting by the studies on mGluR1, the first identified member of GPCR-3 family and looking for protein shared sequences of the extracellular N-terminal domains of the mGluRs, the structure and function of these metabotropic receptors have been elucidated.
As briefly described in chapter 1.5, the extracellular N-terminal domain of mGluRs revealed a bilobate structure. The lobes are separated by a cleft where glutamate binds. In the absence of the ligand these receptor domains are usually in an open state, whereas they assume a closed conformation in the presence of the ligand (Pin *et al*., 2003). An oscillation between the open and closed states was observed also in absence of bound ligand, whereas the ligand binding stabilizes the closed state. This constant equilibrium between the two states of the unbound receptor is crucial for the ligand affinity to the receptor. Because of these structural characteristics, such a protein domain was called Venus Flytrap domain (VFD), in comparison with the mode of insect trapping by the carnivorous Venus Flytrap plants (Pin *et al*., 2003). The first results originated from the deep study of mGluR1. In the open form glutamate exclusively binds lobe 1 (LB1), whereas in the closed state it makes additional contacts with residues of lobe 2 (LB2), stabilizing the closed form of mGluR1 (Pin *et al*.,

2003). VFD can also oscillate from an active to a resting state. Accordingly, in the absence of the ligand, the two VFDs likely will be in an open state, and this orientation correspond to the resting state. Upon binding of the agonist to at least one VFD, this VFD closes to the other, allowing the correct association between the two LB2, stabilizing the active orientation of the dimer. The active orientation can be further stabilized upon binding of the agonist in the second VFD and after the association with a cation (like Ca^{2+}) at the interface between the two LB2 (Figure 8; Pin *et al*., 2003).

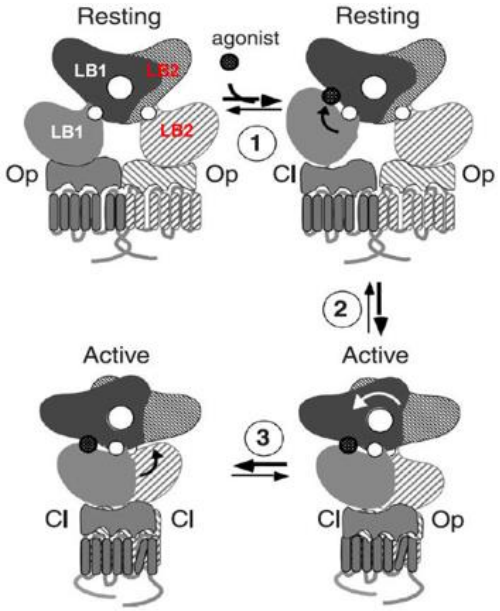

Fig. 8 Schematic representation of the mGluRs dynamics. In the absence of agonist, both VFDs in the dimer are more stable in the open state (Op) (top on the left). Upon agonist binding, at least one VFD dimer shift to a closed state (Cl) (step one, top on the right), allowing the stabilization of the active orientation of the dimer (step 2). This important change in the conformation of the dimer of VFD is transmitted to the dimer of the transmembrane domain. Upon binding of a second agonist and cation, the second VFD closes and further stabilizes the activate state (step 3) (modified from Pin *et al*., 2003).

While the open and closed conformation depends on the distance between the LB1 and LB2 to form a unique VFD domain, the active and resting states are linked to the distance between the two LB2 (Figure 9).

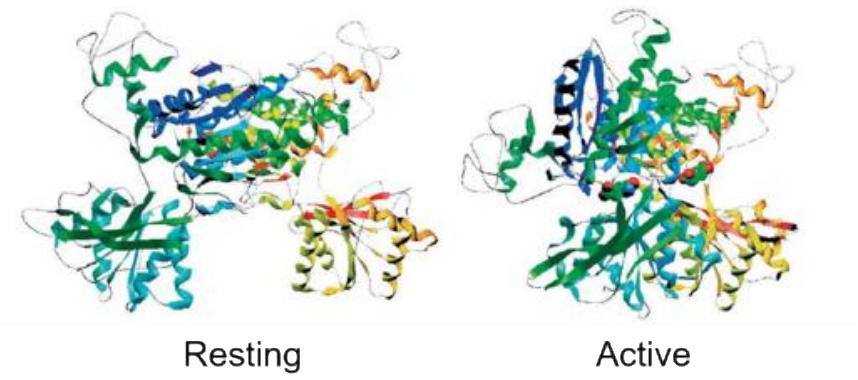

Fig. 9 The different states of the dimer of mGluR1 VFDs. Ribbon views of the empty (left) and glutamate-bound (right) form of the dimer of mGluR1 VFDs. In the presence of glutamate only one VFD closes and the orientation between the VFDs is different from that in the absence of glutamate (Pin *et al*., 2003).

From a pharmacological point of view, several Group I mGluRs agonists have been characterized, among which 3-hydroxyphenylglycine (3-HPG) and *(S)*-3,5-dihydroxyphenylglycine (3,5-DHPG). They selectively activate Group I mGluRs, but not the Group II and III mGluRs. Moreover, mGluR5 can be specifically activated by CHPG (Doherty *et al*., 1997; Conn and Pin, 1997).

Besides the agonists, several antagonists and allosteric modulators can bind Group I mGluRs. Allosteric modulators are molecules that bind at the non orthosteric site of the receptor, typically found in the heptahelical domains of mGluRs, and that can alter the conformational state of the receptors (Stansley and Conn, 2019). These molecules do not directly activate the receptor but potentiate (positive allosteric modulators, PAMs) or decrease (negative allosteric modulators, NAMs) the response to the orthosteric ligand glutamate.

The first negative allosteric modulator of mGluR1 identified was CPCCOEt (Annoura *et al*., 1996), a compound that inhibits mGluR1 signalling without affecting glutamate binding (Litschig, *et al*., 1999). Among mGluR1 antagonists, *(S)*-(+)-α-Amino-4-carboxy-2-methylbenzeneacetic acid (LY367385) emerged as a very potent and selective molecule (Clark *et al*., 1997). Shortly after, a number selective mGluR5 NAMs, such as SIB-1757, SIB-1893 (Varney *et al*., 1999) and Fenobam (Porter *et al*., 2005) were identified. More recently, the mGluR5 non-competitive antagonist 2-methyl-6-(phenylethynyl)-pyridine (MPEP) showed an *in-vitro* protective effect against excitotoxicity induced by AMPA and

NMDA (D'Antoni *et al*., 2011; Takagi *et al*., 2012). As MPEP also 3-[(2-methyl-1,3-thiazol-4-yl) ethynyl] pyridine (MTEP), another mGluR5 antagonist, provides increased potency, selectivity, and brain penetration (Cosford *et al*., 2012). The proposed mechanisms of action of mGluR1 and mGluR5 NAM are schematized in Figure 10.

Several PAMs active at Group I mGluRs have also been developed, including the mGluR5 PAMs, such as [(3-Fluorophenyl)methylene]hydrazone-3-fluorobenzaldehyde (DFB), *N*-{4-chloro-2-[(1,3-dioxo-1,3-dihydro-2*H*-isoindol-2-yl)methyl]phenyl}-2 hydroxybenzamide (CPPHA), 3-cyano-*N*-(1,3-diphenyl-1*H*-pyrazol-5-yl)benzamide (CDDPB), 4-nitro-N-(1,3-diphenyl-1H-pyrazol-5-yl)benzamide (VU29) and [*S*-(4-fluoro-phenyl)-{3-[3-(4-fluoro-phenyl)-[1,2,4]oxadiazol-5-yl]-piperidin-1-yl}-methanone] (ADX47273) and the PAMs specific for mGluR1, such as (*S*)-2-(4-fluorophenyl)-1-(toluene-4-sulfonyl)pyrrolidine (Ro 67-7476), Butyl (9*H*-xanthene-9-carbonyl)carbamate (Ro 67-4853) and 4-nitro-*N*-(1,4-diphenyl-1*H*-pyrazol-5-yl)benzamide (VU71) (Niswender and Conn, 2010).

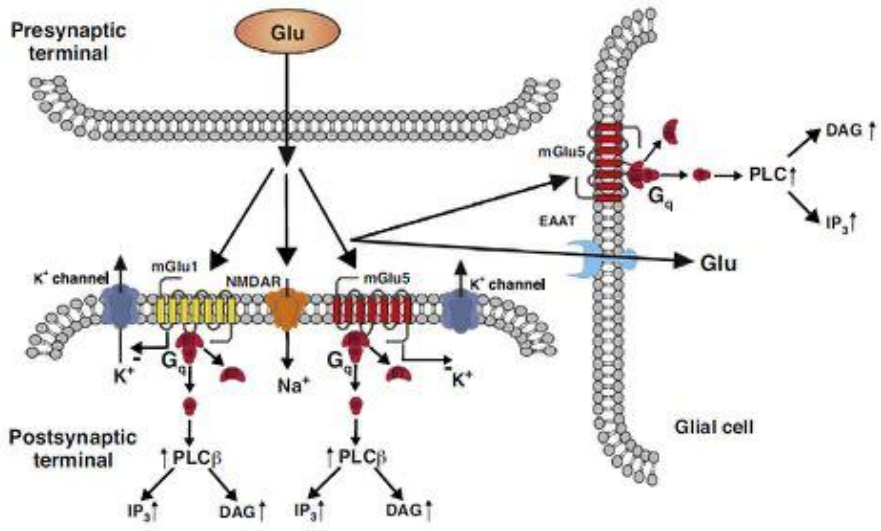

Fig. 10 Proposed molecular mechanisms of action of mGlu1 receptor and mGlu5 receptor NAM. mGluR1 and mGluR5 activate PLCβ leading to an increased production of IP3 and DAG in the postsynaptic nerve terminals and in glial cells. Pharmacological blockade of mGlu1 and mGlu5 receptors with a NAM would reduce excitotoxic damage despite the high levels of ambient glutamate (Battaglia and Bruno, 2018).

1.5.3 Group I metabotropic receptors: regulation and desensitisation

Group I mGluRs undergo to homologous (agonist-dependent) or heterologous (agonist-independent) desensitisation soon after their activation, similarly to what has been observed for the other GPCRs families (De Blasi *et al*., 2001). Multiple mechanisms likely concur in the homologous desensitisation of Group I mGluRs, however, the activation of PKC and the resulting PKC-induced phosphorylation of the intracellular residues of threonine and serine of mGluR1 and mGluR5 plays a major role. This desensitisation mechanism has been confirmed in several systems, including primary neuronal cultures, hippocampal slices, astrocytes and synaptosomes (De Blasi *et al*., 2001) and it might be directly involved in the glutamate release inhibition measured in rats cortical synaptosomes (Herrero *et al*., 1998). Nevertheless, PKC activation does not mediate the whole process of Group I mGluRs desensitisation, since G-protein-coupled receptor kinases (GRKs) are also involved in this phenomenon. These proteins (GRK1-GRK6) are targeted to the membrane by $\beta\gamma$ G protein subunits or by other mechanisms and specifically phosphorylate some residues of the C-terminal domain of the receptor. This allows β-arrestin to bind at the newly generated binding site, to uncouple the receptor from the G protein and to induce internalization of the receptor itself (De Blasi *et al*., 2001). Other proteins involved in Group I mGluRs desensitisation are calmodulin kinase II (CaMKII), huntingtin-binding protein optineurin and second messenger-dependent protein kinases (Dhami and Ferguson, 2006). GPCR and mGluR1 activity can be also attenuated by a proteins family called regulators of G protein signalling (RGS) that recognize specific G protein α-subunits and increase GTP hydrolysis accelerating the G protein conversion from the active to the inactive form (Dhami and Ferguson, 2006). The RGS have more than 20 isoforms. Both RGS2 and RGS4 specifically interact with $G_{\alpha q/11}$-like G proteins and block the downstream activation of PLC (Dhami and Ferguson, 2006).

1.5.4 Group I metabotropic receptors: pathological aspects

Among metabotropic glutamate receptors, Group I mGluRs are considered the only ones that enhance the release of glutamate, while Group II and III provide the neurotransmitter release inhibition. Moreover, mGluRs activate a wide variety of cell-signalling pathways and are broadly distributed in the CNS. Therefore, it is not surprising that Group I mGluRs could be involved in the dysregulation of glutamate neurotransmission and in several

neurodegenerative diseases. Accordingly, they have been found to be impaired or overexpressed in several neurodegenerative disease, like ALS, epilepsy, AD, PD, HD, ischemia and stroke, Fragile x mental disorder, stress disorders and anxiety (Recanses *et al*., 2007; Ribeiro *et al*., 2017). In particular, mGluR5 overexpression has been reported in reactive astrocytes surroundings Aβ plaques, spinal cord lesions, multiple sclerosis (MS) lesions and hippocampal astrocytes from Down syndrome patients and in ALS (Spampinato *et al*., 2018).

As to the involvement of Group I mGluRs in ALS, data show that, in physiological conditions in human, mGluR1 is expressed preferentially in the spinal cord ventral horn neurons and mGluR5 in the dorsal horn neurons (Tomiyama *et al*., 2001; Aronica *et al*, 2001), while astrocytes express low levels of mGluRs. However, reactive glial cells have been shown to express high levels of mGluR1 and mGluR5 in gray and white matter of ALS patient spinal cord (Aronica *et al*, 2001). Accordingly, addition of cerebrospinal fluid (CSF) from ALS patients *in-vitro* to astrocyte cell cultures, significantly increases astrocytes proliferation respect to control CSF (Anneser *et al*., 2004). As a confirmation of this observation, the activation of Group I mGluRs with the non-selective agonist 3,5-DHPG negatively altered the phenotype of astrocytes and microglia that surround motor neurons, whereas the treatment with receptors antagonists inhibited the gliosis (Anneser *et al*., 2004). The overexpression of Group I mGluRs was also observed in striatum, hippocampus, and frontal cortex of $SOD1^{G93A}$ mice during the progression of the disease, accompanied by an increased inflammatory state in the spinal cord and lungs (Brownell *et al*., 2015). The involvement of astrocytes and the link with mGluR5 expression during the progression of ALS were also confirmed by Rossi and colleagues who showed that $SOD1^{G93A}$ astrocytes are very vulnerable to glutamate and undergo cell death mediated by mGluR5 (Rossi *et al*., 2008).

Accordingly, selective blockade of Group I mGluRs have been proposed as therapeutic targets to counteract gliosis, a peculiar feature of ALS, and the ongoing astrocytic degeneration. Accordingly, blocking the receptor *in-vivo* with the non-competitive mGluR5 antagonist MPEP slows down astrocyte degeneration, delays the onset of the disease, and prolongs the $SOD1^{G93A}$ mice survival (Rossi *et al.,* 2008). The protective effect of MPEP was also confirmed in neurons by the reduction of AMPA-mediated toxicity (D'Antoni *et al*., 2011).

An increase of glutamate release in response to Group I mGluRs activation was also showed in synaptosomes isolated from $SOD1^{G93A}$ mice (Giribaldi *et al*., 2013). mGluRs regulate the

glutamate synaptic transmission through several transduction pathways and influence the expression of glutamate transporters GLT-1 and GLAST expressed by astrocytes (Aronica *et al*., 2003). In this context, Vermeiren and colleagues provided *in-vitro* evidence for a crosstalk between mGluR5 and GLT-1 in $SOD1^{G93A}$ rats astrocytes, raising the hypotheses that mGluR5 acts as a sensor of synaptic glutamate concentration which modulates the uptake activity in glial cells (Vermeiren *et al*., 2005). Despite the increased expression of mGluR5 in reactive astrocytes isolated from $SOD1^{G93A}$ rats, stimulation of the receptor failed to activate GLT-1. Therefore, this loss of cross talk has been proposed to enhance glutamate-induced excitotoxicity concurring in the rapid progression of ALS (Vermeiren *et al*., 2006).

1.5.5 Effects of the downregulation of Group I mGluRs in the $SOD1^{G93A}$ mouse model of ALS

On the basis of the previous results obtained by my research group, which demonstrated that abnormal exocytotic glutamate release takes place in pre-symptomatic and late symptomatic $SOD1^{G93A}$ mice (Milanese *et al*., 2011; Bonifacino *et al*., 2016) and the link of this phenomenon with the increased activity and overexpression of Group I mGluRs (Giribaldi *et al*., 2013; Bonifacino *et al*., 2019b), we studied more in dept the role of mGluR1 and mGluR5 in the $SOD1^{G93A}$ mouse model of ALS.

In 2014 my colleagues explored the impact of mGluR1 by downregulating mGluR1 in the $SOD1^{G93A}$ genetic background, generating double mutant mice $SOD1^{G93A}Grm1^{crv4/+}$. The obtained results indicate that the mGluR1 reduction ameliorates the course of the disease, increases the life span, decreases the disease onset and progression, reduces astrogliosis and microgliosis and increases the number of motor neurons still present in the ventral horns of the affected lumbar spinal cords at the late stage of the disease. They also showed that glutamate release induced by 30μM 3,5-DHPG in $SOD1^{G93A}Grm1^{crv4/+}$ and $Grm1^{crv4/+}$ was lower than in WT mice, suggesting that the mGluR1 reduction abolishes the excessive glutamate release measured in $SOD1^{G93A}$ mice. Moreover, they demonstrated that the decreasing of the receptor does not modify the amount of GLT-1 in the spinal cord of double transgenic mice, suggesting that, in our model, the mechanisms leading to an amelioration of the disease progression is independent of GLT-1 function (Milanese *et al*., 2014). Interestingly, halving mGluR1 expression also led to a reduction of mGluR5.

Shortly after these results, we also explored the role of mGluR5 in the pathogenesis of ALS. Similar to the previous work, we generated double transgenic mice carrying the hSOD1^{G93A} mutation and half expression of mGluR5 (SOD1^{G93A}Grm5$^{-/+}$). SOD1^{G93A}Grm5$^{-/+}$ again showed prolonged survival probability and delayed pathology onset, enhanced survival of motor neurons, decreased astrocyte and microglia activation, reduced cytosolic free Ca^{2+} concentration, and regularization of abnormal glutamate release (Bonifacino *et al*., 2017). However, differently from SOD1^{G93A}Grm1$^{crv4/+}$ mice, only male SOD1^{G93A}Grm5$^{-/+}$ mice showed an amelioration of motor skills during progression of the disease. The reason of this divergence is still not clear, even though several hypotheses have raised. Briefly, mGluR1 is involved in the regulation of motor and sensory functions in different brain regions, while mGluR5 is associated to synaptic plasticity, learning memory and cognition process.

Moreover, the existence of mGluR1/mGluR5 heterodimers has been recently demonstrated (Doumazane *et al*., 2011; Pandya *et al*., 2016); thus, altering the mGluR5 but not the mGluR1 expression could affect the association of mGluR1/mGluR5 heterodimers, possibly leading to modification of the pathological traits with different gender impact. Another hypothesis concerns the gender differences. It is worth to note that SOD1^{G93A} female mice performed better than SOD1^{G93A} males both in survival and in motor skills tests, therefore this occurrence could have minimized the beneficial effect of mGluR5 knockdown in SOD1^{G93A}Grm5$^{-/+}$.

To further validate the role of mGluR5 in ALS we recently bred SOD1^{G93A} mice with complete mGluR5 knock out expression (SOD1^{G93A}Grm5$^{-/-}$) (Bonifacino *et al*., 2019a). SOD1^{G93A}Grm5$^{-/-}$ mice exhibited a more favourable clinical course than SOD1^{G93A} and SOD1^{G93A}Grm5$^{-/+}$ littermates. Moreover, no clear differences between female and male SOD1^{G93A}Grm5$^{-/-}$ were observed anymore. These results were accompanied by enhanced motor neuron preservation and decreased astrogliosis and microgliosis. In parallel with this last study, we demonstrated that the expression of mGluR1 and mGluR5 increased in the spinal cord of SOD1^{G93A} mice not only at the end stage of the disease (120 days) but also at the pre-symptomatic (30 and 60 days) and early-symptomatic (90 days) stages. Moreover, also mGluR1- and mGluR5-releasing function is altered in SOD1^{G93A} mice at the end stage and at the early-symptomatic stage of the disease (Bonifacino *et al*., 2019b). These results obtained in SOD1^{G93A} mice emphasize the role of Group I mGluRs in ALS, supporting the idea that their hyperactivity could represent a central mechanism contributing to disease progression. Moreover, these genetically based evidence underly the importance of verifying

whether also the pharmacological blockade of mGluR1 and/or mGluR5 can represent a valid approach for the treatment of ALS.

1.6 Therapies for Amyotrophic Lateral Sclerosis

ALS, as already discussed in the previous chapters, is a very complex disease. This is the reason why it was so difficult to find and effective therapy which could counteract the several and pathological causes of the disease and their relationships taking place during ALS initiation and progression. To date, only two drugs were approved by FDA for ALS treatment: Riluzole and Edavarone.

Riluzole was approved in 1995 and initially showed a great effect in the transgenic SOD1 mouse models, significantly delaying the symptoms onset and slightly improving survival (Gurney, 1997). However, it only prolongs survival for up to 2-3 months in patients and exerts its beneficial effect exclusively in the first months of therapy. When launched Riluzole was hypothesized to modulate the glutamatergic transmission by blocking voltagedependent Na^{2+} channels and reducing release of the neurotransmitter (Bensimon *et al*., 1994; Bellingham, 2011). However, it has been showed that Riluzole also affect glutamate receptors and that the mechanisms of action are more complex and varied (Bellingham, 2011). Also other anti-glutamatergic compounds, such as Ceftriaxone (an approved antibiotic which reduces the expression of GLT-1 in rodents and EAAT2 in humans), Memantine (an NMDA receptor antagonist) and Talampanel (a non-competitive antagonist of AMPA receptors) failed to show efficacy in ALS clinical trials (De Carvalho *et al*., 2010; Pascuzzi *et al*., 2010; Cudkowic *et al*., 2014).

Only after 22 years, in 2017, another drug for ALS treatment was approved, Edaravone, but only for use in Japan, South Korea and the United States. It was introduced in Europe as an off-label drug, but its distribution was suspended in July 2020 by EMA due to lack of proven efficacy. Edaravone has been marketed for many years to treat ischemic stroke. It is an antioxidative compound proposed to function by reducing oxidative stress, but its exact mechanism is still unknown (Mejzini *et al*., 2019). Although the preclinical trials in ALS mouse models demonstrated beneficial effects of the drug (Yoshino and Kimura, 2006), the first human trial did not show a significant improvement in Edavarone-treated patients (Abe *et al*., 2014). However, a post-hoc analysis of the previous study revealed that the drug is effective at an early stage of the disease (Abe *et al*., 2017).

Besides Edavarone, several other drugs are being tested to act on oxidative stress, such as Methylcobalamin, that inhibits neuronal degeneration by decreasing levels of homocysteine and Verdiperstat, an irreversible inhibitor of myeloperoxidase (MPO), an enzyme which acts as key driver in pathological oxidative stress and inflammation in the brain. A phase 3 human study is now ongoing for Methylcobalamin and under enrolment for Verdiperstat (Chiò *et al*., 2020). In parallel other two compounds are being studied in phase II trials: Ranolazine, already approved for angina, which inhibits the late Na^+ current and the intracellular Ca^{2+} accumulation, and Inosine that elevates urate levels improving the endogenous defence against oxidative stress (Chiò *et al*., 2020).

Another therapeutic approach consists in targeting the mitochondrial dysfunction. Unfortunately, the investigated drug Rasagiline, a monoamine oxidase B (MAOB) inhibitor, failed the phase II trials (Chiò *et al*., 2020), even though it was found to be effective in prolonging survival of $SOD1^{G93A}$ mice (Waibel *et al*., 2004). However, evidence showed that it might positively modify disease progression in a subset of ALS patients, therefore a post-hoc analysis is being carried on to better stratify the participants to the trial.

A hydroxylamine derivative, Arimoclomol, is now in phase III trial with sporadic and familial ALS patient to counteract autophagy and improve protein quality control in ALS. Arimoclomol reduces the level of protein aggregates in the motor nerves by boosting heat shock proteins (Hsp70 and Hsp90) expression and by inducing the overexpression of the heat-shock factor 1 which is directly linked to TDP-43 aggregate reduction (Wang *et al*., 2017).

Tauroursodeoxycholic acid and sodium phenylbutyrate are being tested in combination in a phase II trial with the aim to counteract apoptosis, another pathological feature of ALS. In particular, they should reduce the caspase activity, abnormally increased, and negatively modulate the mitochondrial pathway by inhibiting Bax translocation, ROS formation, cytochrome-*c* release and caspase-3 activation (Waibel *et al*., 2004).

Neuroinflammation is another peculiar feature of ALS. For this reason, several studies are trying to target this phenomenon to treat the disease. In particular, two drugs acting on Complement component 5 (C5) have been planned for trials in ALS: Ravulizumab and Zilucoplan. The first drug is a humanized monoclonal antibody which inhibits C5 and a phase III placebo-controlled trial in ALS has recently started (McKeage, 2019; Stern and Connel, 2019). Zilucoplan, is a synthetic peptide that binds C5 and inhibits its cleavage into C5a and C5b, thus preventing the overactivation of the complement system. For this drug, a phase II trial in ALS has started in July 2020 (Waibel *et al*., 2004).

Ibudilast is another anti-inflammatory and neuroprotective oral agent acting as an inhibitor of phosphodiesterase-4 and -10 (PDE-4 and PDE-10) as well as a macrophage migration inhibitory factor (MIF). A phase II trial on ALS patients showed that this compound has potential and beneficial effects on survival, therefore the drug is now in a phase III trial.

Toclizumab, an interleukin 6 (IL-6) receptor antibody, already approved for the treatment of rheumatoid arthritis, showed to downregulate inflammatory genes (in particular IL-1β) (Fiala *et al*., 2013) in a study carried on sporadic ALS patients. A phase II study has been performed in U.S.A but the results of the trial have not been published yet.

A compound which demonstrated promising preclinical activity in $SOD1^{G93A}$ rat model of ALS, is Masitinib, an oral tyrosine kinase inhibitor. It exerts its neuroprotective function mainly targeting microglia, macrophage, and mast cells activity. Moreover, it regulates the stem cell factor (SCF) receptor c-kit (Dubreuil *et al*., 2009). A phase II/III trial has started.

Another therapeutic approach that resulted in a phase I trial in ALS involves selective inhibitors of nuclear transport (SINEs) (Archbold *et al*., 2018). SINEs can prevent TDP-43 nuclear export thus slowing neurodegeneration in models of both ALS and FTD (Waibel *et al*., 2004).

Drugs affecting other biological mechanisms operating in ALS, such as stress granule dynamics, RNA splicing/metabolism, cytoskeleton integrity and axonal trafficking are currently no under clinical trial studies.

In the last decade, several mGluR5 antagonists or NAMs have been synthetized and showed promising pharmacokinetics for *in-vivo* application (Arsova *et al*., 2020). An example is represented by 2-chloro-4-((2,5-dimethyl-1-(4-((trifluoromethoxy)phenyl)-1H-imidazol-4-yl(ethynyl)pyridine (CTEP), an oral bioavailable mGluR5 NAM optimized for chronic *in-vivo* treatments in rodents (Lindemann *et al*., 2011) and already tested in mouse models of Huntington's and Parkinson's diseases (Abd-Elrahman *et al*., 2017; Farmer *et al*., 2020). We have submitted a paper, now under revision, investigating the pharmacological effects of the *in-vivo* chronic treatment of $SOD1^{G93A}$ mice with this compound, starting after the onset of the clinical symptoms of the disease (90 days) (Milanese *et al*., under revision). Results demonstrated that CTEP treatment, increases survival probability, ameliorates the ALS-linked motorial parameters during disease progression, reduces microgliosis and astrogliosis, normalizes the excessive glutamate release and preserves spinal cord motor neurons from death. These results support the idea that the selective modulation of mGluR5 represent an effective therapeutic approach with clinical perspective in ALS. Of note, other mGluR5 NAMs have been synthetized and tested in human clinical studies for the treatment

of depression, fragile X syndrome, Huntington's disease, and levodopa-induced dyskinesia (Reilmann *et al*., 2015; Trenkwalder *et al*., 2016). For example, Basimglurant, an imidazole derivative analogue of CTEP that has been optimized for human studies, showed favourable pharmacokinetic and toxicological facets (Jaeschke *et al*., 2015; Lindemann *et al*., 2015) and has been successfully studied in clinical trials for the cure of depression and fragile X syndrome (Quiroz *et al*., 2016; Youssef *et al*., 2018).

1.6.1 Innovative therapeutic approaches

In addition to the study of chemical compounds, alternative therapeutic strategies are under development to treat ALS. A first example is represented by gene therapy. This approach consists in targeting, with different biological tools, the abnormal function of certain genes. Although in ALS only 10% of cases are familial, the removal of the initial cause of the disease can be effective respect to fight with consequences (Ustyantseva *et al*., 2020). One proposed method is based on mRNA binding with antisense oligonucleotides (ASOs) that inhibit translation and promote mRNA degradation. The first ASO drug in clinical development for ALS was developed by Ionis and targeted mutant SOD1, because this protein provokes ALS development more likely through a gain-of function mechanism that causes its aggregation. After the encouraging results obtained both *in-vitro* (Nizzardo *et al*., 2016) and *in-vivo* (Winer *et al*., 2013), the first human trial started in 2013 (Miller *et al*., 2013). Unfortunately, the delivery of ASOs became a major problem because it required intrathecal injection that is too invasive for patients. However, up to date a large international trial with a second generation SOD1-targeting ASO, BIIB067 (IONIS-SOD1$_{RX}$), is recruiting patients for ASO efficiency testing (ClinicalTrial.gov identifier: NCT02623699). Pre-clinical studies of ASO targeting C9orf72 are also ongoing (Mejzini *et al*., 2019). In addition, an ASO treatment directed to ataxin-2, a protein that regulates stress granule formation of TDP-43 aggregates, was also tested in mice expressing human TDP-43. This treatment showed to reduce the formation of TDP-43 aggregates, slowed disease progression, and extended lifespan (Becker *et al*., 2017).

Another method of mRNA silencing consists in the use of short interfering RNA (siRNA). These siRNA are small RNA molecules (21-23 nucleotides) that make a complex with a target mRNA causing its subsequent degradation by the RNA-induced silencing complex (RISC) protein complex (Fire *et al*., 1998). Several preclinical studies targeting SOD1 with

siRNA showed positive phenotypical effects, but unfortunately these effects tend to disappear with age (Ralph *et al*., 2005) and none of them have reached clinical trials yet (Ding *et al*., 2003, Nishimura *et al*., 2014).

Therapy based on virus vectors is also arriving to human trials in ALS. The goal of this treatment is the mRNA or cDNA delivery aimed to replace the missing gene in the loss-of-function mutations (Chiò *et al.,* 2020). An encouraging example of this kind of treatment is the administration of the adeno-associated virus 9 (AAV9) capsid carrying the short hairpin RNA (shRNA) specific for SOD1 (AAV9-SOD1-shRNA), called AVXS-301. The administration of this virus appeared safe and well tolerated both in $SOD1^{G93A}$ mice and in non-human primates. Moreover, a single lumbar intrathecal administration resulted in efficient transduction and SOD1 downregulation in the entire CNS. A phase 1 trial on AVXS-301 in SOD1 mutated patients is going to start (Chiò *et al.,* 2020).

Although gene therapy of ALS through gene sequence correction (gene editing) has not been achieved yet, it could represent another potential approach for ALS treatment. This method can have two outcomes: gene knock out or gene correction. The first is beneficial in case of the gain-of-function mechanism and can be an alternative to RNA silencing. The second aims to restore the wild-type gene sequence of the protein and provides its normal function (Ustyantseva *et al*., 2020). Some attempts to apply gene editing strategy have already been made using Transcription activator-like effector nucleases (TALENs) and Clustered Regularly Interspaced Short Palindromic Repeat/CRISPR associated system 9 (CRISPR/Cas9) to treat some monogenic diseases among which β-Thalassemia, Duchenne muscular dystrophy, Cystic fibrosis, Haemophilia A and Epidermolysis bullosa (Osborn *et al*., 2013; Schwank *et al*., 2013; Park *et al*., 2014; Ousterout *et al*., 2015). However, still a number of questions remain open, including tolerability, safety and delivery of this procedure in humans.

ALS is a non-cell autonomous disease, therefore multiple cellular components and different cell type are compromised in the pathology. Moreover, dying motor neurons cannot be fully replaced. For these reasons, the only therapeutical approach to counteract ALS is to preserve motor neurons by either correcting altered processes or giving additional support. Cell-based therapy is now mostly focused on providing additional factors that support motor neurons survival through non-cell autonomous mechanisms (Lepore *et al*., 2008; Teng *et al*., 2012; Xu *et al*., 2006). Various cell types have been studied to ameliorate ALS course, among

which Mesenchymal Stem Cells (MSCs), Induced Pluripotent Stem Cells (IPSCs) and NPCs.

MSCs are multipotent stem cells that can be derived from various connective tissues, such as adipose tissue, bone marrow or umbilical cord. They can be easily expanded *in-vitro* and differentiate into several other cell types. Low immunogenic rate of MSCs permits their use for allogenic transplantation together with their positive effect on neuronal tissue repair (Lewis and Suzuki, 2014). In rodent models their intrathecal administration, spinal, or intravenous injection results in better survival of motor neurons, improved motor function (Forostyak *et al*., 2013; Uccelli *et al*., 2012) and prolonged survival (Kim *et al*., 2010). Up to date a phase II clinical trial with MSCs in ALS is ongoing and estimated to be finished in 2022. However, the main therapeutic effect of these cells is still considered to be their local secretion of growth factors (Forostyak *et al*., 2013). We recently investigated the role of microRNA (miRNAs) present in exosomes derived from IFN-γ-primed mouse MSCs in the modulation of microglia activation (Giunti *et al*., 2020 revised). Three miRNAs have been found to modulate the pro-inflammatory phenotype of N9 microglia and of primary microglia isolated from $SOD1^{G93A}$ mice. This suggests that exosome-mediated transfer of functional miRNAs could be one mode of action through which MSCs exert their therapeutic effect in ALS by downregulating neuroinflammatory microglia.

Due to their ability to differentiate into any derived cell type IPSCs rapidly became of great value in various studies. These cells are produced by reprogramming adult human fibroblasts to induce pluripotent stem cells by the use of selected transcription factors (Takahashi *et al*., 2007). Therefore, these cells can differentiate into multiple cell types, including neurons and glia and represent an important tool for the study of the familial and the sporadic forms of ALS. Even if IPSCs-derived motor neuron cannot replace dying neurons because cannot project long axons towards target muscle cell, they showed beneficial effects in several studies (Kallur *et al*., 2006). It has been reported that injection of stem cells-derived glial progenitors led to attenuated motor neuron death, reduced microgliosis, prolonged survival and conserved motor function in $SOD1^{G93A}$ mice (Lepore *et al.,* 2008). IPSCs technology has already applied to several other neurodegenerative diseases; among which, AD, Down's syndrome, schizophrenia and Rett syndrome. However, it is still unclear whether these cells are efficacious in affecting the characteristics of each disease. Moreover, the long process to obtain IPSCs, their variability and the epigenetic modifications during the reprogramming lead to some limitations on their use (Ferraiuolo, 2014).

Recent advances have led to the development of an efficient and direct conversion of mice and patients' fibroblasts into tripotent iNPCs which can be differentiated into oligodendrocytes, astrocytes, and neurons (Kim *et al.,* 2011; Meyer *et al*., 2014). Interestingly, a recent study showed that human NPCs (hNPCs) engineered to express GDNF and differentiated *in-vitro* into astrocytes, ameliorated the condition of upper MNs, supported lower MN survival, delayed paralysis and extended lifespan when transplanted in the cortex of $SOD1^{G93A}$ rats. These cells have been approved from FDA to proceed with clinical trials to explore their safety and efficacy in ALS patients (ClinicalTrials.gov Identifier: NCT02943850) (Thomsen *et al*., 2018).

2 AIM OF THE THESIS

This project bases on two main themes: i) the primary role of glutamate excitotoxicity in ALS and the involvement of Group I metabotropic receptors in glutamate transmission disarrangement; ii) the important role played by non-neuronal cells, in particular astrocytes, in ALS, which is a non-cell autonomous disease. A third theme taken into consideration and only partly developed concerns the important role played also by microglia in shaping ALS features.

As to the first theme, several studies support the notion that altered excitatory transmission in spinal cord and excitotoxicity, based on high extra-cellular levels of glutamate, abnormal functions of postsynaptic glutamate receptors expressed by lower MNs, and impairment of the neurotransmitter transporters, play a key role in ALS progression and cell death (Shaw and Eggett, 2000; Van Den Bosch *et al*., 2000; Kuner *et al*., 2005; Tortarolo *et al*., 2006). Elevated glutamate concentrations have been documented in plasma and in the CSF of ALS patients (Perry *et al*., 1990; Rothstein *et al*., 1990; Shaw *et al*., 1995; Spreux-Varoquaux *et al*., 2002; Fiszman *et al*., 2010) and impaired clearance of the excitatory neurotransmitter by astrocyte uptake, due to reduced expression of GLT1, has been proposed as a causative factor (Cleveland and Rothstein 2001; Rothstein *et al*., 1995). My group of research has also demonstrated that glutamate release is enhanced in the spinal cord of $SOD1^{G93A}$ mouse model of the disease both at the pre- and the late symptomatic stages of ALS (Raiteri *et al*., 2003; Raiteri *et al*., 2004; Milanese *et al*., 2010; Milanese *et al*., 2011; Giribaldi *et al*., 2013; Bonifacino *et al*., 2016). Altered function of AMPAR, which become permeable to Ca^{2+} in ALS, has been proposed as a cause of excitotoxicity (Takuma *et al*.,1999; Van den Bosch *et al*., 2000; see also review of Van Damme *et al*., 2005 and Van den Bosch *et al*., 2006). Also, Group I metabotropic receptors, mGluR1 and mGluR5, are overexpressed and hyperactive in spinal cord of both fALS and sALS patients and in $SOD1^{G93A}$ mice (Anneser *et al*., 1999; Aronica *et al*., 2001; Anneser *et al*., 2004; Rossi *et al*., 2008; Brownell *et al*., 2015; Bonifacino *et al*., 2019b). As a proof of concept of the impact of mGluR1 and mGluR5 in ALS, my group of research recently showed that the constitutive genetic reduction or ablation of mGluR1 or mGluR5 in $SOD1^{G93A}$ mice overall ameliorates survival and disease progression (Milanese *et al*., 2014; Bonifacino *et al*., 2017; Bonifacino *et al*., 2019a). In particular, the genetic knock out of mGluR5 delayed the disease onset, significantly increased survival probability, and slowed down the disease progression by ameliorating motor coordination, motor skills and muscle strength in $SOD1^{G93A}$ mice. These effects were also associated with enhanced number of preserved motor neurons, decreased astrogliosis

and microgliosis, and reduction of the excessive glutamate release in spinal cord of $SOD1^{G93A}$ mice (Bonifacino *et al*., 2019a).

Based on this encouraging genetic proof of concept, we also verified the pharmacological effects of the *in-vivo* chronic treatment of $SOD1^{G93A}$ mice with CTEP, a negative allosteric modulator of mGluR5. Results demonstrated that CTEP treatment, as in the genetically mGluR5 deficient $SOD1^{G93A}$ mice, increased survival probability, ameliorated the ALS-linked motorial parameters during disease progression, reduced astrogliosis and microgliosis, normalized the excessive glutamate release and preserved spinal cord motor neurons from death (Milanese *et al*., under revision).

Taking together these results support the importance of Group I metabotropic receptors in contributing to ALS and makes them possible therapeutic targets to counteract the disease.

The second theme bases on the important role of astrocytes in ALS. Astrocytes have several physiological functions in CNS. They, as part of the tri-partite synapse, remove toxin metabolites, control ions levels and neurotransmitters in the extracellular space, release trophic factors and nutrients which sustain the synaptogenesis, lead to synapse maturation, enhance the pre- and postsynaptic function (Barres, 2008). Moreover, they promote the correct structure of blood vessels and blood-brain barrier (Volterra and Maldolesi, 2005; Sykova and Chavatal, 1993), sustain the neuronal energy demands (Magistretti, 2006; Tsacopoulus and Magistretti, 1996) and regulate the immune response (Philips *et al*., 2014). During neurodegeneration, astrocytes get into a reactive state, called astrogliosis, and change their morphology and gene expression profile (Liddelow and Barres, 2015; Liddelow *et al*., 2017). Accordingly, several changes in astrocytic phenotype have been found in SOD1-ALS models (Rossi *et al*., 2008; Diaz-Amarilla *et al*., 2011; Papadeas *et al*., 2011; Lepore *et al*., 2008; Yamanaka and Komine, 2018; Guttenplan *et al*., 2020) and in ALS patients' tissues (Hamby and Sofroniew, 2010; Rossi and Volterra, 2009).

An interesting link between these cells and glutamate excitotoxicity is represented by the overexpression of Group I metabotropic receptors in activated astrocytes (Aronica *et al*, 2001). Moreover, the activation of these receptors negatively alters the phenotype of astrocytes surrounding motor neurons, whereas a treatment with receptors antagonist reduces astrogliosis, slows down astrocytic degeneration and prolongs $SOD1^{G93A}$ mice survival (Anneser *et al*., 2004; Rossi *et al*., 2008).

Based on these data and focussing on our encouraging results indicating a reduced astrogliosis after the *in-vivo* knocking down and knocking out of mGluR5 in $SOD1^{G93A}$ mice

(Bonifacino *et al*., 2017; Bonifacino *et al*., 2019a), the impact of mGluR5 activity reduction on astrocytes characteristics was planned to investigate. At this purpose, we characterize in detail the phenotype of primary astrocytes cultured from spinal cord of $SOD1^{G93A}$ mice partially expressing mGluR5 ($SOD1^{G93A}Grm5^{-/+}$ mice) at the late stage of the disease (120 days). The mGluR5 activity was also reduced by treating *in-vitro* astrocytes from adult $SOD1^{G93A}$ mice with the negative allosteric modulator CTEP. The pharmacological effect was also mimicked by the genetic knocking down of mGluR5 by acute exposure of adult $SOD1^{G93A}$ astrocytes in culture to an antisense oligonucleotide selective for mGluR5 mRNA. Finally, we verified whether the modifications registered in mGluR5-lacking astrocyte could impact on the MN status, studying the survival of MNs from $SOD1^{G93A}$ mouse embryos when co-cultured with adult $SOD1^{G93A}Grm5^{-/+}$ or $SOD1^{G93A}$ astrocytes.

In the frame of the international curriculum of my PhD, I spent six months at the School for Mental Health and Neuroscience (Maastricht University, Netherlands) in the laboratory of Professor Prickaerts and in the laboratory of his collaborator Dr. Vanmierlo, at the Biomedical Research Institute (Hasselt University, Belgium). In these laboratories the role of knocking down mGluR5 in $SOD1^{G93A}$ mice on the microglia phenotype was investigated. Microglia represent another important non neuronal cell population actively involved in ALS pathogenesis. During the progression of ALS, microglia start proliferating more and acquire a toxic profile (Liao *et al*., 2012; Chiu *et al.*, 2013). Accordingly, several studies carried in animal models of ALS showed a shift of microglia from an anti-inflammatory (M2-like) profile, characterized by an overexpression and release of anti-inflammatory factors and cytokines (Gravel *et al*., 2016; Beers *et al*., 2011a) and typical of the pre-onset stages of ALS, to a pro-inflammatory (M1-like) phenotype typical of the late stage of the disease and characterized by high levels of inflammatory factors (Beers *et al*., 2011a). Other studies carried in $SOD1^{G93A}$ mice also showed that microglia expressing the mutated SOD1 produced high levels of peroxides, nitrates, and nitrites compared to WT microglia causing an exacerbation of the progression of the disease and an increase of MN death (Beers *et al*., 2006).

Based on preliminary results obtained in the laboratory at the University of Genoa, investigating the effect of dampening mGluR5 on the balance between pro- and anti-inflammatory microglia phenotype acutely purified from the involved in neuroinflammation

brain and spinal cord of $SOD1^{G93A}Grm5^{-/+}$mice, the profile of these cells by detecting the mRNA expression of some pro- and anti-inflammatory relevant markers expressed by microglia acutely isolated from the brain and spinal cord of WT, $Grm5^{-/+}$, $SOD1^{G93A}$ and $SOD1^{G93A}Grm5^{-/+}$ mice was investigated here at the early (90 days) and late symptomatic (120 days) stages of ALS.

3. MATERIALS AND METHODS

3.1 Animals

Both $Grm5^{-/+}$ and $SOD1^{G93A}$ mice were originally obtained from Jackson Laboratories (Bar Harbor, ME, USA).

$Grm5^{-/+}$ mice (B6.129-$Grm5^{tm1Rod/J}$) carry a partial ablation of the Grm5 gene only on one allele of chromosome 11. This gene codes for mGlu5 receptor (Nagy *et al*., 1993) therefore $Grm5^{-/+}$ mice express only half mGluR5 *in-vivo*. Phenotypically, $Grm5^{-/+}$ mice do not differ from WT mice and do not show changes of body weight and behavioural test performances (Lu *et al*., 1997). The genotype of $Grm5^{-/+}$ mice was, instead, identified by polymerase chain reaction (PCR) using specific primers according to the Jackson Laboratory protocols with minor modifications. Briefly, DNA was extracted from mice tails according to the manufacturer's protocol (KAPA Mouse Genotyping Kits, Kapa Biosystems, Woburn, MA, USA) and amplified using 2 couples of primers. The first couple of primers (5'-CACATGCCAGGTGACATTAT-3' and 5'-CCATGCTGGTTGCAGAGTAA-3') amplifies a product of 442 bp for the WT alleles. The second couple of primers (5'-CCCTAGAGCAAAGCATTGAGTT-3' and 5'-GCCAGAGGCCACTTGTGTAG-3') amplifies a genomic fragment of 254 bp specific for the gene target insertion of the Grm5 null gene.

B6SJL-TgN ((SOD^{G93A}) 1Gur) male mice, expressing a high copy number of mutant human SOD1 with the Gly93Ala substitution ($SOD1^{G93A}$; Gurney *et al*., 1994) were bred with background-matched B6SJL wild-type (WT) females at the animal facility of the Pharmacology and Toxicology Unit, Department of Pharmacy in Genoa. The selective breeding preserved the transgene in the hemizygous state. Mice carrying the $SOD1^{G93A}$ mutation were identified analysing tissue extracts from tail tips, as previously described (Bonifacino *et al*., 2017): tissue was homogenized in phosphate-buffer saline (PBS), freeze/thawed twice, and centrifuged at 23,000 x g for 15 minutes (min) at 4 °C and the SOD1 level was evaluated by staining for its enzymatic activity after 10% non-denaturing polyacrylamide gel electrophoresis.

$SOD1^{G93A}$ male mice (with the mixed background C57BL6J) were bred with $Grm5^{-/+}$ females (with the background B6;129) to generate $SOD1^{G93A}Grm5^{-/+}$ double-mutant mice heterozygous for $Grm5^{-/+}$ and carrying the SOD1*G93A transgene. All experiments were conducted on littermates derived from this last breeding (Figure 10).

Animals were housed at relative humidity (50%) and constant temperature (22 ± 1 °C) with a regular 12 hours (h)-12 h light cycle (light 7 a.m.-7 p.m.); water and food (type 4RF21 standard diet obtained from Mucedola, Settimo Milanese, Milan, Italy) were freely available. The number of animals of each sex was balanced in each experimental group to avoid bias due to intrinsic sex-related differences. Experiments were carried out in accordance with the guidelines established by the European Communities Council (EU Directive 114 2010/63/EU) and with the Italian D.L. n. 26/2014 and were approved by the local Ethical Committee and by the Italian Ministry of Health (Project Aut. Prot. No. 97/2017-PR). All efforts were made to minimize animal suffering and to use only the number of animals necessary to produce reliable results. In particular, the use of primary cell cultures leads to a reduction in the number of utilized animals. Indeed, our optimised protocol for isolation and culture of astrocytes from adult mouse spinal cord allowed to study diverse parameters by multiple techniques from cells prepared from a single mouse. For experimental use animals were killed at a late stage of disease, around 120 days old.

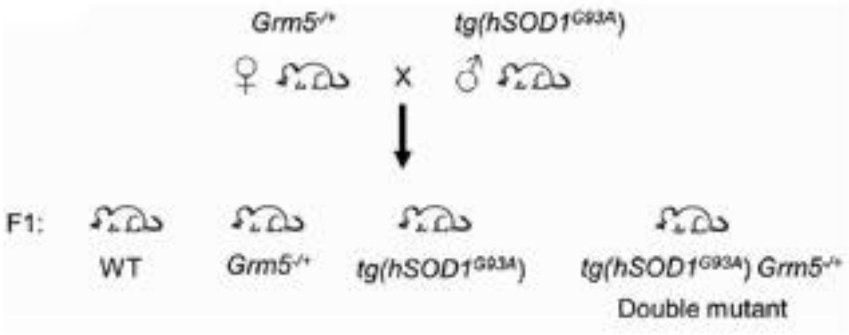

Fig. 10 Schematic representation of animal crossing. SOD1^{G93A} male mice were bred with Grm5$^{-/+}$ females to generate four genetically distinct mouse littermates (WT, Grm5$^{-/+}$, SOD1^{G93A} and SOD1^{G93A}Grm5$^{-/+}$). SOD1^{G93A}Grm5$^{-/+}$ are the transgenic mice carrying both the Grm5$^{-/+}$ heterozygous mutation and the SOD1*G93A transgene. All experiments were conducted on littermates derived from F1 crossing (Bonifacino *et al*., 2017).

3.2 Preparation of astrocyte primary cultures

WT, $SOD1^{G93A}$ and $SOD1^{G93A}$ $Grm5^{-/+}$ mice (120 days old) were euthanized by cervical dislocation, without prior anaesthesia by personnel well-trained with this technique. Spinal cords were quickly removed, cleaned by meninges, and put in ice at 4 °C. Primary astrocytes were prepared according to a protocol optimised in our laboratory. Tissue was chopped with a scalpel under sterile conditions to facilitate the next step of mechanical dissociation of spinal cord. Dissociated tissue was transferred in a 15 mL tube containing 1 mL of cell culture medium, composed by Dulbecco's Modified Eagle Medium High Glucose (DMEM; Euroclone, Cat# ECM0728L), 2 % Glutamine (Euroclone, Cat# ECB3004D), 1 % Penicillin-Streptomycin (Euroclone, Cat# ECB3001D) and 10 % fetal bovine serum (Euroclone, Cat# ECS0180L), then the tissue was further dissociated by gently pipetting up and down until reaching a homogenous preparation.

The cell suspension derived from $SOD1^{G93A}$ and $SOD1^{G93A}Grm5^{-/+}$ mice was plated onto poly-L-ornithine hydrocloride- (1.5 µg/mL, Sigma-Aldrich, Cat# P2533) and laminin- (3 µg/mL; Sigma-Aldrich, Cat# L2020) coated 6-well plates (2 wells/mouse) and WT astrocytes were plated onto pre-coated 35mm dishes (1 dish/mouse). All the preparations were incubated at 37 °C in humified 5 % CO_2 for three days, then, after washing with PBS 1X, the medium containing the tissue fragments was replaced with fresh complete DMEM. Medium was replaced three days/week and after 7-10 days *in-vitro* (DIV) cells were detached by incubation at 37 °C for 15 min with Trypsin-EDTA 1X (Euroclone, Cat# ECB3052B). Trypsin was then neutralized with 4 volumes of DMEM and centrifuged for 5 min at 700 x g at room temperature (RT). The cell pellet was re-suspended, a cell aliquot was diluted 2X in Trypan Blue (Euroclone, Cat# ECM0990D) to be counted.

Astrocytes were seeded at the optimal density of 1 x 10^5 cells in pre-coated 6-well plates for qPCR and western blot or in pre-coated 35mm dishes for astrocyte-MN co-culture. Astrocytes were also seeded at a density of 3 x 10^4 cells/well in 24-well plates containing 12 mm diameter pre-coated glass coverslips, for confocal microscopy analysis. After 20 DIV, when astrocytes reached the confluence, they were used for the analyses (Figure 11).

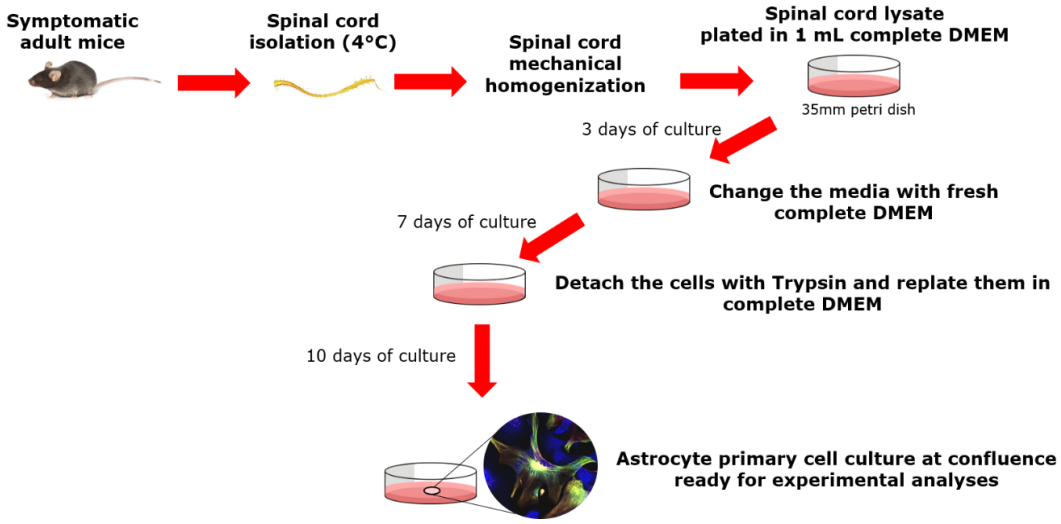

Fig. 11 Schematic representation of the protocol to plate spinal cord primary astrocytes.

3.3 Quantitative reverse transcription polymerase chain reaction (RT-qPCR)

RT-qPCR was used to determine mGluR5 mRNA expression. After about 20 DIV, WT, Grm5$^{-/+}$, SOD1^{G93A}, and SOD1^{G93A} Grm5$^{-/+}$ astrocytes were detached with Accutase® (Euroclone, Cat# ECB3056D) for 10 min at 37 ºC. Then, Accutase was blocked by adding 3 volumes of complete DMEM and cell suspension was centrifuged at 700 x g for 5 min at RT. Cell pellet was washed with PBS 1X and centrifuged again at 17,000 x g for 5 min at 4 ºC. RNA was obtained using 500 µL TRIzol (Invitrogen, Cat# 15596026), then purified with ReliaPrep™ RNA Cell Miniprep System (Promega, Cat# Z6010), and quantified by measuring the optical density (NanoDrop ND-2000 Spectrophotometer, NanoDrop Technologies). cDNA was prepared from 0.6 µg RNA using the iScript™ Reverse Transcription Supermix for RT-qPCR Kit (Bio-Rad, Cat# 1708840). Real-time PCR was performed in an IQ5 Multicolor Real-Time PCR Detection System (Bio-Rad Laboratories, Hercules, California, United States) using iQ SYBR Green Supermix (Bio-Rad Laboratories, Cat# 1708882), as previously described (Rossi *et al*., 2013). Briefly, PCR amplifications were done in triplicate using 1:2 diluted cDNA in 25 µL final reaction mixture. Mouse

glyceraldehyde-3-phosphate dehydrogenase (GAPDH) cDNA was used as housekeeping gene. The following primers were used: Grm5 (Grm5_F1: 5'-AGCAAGTGATCAGAAAGACTCG-3' and Grm5_R1: 5'-GTCACAGACTGCAGCAGAGC-3'); GAPDH (GAPDH_F3: 5'-ATTGTCAGCAATGCATCCTG-3' and GAPDH_R3: 5'-ATGGACTGTGGTCATGAGCC-3') The RT-qPCR conditions were: 95 °C for 10 seconds (s), 60 °C for 30 s, 72 °C for 30 s, for 40 cycles. The expression level of mRNA was calculated using the ΔΔCt method (Livak and Schmittgen, 2001), normalizing to GAPDH. Data from ASO- and scramble-treated mice were compared to WT, which were normalized to 100%.

3.4 Immunofluorescence assay

WT, $SOD1^{G93A}$ and $SOD1^{G93A}Grm5^{-/+}$ astrocytes, seeded on coated 12 mm diameter glass coverslips were washed three times with PBS 1X and fixed with 4% paraformaldehyde (PFA, Sigma-Aldrich, Cat# 47608) for 15 min at RT, in the dark. After fixing, cells were permeabilized with methanol for 5 min at -20 °C, washed three times with PBS 1X (3 x 5 min) and treated with a solution of 0.5% bovine serum albumin (BSA) in PBS 1X (0.5% PBS/BSA) for 15 min at RT. Primary antibodies were properly diluted in 3% PBS/BSA and incubation was performed overnight at 4 °C. The list of antibodies and their final dilutions are reported in Table 4. The day after, astrocytes were washed three times with 0.5% PBS/BSA (3 x 5 min) and labelled with secondary antibodies diluted 1:3000 in 3% PBS/BSA for 1 h at RT (Table 4). Cells were washed three times with PBS 1X, and the coverslips were assembled on a microscopy glass slide by using Fluoroshield™ containing DAPI (Sigma-Aldrich, Cat# F6057), to label nuclei.

Fluorescence image (512 x 512 x 8 bit) acquisition was performed by a three-channel TCS SP5 laser-scanning confocal microscope (Leica, Wetzlar, Germany) equipped with 458, 476, 488, 514 and 633 nm excitation lines, through a plan-apochromatic oil immersion objective 63x/1.4. Light collection was optimized according to the combination of the chosen fluorochromes, and sequential channel acquisition was performed to avoid crosstalk. The Leica "LAS AF" software package was used for image acquisition. The quantitative analyses of co-localization and the relative protein expression level were obtained by calculating co-localization coefficients (Manders *et al.*, 1992) and normalizing the results with the

expression of glyceraldehyde 3-phosphate dehydrogenase (GAPDH), the housekeeping marker.

PRIMARY ANTIBODY	WORKING DILUTION	PRODUCER AND CATALOGUE NUMBER
mouse monoclonal anti-glial fibrillary acid protein (GFAP) antibody	1:1000	Sigma Aldrich, Cat# G3893
mouse monoclonal anti-S100β antibody	1:500	Merck Millipore, Cat# MAB079
goat polyclonal anti-IL-1β antibody	1:1000	Sigma Aldrich, Cat# I3767
goat polyclonal anti-TNF-α antibody	1:300	Sigma Aldrich, Cat# T0938
chicken polyclonal anti-IL-6 antibody	1:500	Sigma Aldrich, Cat# GW22495
mouse monoclonal anti-glyceraldehyde 3-phosphate dehydrogenase (GAPDH) antibody	1:1000	Sigma Aldrich, Cat# G8795
rabbit polyclonal anti-glyceraldehyde 3-phosphate dehydrogenase (GAPDH) antibody	1:1000	Sigma Aldrich, Cat# G9545
rabbit polyclonal ant-mGluR5 antibody	1:500	Abcam, Cat# ab53090
rabbit polyclonal anti-human superoxide dismutase 1 (hSOD1) antibody	1:100	Chemicon, Cat# AB5480
mouse monoclonal anti-misfolded human superoxide dismutase 1 (hSOD1) antibody	1:100	Medimabs, Cat# B8H10
rabbit monoclonal anti-LC3 A/B antibody	1:100	Cell Signaling Technology, Cat# D3U4C
SECONDARY ANTIBODY	**WORKING DILUTION**	**PRODUCER AND CATALOGUE NUMBER**
donkey anti-rabbit Alexa Fluor A488-conjugated	1:3000	Thermo fisher Scientific, Cat# R37118
donkey anti-mouse Alexa Fluor A488-conjugated	1:3000	Thermo fisher Scientific, Cat# A21202
donkey anti-goat Alexa Fluor A488-conjugated	1:3000	Thermo fisher Scientific, Cat# A11055
goat anti-chicken Alexa Fluor A488-conjugated	1:3000	Thermo fisher Scientific, Cat# A11039
donkey anti-mouse Alexa Fluor A647-conjugated	1:3000	Thermo fisher Scientific, Cat# A31571
donkey anti-rabbit Alexa Fluor A647-conjugated	1:3000	Thermo fisher Scientific, Cat# A31573

Table 4 List of primary and secondary antibodies with the respective working dilution, the supplier company, and the catalogue number.

3.5 Western blot

After about 20 DIV, WT, SOD1^{G93A} and SOD1^{G93A}Grm5$^{-/+}$ astrocytes were detached with Trypsin-EDTA 1X, diluted in 3 volumes complete DMEM to block the enzymatic activity and centrifuged at 700 x g for 5 min at RT. Pellet was washed in PBS 1X and centrifuged at 17,000 x g for 5 min at 4°C. PBS was removed and cell pellet stored at -80°C. Western blot analyses were conducted using standard procedures. Cell pellets were lysed using lysis Buffer (150 mM NaCl, 20 mM TRIS-HCl pH 7.4, 2 mM EDTA and 1 % NP40) containing a protease inhibitor cocktail for mammalian cells (Sigma Aldrich, Cat# P8340) and total protein was measured by Bradford assay (Bradford MM, 1976). Samples were incubated with a denaturing solution containing: 8% w/v SDS, 125 mM Tris-HCl (pH 6.8), and 1.25% v/v DTT. After 10 min of incubation at 37 ºC, the sample was boiled for 5 min and 40% w/v sucrose and 0.008% bromophenol blue were added.

Electrophoresis was carried out using a Mini Protean III (Bio-Rad Laboratories, Hercules, CA, USA) apparatus, in which both faces of the gel sandwich were immersed in the buffer. To a better resolution of both middle and low-molecular weight proteins, 4-20% precast gradient gels (Bio-Rad, Cat# 4568094) were used. The electrophoretic run was performed at 4 ºC, setting constant current at 70 mA, with denaturing running buffer. Proteins separated by SDS-PAGE were transferred onto nitrocellulose membrane (NC, Bio-Rad Laboratories) by electroblotting at 400 mA for 2 h in Tris-glycine buffer (50 mM Tris, 380 mM glycine) plus 20% methanol. The membrane was blocked with PBS/0.1% Tween 20 (PBSt) containing 5% non-fat dry milk for 1 h and incubated over night at 4 °C with primary antibodies (Table 5), The list of antibodies and their final dilutions are reported in Table 3. After 3 washes with PBSt, NC was incubated for 1 h at RT with specific secondary antibodies conjugated with horse radish peroxidase (HRP) (Bio-Rad Laboratories) and developed with Clarity Western ECL Substrate (Bio-Rad Laboratories). Bands were detected and analyzed for density using the Alliance 6.7 WL 20 M enhanced chemiluminescence system and UV1D software (UVITEC, Cambridge, UK). Each band was converted by into a densitometric trace allowing calculations of intensity; signals were normalized to the signal of GAPDH and results expressed as Relative Optical Density (R.O.D.).

PRIMARY ANTIBODY	WORKING DILUTION	PRODUCER AND CATALOGUE NUMBER
mouse monoclonal anti-glial fibrillary acid protein (GFAP) antibody	1:1000	Sigma Aldrich, Cat# G3893
mouse monoclonal anti-S100β antibody	1:100	Merck Millipore, Cat# MAB079
rabbit recombinant monoclonal anti-NLRP3 antibody	1:500	Abcam, Cat# ab210491
goat polyclonal anti-IL-1β antibody	1:500	Sigma Aldrich, Cat# I3767
goat polyclonal anti-TNF-α antibody	1:1000	Sigma Aldrich, Cat# T0938
chicken polyclonal anti-IL-6 antibody	1:500	Sigma Aldrich, Cat# GW22495
mouse monoclonal anti-glyceraldehyde 3-phosphate dehydrogenase (GAPDH) antibody	1:10000	Sigma Aldrich, Cat# G8795
rabbit polyclonal anti-glyceraldehyde 3-phosphate dehydrogenase (GAPDH) antibody	1:10000	Sigma Aldrich, Cat# G9545
rabbit polyclonal ant-mGluR5 antibody	1:500	Abcam, Cat# ab53090
rabbit polyclonal anti-human superoxide dismutase 1 (hSOD1) antibody	1:500	Chemicon, Cat# AB5480
mouse monoclonal anti-misfolded human superoxide dismutase 1 (hSOD1) antibody	1:1000	Cell Signaling Technology, Cat# 4108
rabbit monoclonal anti-LC3 A/B antibody	1:100	Cell Signaling Technology, Cat# D3U4C
SECONDARY ANTIBODY	**WORKING DILUTION**	**PRODUCER AND CATALOGUE NUMBER**
goat polyclonal anti-mouse IgG (HRP) antibody	1:5000	Bio-Rad, Cat# 0300-0108P
goat polyclonal anti-rabbit IgG (HRP) antibody	1:5000	Bio-Rad, Cat# STAR124P
rabbit polyclonal anti-goat IgG (HRP) antibody	1:5000	Bio-Rad, Cat# 5160-2104
goat polyclonal anti-chicken IgG (HRP) antibody	1:5000	Bio-Rad, Cat# AAI29
goat polyclonal anti-guinea pig IgG (HRP) antibody	1:5000	Bio-Rad, Cat# AHP863F

Table 5 List of primary and secondary antibodies used to perform western blot analysis, reporting the working dilution, the supplier company and the catalogue number.

3.6 Cytosolic Calcium concentration

To determine the $[Ca^{2+}]_c$, WT, $SOD1^{G93A}$ and $SOD1^{G93A}Grm5^{-/+}$ astrocytes were seeded on 12 mm diameter coated coverslips inside 24-well plates. After 20 DIV astrocytes were incubated for 40 min at 37 ºC in complete DMEM supplemented by 10 µM od the fluorescent dye Fura-2/AM (Grynkiewicz G *et al*., 1985) previously solubilized in 0.5% Dimethyl-sulfoxide (DMSO, Sigma Aldrich, Cat# D2650). Astrocytes incubated with complete DMEM supplemented only by 0.5% DMSO were used to measure the auto-fluorescence. After the incubation, cells were washed with PBS 1X with 0.9 mM $CaCl_2 \cdot 2\ H_2O$ (Sigma Aldrich, Cat# D8662-500ML) to remove the excess of Fura-2/AM. The same solution was used to measure $[Ca^{2+}]_c$. The $[Ca^{2+}]_c$ measurements were performed at 37 ºC by a RF-5301PC dual wavelength spectrofluorophotometer (Shimadzu Corporation, Milan, Italy) by alternating the excitation wavelengths of 340 and 380 nm. Fluorescent emission was monitored at 510 nm. Basal fluorescence was recorded for 1 minute, then astrocytes were exposed to 30 µM 3,5-DHPG, a non-selective agonist of mGluRs. Calibration of the fluorescent signal was done at the end of each measure by adding 10 µM Ionomycin to obtain the maximum fluorescence signal (F_{max}), followed by 10 mM EDTA adjusted to pH 8.0 and buffered with 3 mM Tris, to obtain the minimum fluorescence signal (F_{min}). After correcting for extracellular dye, $[Ca^{2+}]_c$ was calculated by the equation of Grynkiewicz and colleagues (Grynkiewicz G *et al*., 1985) using a K_D of 224 nM for the Ca^{2+} - Fura-2 complex. Measures were performed within 2 h from astrocyte labelling.

3.7 Evaluation of aerobic metabolism and lactate fermentation

3.7.1 Evaluation of oxygen consumption rate (OCR)

O_2 consumption was evaluated in WT, $SOD1^{G93A}$ and $SOD1^{G93A}Grm5^{-/+}$ astrocytes by a thermostatically controlled (37°C) oxygraph apparatus equipped with an amperometric electrode (Unisense-Microrespiration, Unisense A/S, Denmark). For each experiment, 1 x 10^5 cells permeabilized with 0.03% digitonin for 10 min were used. After permeabilization, cells were suspended in the respiration medium containing 137 mM NaCl, 5 mM KCl, 0.7 mM KH_2PO_4, 25 mM Tris–HCl pH 7.4, and 25 mg/mL ampicillin. The respiring substrates, Pyruvate (10mM) and Malate (5mM) or Succinate (20mM) were added, using a Hamilton syringe, to study the Complexes I, III, IV or Complex II, III, IV pathways, respectively. 0.1

mM ADP was added after the addition of the respiratory substrates. The respiratory rates were expressed as nmol O/min/10^6 cells (Ravera *et al*., 2018b).

3.7.2 Assay of Fo-F1 ATP synthase activity

Fo-F1 ATP synthase activity was evaluated in WT, $SOD1^{G93A}$ and $SOD1^{G93A}Grm5^{-/+}$ astrocytes. For each experiment 1 x 10^5 cells were incubated for 10 min at 37°C in a medium containing: 10 mM Tris-HCl pH 7.4, 100 mM KCl, 5 mM KH_2PO_4, 1 mM EGTA, 2.5 mM EDTA, 5 mM $MgCl_2$, 0.6 mM ouabain, 0.3 mM P1, P5-Di (adenosine-5′) pentaphosphate and 25 mg/mL ampicillin. ATP synthesis was induced by addition of the following metabolic substrates: pyruvate (10 mM) + malate (5 mM) or succinate (20 mM). The reaction was monitored for two min, every 30 seconds, in a luminometer (GloMax® 20/20n Luminometer, Promega Italia, Milano, Italy), by the luciferin/luciferase chemiluminescent method, with ATP standard solutions between
10^{-8}M and 10^{-5}M (luciferin/luciferase ATP bioluminescence assay kit CLSII, Roche, Basel, Switzerland). Data were expressed as nmol ATP produced/min/10^6 cells (Ravera *et al*., 2018b).

3.7.3 Evaluation of OxPhos efficiency

The oxidative phosphorylation efficiency was calculated as the ratio between the concentration of the produced ATP (as in Chapter 3.7.2) and the amount of consumed oxygen in the presence of pyruvate + malate or succinate and ADP (as in Chapter 3.7.1; P/O ratio). When the oxygen consumption is completed devoted to the energy production, the P/O ratio should be around 2.5 and 1.5 after pyruvate + malate or succinate addition, respectively (Hinkle, 2005).

3.7.4 Glucose consumption assay

To evaluate glucose consumption, the glucose content in the growth medium of WT, $SOD1^{G93A}$ and $SOD1^{G93A}Grm5^{-/+}$ astrocytes was evaluated in a double beam spectrophotometer (UNICAM UV2, Analytical S.n.c., Italy) by the hexokinase (HK) and glucose 6 phosphate dehydrogenase (G6PD) coupling system, following the reduction of NADP at 340 nm (NADH/NADPH molar extinction coefficient was considered:

6.22 x 10^{-3} M x 1 cm^{-1} at 340 nm, Bianchi *et al*., 2015). The assay medium contained: 100 mM Tris-HCl pH 7.4, 2 mM ATP, 10 mM NADP, 2 mM $MgCl_2$, 2 IU of hexokinase and 2 IU of glucose 6-phopshate dehydrogenase. Data was normalized to the cell number and expressed as mM glucose consumed/10^6 cells (Ravera *et al*., 2018c).

3.7.5 Lactate release assay

Lactate concentration was assayed spectrophotometrically in the growth medium of WT, $SOD1^{G93A}$ and $SOD1^{G93A}Grm5^{-/+}$ astrocytes, following the reduction of NAD^+ at 340 nm (Bianchi *et al*., 2015). The assay medium contained: 100 mM Tris-HCl at pH 8, 5mM NAD^+ and 1 IU/ml of lactate dehydrogenase (LDH). Samples were analysed before and after the addition of 4 µg purified LDH. Data was normalized to the cell number and expressed as mM lactate released/10^6 cells (Ravera *et al*., 2018c).

3.8 Enzyme-linked immunosorbent assay

The conditioned medium of 20 DIV WT, $SOD1^{G93A}$ and $SOD1^{G93A}Grm5^{-/+}$ astrocytes, was collected after 24 h and filtered with 0.22 µm sterile filter. Then, TNF-α, IL-1β and IL-6 concentrations were measured with a specific enzyme-linked immunosorbent assay (ELISA) kit (R&D Systems, Cat# DY401, DY410 and DY406, respectively) according to the manufacturer's protocol.

ELISA 96-well plates were pre-treated with the capture antibody for TNF-α (1:50), IL-1β (1:50) or IL-6 (1:50) for 24 h at RT; then the excess of antibody was washed out using the supplied Wash Buffer (R&D systems, Cat# WA126) and the plate was incubated for 1 h with the supplied Reagent Diluent (R&D systems, Cat# DY995).

At this point, standards and samples were added. Standard solution was prepared by diluting recombinant TNF-α, IL-1β or IL-6 in Reagent Diluent to obtain the standard curves. Seven-point standard curves were generated using 2-fold serial dilutions in Reagent Diluent. Standard curves extend over 1000 pg/mL and 15.6 pg/mL in the case of TNF-α; 2000 pg/mL and 31.25 pg/mL in the case of IL-1β; 1000 pg/mL and 15.6 pg/mL in the case of IL-6. Triplicate standard curve points were obtained by adding 100 µL of the standards at the diverse concentrations in the proper plate wells. For the analysis, 150-200 µL of filtered cell supernatant/well was added. Each sample was run in duplicate. Three wells were used as

blank and were added with 100 µL filtered water. Plates were incubated for 2 h at RT to allow the binding of cytokine to the antibody. After incubation, medium was harvested, and wells were washed three times with Wash Buffer. Samples were incubated with 100 µL of the detection antibody for TNF-α, IL-1β and IL-6 per well, each diluted 1:60 in Reagent Diluent for 2 h at RT, as appropriate.

Wells were washed three times with Wash Buffer and 100 µL Streptavidin-HRP (1:40 in Reagent Diluent) were added to each well for 20 min, protected from light. Streptavidin-HRP was harvested, and wells were washed three times with Wash Buffer and added with 100 µL Substrate Solution, composed by 1:1 mixture of Colour Reagent A (H_2O_2) and Colour Reagent B (Tetramethylbenzidine) (R&D systems, Cat# DY999]. Plates were incubated 20 min at RT, protected from light. Finally, 50 µL Stop Solution (2N H_2SO_4; R&D systems, Cat# DY994) was used to block the reaction.

Cytokine amount was measured by Spectrophotometry. Absorbance was measured at 450 nm with a microplate reader (SpectraMax 340PC Microplate Reader, Molecular devices, San Jose, California, USA). The standard curves were fitted from the averaged absorbance values of each concentration. Sample quantification was obtained from the averaged absorbance values by regression analysis based on the standard curve.

3.9 Motor neuron co-culture

MNs were prepared from spinal cord of WT and $SOD1^{G93A}$ E13.5 mouse embryos (Vandenberghe *et al*., 1998; Wiese *et al*., 2009). Spinal cord was isolated by microscopy dissection, then meninges and the dorsal root ganglia were removed. Ventral spinal cord was cut with scalpel in small pieces and digested with 2.5% trypsin (Sigma-Aldrich, Cat# T4799) in Hank's Balance Salt Solution (HBSS, Euroclone, Cat# ECM0507L) for 15 min at 37 °C. Then, trypsin solution was replaced with 0.02 mg/mL Deoxyribonuclease I (DNAse; Sigma-Aldrich, Cat#DN25), 0.4% BSA (Sigma-Aldrich, Cat# A3311) and F1 culture medium composed by Leibovitz-15 medium (Sigma-Aldrich, Cat# L5520), 3.6 mg/mL Glucose, 100 µg/mL Penicillin-Streptomycin (Euroclone, Cat# ECB3001D), 20 nM Progesterone (Sigma Aldrich, Cat# P8783), 2% Horse serum (Gibco, Cat# 16050130), 1% Glutamine (Euroclone, Cat# ECB3004D) and IPCS mix [5µg/mL Insulin from bovine pancreas (Sigma Aldrich, Cat# I6634-50mg), 0.1mM Putrescine dihydrochloride (Sigma Aldrich, Cat# P5780-5g), 0.1mg/mL Conalbumin (Sigma Aldrich, Cat# C7786-1g) and 30 nM Sodium Selenite

(Sigma Aldrich, Cat# S5261)] and gently dispersed with P1000 pipette. The tissue homogenate was stratified on 6.2% OptiPrep (Sigma-Aldrich, Cat# D1556) cushion and centrifuged 500 x g for 15 min at RT. After centrifuging, the MN-enriched cell population was localized at the interface between the OptiPrep solution and the medium. The MN band was collected and re-suspended in 3 mL F1 culture medium. Cell suspension was layered on top of a 1 mL BSA (4%) gradient containing 20 µL DNAse (1 mg/mL) and centrifuged at 75 x g for 20 min to remove Optiprep impurity. The pellet containing MNs was diluted in 1 mL F1 culture medium supplemented by Sodium Bicarbonate solution (Sigma Aldrich, Cat# S8761-100 mL) and 50 µL of Chick Embryo Extract (US Biological, Cat# C3999). $5x10^4$ MNs were seeded in a 35 mm Petri dish on a confluent adult astrocytes layer prepared from 120 days-old WT, $SOD1^{G93A}$ or $SOD1^{G93A}Grm5^{-/+}$ mice. After 3 days medium was removed and replaced with fresh MN medium. After that, medium was changed three times a week. Four day after seeding, MNs present in an area of $1cm^2$ were counted to assess viability. The number of MNs was recorded three times a week for 14 days. The number of MNs at day 4 were taken as 100% of survival. The percentage of survival at the other time-points was calculated as percentage of the number of MNs at day 4, in the same area of the same dish.

3.10 Acute treatment with antisense oligonucleotide

After about 20 DIV, $SOD1^{G93A}$ astrocytes were seeded at a density of 2-3 x 10^4 cells/well in 24-well plates containing 12 mm diameter pre-coated glass coverslip and treated with 10 µM of a mGluR5 directed antisense oligonucleotide (ASO, Ionis™ Pharmaceuticals) or with 10 µM scramble oligonucleotide for 48 h. Then, cells were washed with PBS 1X and fresh complete DMEM was added for further 5 days. After 7 days from starting of treatment, $SOD1^{G93A}$ astrocytes were either detached and collected to perform qPCR analysis aimed at evaluating the mGluR5 mRNA expression or fixed in 4% PFA to proceed with immunofluorescence analysis aimed at investigating the expression of two markers of astrogliosis, such as S100β and GFAP.

3.11 Pharmacological treatment with CTEP

After about 20 DIV $SOD1^{G93A}$ astrocytes were seeded at a density of 2-3 x 10^4 cells/well in 24-well plates containing 12 mm diameter pre-coated glass coverslips. The pharmacological treatment with CTEP, synthetized, purified, and kindly provided by Prof. Silvana Alfei

[Organic Chemistry Unit of the Department of Pharmacy, University of Genoa (Alfei and Baig, 2017)], was performed as follows: three days after plating, $SOD1^{G93A}$ astrocytes were treated for seven days either with 0.1 µM CTEP dissolved in 140 µM DMSO or with vehicle. CTEP/DMSO and DMSO were diluted in complete DMEM to the correct final concentration and replaced every 48 h. On day 7 cells were washed twice with PBS 1X and complete DMEM was added for further 24 h. Then, $SOD1^{G93A}$ astrocytes were fixed with 4% PFA and immunofluorescence analysis of S100β and GFAP expression was performed, as previously described, to investigate astrogliosis.

3.12 Statistical analyses

Data are expressed as the mean ± s.e.m. and P value < 0.05 was considered significant. Statistical comparison of two means were performed by unpaired two-tailed Student's *t*-test; multiple comparisons were done using the analysis of variance (one-way ANOVA) followed by the Bonferroni's post hoc test. Analyses were performed by means of Sigma Stat software (Systat Software, Inc., San Jose, CA, USA). LRT-qPCR data were analyzed by Kruscal-Wallis test followed by Dunn's Multiple Comparison.

3.13 Preparation of *enriched* microglia

Enriched microglia samples were prepared at the University of Genoa following the protocol of Norden and colleagues (Norden *et al*., 2014) and De Haas and colleagues (De Haas *et al*., 2008) with little modifications. WT, $Grm5^{-/+}$, $SOD1^{G93A}$ and $SOD1^{G93A}Grm5^{-/+}$ mice were sacrificed at the early and late symptomatic stages of the disease (90 and 120 days, respectively). Brain or spinal cord were homogenized in 2 mL of ice-cold "Medium A" composed of 50 mL Hanks' balanced salt solution 1X (HBSS 1X, Euroclone, Cat# ECM0507L) 1.3% glucose (Sigma Aldrich, Cat# G8769) 750 µL N-2-hydroxyethylpiperazine-N0-2-ethanesulfonic acid 1 M (HEPES 1M, Euroclone, Cat# ECM0180D) and 10% heat inactivated fetal bovine serum (FBS, Euroclone, Cat# ECS0180L) and filtered with 106 µm and 75 µm sieves. The preparation was transferred in a 50 mL tube on ice and filtered under the sterile hood using a 70 µm filter. Medium A was added reaching the volume of 20 mL/brain or spinal cord and centrifuged at 900 x g for 10 min at 4 °C (acceleration 9, brake 6). Cell pellet was resuspended in 20 mL Medium A without FBS and centrifuged again as before. Next, the cell pellets were resuspended in less

than 3 mL of 75% Percoll Solution (37,5 mL Percoll 100% and 12.5 mL PBS1X), transferred to another cleaned tube and put in ice to gently create the complete gradient with 3 mL of 50% Percoll Solution, 3 mL of 25% Percoll Solution and 3 mL of PBS1X. Gradient was centrifuged at 2000 x g for 20 min at 4 ℃ (acceleration 4, brake 0). Microglia (the band between 75% and 50% gradient interface) were transferred into a new tube and PBS1X was added reaching a volume of 30 mL. To clean cell suspension from Percoll, samples were centrifuged at 900 x g for 10 min at 4 ℃ (acceleration 9, brake 6, this step was repeated twice). Finally, the cell pellets were resuspended in 1 mL of PBS and an aliquot of 50 µL was mixed with Guava ViaCount (Luminex Corporation, Cat# 4000-0040) to proceed with cell counting at flow cytometer (Guava EasyCyte, Merck Millipore). Microglia were lastly centrifuged at 3000 x g for 5 min at 4 ℃ and pellet resuspended in 500 µL QIAzol. Samples were immediately stored in -80 °C and shipped to Hasselt University in dry ice to proceed with the analyses.

3.14 RNA extraction

Enriched microglia samples shipped from Italy were stored at -80 ℃ or immediately processed to extract RNA. RNA extraction was performed following the optimized phenol-chloroform protocol of Toni and colleagues (Toni *et al*., 2018) with minor modifications. Cells were gently resuspended up and down and 100 µL pure RNase-free chloroform were added to each tube. Samples were vigorously inverted by hand for 15 times up and down, let sit for 3-15 min at RT and centrifuged at 12,000 x g for 15 min at 4 °C. The RNA-containing upper aqueous phase (clear supernatant) was transferred into a new 1.5 mL tube where a chloroform extraction was repeated one more time. Then, for the RNA precipitation, new 1.5 mL tubes were prepared containing 2 µL glycogen (5 µg/µL, Sigma Aldrich, Cat# 361507-1ML) and 250 µL pure RNase-free isopropanol. The RNA-containing upper aqueous phase was added into the new tubes, samples were inverted by hand 10-20 times, let sit at RT for 10 min and centrifuged at 12,000 x g for 10 min at 4 °C. RNA pellet was washed with 1mL of 75% ethanol (EtOH), vortex and centrifuged at 7,500 x g for 5 min at 4 °C. This step was repeated three times. RNA samples were pulse spin at RT, the supernatant was carefully removed, and tubes were let opened for 3-5 min at RT to make EtOH evaporate. RNA was resuspended in 15-20 µL nuclease-free water and heated at 65 ℃ for 2-5 min to make RNA solubilized. Then, samples were vortex for 5-10 seconds, pulse spin and put immediately on ice. RNA was treated with DNase (Heat & Run gDNA removal

kit, ArcticZymes Technologies, Cat# 80200-250) to remove genomic DNA (gDNA) contamination and then quantified and analysed for purity at the spectrophotometer (NanoDrop 2000, Thermo Scientific). The RNA integrity was tested at Agilent 2100 Bioanalyzer System (Agilent, Santa Clara, United States) with Agilent RNA 6000 Pico Kit (capacity of 50-5000 pg/µL, Agilent), starting with 5 ng RNA.

3.15 RT-qPCR

To retro-transcribed the RNA to cDNA it was followed the protocol set in the group of Dr. Tim Vanmierlo at Biomedical Research Institute (BIOMED, Hasselt University, Belgium). Briefly, after RNA quantification at Nanodrop 2000, 100 ng RNA were retro-transcribed to cDNA (16 µL final volume) and 4 µL Qscript cDNA supermix (Quanta Biosciences, Cat# 95047) were added to each 200 µL strip tube (20 µL final volume), samples were mixed, quickly spin and retro-transcribed to cDNA with a thermocycler following this protocol: 5 min at 25 °C, 30 min at 42 °C, 5 min at 85 °C, Hold at 4 °C. cDNA samples were stored in -20 °C or immediately used for qPCR analyses.

For qPCR experiments it was followed the protocol already set in the group of Dr. Vanmierlo (BIOMED, Hasselt University, Belgium). qPCR reactions were performed in a total volume of 10 µL, comprising 5 µL Fast SYBR Green Master Mix (Thermo Fisher Scientific, Cat#4385612), 0.3 µL forward and 0.3 µL reverse primers (300 nM final concentration, Table 6) and variable cDNA content (5-12.5 ng) in 96-well white plates (MicroAmpFastOptical 96-well Reaction Plate with Barcode 0.1 mL, Applied Biosystem) which were quicky spin at 1,200 x g for 2 min before loading in the QuantStudio 3 qPCR instrument (Applied Biosystem).

Thermocycling conditions set by Vanhauwaert and colleagues were performed with minor modifications (Vanhauwaert *et al.,* 2014):

- 95 °C for 10 min.
- 95 °C for 15 seconds, 60 °C for 30 seconds, 72 °C for 12 seconds.
- Melting curve: 95 °C for 5 seconds, 60 °C for 1min, gradual heating to 95 °C (10 seconds) at a ramp-rate of 0.11 °C/second, cooling to 37 °C for 3 min.

To investigate the anti-inflammatory "M2-like" microglia phenotype we selected the following genes: Arginase 1 (Arg1), interleukin 10 (IL-10), cluster of differentiation 206

(CD206), interleukin 4 (IL-4). For the activated "M2-like" microglia phenotype we studied the following targets: interleukin 1β (IL-1β), cluster of differentiation 86 (CD86), inducible nitric oxide synthase (iNOS), tumor necrosis factor α (TNF-α), and interleukin 6 (IL-6).

The most stable endogenous reference genes and Expressed Repetitive Elements (EREs) (Table 6, primers selected in red) were selected using geNorm software. Exon-exon junction primers were designed with the *Primer design Tool* of NCBI (https://www.ncbi.nlm.nih.gov/tools/primerblast/index.cgi?ORGANISM=9606&INPUT_SEQUENCE=NM_001618.3) and EREs were selected from literature (Renard *et al*., 2018). EREs primers efficiency was tested using standard dilution series: RNA extracted from the brain of a WT mouse was converted to cDNA to make standard dilution series (5X) ranging from 12.5 ng to 0.1 ng. The efficiency of other primers was tested previously in the laboratory.

PRO-INFLAMMATORY GENES	FORWARD PRIMER (5'-3')	REVERSE PRIMER (5'-3')
TNF-α	ATGGCCTCCCTCTCATCAGT	CTTGGTGGTTTGCTACGACG
iNOS	CCCTTCAATGGTTGGTACATGG	ACATTGATCTCCGTGACAGCC
IL-1β	GCTGAAAGCTCTCCACCTCA	AGGCCACAGGTATTTTGTCG
CD86	TCAGTGATCGCCAACTTCAG	TTAGGTTTCGGGTGACCTTG
IL-6	TGTCTATACCACTTCACAAGTCGGAG	GCACAACTCTTTTCTCATTTCCAC
ANTI-INFLAMMATORY GENES	**FORWARD PRIMER (5'-3')**	**REVERSE PRIMER (5'-3')**
IL-10	AATAACTGCACCCACTTCCCA	CAGCTGGTCCTTTGTTTGAAAG
Arg-1	GTGAAGAACCCACGGTCTGT	GCCAGAGATGCTTCCAACTG
CD206	CTTCGGGCCTTTGGAATAAT	TAGAAGAGCCCTTGGGTTGA
IL-4	CTCACAGCAACGAAGAACACCA	AAGCCCGAAAGAGTCTCTGCA
REFERENCE GENES/EREs	**FORWARD PRIMER (5'-3')**	**REVERSE PRIMER (5'-3')**
GAPDH	GGCCTTCCGTGTTCCTAC	TGTCATCATATCTGGCAGGTT
ACT-β	GGCTGTATTCCCCTCCATCG	CAGTTGGTAACAATGCCATGT
CYPA	**GCGTCTCCTTCGAGCTGTT**	**AAGTCACCACCCTGGCA**
TBP	ATGGTGTGCACAGGAGCCAAG	TCATAGCTACTGAACTGCTG
PGK1	GAAGGGAAGGGAAAAGATGC	GCTATGGGCTCGGTGTGC
RPL13a	GGATCCCTCCACCCTATGACA	CTGGTACTTCCACCCGACCTC
18s	ACGGACCAGAGCGAAAGCAT	TGTCAATCCTGTCCGTGTCC
Ervb4_1B_LTR_Mm	AGCCTAATAAACGAGACCTTGAT	CCGCGGGATTCAGTTATTCG
Ervb7_1-I_Mm	AAAGTGTTGCTGAGGATGCG	TTCCACCTAAGCAGCTTCCT
Iap1_Mm	TGGGAGGTATGTCTGATTGCA	TGATCCCCAGTGTGCAGAAA
Ltris3	ATTGCTGGAACCCACTATGC	GCCCCGAGTAGCTGAGTAAG
Orr1a0	**GGTTGGAATGGGTGTGTCAC**	**TGGCTTACAGGTTCAGAGGT**
Rltr2aiap_Mm	CATGTGCCAAGGGTAGTTCTC	GCAAGAGAGAGAATGGCGAAAC
Rltr4_Mm	GTAACGCCATTTTGCAAGGC	CCATCTGTTCTTTGGCCCTG
Rltr4i_Mm	TCAGGACAAGGGTGGTTTGA	GGCCTGCACTACCGAAATTC
Rltr10b2	CCAATCCGGGTGTGAGACA	CTGACTCGCCAGCAAGAAC
Rltr13a3	ACAGACTACATTCCATGCCAAG	GCCAGGCAAGAGTTTTACAC
Rltr13b3	TCCGGCTGTGGTTTTAGAGT	TGAAAACGCAAAGACTGGCA

Table 6 Forward and reverse primers of pro- and inflammatory genes and of reference genes. The most stable reference gene and ERE used for the final analysis are selected in red.

3.16 Data Analysis

geNorm software was used to compute expression stability values for all reference targets. As input for geNorm analysis, Ct values were exported directly from QuantStudio3 software. geNorm calculated the gene expression stability measure (M-value) for a reference gene as the average pairwise variation V for that gene with all other tested reference genes. Stepwise exclusion of the gene with the highest M value allows ranking of the tested genes according to their expression stability. qPCR data were accomplished using comparative Ct method. Data were normalized to the most stable reference genes/ERE, determined by geNorm: cyclophilin A (CYPA) and *Orr1a0*.

3.17 L929 conditioned medium (LCM-enriched medium) production

L929 cell line (Merck Millipore, Cat# 85011425) derives from normal subcutaneous connective tissue of an adult C3H strain mouse. The conditioned medium of these cells contains high amounts of macrophage colony-stimulating factor (M-CSF) which activates microglia proliferation (Sawada *et al*., 1977). Therefore, the laboratories of Biomedical Research Institute (BIOMED, Hasselt University, Belgium) use this enriched medium to expand neonatal primary microglia.

Cells were thawed in 9 mL of pre-warmed complete DMEM (DMEM high glucose, 10% FBS, 1% Glutamine and 1% Penicillin/Streptomycin), spin down for 5 min at 1,200 rpm at RT and plate in T175 culture flasks with 25 mL complete DMEM. As L929 reached the confluence, they were split into three T175 culture flasks (1:3). 2-4 days after, they were split again into nine T175 culture flasks (1 flask into three, 1:3). 2-4 days after the second split, 15 mL pre-warmed complete DMEM was added in each flask to reach a final volume of 40 mL. Ten-to-eleven days after, L929 conditioned medium (LCM) was collected, filtered with a 0.2 µm filter, aliquoted and stored at -20ºC. Cells were frozen or used for a second collection of LCM. To proceed with a second collection of LCM, 40 mL complete DMEM were added in each flask and 10-11 days after, a second collection was performed (as described before). Cells cannot be used for a third LCM collection because the quality of the medium will decrease, and more cell debris will be present in the medium.

3.18 Culture of neonatal primary microglia

Neonatal primary microglia were prepared following the protocol set by the host laboratory with minor modifications. T25 or T75 flat bottomed flasks were coated with 1 mg/mL Poly-L-Lysine (PDL, Merck Millipore P7280-5 mg) diluted in PBS 1X and incubated at 37 ºC for, at least, 1 h. Postnatal mice (P0-P2) were decapitated, skin was cut from head to the tail and ribs were cut starting from the cervical side to the tail. The lumbar side of spinal cord was cut very near the start of the tail. A small syringe capped with a P20 tip and full of PBS 1X was used to flush out spinal cord and remove meninges. Spinal cords of, at least, 3 neonatal mice were pooled together in a 15 mL tube with cold and pure DMEM (without FBS, Glutamine and Penicillin/Streptomycin) and conserved in ice. A solution containing 1 mL Papain (20 Units/mL, Merck Millipore P4762-100MG) was supplemented by 40 µg/mL DNase and placed in the warm bath at 37 ºC. Meantime, the medium was removed from

spinal cords up to +/- 1mL on top of spinal cords, tissue was homogenized with a P1000 pipette and centrifuged at 300 x g for 5 min at RT. The pellet was resuspended in the Papain-DNase solution previously prepared and placed in the warm bath at 37 ºC for 20 min, by inverting the tube up and down every 5 min. Papain-DNase solution was inhibited by adding 9 mL cold and complete DMEM (DMEM high glucose, 1% Glutamine, 1% Penicillin/Streptomycin, 10% FBS) and cell suspension was centrifuged at 300 x g for 8 min at RT. Then, the supernatant was carefully removed, and the cell pellets were resuspended in 2 mL complete DMEM and gently passed through a 21 g needle few times to avoid having cell clumps. The PLL coating was removed from flasks and cells were plated in 10 mL pre-warmed complete DMEM. At day 4, 7, and 11 after plating the old medium was removed from flasks and replaced by the new medium supplemented with 1/3 LCM. At day 14 after plating, flasks containing mixed glial cells were placed in an orbital shaker for 2h at 37 °C and agitated at 200 rpm. Medium containing microglia was collected from flasks and centrifuged at 300 x g for 8 min at RT. Cell pellet was resuspended in complete DMEM supplemented by 15% of LCM-enriched medium. Cell counting was performed by diluting 10X a cells aliquot in Trypan Blue (Euroclone, Cat# ECM0990D) with Fuchs Rosenthal counting chamber. Cells were then seeded in PLL-pre-coated flasks (from 1-10 x 10^6 cells/T75 cm^2 flask) to expand microglia (for about one month) or in 24 well plate (5 x 10^4-2.5 x 10^5 cells/well) to proceed with immunofluorescence staining or RNA extraction (Figure 12).

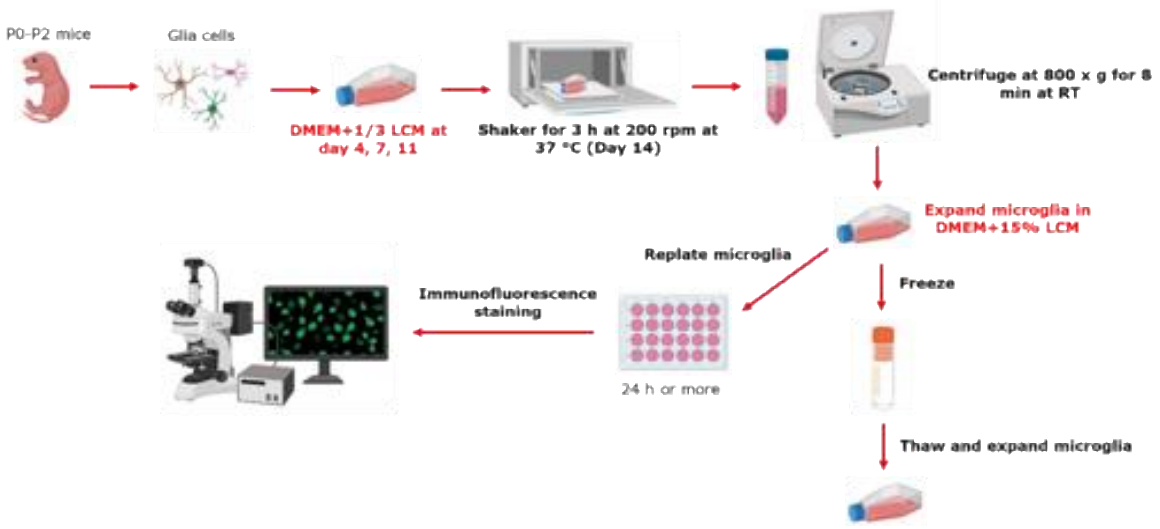

Fig. 12 Protocol to grow and expand neonatal microglia in culture (pictures were modified from BioRender).

3.19 Freezing and thawing of neonatal primary microglia and astrocytes

To freeze primary microglia and astrocytes, cells were detached as previously described in chapter 3.2. After Trypsin-EDTA inhibition with complete DMEM, microglia and astrocytes were centrifuged at 300 x g for 8 min at RT and cell pellets were resuspended in the cold freezing medium composed by 10% DMSO, 10% FBS and 80% pure DMEM. Cells were aliquot in 1 mL cryovials (at least 1 x 10^6 cells/cryovial), quickly stored in Mr. Frosty™ Freezing Container (Thermo Fisher Scientific, Cat# 5100-0001) and put at -80 ºC for 1-2 days. Then, the cryovials were transferred in liquid nitrogen.

To thaw primary microglia and astrocytes, cryovials containing cells were put in the warm bath at 37 °C until freezing medium was almost thawed. Cell suspension was transferred in 15 mL tubes, resuspended in 10 mL pre-warmed complete DMEM and centrifuged at 300 x g for 8 min at RT. Then, microglia pellet was resuspended in 5 mL complete DMEM supplemented by 15% LCM-enriched medium (astrocytes were cultured without LCM). Both glial cell types were plated in PLL- pre-coated T25 flasks and incubated at 37 °C in 5% CO_2 humified incubator. The day after microglia and astrocytes were attached and able to grow for weeks in culture.

3.20 Staining of neonatal primary microglia

To check the purity of microglia culture after thawing, cells were labelled with Ionized calcium-binding adaptor molecule 1 (IBA1, 1:500 rabbit anti-IBA1, Wako, Cat# 019-19741), a specific microglial marker, and for the astrocytic marker GFAP (1:200 goat anti-GFAP antibody, Santa-Cruz, Cat# sc-6170). As positive control primary microglia isolated from brain of P0-P2 mice and never frozen/thawed were stained for the same markers.
Microglia culture was also checked for purity after shaking from astrocytes by staining cells with the markers described above. In parallel, the same immunofluorescent labelling was performed for the spinal cord primary astrocytes to check the microglia yield still attached to the original flask.
Glass coverslips were washed first with 70% EtOH (1 time) and then with deionized H_2O (3 times) and PBS 1X (3 times). Then, coating was performed with 20 µg/mL PLL for 1 h at 37 °C, let completely dry under the sterile hood and put inside 24 well-plates. 2 x 10^5 microglia were seeded in each well by performing 80 µL droplet in the middle of the coverslip and incubated at 37 °C in 5% CO_2 humified incubator. As soon as microglia attached (30 min), complete DMEM was added in each well and immunofluorescence analyses were performed 24 h later. DMEM was removed from the cells and the coverslips were gently washed with PBS (3 times) and fixed with 4% PFA for 15 min at RT. After fixation, the coverslips were washed again with PBS (3 times) and blocked with PBS-Protein Blocker 20% (Protein Block Serum-Free Ready to Use, Dako, Cat#X0909) for 1 h at RT. Cells were then incubated overnight at 4 °C in the dark with primary antibodies (1:200 goat anti-GFAP antibody, Santa-Cruz, Cat# sc-6170 and 1:500 rabbit anti-IBA1 antibody, Wako, Cat# 019-19741) diluted in PBS-Protein Blocker 1% -Triton X-100-0.5%. The day after, cells were washed with PBS 1X (3 times x 10 min). Secondary antibodies (anti-rabbit in donkey-555, Thermo Fisher Scientific, Cat#A31572 and anti-goat in donkey-488, Thermo Fisher Scientific, Cat#A11055) were centrifuged at 5,000 rpm for 5 min to precipitate colour crystals, diluted 1:600 in PBS-PB 1% -Triton X-100-0.5% and incubated with cells for 1 h at RT. Cells were washed with PBS 1X (3 times x 5 min) and stained for DAPI for 15 min at RT. Then, after washing with PBS 1X, coverlips were reverse mounted on the mounting medium (Fluoromount-G™, Thermo Fisher Scientific, Cat# 00-4958-02) previously put on the microscope slides. Slides were let dried for few hours at RT in a dark box and then store

at 4 °C until analyses. Pictures were obtained with a fluorescent microscopy (Nikon eclipse 80i) using the 20X objective. Staining analyses were performed with ImageJ. Cells which were positive for IBA-1 or GFAP were counted manually.

4. RESULTS

4.1 Expression level of mGluR5 in WT, SOD1^{G93A} and SOD1^{G93A}Grm5$^{-/+}$ astrocytes

To verify the impact of the genetic reduction of mGluR5 the expression of the receptor was studied in WT, SOD1^{G93A} and SOD1^{G93A}Grm5$^{-/+}$ primary astrocytes. Cells were analysed by western blot (Figure 13) and RT-qPCR (Figure 14).

Western blot analysis evidentiated an overexpression of mGluR5 in SOD1^{G93A} astrocytes compared to WT astrocytes (401% increase; P<0.001, $F_{(2,6)}$= 252.791). SOD1^{G93A}Grm5$^{-/+}$ astrocytes showed a significative decrease of mGluR5 overexpression (48% decrease; P<0.001, $F_{(2,6)}$= 252.791); the latter was still significantly different compared to WT astrocytes (207% increase; P<0.001, $F_{(2,6)}$= 252.791). Figure 13 panel A shows a representative blot; panel B shows the quantification of mGluR5 changes.

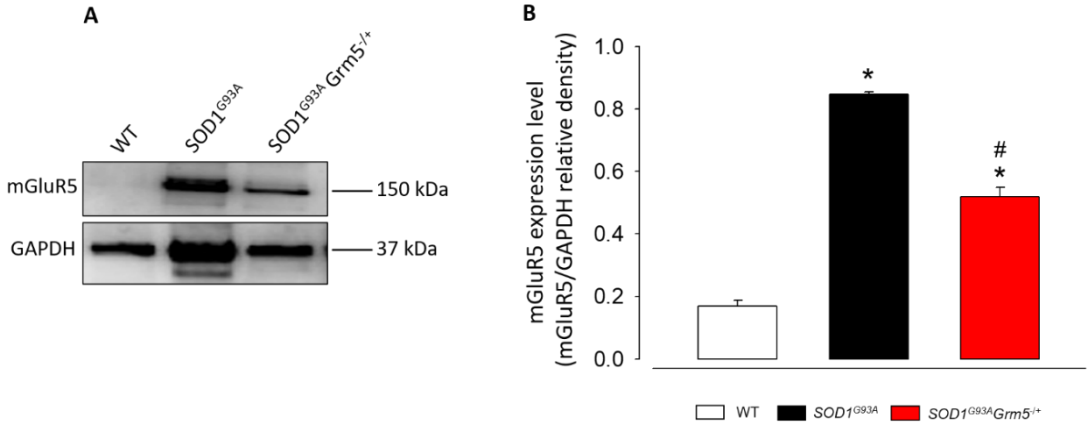

Fig. 13 Western blot quantification of mGluR5 expression in cell lysates from primary cultures of spinal cord astrocytes from WT, SOD1^{G93A} and SOD1^{G93A}Grm5$^{-/+}$ adult mice. (A) Representative immunoreactive bands for mGluR5 and GAPDH. (**B**) Quantification of protein expression as per scanned band density in WT, SOD1^{G93A}, and SOD1^{G93A}Grm5$^{-/+}$ astrocytes. Protein expression level was calculated as relative density, normalized to the housekeeping protein GAPDH. Data presented are means ± s.e.m of three independent experiments. *P<0.001 vs WT astrocytes; $^{\#}$P<0.001 vs SOD1^{G93A} astrocytes (One-way ANOVA followed by Bonferroni post hoc-test).

Data at the protein level were confirmed by qPCR experiments, that revealed the efficacy of the genetic ablation of mGluR5 in $Grm5^{-/+}$ and $SOD1^{G93A}Grm5^{-/+}$ astrocytes: mRNA expression of mGluR5 was significantly decreased in $Grm5^{-/+}$ astrocytes respect to WT astrocytes (47% decrease; $P<0.05$, $t_{(4)}= 8.309$) (Figure 14A) and the same was observed for double mutant astrocytes respect to $SOD1^{G93A}$ astrocytes (42% decrease; $P<0.01$, $t_{(4)}= 7.425$) (Figure 14B).

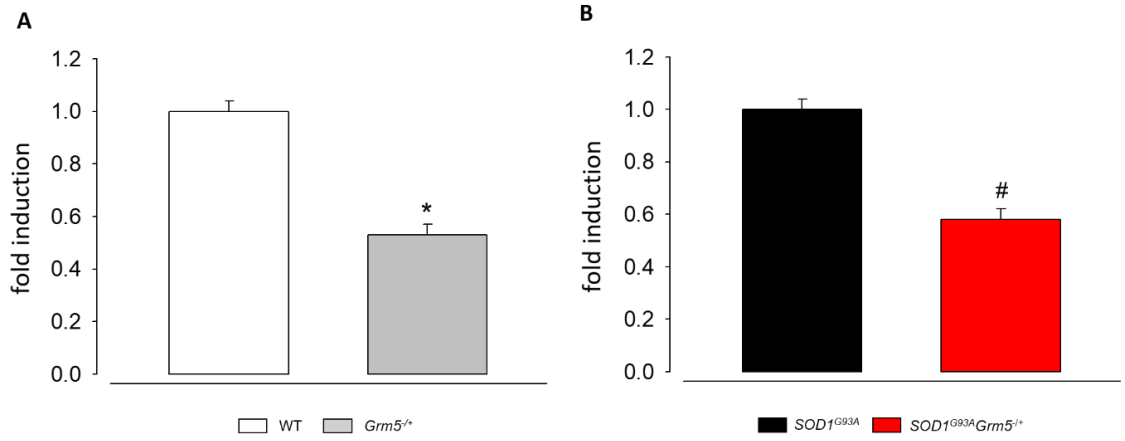

Fig. 14 RT-PCR quantification of mGluR5 mRNA in WT, $Grm5^{-/+}$, $SOD1^{G93A}$ and $SOD1^{G93A}Grm5^{-/+}$ astrocytes. (**A**) WT and $Grm5^{-/+}$ astrocytes; (**B**) $SOD1^{G93A}$ and $SOD1^{G93A}Grm5^{-/+}$ astrocytes. Data represent the mean ± s.e.m of three independent experiments run in triplicate. The mRNA expression of mGluR5 of WT and $SOD1^{G93A}$ astrocytes is reported as 1. $^{*}P<0.05$ vs WT astrocytes and $^{\#}P<0.01$ vs. $SOD1^{G93A}$ astrocytes (two-tailed Student's t-test).

4.2 Altered Ca^{2+} homeostasis in $SOD1^{G93A}$ primary astrocyte cultures is ameliorated in $SOD1^{G93A}Grm5^{-/+}$astrocytes

My group of research has previously showed that $[Ca^{2+}]_c$ was increased in the cytoplasm of spinal cord nerve terminals of $SOD1^{G93A}$ mice, both at pre-symptomatic and symptomatic stages of disease (Bonifacino *et al.*, 2016; Milanese *et al.*, 2011). Moreover, they demonstrated that knocking down mGluR5 in $SOD1^{G93A}$ mice significantly diminished the abnormal $[Ca^{2+}]_c$ both under basal and after 3,5-DHPG or KCl stimulation in spinal cord synaptosomes, suggesting that mGluR5 plays a key role in shaping intra-terminal $[Ca^{2+}]_c$ fluxes (Bonifacino *et al.*, 2017). Based on these results we here investigated whether the same effect could be seen in $SOD1^{G93A}Grm5^{-/+}$ astrocytes. $[Ca^{2+}]_c$ was measured in WT,

SOD1^{G93A} and SOD1^{G93A}Grm5$^{-/+}$ primary astrocytes by means of the fluorescent dye FURA-2/AM both under basal condition and after stimulus with 30 µM 3,5-DHPG.

$[Ca^{2+}]_c$ in WT astrocytes amounted to 153.78 nM under basal conditions. Basal $[Ca^{2+}]_c$ was almost doubled (81% increase) in SOD1^{G93A} astrocytes (279.08 nM; P <0.001, $F_{(2,30)}$= 127.623) compared to WT astrocytes. This elevated basal $[Ca^{2+}]_c$ was, in turn, significantly reduced (36% reduction) in SOD1^{G93A}Grm5$^{-/+}$ (234.59 nM; P<0.001, $F_{(2,30)}$= 127.623) respect to SOD1^{G93A} astrocytes but remained statistically higher compared to WT astrocytes (53% increase; P<0.001, $F_{(2,30)}$= 127.623) (Figure 15A).

The effects of the mixed mGluR1/5 agonist on $[Ca^{2+}]_c$ were then measured. Figure 15B shows the net increase of $[Ca^{2+}]_c$ over the basal level. Exposure to 30 µM 3,5-DHPG produced an increase of $[Ca^{2+}]_c$ of 206.33 nM in WT astrocytes. In SOD1^{G93A} astrocytes 3,5-DHPG stimulation enhanced $[Ca^{2+}]_c$ even to a greater extent (350.17 nM; 70% increase; P<0.001, $F_{(2,15)}$= 37.698) and this effect was significantly reduced in SOD1^{G93A}Grm5$^{-/+}$ astrocytes (288.67 nM; 43% decrease; P<0.01, $F_{(2,15)}$= 37.698) vs. SOD1^{G93A} astrocytes. Additionally, the 3,5-DHPG $[Ca^{2+}]_c$ in SOD1^{G93A}Grm5$^{-/+}$ astrocytes was statistically more elevated than in WT astrocytes (40% increase, P<0.001, $F_{(2,15)}$= 37.698).

These results indicate that $[Ca^{2+}]_c$, which is constitutively higher in SOD1^{G93A} astrocytes, is reduced by reducing mGluR5 expression.

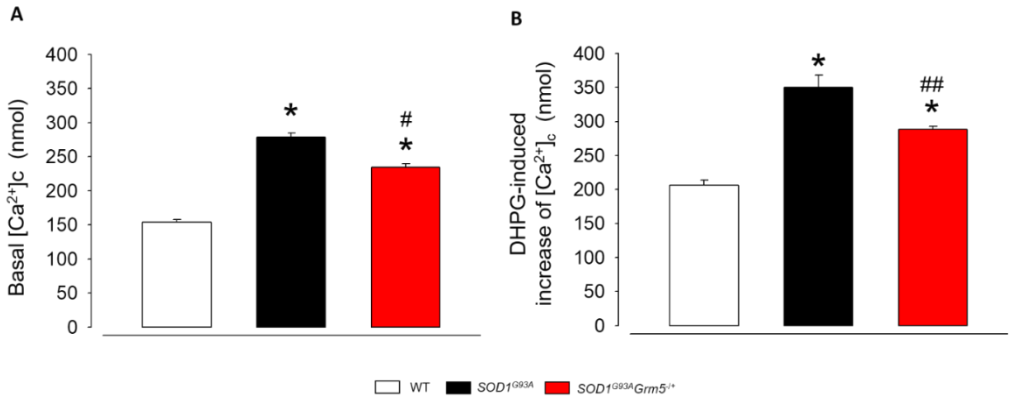

Fig. 15 $[Ca^{2+}]_C$ under basal condition (A) and after stimulation with the mGluR1/5 agonist 3,5-DHPG (30 µM) (B) in primary spinal cord astrocyte cultures of WT, SOD1^{G93A} and SOD1^{G93A}Grm5$^{-/+}$ astrocytes. $[Ca^{2+}]_C$ was determined by labelling astrocytes with the fluorescent dye Fura2-AM. Results are expressed as nM concentration of Ca^{2+}. Results represent the average ± s.e.m. of six independent experiments carried in triplicate *P<0.001 vs WT; $^{\#}$P<0.001 and $^{\#\#}$P<0.01 vs SOD1^{G93A} (One-way ANOVA followed by Bonferroni post hoc-test).

4.3 Knocking down mGluR5 reduces astrogliosis in SOD1^{G93A}Grm5$^{-/+}$ astrocytes

Astrogliosis is a key feature of ALS (Rossi *et al*., 2008, Lasiene and Yamanaka, 2011), often characterized by overexpression of GFAP and S100β proteins (Benninger *et al*., 2016). Accordingly, the mis-regulated expression of these two markers is related to the reactive and proliferative state of astrocytes in ALS (Schiffer *et al*., 1996).

Here, the expression of GFAP and S100β was quantified in WT, SOD1^{G93A} and SOD1^{G93A}Grm5$^{-/+}$ astrocytes by western blot (Figure 16) and immunocytochemical analysis (Figure 17).

A representative WB of the expression of GFAP and S100β in WT, SOD1^{G93A} and SOD1^{G93A}Grm5$^{-/+}$ astrocytes is shown in Figure 16A. Western blot analysis showed that GFAP was significantly upregulated in SOD1^{G93A} astrocytes compared to WT astrocytes (440% increase; $P<0.001$, $F_{(2,6)}= 412.059$) (Figure 16B). Figure 16B also shows that knocking down mGluR5 significantly reduced the overexpression of GFAP (20% decrease; $P<0.01$, $F_{(2,6)}= 412.059$); although a significant upregulation was still present respect to WT astrocytes (352% increase; $P<0.001$, $F_{(2,6)}= 412.059$).

S100β was also significantly upregulated in SOD1^{G93A} astrocytes (262% increase; $P<0.001$, $F_{(2,6)}= 59.016$) and the overexpression was abolished in SOD1^{G93A}Grm5$^{-/+}$ astrocytes (100% decrease; $P<0.001$, $F_{(2,6)}= 59.016$) (Figure 16C).

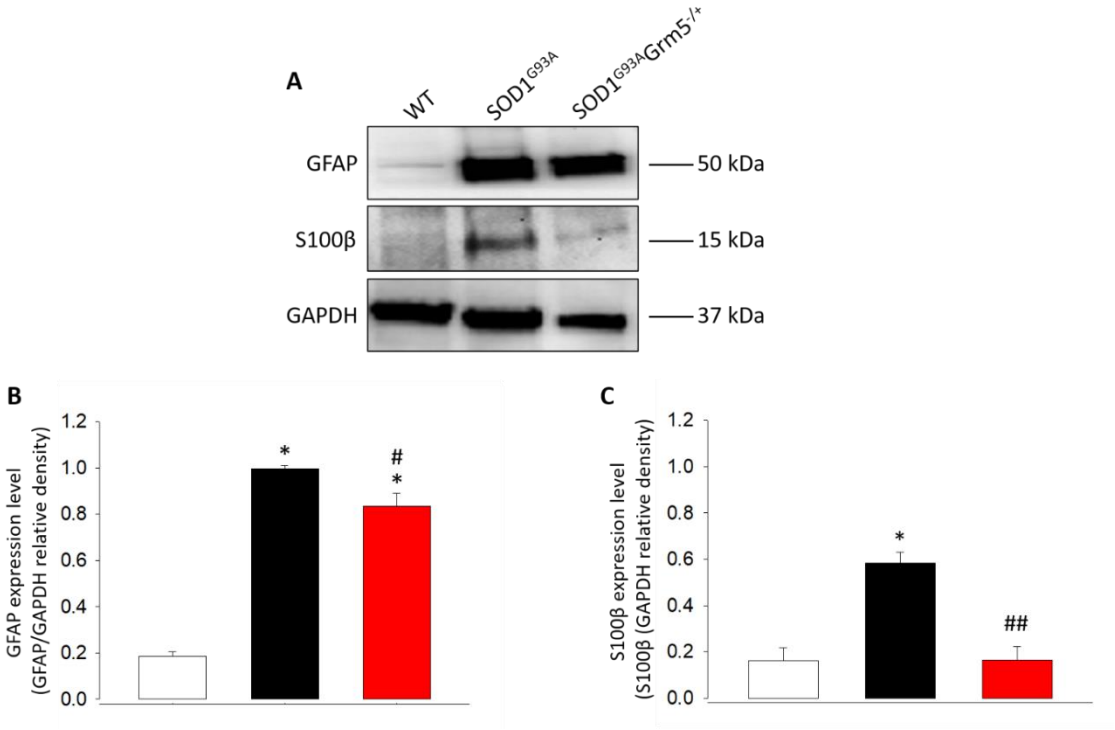

Fig. 16 Western blot quantification of GFAP and S100β expression in cell lysates from primary cultures of spinal cord astrocytes from WT, SOD1^{G93A} and SOD1^{G93A}Grm5$^{-/+}$ adult mice. (A) Representative immunoreactive bands for GFAP, S100β, and GAPDH; (**B**, **C**) Quantification of protein expression as per scanned band density in WT, SOD1^{G93A}, and SOD1^{G93A}Grm5$^{-/+}$ astrocytes. Protein expression level was calculated as relative density, normalized to the housekeeping protein GAPDH. Data presented are means ± s.e.m of three independent experiments. *P<0.001 vs. WT astrocytes; $^{\#}$P<0.01 and $^{\#\#}$P<0.001 vs. SOD1^{G93A} astrocytes (One-way ANOVA followed by Bonferroni post hoc-test).

The same GFAP and S100β expression trend was confirmed by immunocytochemical analysis. Accordingly, Figure 17A shows representative immunocytochemical images of GAPDH (red) and GFAP (green) expression and co-localization (yellow) in WT, SOD1^{G93A} and SOD1^{G93A}Grm5$^{-/+}$ astrocytes). Quantization of immunocytochemical images revealed that the expression of GFAP in SOD1^{G93A} astrocytes was augmented compared to WT astrocytes (82% increase; P<0.001, $t_{(4)}$= -18.336), while SOD1^{G93A}Grm5$^{-/+}$ astrocytes displayed a significantly reduced level of the protein (50% decrease; P<0.01, $t_{(4)}$= 7.248) being the residual overexpression still significantly different from WT astrocytes (41% increase; P<0.001, $t_{(4)}$= -9.168) (Figure 17B).

Figure 17 C shows representative immunocytochemical images of GAPDH (red) and S100β (green) expression and co-localization (yellow) in WT, SOD1^{G93A} and SOD1^{G93A}Grm5$^{-/+}$

astrocytes. As shown in Figure 17D, also the S100β level was upregulated in SOD1^{G93A} astrocytes (32% increase; $P<0.01$, $t_{(4)}= -5.261$), and its overexpression was reduced in double mutant astrocytes (72% decrease; $P<0.05$, $t_{(4)}= 3.190$).

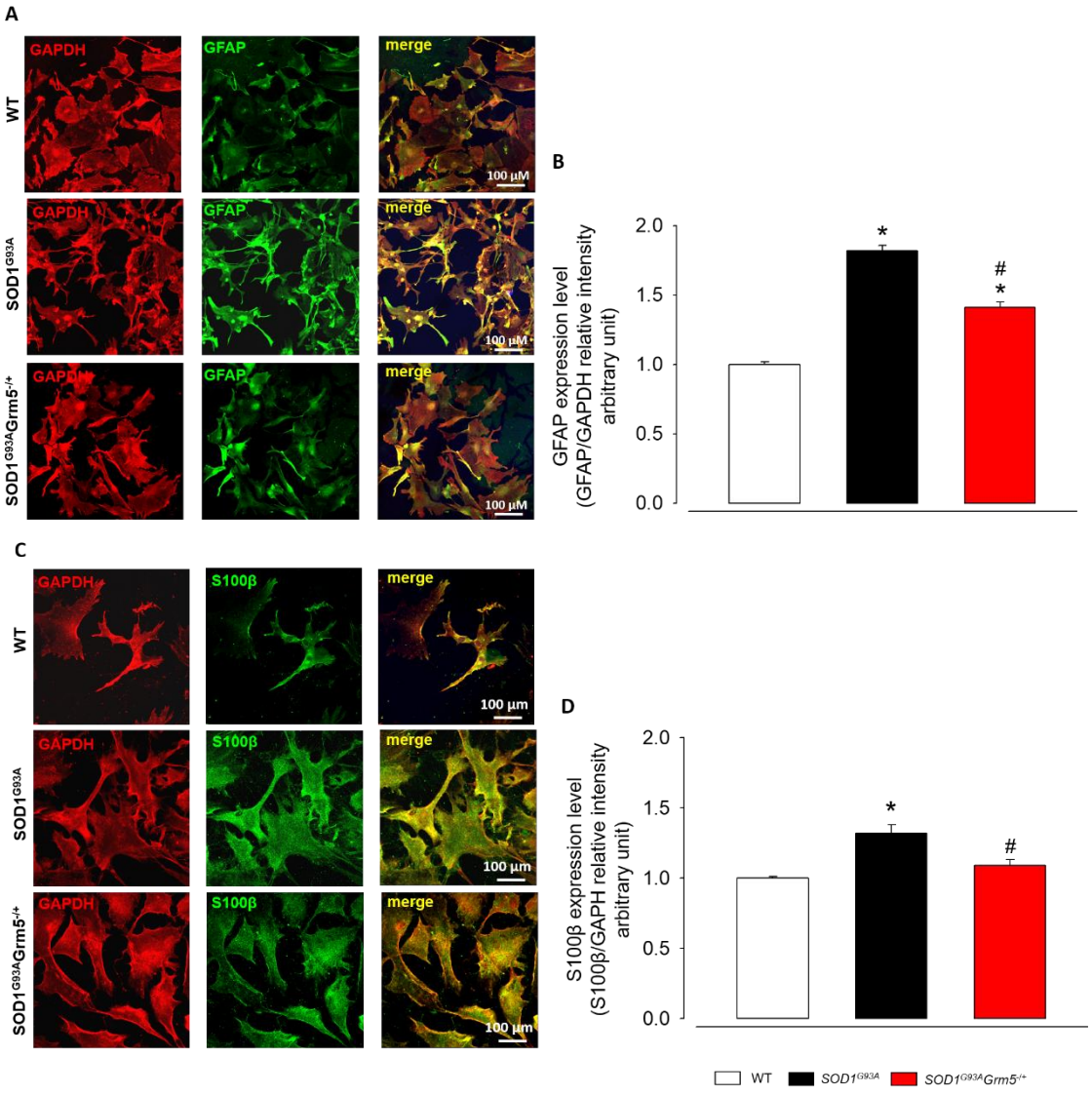

Fig. 17 Immunocytochemical quantification of GFAP and S100β expression in primary cultures of spinal cord astrocytes from WT, SOD1^{G93A} and SOD1^{G93A}Grm5$^{-/+}$ adult mice. (A) Representative confocal microscopy immunocytochemical images of GFAP (green) and GAPDH (red), (**C**) S100β (green) and GAPDH (red) in WT, SOD1^{G93A} and SOD1^{G93A}Grm5$^{-/+}$ astrocytes cultured on coverslip and labelled with the appropriate primary and secondary antibodies. The merge panels represent the co-expression of GFAP and GAPDH, or of S100β and GAPDH, respectively. Scale bar: 100 µm. (**B, D**) Quantification of protein expression, as per relative fluorescence intensity, was performed calculating the co-localization coefficients (Manders *et al*., 1992) using Image-J software analyses. Data are expressed as relative fluorescence intensity of GFAP or S100β normalized respect to the fluorescence intensity of the housekeeping protein GAPDH. The relative intensity of control WT astrocytes is reported as 1. Data presented are means ± s.e.m of three independent experiments run in triplicate (three different coverslips for each experimental condition); statistical analysis was performed by one-way ANOVA followed by Bonferroni post hoc-test. *P<0.001 vs. WT astrocytes; $^{\#}$P<0.01 vs. SOD1^{G93A} astrocytes.

4.4 Dampening mGluR5 normalizes NLRP3 inflammasome overexpression in SOD1^{G93A}Grm5$^{-/+}$astrocytes

NLRP3 is a protein complex strictly related to inflammation. Its assembly determines the cleavage of IL-1β and IL-18 through caspase-1 and the subsequently conversion of these cytokines into their active form, exacerbating neuroinflammation and inducing cell apoptosis and necroptosis (Mangan *et al*., 2018).

We here investigated NLRP3 expression in WT, SOD1^{G93A} and SOD1^{G93A}Grm5$^{-/+}$ astrocytes by western blot. Figure 18A shows a representative WB. Protein expression quantification is illustrated in Figure 18B and highlighted the higher levels of NLRP3 in SOD1^{G93A} astrocytes respect to WT astrocytes (393% increase; P<0.001, $F_{(2,6)}$=50.653). Conversely, SOD1^{G93A}Grm5$^{-/+}$ astrocytes revealed a lower expression of NLRP3 compared to SOD1^{G93A} astrocytes (34% decrease; P<0.05, $F_{(2,6)}$=50.653). However, the partial deletion of mGluR5 did not completely reverse the NLRP3 overexpression of SOD1^{G93A}Grm5$^{-/+}$ astrocytes compared to WT astrocytes (260% increase; P<0.01, $F_{(2,6)}$=50.653) (Figure 18B).

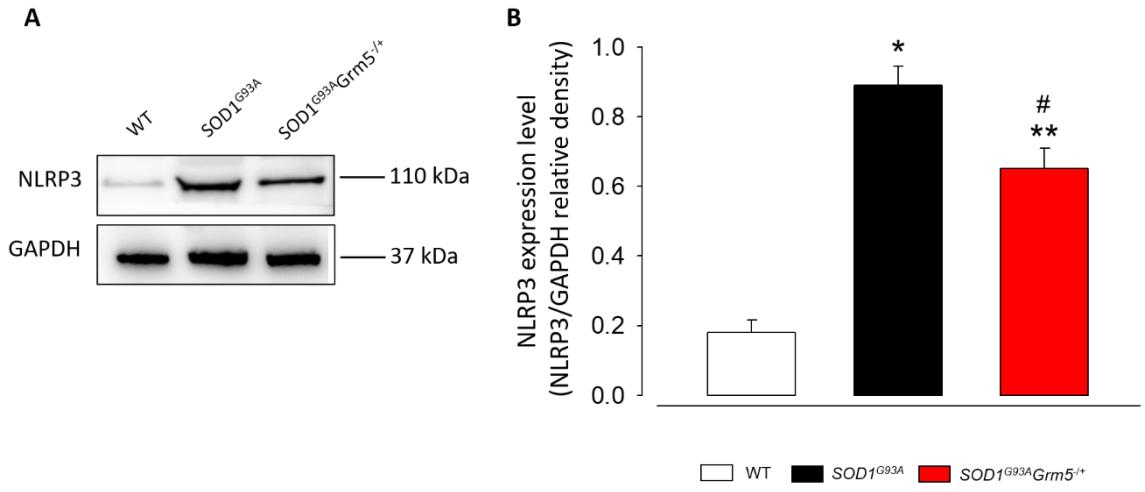

Fig. 18 Western blot quantification of NLRP3 in cell lysates of primary cultures of spinal cord astrocytes from WT, SOD1^{G93A} and SOD1^{G93A}Grm5$^{-/+}$ adult mice. (A) Representative immunoreactive bands for NLRP3 and GAPDH; (**B**) Quantification of protein expression as per scanned band density in WT, SOD1^{G93A}, and SOD1^{G93A}Grm5$^{-/+}$ astrocytes. Protein expression level was calculated as relative density, normalized to the housekeeping protein GAPDH. Data presented are means ± s.e.m of three independent experiments. *P<0.001 and **P<0.01 vs WT astrocytes, $^{\#}$P<0.05 vs SOD1^{G93A} astrocytes (One-way ANOVA followed by Bonferroni post hoc-test).

4.5 The partial ablation of mGluR5 reduces the misfolded SOD1 level in SOD1^{G93A}Grm5$^{-/+}$astrocytes

Because of the importance of SOD1 during ALS development, especially in our mouse model of the disease, and due to the well demonstrated presence of misfolded proteins in ALS astrocytes (Forsberg *et al*., 2011), the misfolded SOD1 level was evaluated in WT, SOD1^{G93A} and SOD1^{G93A}Grm5$^{-/+}$ astrocytes with western blot (Figure 19) and immunocytochemical analysis (Figure 20).

Figure 19A displays a representative WB of misfolded SOD1 in WT, SOD1^{G93A} and SOD1^{G93A}Grm5$^{-/+}$ astrocytes. -Figure 19B shows that misfolded SOD1 level in SOD1^{G93A} astrocytes was dramatically increased respect to WT astrocytes (800% increase; P<0.001, $F_{(2,6)}$= 111.361), confirming the results of literature. Conversely, SOD1^{G93A}Grm5$^{-/+}$ astrocytes displayed a significative reduction of misfolded SOD1 expression (65% decrease; P<0.001, $F_{(2,6)}$= 111). The overexpression of the misfolded protein was not completely reversed by knocking down mGluR5 in SOD1^{G93A} astrocytes (278% increase; P<0.01, $F_{(2,6)}$= 111.361) (Figure 19B).

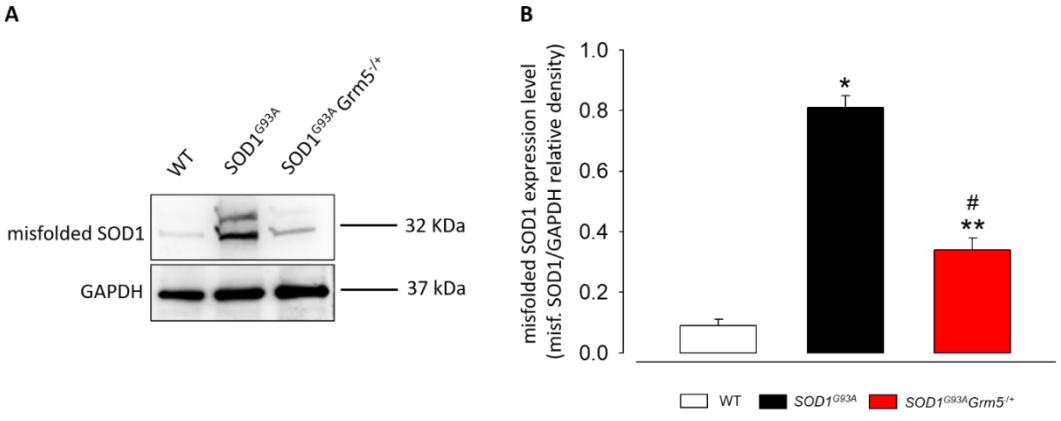

Fig. 19 Western blot quantification of misfolded SOD1 in cell lysates of primary cultures of spinal cord astrocytes from WT, SOD1^{G93A} and SOD1^{G93A}Grm5$^{-/+}$ adult mice. (A) Representative immunoreactive bands for misfolded SOD1 and GAPDH; (**B**) Quantification of protein expression as per scanned band density in WT, SOD1^{G93A}, and SOD1^{G93A}Grm5$^{-/+}$ astrocytes. Protein expression level was calculated as relative density, normalized to the housekeeping protein GAPDH. Data presented are means ± s.e.m of three independent experiments. *P<0.001 and **P<0.01 vs WT astrocytes, $^{\#}$P<0.001 vs SOD1^{G93A} astrocytes (One-way ANOVA followed by Bonferroni post hoc-test).

Figure 20 reports the immunocytochemical analysis of misfolded SOD1 expression. Figure 20A shows representative immunocytochemical images of GAPDH (red) and misfolded SOD1 (green) expression and co-localization (yellow) in WT, $SOD1^{G93A}$ and $SOD1^{G93A}Grm5^{-/+}$ astrocytes. In accordance to western blot results, $SOD1^{G93A}$ astrocytes displayed an overexpression of misfolded SOD1 compared to WT astrocytes (114% increase; $P<0.001$, $F_{(2,6)}= 45.685$), whereas a significant reduction of the misfolded protein was detected in $SOD1^{G93A}Grm5^{-/+}$ astrocytes (60% decrease; $P<0.01$, $F_{(2,6)}= 45.685$) (Figure 20B). Also in this case, however, the protein expression level was still statistically different from WT astrocytes (46% increase; $P<0.05$, $F_{(2,6)}= 45.685$).

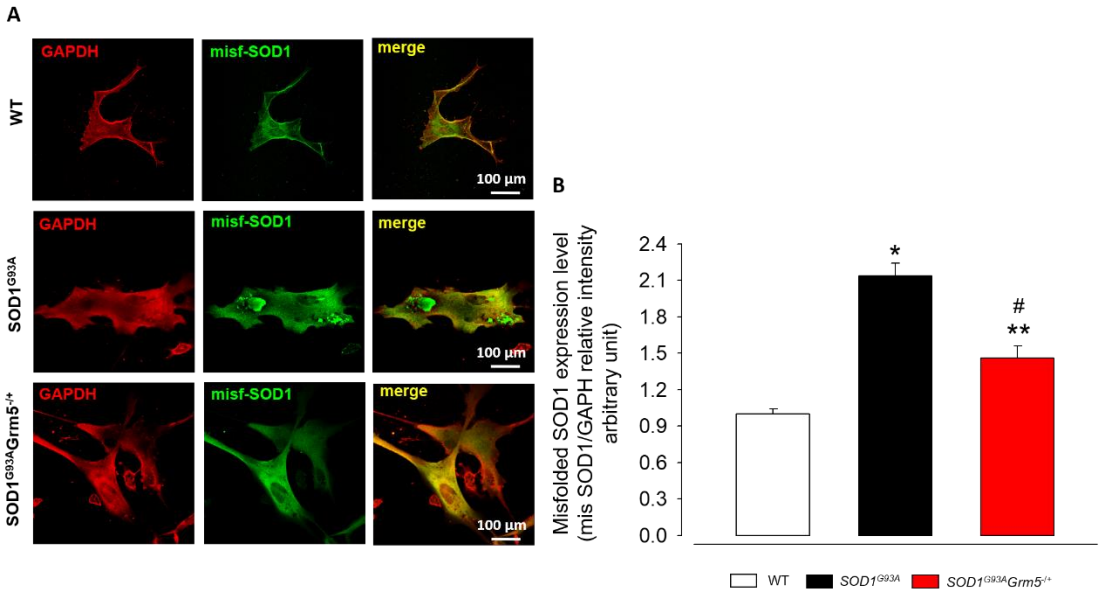

Fig. 20 Immunocytochemical quantification of misfolded SOD1 expression in primary cultures of spinal cord astrocytes from WT, $SOD1^{G93A}$ and $SOD1^{G93A}Grm5^{-/+}$ adult mice. (**A**) Representative confocal microscopy immunocytochemical images of misfolded SOD1 (green) and GAPDH (red), in WT, $SOD1^{G93A}$ and $SOD1^{G93A}Grm5^{-/+}$ astrocytes. cultured on coverslip and labelled with the appropriate primary and secondary antibodies. The merge panels represent the co-expression of misfolded SOD1 and GAPDH. Scale bar: 100 µm. (**B**) Quantification of protein expression, as per relative fluorescence intensity, was performed calculating the co-localization coefficients (Manders *et al.*, 1992) using Image-J software analyses. Data are expressed as relative fluorescence intensity of misfolded SOD1normalized respect to the fluorescence intensity of the housekeeping protein GAPDH. The relative intensity of control WT astrocytes is reported as 1. Data presented are means ± s.e.m of three independent experiments run in triplicate (three different coverslips for each experimental condition); statistical analysis was performed by one-way ANOVA followed by Bonferroni post hoc-test. *$P<0.01$ and *$P< 0.05$ vs. WT astrocytes; $^{\#}P<0.01$ vs. $SOD1^{G93A}$ astrocytes.

4.6 The LC3 expression was decreased after the partial ablation of mGluR5 in SOD1^{G93A}Grm5$^{-/+}$astrocytes

LC3 is one of the main protein markers of autophagy in eukaryotes. It is processed to LC3-I in the cytosol and converted to LC3-II which is recruited to autophagosomal membranes during the autophagosomes formation (Kabeya *et al.*, 2000; Munz, 2006). Therefore, the amount of LC3-II is indicative of the extent of autophagosomes formation and is often used both *in-vitro* and *in-vivo* to detect neuron damage and repair assessment (Mizushima, 2004; Rubinsztein *et al*., 2005).

Due to the important role of LC3 in SOD1^{G93A} mouse model, its expression in SOD1^{G93A} astrocytes and the modifications in SOD1^{G93A}Grm5$^{-/+}$ astrocytes was here investigated, by western blot and immunocytochemical analyses (Figure 21).

Figure 21A displays a representative western blot showing the bands of LC3-I and LC3-II in WT, SOD1^{G93A} and SOD1^{G93A}Grm5$^{-/+}$ astrocytes. Figure 21B shows that the LC3 total expression was increased in SOD1^{G93A} astrocytes respect to WT astrocytes (95% increase; $P<0.001$, $t_{(4)}= -17.964$). SOD1^{G93A}Grm5$^{-/+}$astrocytes displayed a decrease of the protein expression (27% decrease; $P<0.05$, $t_{(4)}= 4.584$). However, this latter significantly differed from WT astrocytes (69% increase; $P<0.001$, $t_{(4)}= -9.198$) (Figure 21B).

The expression level of the specific LC3-II isoform was quantified in Figure 21C. The results obtained outlined the tendency to a reduction of the LC3-II/LC3-I ratio in SOD1^{G93A} astrocytes and a reversion of this occurrence in SOD1^{G93A}Grm5$^{-/+}$ astrocytes. Unexpectedly, these results are not in line with the data of the literature, but it should be outlined that the differences observed were not statistically significant.

Immunocytochemical analysis confirmed the results obtained with WB, as to the expression of total LC3. Figure 21D reports representative immunocytochemical images of GAPDH (red) and LC3 (green) expression and co-localization (yellow) in WT, SOD1^{G93A} and SOD1^{G93A}Grm5$^{-/+}$ astrocytes. The quantization of the protein expression is reported in Figure 21E and shows that SOD1^{G93A} astrocytes expressed a higher level of LC3 respect to WT astrocytes (63% increase; $P<0.001$, $F_{(2,6)}= 83.528$). Conversely, SOD1^{G93A}Grm5$^{-/+}$ astrocytes displayed a significant reduction of the autophagic protein expression (41% decrease; $P<0.01$, $F_{(2,6)}= 83.528$), The expression of LC3 was still significantly higher than in WT astrocytes (37% increase; $P<0.001$, $F_{(2,6)}= 83.528$).

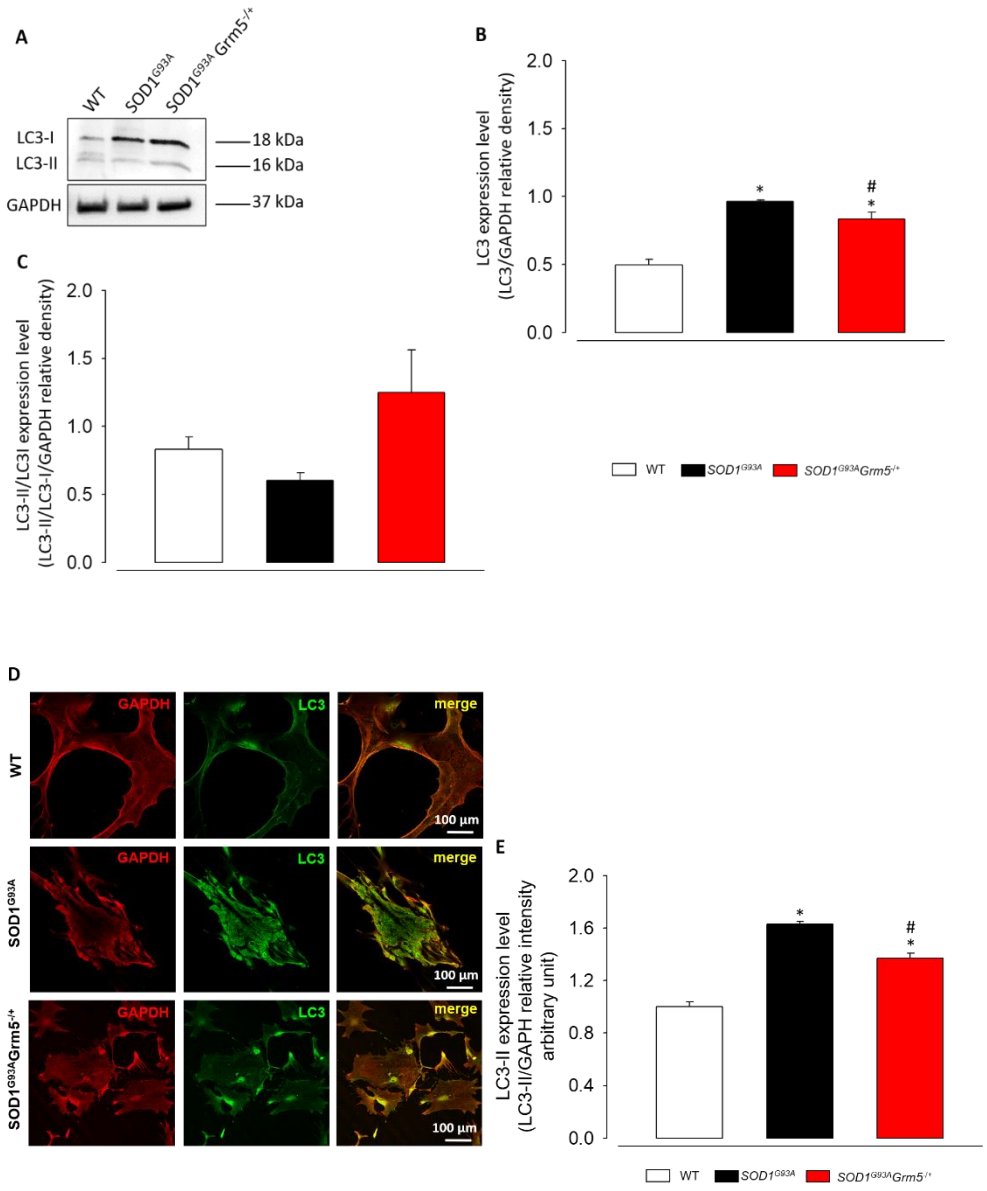

Fig. 21 Western blot and immunocytochemical quantification of LC3 in primary cultures of spinal cord astrocytes from WT, SOD1^{G93A} and SOD1^{G93A}Grm5$^{-/+}$ adult mice. (**A**) Representative immunoreactive bands for LC3-I, LC3-II and GAPDH in cell lysate from WT, SOD1^{G93A} and SOD1^{G93A}Grm5$^{-/+}$ astrocytes; (**B**) Quantification of total protein expression and (**C**) of specific LC3-II form as per scanned band density in WT, SOD1^{G93A}, and SOD1^{G93A}Grm5$^{-/+}$ astrocytes. Protein expression level was calculated as relative density, normalized to the housekeeping protein GAPDH. Data presented are means ± s.e.m of three independent experiments. *P<0.001 vs. WT astrocytes, $^{\#}$P<0.05 vs. SOD1^{G93A} astrocytes (two-tailed Student's t-test). (**D**) Representative confocal microscopy immunocytochemical images of LC3 (green) and GAPDH (red) in WT, SOD1^{G93A} and SOD1^{G93A}Grm5$^{-/+}$ astrocytes cultured on coverslip and labelled with the appropriate primary and secondary antibodies. The merge panels represent the co-expression of LC3 and GAPDH. Scale bar: 100 µm. (**E**) Quantification of protein expression, as per relative fluorescence intensity, was performed calculating the co-localization coefficients (Manders *et al.*, 1992) using Image-J software analyses. Data are expressed as relative fluorescence intensity of LC3 normalized respect to the fluorescence intensity of the housekeeping protein GAPDH. The relative intensity of control WT astrocytes is reported as 1. Data presented are means ± s.e.m of three independent experiments run in triplicate (three different coverslips for each experimental condition); statistical analysis was performed by one-way ANOVA followed by Bonferroni post hoc-test. *P<0.001 vs. WT astrocytes; $^{\#}$P<0.01 vs. SOD1^{G93A} astrocytes.

4.7 Effects of partial deletion of mGluR5 on energy metabolism of SOD1^{G93A} astrocytes

Since is known that ALS is associated with altered mitochondrial aerobic metabolism (Tefera *et al*., 2016), we assayed the OCR and the ATP synthesis by the Fo-F1 ATP synthase in WT, SOD1^{G93A}, and SOD1^{G93A}Grm5$^{-/+}$ astrocytes.

Figure 22 shows that SOD1^{G93A} astrocytes displayed a significant reduction of the OCR, in presence of pyruvate/malate (48% decrease; P<0.01, $t_{(4)}$= 4.697) or succinate (61% decrease; P<0.01, $t_{(4)}$= 7.034), as respiration substrates, in comparison to WT astrocytes. This alteration was partially reverted in SOD1^{G93A}Grm5$^{-/+}$ astrocytes, but only when the respiration was stimulated by pyruvate/malate (57% increase; P<0.05, $t_{(4)}$= -2.791) (Figure 22), the substrates that activate the pathway involving Complexes I, III, and IV.

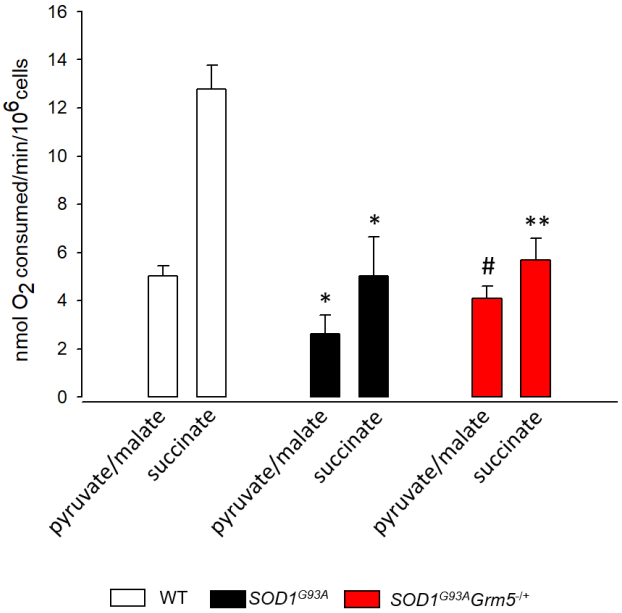

Fig 22 Effect of mGluR5 downregulation on oxygen consumption rate of astrocytes. After permeabilization with 0.03% digitonin, WT, SOD1^{G93A} and SOD1^{G93A}Grm5$^{-/+}$ astrocytes were resuspended in a respiration medium and stimulated with pyruvate (10 mM) + malate (5 mM) and ADP (0.1 mM) to study the Complexes I, III, IV, or with succinate (20 mM) and ADP (0.1mM) to investigate the activity of Complexes II, III, IV. The respiratory rates were expressed as nmol O_2/min/10^6 cells. Data represent the means ± s.e.m of three independent experiments. *P<0.01 and **P<0.001 vs. WT astrocytes; $^{\#}$P<0.05 vs. SOD1^{G93A} astrocytes (two-tailed Student's t-test).

A similar trend was observed in Figure 23, in which the aerobic ATP synthesis results are represented. Accordingly, SOD1^{G93A} astrocytes displayed a significant reduction of the ATP production in presence of pyruvate/malate (72% decrease; P<0.001, $t_{(4)}$= 15.534) or succinate (79% decrease; P<0.001, $t_{(4)}$= 14.937) in comparison to WT astrocytes (Figure 23). This alteration was partially reverted in SOD1^{G93A}Grm5$^{-/+}$ astrocytes both after stimulation with pyruvate/malate (143% increase; P<0.01, $t_{(4)}$= -6.197), and with succinate (107% increase; P<0.05, $t_{(4)}$= -4.223), which stimulates the energy production through the pathway involving -Complex II.

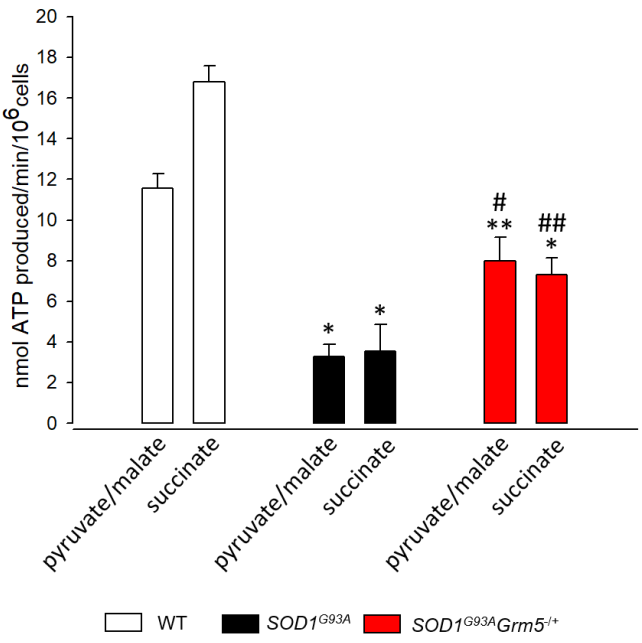

Fig. 23 Effect of mGluR5 downregulation on ATP synthesis by astrocytes. The activity of F0-F1 ATP synthase was evaluated in WT, SOD1^{G93A} and SOD1^{G93A}Grm5$^{-/+}$ astrocytes after stimulation with pyruvate (10 mM) and malate (5 mM) or with succinate (20 mM). Data were expressed as nmol ATP produced/min/10^6 cells and represented the means ± s.e.m of three independent experiments. *P<0.001 and **P<0.05 vs. WT astrocytes; $^{\#}$P<0.01 and $^{\#\#}$P<0.05 vs. SOD1^{G93A} astrocytes (two-tailed Student's t-test).

In Figure 24 it is represented the oxidative phosphorylation efficiency, in terms of P/O values. Interestingly, we observed that WT and SOD1^{G93A}Grm5$^{-/+}$ astrocytes displayed similar values to the maximal efficiency for both respiratory pathways. Conversely, SOD1^{G93A} astrocytes were characterized by very low P/O values (Figure 24).

SOD1^{G93A} astrocytes showed a significative reduction of the OxPhos efficiency respect to WT astrocytes, both after stimulus with pyruvate/malate (46% decrease; P<0.01, $t_{(4)}$= 5.582), and with succinate (46% decrease P<0.05, $t_{(4)}$= 3.585) (Figure 24). Conversely, these values were significantly increased in SOD1^{G93A}Grm5$^{-/+}$ respect to SOD1^{G93A} astrocytes, but only after the pyruvate/malate stimulus (55% increase; P<0.05, $t_{(4)}$= -3.831), while the reversion of P/O observed after the succinate stimulation did not reach the statistical significance (Figure 24). However, the values of oxidative phosphorylation efficiency displayed similar values in WT and SOD1^{G93A}Grm5$^{-/+}$ astrocytes also in the case of succinate.

This analysis suggests that the ALS samples are characterized by the uncoupling between oxygen consumption and ATP synthesis, which is reverted by the partial reduction of mGluR5.

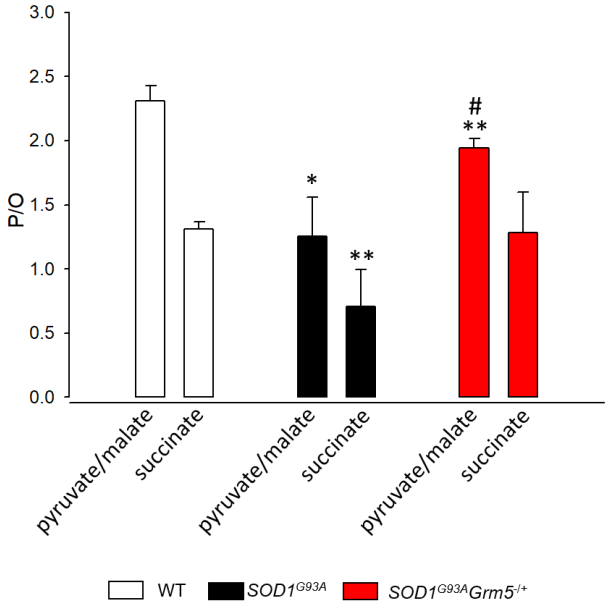

Fig. 24 Effect of mGluR5 downregulation on the oxidative phosphorylation efficiency in WT, SOD1^{G93A} and SOD1^{G93A}Grm5$^{-/+}$ astrocytes. The P/O was calculated in WT, SOD1^{G93A} and SOD1^{G93A}Grm5$^{-/+}$ astrocytes as the ratio between the concentration of the produced ATP (P) and the amount of consumed oxygen (O) in the presence of pyruvate (10 mM) + malate (5 mM) or succinate (20 mM) and ADP (0.1 mM). Data represent the means ± s.e.m of three independent experiments. *P<0.01 and **P<0.05 vs. WT astrocytes; $^{\#}$P<0.05 vs. SOD1^{G93A} astrocytes (two-tailed Student's t-test).

In addition to these results, Figure 25 shows the glucose consumption and the lactate release of WT, SOD1^{G93A} and SOD1^{G93A}Grm5$^{-/+}$ astrocytes. Figure 25A shows that lactate content was augmented in the culture medium of SOD^{G93A} compared to WT astrocytes (72% increase; P<0.01, $F_{(2,6)}$= 21.453). SOD1^{G93A}Grm5$^{-/+}$ astrocytes, instead, were characterized by decreased lactate release (79% decrease; P<0.01, $F_{(2,6)}$= 21.453) which reached the WT levels.

Conversely, a similar glucose culture medium content was measured in all the astrocyte genotypes (Figure 25B).

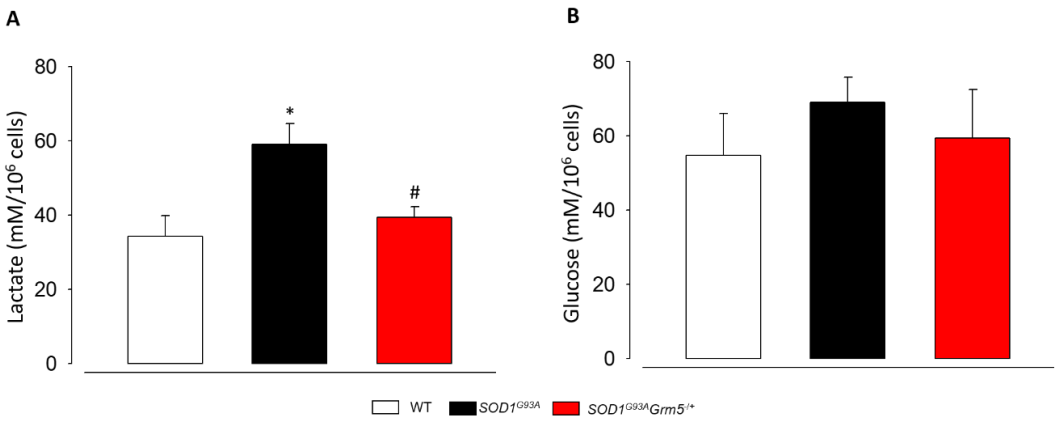

Fig. 25 Effects of mGluR5 downregulation on lactate and glucose consumption in astrocytes. (**A**) Lactate e and (**B**) glucose concentrations were assayed spectrophotometrically in the culture medium of WT, SOD1^{G93A} and SOD1^{G93A}Grm5$^{-/+}$ astrocytes. Data are expressed as mM per 10^6 cells and are means ± s.e.m of three independent experiments. *P<0.01 vs. WT astrocytes; $^{\#}$P<0.01 vs. SOD1^{G93A} astrocytes (One-way ANOVA followed by Bonferroni post hoc-test).

4.8 The overexpression and the abnormal release of pro-inflammatory cytokines in SOD1^{G93A} astrocytes are partially rescued by knocking down mGluR5

Astrocytes secrete various pro-inflammatory cytokines. A dysregulation of cytokine production and secretion has been observed in several neurodegenerative diseases, including in ALS (Farina *et al*., 2007; Holden, 2007). To verify the possible modulation of the pro-

inflammatory phenotype of SOD1^{G93A} astrocytes exerted by the knock-down of mGluR5, it was analysed the expression and release of IL-1β, TNF-α and IL-6 by western blot (Figure 26) and ELISA assay (Figure 27), respectively.

Figure 26 panel A shows a representative western blot of IL-1β, TNF-α and IL-6 in WT, SOD1^{G93A} and SOD1^{G93A}Grm5$^{-/+}$ astrocytes. Figure 26B quantify the expression level of IL-1β which was dramatically increased in SOD1^{G93A} compared to WT astrocytes (1667% increase, $P<0.001$, $F_{(2,6)}= 68.838$). Conversely, SOD1^{G93A}Grm5$^{-/+}$ astrocytes showed a significant reduction of IL-1β (44% decrease; $P<0.01$, $F_{(2,6)}=68.838$) (Figure 26 panel B), even if this level significantly differs from WT (940% increase; $P<0.01$, $F_{(2,6)}=68.838$).

Similar results were observed in Figure 26C as to TNF-α expression: SOD1^{G93A} astrocytes displayed a high increase of the cytokine expression compared to WT cells (395% increase, $P<0.001$, $F_{(2,6)}= 105.741$), while double mutant astrocytes showed a significantly decreased expression (27% decrease; $P<0.05$, $F_{(2,6)}= 105.741$) (Figure 26C). TNF-α expression level persisted higher than in WT astrocytes (288% increase; $P<0.001$, $F_{(2,6)}= 105.741$) (Figure 26C).

Last, Figure 26D shows IL-6 quantification; IL-6. IL-6 expression was also increased in SOD1^{G93A} compared to WT astrocytes (4220% increase; $P<0.001$, $F_{(2,6)}=252.135$). The partial ablation of mGluR5 reduced this level (85% decrease; $P<0.001$, $F_{(2,6)}=252.135$), not statistically different from WT astrocytes.

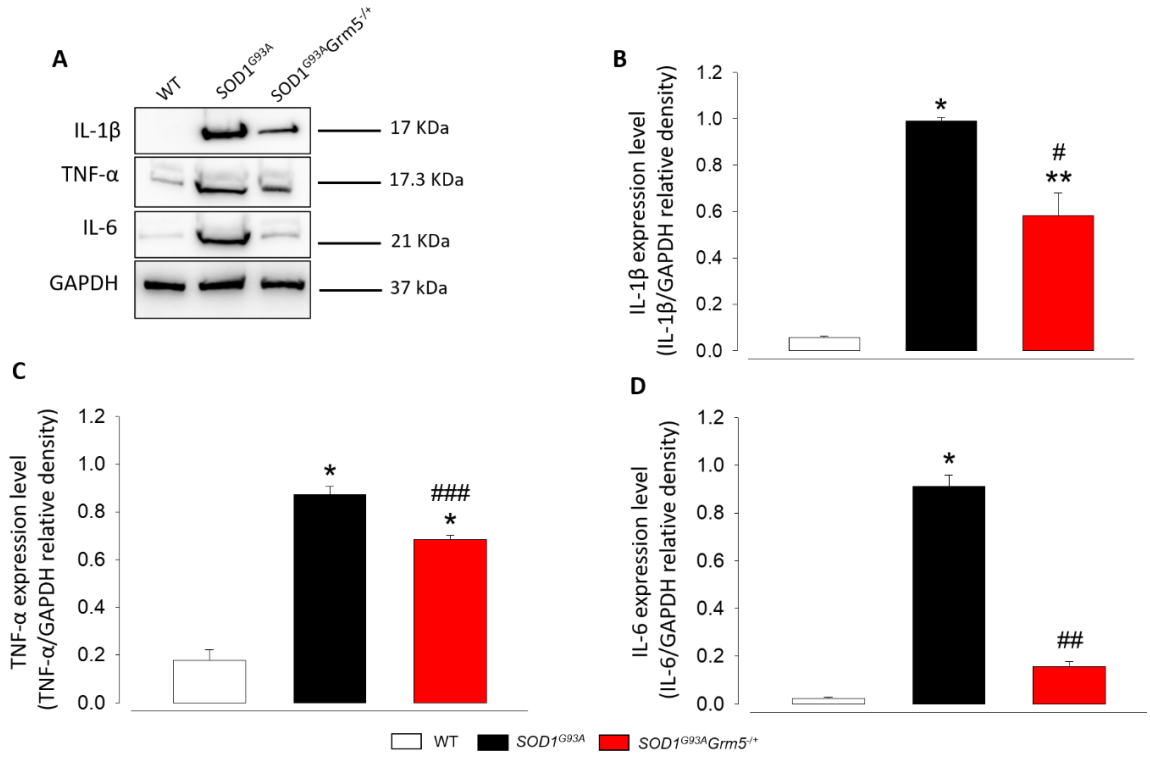

Fig. 26 Western blot quantification of IL-1β, TNF-α and IL-6 in cell lysates of primary cultures of spinal cord astrocytes from WT, SOD1^{G93A} and SOD1^{G93A}Grm5$^{-/+}$ adult mice. (A) Representative immunoreactive bands of IL-1β, TNF-α, IL-6 and GAPDH. (**B, C, D**) Quantification of protein expression as per scanned band density in WT, SOD1^{G93A}, and SOD1^{G93A}Grm5$^{-/+}$ astrocytes. Protein expression level was calculated as relative density, normalized to the housekeeping protein GAPDH. Data presented are means ± s.e.m of three independent experiments. *P<0.001 and **P<0.01 vs. WT astrocytes, $^{\#}$P<0.01, $^{\#\#}$P<0.001 and $^{\#\#\#}$P<0.001 vs. SOD1^{G93A} astrocytes (One-way ANOVA followed by Bonferroni post hoc-test).

The release of IL-1β, TNF-α and IL-6 in the culture medium was also investigate. At this purpose, culture medium of WT, SOD1^{G93A} and SOD1^{G93A} Grm5$^{-/+}$ astrocytes was analysed for cytokine presence at 24h time interval by ELISA (Figure 27)..

The level of IL-1β, illustrated in Figure 27A, was massively augmented in the conditioned medium of SOD1^{G93A} compared to WT astrocytes (395% increase, P<0.001, $F_{(2,15)}$=585.945). Conversely, the release of IL-1β by SOD1^{G93A}Grm5$^{-/+}$ astrocytes was strongly reduced (83% decrease, P<0.001, $F_{(2,15)}$=585.945). The residual amount of IL-1β released by SOD1^{G93A}Grm5$^{-/+}$ astrocytes was still significantly differed from WT astrocytes (66% increase; P<0.001, $F_{(2,15)}$=585.945) (Figure 27A).

TNF-α showed the same trend, displaying a dramatic increase in the culture medium of $SOD1^{G93A}$ astrocytes (475% increase; $P<0.001$, $F_{(2,15)}=624.699$) and an elevated release reduction in the double mutant astrocytes (85% decrease; $P<0.001$, $F_{(2,15)}=624.699$) (Figure 27B). Despite the massive release reduction, also in this case the partial ablation of mGluR5 did not completely revert the cytokine release respect to WT astrocytes (73% increase; $P<0.001$, $F_{(2,15)}=624.699$).

Figure 27C shows the release of the pro-inflammatory cytokine IL-6 release from WT, $SOD1^{G93A}$ and $SOD1^{G93A}Grm5^{-/+}$. $SOD1^{G93A}$ astrocytes released also high levels of IL-6 (775% increase; $P<0.001$, $F_{(2,15)}= 1786.465$), which, instead, was significantly diminished in the culture medium of double mutant astrocytes (83% decrease; $P<0.001$, $F_{(2,15)}= 1786.465$) (Figure 26C). Compared to WT astrocytes, $SOD1^{G93A}Grm5^{-/+}$ astrocytes still released higher level of IL-6 (128% increase ($P<0.001$, $F_{(2,15)}= 1786.465$).

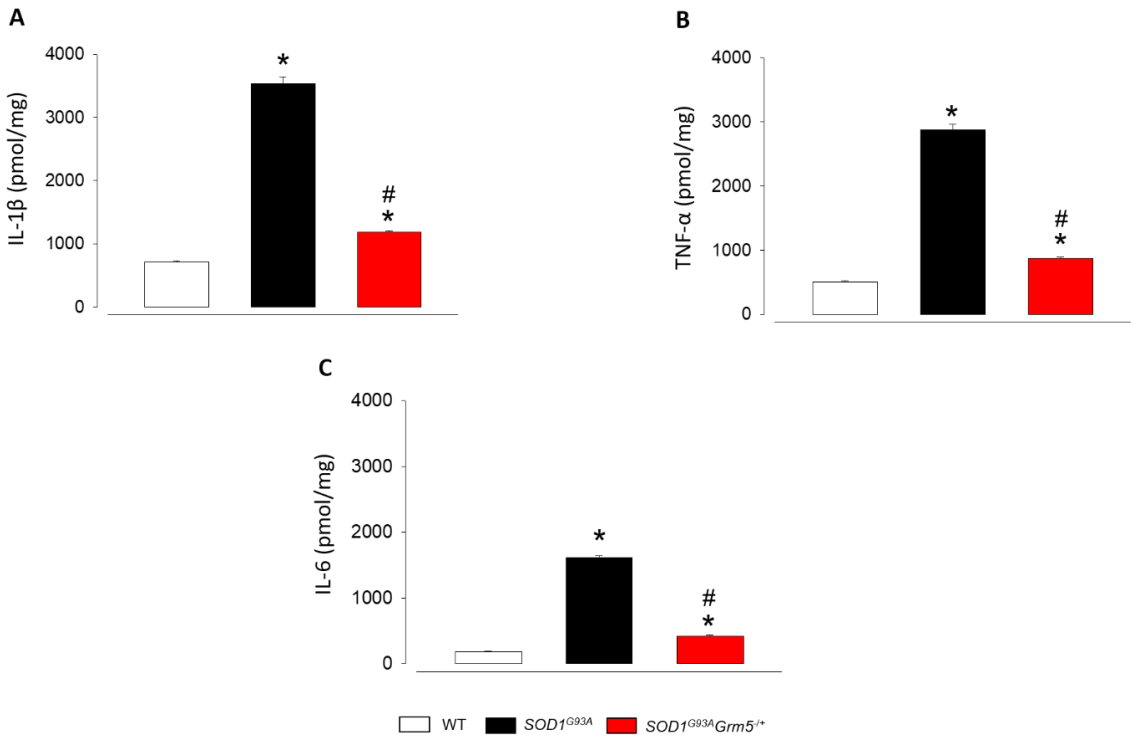

Fig. 27 Immuno-enzymatic quantification of IL-1β, TNF-α and IL-6 concentration in the culture medium of primary cultures of spinal cord astrocytes from WT, SOD1^{G93A} and SOD1^{G93A}Grm5$^{-/+}$ adult mice. Bar plots report the concentration of the pro-inflammatory cytokines (**A**) IL-1β, (**B**) TNF-α**,** and (**C**) IL-6 in the supernatant of WT, SOD1^{G93A} and SOD1^{G93A}Grm5$^{-/+}$ astrocytes. Protein concentration was determined as per specific ELISA commercial kits. Data presented are means ± s.e.m of six independent experiments run in triplicate (three analyses for each experimental condition). *P<0.001 vs. WT astrocytes; $^{\#}$P<0.001 vs. SOD1^{G93A} astrocytes (One-way ANOVA followed by Bonferroni post-hoc test).

4.9 SOD1^{G93A}Grm5$^{-/+}$ astrocytes exert a positive impact on motor neuron viability

To investigate whether the phenotypic amelioration of SOD1^{G93A}Grm5$^{-/+}$ astrocytes could exert a positive impact on MN survival, experiments were performed with co-cultures of motor neurons isolated from WT or SOD1^{G93A} mouse embryos and adult WT, SOD1^{G93A} and SOD1^{G93A}Grm5$^{-/+}$ astrocytes med.

Figure 28A, B and C represent phase-contrast microscope images of the different co-cultures after 10DIV. Figure 28D showed the MN viability which was assessed starting 4 days after MN seeding on the different astrocyte phenotypes and followed for further 10 days. When analysing the viability of WT MNs co-cultured with WT astrocytes, we observed a constant

and fast decrease of MN number during the experimental time (day 4: 100% viability; day 6: 87% viability; day 8: 56% viability; day 10: 25% viability; day 12: 14% viability; day 14: 10% viability) (Figure 28D). Co culture of $SOD1^{G93A}$ astrocytes with $SOD1^{G93A}$ MNs induced an even higher and faster death of MNs (day 4: 100% viability; day 6: 68% viability, $P<0.05$, $t_{(16)}= 2.221$; day 8: 36% viability, $P<0.001$, $t_{(16)}= 4.149$; day 10: 16% viability, $P<0.01$, $t_{(16)}= 3.396$; day 12: 7% viability, $P<0.05$, $t_{(16)}= 2.905$; day 14: 3.5% viability, $P<0.001$, $t_{(16)}= 4.516$) (Figure 28D). Finally, $SOD1^{G93A}$ MNs displayed a significative amelioration in viability, compared to the co-culture with $SOD1^{G93A}$ astrocytes, when co-cultured with $SOD1^{G93A}Grm5^{-/+}$ astrocytes reaching the values obtained for the WT astrocytes/WT MNs co-cultures (day 4: 100% viability; day 6: 87% viability, $P<0.01$, $t_{(16)}= -3.259$; day 8: 54% viability, $P<0.05$, $t_{(16)}= -2.532$; day 10: 29% viability, $P<0.05$, $t_{(16)}= -2.429$; day 12: 17% viability, $P<0.05$, $t_{(16)}= -2.727$; day 14: 6% viability, not significant) (Figure 28D). Significance was calculated vs. the survival of WT MNs co-cultured with WT astrocytes or vs. survival of $SOD1^{G93A}$ MNs co-cultured with $SOD1^{G93A}$ astrocytes at the respective time point.

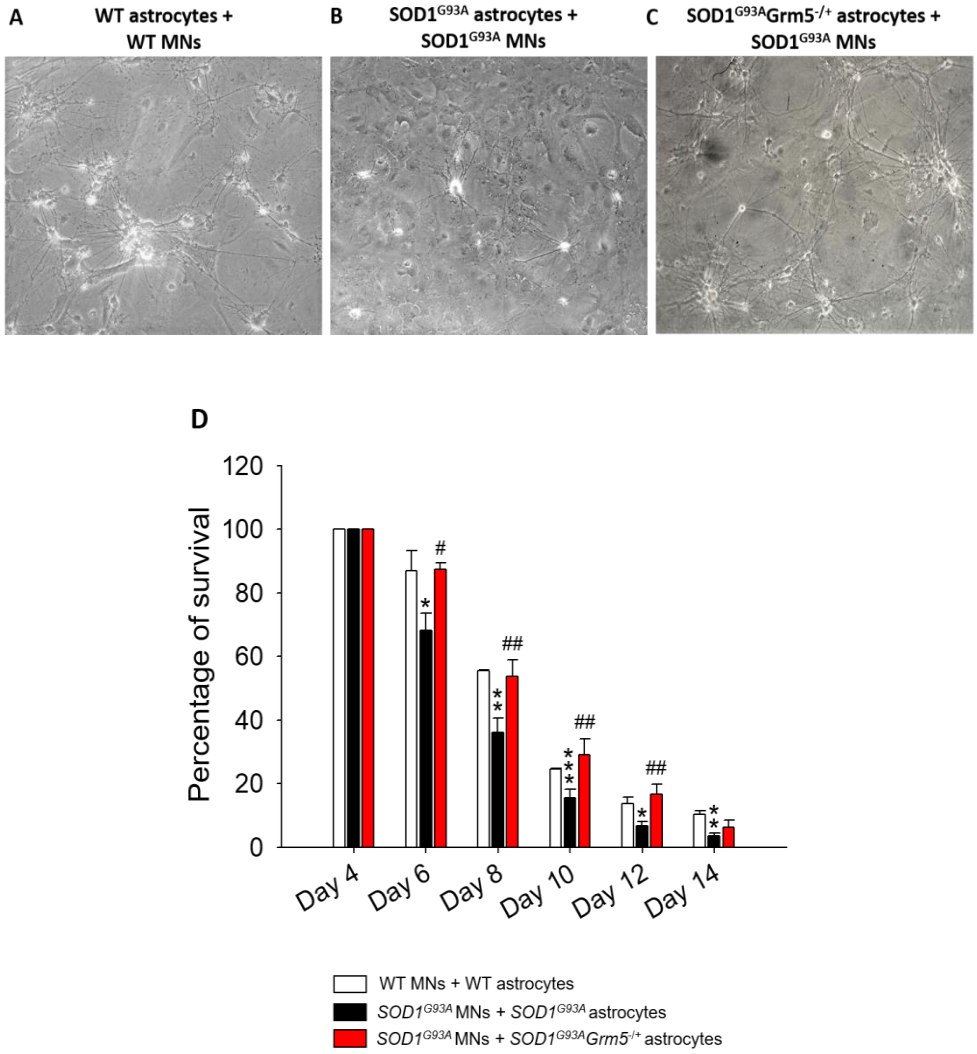

Fig. 28 Viability of WT and SOD1^{G93A} motor neurons co-cultured in the presence of spinal cord astrocytes from WT, SOD1^{G93A} or SOD1^{G93A} Grm5$^{-/+}$ adult mice. Representative phase-contrast microscopy images (10x) at day 10 after seeding (**A**) WT MNs on WT astrocytes, (**B**) SOD1^{G93A} MNs on SOD1^{G93A} astrocytes, or (**C**) SOD1^{G93A} MNs on SOD1^{G93A} Grm5$^{-/+}$ astrocytes.
(**D**) Quantitative analysis of MN viability. The analysis was performed by directly counting viable MNs in a previously defined area (1 square centimeter divided in 100 quadrants). MN viability was expressed as % survival of SOD1^{G93A} MNs co-cultured with SOD1^{G93A} astrocytes vs. survival of WT MNs co-cultured with WT astrocytes or as % survival of SOD1^{G93A} MNs co-culture with SOD1^{G93A}Grm5$^{-/+}$ astrocytes vs. survival of SOD1^{G93A} MNs co-cultured with SOD1^{G93A} astrocytes. Data represent the means ± s.e.m of nine independent experiments. *P<0.05, **P<0.001 and ***P<0.01 vs WT MNs co-cultured with WT astrocytes; $^{\#}$P<0.001 and $^{\#\#}$P<0.05 vs. SOD1^{G93A} MNs co-cultured with SOD1^{G93A} astrocytes (two-tailed Student's t-test).

4.10 The acute treatment with mGluR5-directed ASO reduced the mGluR5 expression and the astrogliosis in SOD1^{G93A} astrocytes

An innovative therapeutic strategy currently studied to counteract ALS is the use of antisense oligonucleotides which inhibits mRNA translation and promote mRNA degradation (see review of Ly and Miller, 2018).

Here, the acute effect of a mGluR5 specific ASO was tested, investigating both the mGluR5 expression in SOD1^{G93A} astrocytes and the modulation of astrogliosis in these cells. Astrocyte were exposed to the ASO for 48 h and measures were obtained 7 days after starting the treatment.

The quantitative RT-PCR results represented in Figure 29, shows that SOD1^{G93A} astrocytes treated with the ASO evidenced a significant decrease of the mRNA of mGluR5 respect to the SOD1^{G93A} astrocytes treated with scramble (90% decrease; $P<0.05$, $t_{(4)}= 2.997$).

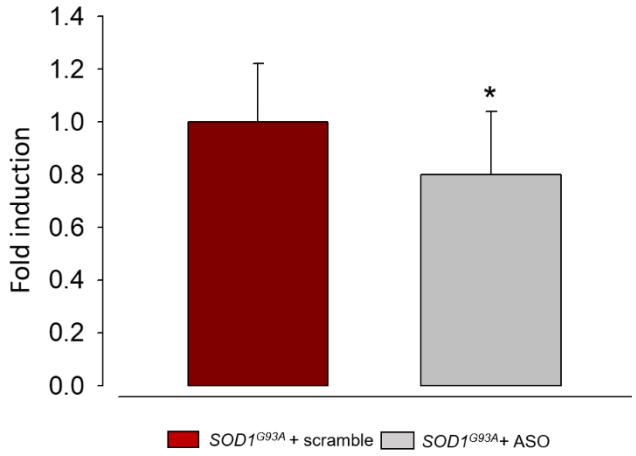

Fig. 29 RT-PCR quantification of mGluR5 mRNA present in SOD1^{G93A} after treatment with scramble or mGluR5-directed ASO. Astrocytes we exposed to scramble or ASO for 48 h, measures were performed five days after ASO washout. Data represent the mean ± s.e.m of three independent experiments run in triplicate. The mRNA expression of mGluR5 of SOD1^{G93A} astrocytes treated with scramble is reported as 1. $^{*}P<0.05$ vs. SOD1^{G93A} astrocytes treated with scramble (two-tailed Student's t-test).

Most interesting, the ASO treatment showed a positive effect in modulating astrogliosis of $SOD1^{G93A}$ astrocytes. Figure 30A reports representative immunocytochemical images of GAPDH (red) and GFAP (green) expression and co-localization (yellow) in $SOD1^{G93A}$ astrocytes treated with the ASO or scramble. Figure 30B outlines that the GFAP expression was reduced in astrocytes treated with ASO respect to scramble (37% decrease; $P<0.001$, $t_{(10)}= 4.992$).

Figure 30C shows representative immunocytochemical images of GAPDH (red) and S100β (green) expression and co-localization (yellow) in $SOD1^{G93A}$ astrocytes treated with the ASO or scramble. Results similar to GFAP were obtained for S100β: again S100β expression was reduced in astrocytes treated with ASO respect to scramble (30% decrease; $P<0.01$, $t_{(10)}= 3.964$) (Figure 30D).

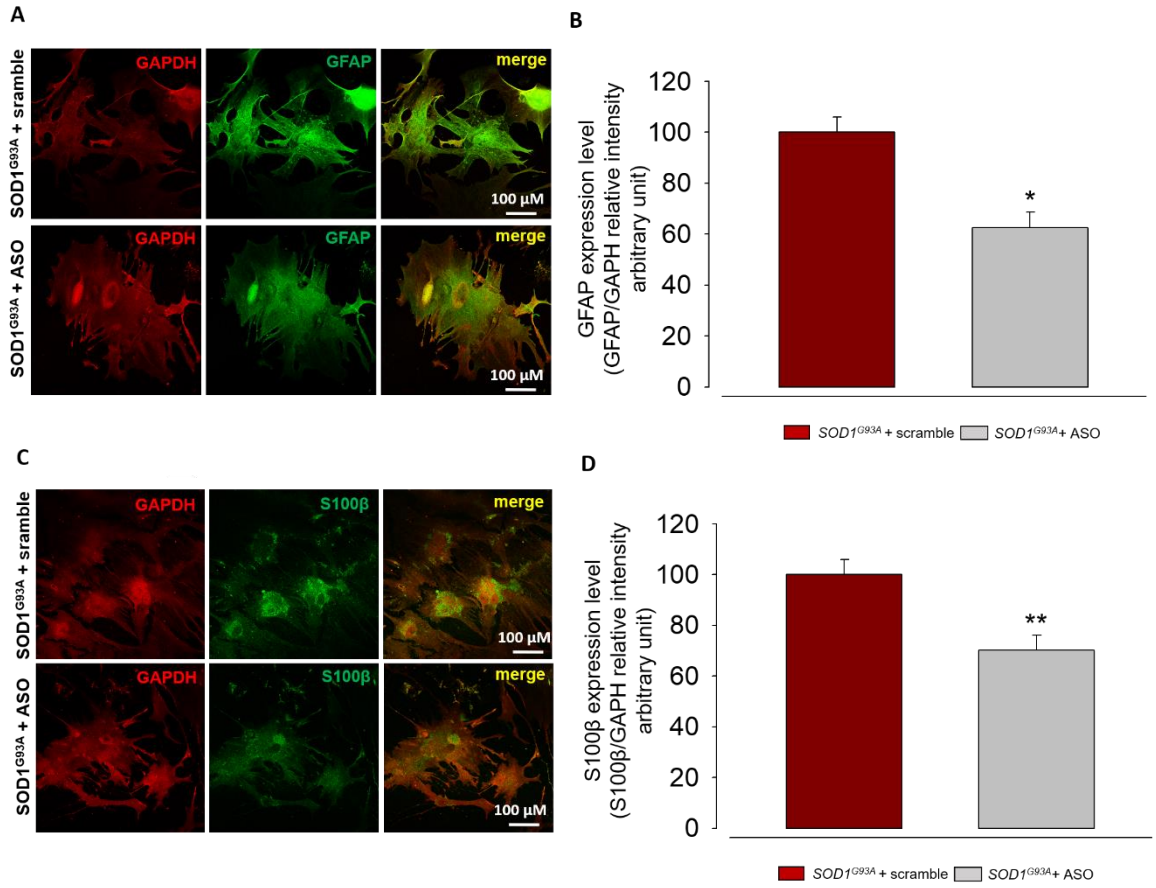

Fig. 30 Immunocytochemical quantification of GFAP and S100β in SOD1^{G93A} astrocytes treated with scramble or ASO. (**A**) Representative confocal microscopy immunocytochemical images of GFAP (green) and GAPDH (red) and of (**C**) S100β (green) and GAPDH (red) in SOD1^{G93A} astrocytes treated with scramble or ASO, cultured on coverslip and labelled with the appropriate primary and secondary antibodies. The merge panels represent the co-expression of GFAP or S100β and GAPDH. Scale bar: 100 µm. (**B**) Quantification of GFAP expression, as per relative fluorescence intensity, was performed calculating the co-localization coefficients (Manders *et al*., 1992) using Image-J software analyses. (**D**) Quantification of S100β expression. Data are expressed as relative fluorescence intensity of GFAP or S100β normalized respect to the fluorescence intensity of the housekeeping protein GAPDH. The relative intensity of SOD1^{G93A} astrocytes treated with scramble is reported as 1. Data presented are means ± s.e.m of three independent experiments run in triplicate (three different coverslips for each experimental condition). Statistical analysis was performed by two-tailed Student's t-test. *P<0.001 and **P<0.01 vs. SOD1^{G93A} astrocytes treated with scramble.

4.11 The pharmacological treatment with CTEP reduced the astrogliosis in SOD1^{G93A} astrocytes

CTEP is a non-allosteric modulator of mGluR5 optimized for *in-vivo* treatments in rodents (Lindemann *et al*., 2011) and already tested in mouse models of a number of neurodegenerative diseases (Abd-Elrahman *et al*., 2017; Farmer *et al*., 2020). Moreover, it showed positive *in-vivo* results in SOD1^{G93A} mouse model of ALS (Milanese *et al*., submitted in 2020) reducing also astrogliosis and microgliosis. The aim of the present experiments was to verify whether the positive effects of CTEP obtained *in-vivo* could also reflect on SOD1^{G93A} astrocyte phenotype amelioration. SOD1^{G93A} astrocytes were exposed to the drug for seven days *in-vitro*. Then, the reactive phenotype of the treated cells was analysed by immunocytochemical analysis checking the expression of GFAP or S100β. Figure 31 panel A represents immunocytochemical images of GAPDH (red) and GFAP (green) expression and co-localization (yellow) in SOD1^{G93A} astrocytes treated with the CTEP or DMSO. The treatment with CTEP significantly reduced the expression level of GFAP (15% increase; $P<0.05$, $t_{(4)}= 2.958$) (Figure 31 panel B) respect to the cell treatment with DMSO.

Figure 31 panel C represents immunocytochemical images of GAPDH (red) and S100β (green) expression and co-localization (yellow) in SOD1^{G93A} astrocytes treated with CTEP or DMSO. The expression level of S100β was also reduced after the treatment with the drug (20% decrease; $P<0.05$, $t_{(4)}= 2.958$) (Figure 31 panel D).

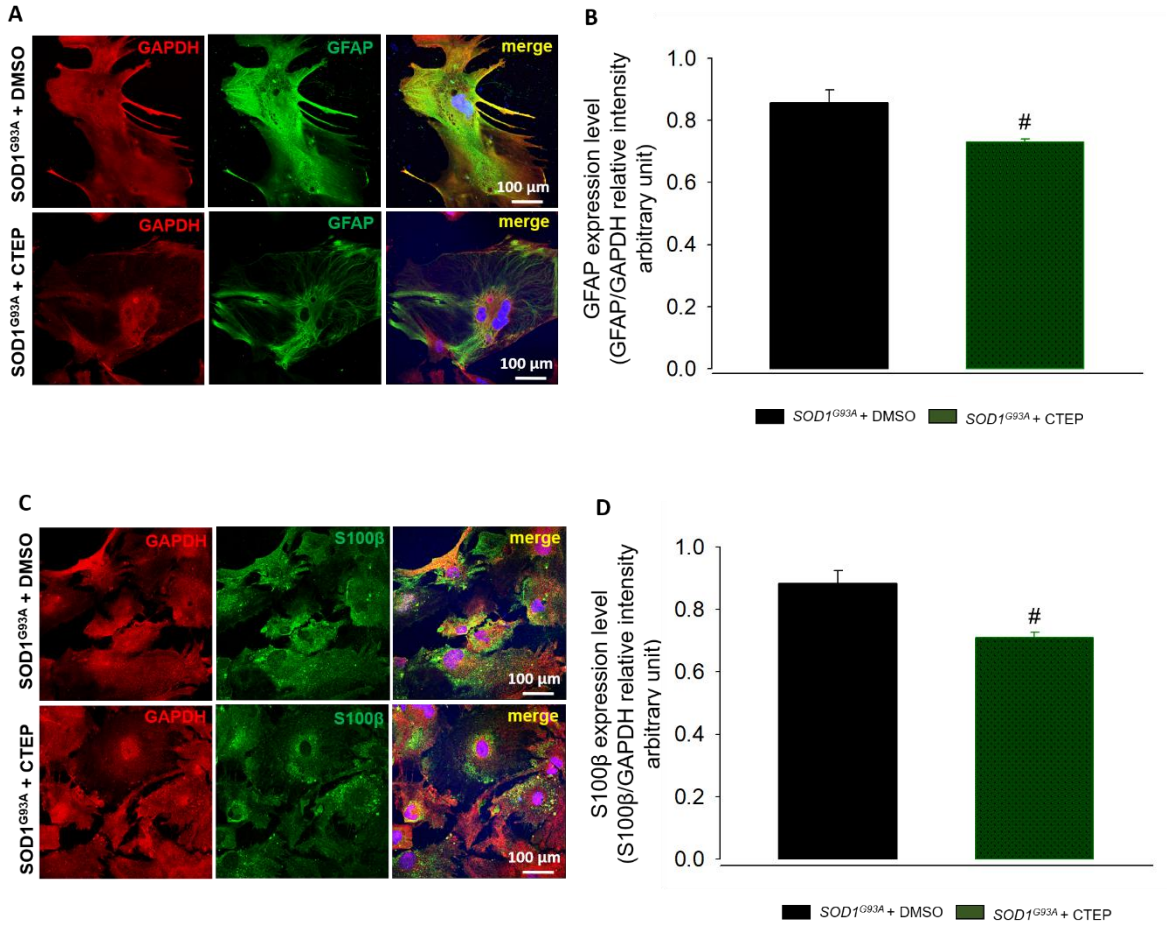

Fig. 31 Immunocytochemical quantification of GFAP and S100β expression in SOD1^{G93A} astrocytes treated with DMSO or CTEP. Representative confocal microscopy immunocytochemical images of (**A**) GFAP (green) and GAPDH (red) and of (**C**) S100β (green) and GAPDH in SOD1^{G93A} astrocytes treated with DMSO or CTEP and cultured on coverslip and labelled with the appropriate primary and secondary antibodies. The merge panels represent the co-expression of GFAP or S100β and GAPDH. Scale bar: 100 µm. (**B, D**) Quantification of protein expression, as per relative fluorescence intensity, was performed calculating the co-localization coefficients (Manders *et al*., 1992) using Image-J software analyses. Data are expressed as relative fluorescence intensity of GFAP or S100β normalized respect to the fluorescence intensity of the housekeeping protein GAPDH. Data presented are means ± s.e.m of three independent experiments run in triplicate (three different coverslips for each experimental condition); statistical analysis was performed by two-tailed Student's t-test. $^{\#}P<0.05$ vs. SOD1^{G93A} astrocytes treated with DMSO.

4.12 Studies on the reactive microglia phenotype in WT, SOD1^{G93A}, Grm5$^{-/+}$, and SOD1^{G93A}Grm5$^{-/+}$ mice

In Prof. Bonanno's laboratory, we are investigating the expression of mGluR5 and the effect of dampening this receptor on the balance between pro- (M1-like) and anti- (M2-like) inflammatory phenotype in microglia acutely purified from the brain and spinal cord of SOD1^{G93A} mice at pre (30 days), early (90 days) and late (120 days) symptomatic stages of ALS. Since these experiments are measuring the expression of relevant markers at the protein level, my work in Maastricht and Hasselt University, in the laboratory of Professor Prickaerts and Dr. Vanmierlo, respectively, focused on the detection of the expression of the same markers at the mRNA level.

Enriched microglia samples acutely isolated from the brain and spinal cord of WT, SOD1^{G93A}, Grm5$^{-/+}$, and SOD1^{G93A}Grm5$^{-/+}$ mice at the early and late symptomatic stages of the disease (90 and 120 days, respectively) have been prepared in Genoa and sent to Maastricht and Hasselt for RT-qPCR analyses.

4.12.1 Quantitative RT-PCR

The first step to proceed with RT-qPCR experiments was to select the best RNA isolation protocol. We chose the phenol-chloroform protocol (Toni *et al*., 2018) with minor modification to retain highest RNA yields. The quantification and purity of RNA was detected by Nanodrop 2000 (ThermoFisher Scientific, Waltham, Massachusetts, USA) and quality was assessed using the Bionalyzer (Agilent Technologies, Santa Clara, California, USA). The total RNA amount measured ranged from 120 to 455 ng and the 260/230 ratio was always lower than the expected value (2.0-2.2) ranging from a minimum of 0.02 to a maximum of 1.17, indicating possible contaminations by phenols, alcohols, and carbohydrates. To clean the samples from impurities, we heated RNA at 65 °C for 5 min.

For each sample, the same amount of RNA was retro-transcribed to cDNA and the first qPCR experiments were carried on using both 5 and 12.5 ng cDNA to set the best experimental condition. As negative control, nuclease-free water and no retro-transcribed RNA were used. As positive control, cDNA derived from cultured OPCs and microglia, already tested for qPCR efficiency in Dr. Vanmierlo laboratory, was used. The endogenous reference genes were selected searching in the literature, using Primer3Plus and Primer-BLAST (National Center for Biotechnology Information, NCBI) platforms and based on the

experience of the host laboratory. Samples from Genoa were used to select the best reference genes.

Unfortunately, the expression of the reference genes was not stable in the different samples (difference > 0.5 Ct value) and the Ct values needed for reveal mRNAs ranged from 30 to 37 cycles or were even undetectable. Therefore, to increase signal detection, we added 5 cycles (45-50) to the PCR protocol. Moreover, to avoid primers-dimers event and to limit background signal, we diluted primers twice and always run the higher amount of cDNA (12.5 ng). Notwithstanding these modifications, also the subsequent experiment produced instable results and the expression of pro- and anti-inflammatory genes was not detectable. Therefore, we checked again primers and re-designed them to have better exon-exon junction primers. In addition, we checked again the PCR annealing temperature and the melting temperature (Tm) of the primers.

In parallel, by searching the literature, the use of *Expressed repetitive elements* (EREs) or *Expressed Alu Repeat* (EAR, the homologous of EREs in humans) became manifest as an alternative to the classic normalization of PCR data, since the different expression of a number of genes in the target tissues or cells does not influence the EREs/EARs abundance in the transcriptome (Marullo *et al*., 2010; Renard *et al*., 2018; Rihani *et al*., 2013; Janssens *et al*., 2019; Figure 32).

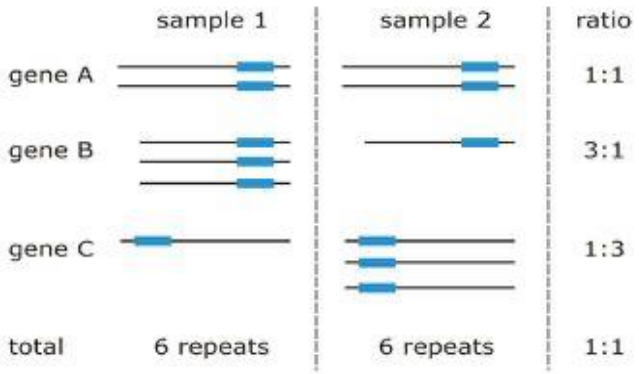

Fig. 32 Schematic representation EREs/EARs rationale. Repeat sequences are present in the UTR of many genes, and the differential expression of a small number of genes does not influence the overall repeat abundance in the transcriptome (picture was taken from *qPCR training* course, Biogazelle).

Renard and colleagues (Renard *et al*., 2018) compared the expression stability of 11 EREs and 8 commonly used endogenous reference genes in different organs of healthy and transgenic mice and in a cell line. In all the experimental conditions three to eight EREs resulted most stable among all the 11 EREs and the other tested reference genes. Therefore, we checked the efficiency and stability of the same 11 EREs in our experimental conditions, compared to the previous utilized reference genes, by performing standard dilution series (standard curve) and using geNorm software. Figure 33A shows the PCR efficiency of *Orr1A0*, which gave the best results [Efficiency (%) = 100.78%; slope of -3.30; base exponential amplification (E) = 2.01]. Figure 33B shows the geNorm analysis performed with enriched microglia samples isolated from brain and spinal cord of 120 days old mice to evaluate the most stable sequence and reference genes. *Orr1A0* (named as "3" in the picture) resulted the most stable sequence among the 11 EREs, even if with an M-value >0.5. CYPA, on the other hand, resulted as one of the most stable reference genes (M-value <0.5), also compared to the EREs (Figure 33B). Therefore, *Orr1A0* and CYPA were selected for the following qPCR experiments.

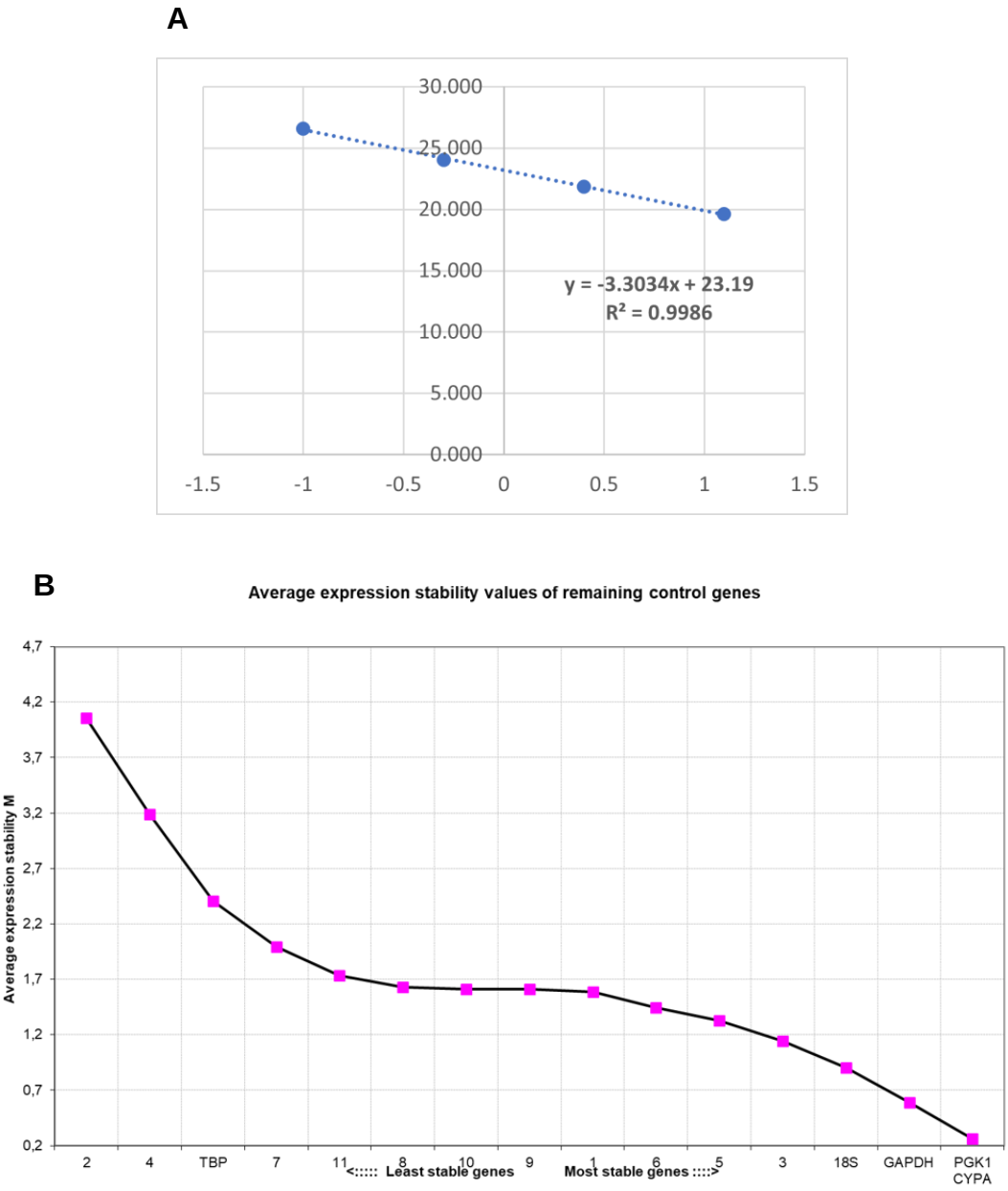

Fig. 33 Results obtained after PCR efficiency calculation (A) and geNorm analyses of the most stable reference genes/ EREs sequence (B). (**A**) The PCR efficiency was calculated with standard dilution series of a sample with known concentration. On the horizontal axis it is reported the Log_{10} cDNA amount (12.5 - 0.1 ng) and on the vertical axis the Cq values. The PCR efficiency was calculated as follows: $E= 10^{-(1/a)-1}$. (**B**) The geNorm analysis compared all the tested reference genes and the 11 EREs for their stability with enriched microglia samples isolated from brain and spinal cord of 120 days old mice. The most stable genes/sequence are represented on the right part of the graph (M-value <0.5). *Orr1a0* (named as "3" in the graph) was the most stable sequence among all the 11 EREs.

Notwithstanding the above encouraging results, we again did not obtain stable expression among different samples of enriched microglia from the four WT, $Grm5^{-/+}$, $SOD1^{G93A}$ and $SOD1^{G93A}Grm5^{-/+}$ mouse groups. Therefore, we decided to assess the RNA integrity of the original samples, a critical step to obtain reliable gene expression data. RNA integrity of microglia samples was assessed by electrophoretic separation on chips via laser induced fluorescence detection (2100 Bioanalyzer System, Agilent, Santa Clara, United States). Figure 34 shows a representative electropherogram image detailing size distribution of RNA fragments, sample concentration, ribosomal ratio, and the RNA integrity number (RIN) which classifies the total RNA quality on the basis of a 1-10 scale, 1 being the most degraded profile and 10 the most intact. As RNA degradation proceeds, 18S to 28S ribosomal band ratio decreases and baseline signal between the two ribosomal peaks increases (Figure 35).

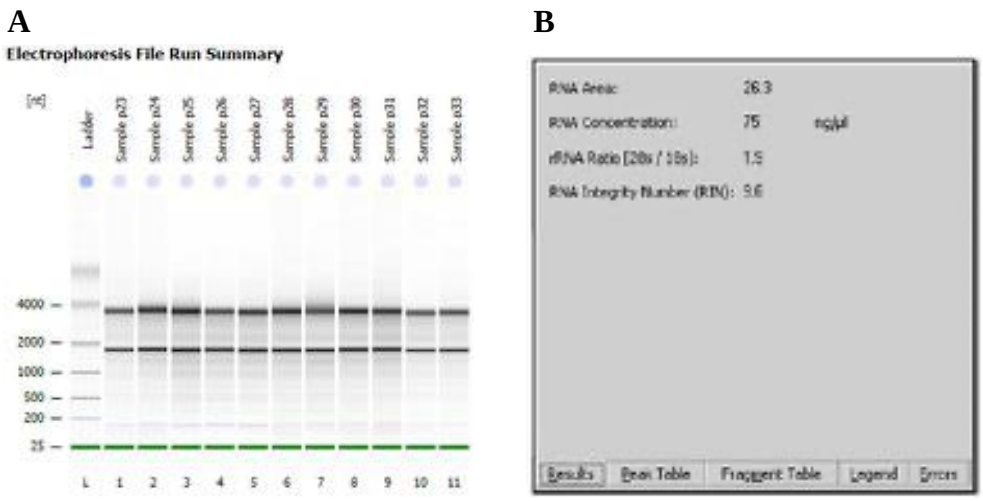

Fig. 34 Preview of the results showed by 2100 Bioanalyzer. (**A**) The gel-liked image generated by the instrument shows the RNA profile of different samples. (**B**) All the information about the RNA profile (including RIN) are summarized in the results table (Agilent, Santa Clara, United States).

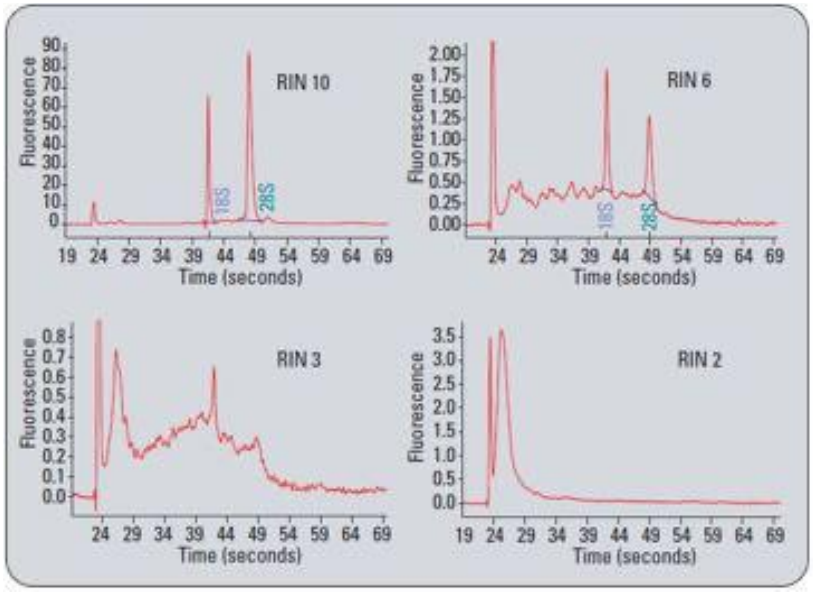

Fig. 35 Sample electropherograms used to train the RNA Integrity Number (RIN) software. Samples range from intact (RIN 10), to degraded (RIN 2) (Agilent, Santa Clara, United States).

RNA integrity analyses were performed. We compared RNA samples deriving from microglia isolated from both male and female mice of different genotypes (WT, $Grm5^{-/+}$, $SOD1^{G93A,}$ $SOD1^{G93A}$ $Grm5^{-/+}$) after two different RNA extraction protocols, e.g., RNeasy Mini Kit (QIAGEN, Cat#74106) or phenol-chloroform protocol (Table 7), described in detail in the *Materials and Methods* section. Results showed high degradation of RNA (Table 7 and Figure 36). Moreover, a lower RNA concentration than expected was obtained (< 5 ng, Table 7). The hypothesis is that the RNA quantification obtained soon after RNA isolation at Nanodrop 2000 was overestimated.

Sample N°	Genotype	Mice sex	Age (days old)	Tissue	RNA isolation protocol	RNA concentration (ng/µL)	RIN
5	WT	M	120	Spinal cord	RNeasy Mini Kit protocol	0.086	1
7	WT	M	120	Spinal cord	Phenol-chloroform protocol	0.268	N/A
8	$SOD1^{G93A}$	M	120	Spinal cord	RNeasy Mini Kit protocol	0.045	2.10
10	$SOD1^{G93A}$	F	120	Spinal cord	Phenol-chloroform protocol	0.397	2.50
11	$SOD1^{G93A}$	F	120	Spinal cord	Phenol-chloroform protocol	0.235	2.50
2+3 (two mice pooled together)	$SOD1^{G93A}$ $Grm5^{-/+}$	M	120	Spinal cord	RNeasy Mini Kit protocol	0.053	1
12	$SOD1^{G93A}$ $Grm5^{-/+}$	F	120	Spinal cord	RNeasy Mini Kit protocol	0.110	2.60
13	$SOD1^{G93A}$ $Grm5^{-/+}$	F	120	Spinal cord	Phenol-chloroform protocol	0.112	2.80
14	$SOD1^{G93A}$ $Grm5^{-/+}$	M	120	Spinal cord	Phenol-chloroform protocol	0.322	2.70
15	$Grm5^{-/+}$	F	120	Spinal cord	RNeasy Mini Kit protocol	0.001	N/A
17	$Grm5^{-/+}$	M	120	Spinal cord	Phenol-chloroform protocol	0.039	1

Table 7 Analysis of RNA integrity. Data were obtained by 2100 Bioanalyzer Instrument at Hasselt University. All the samples showed very low RIN, indicating a high level of degradation.

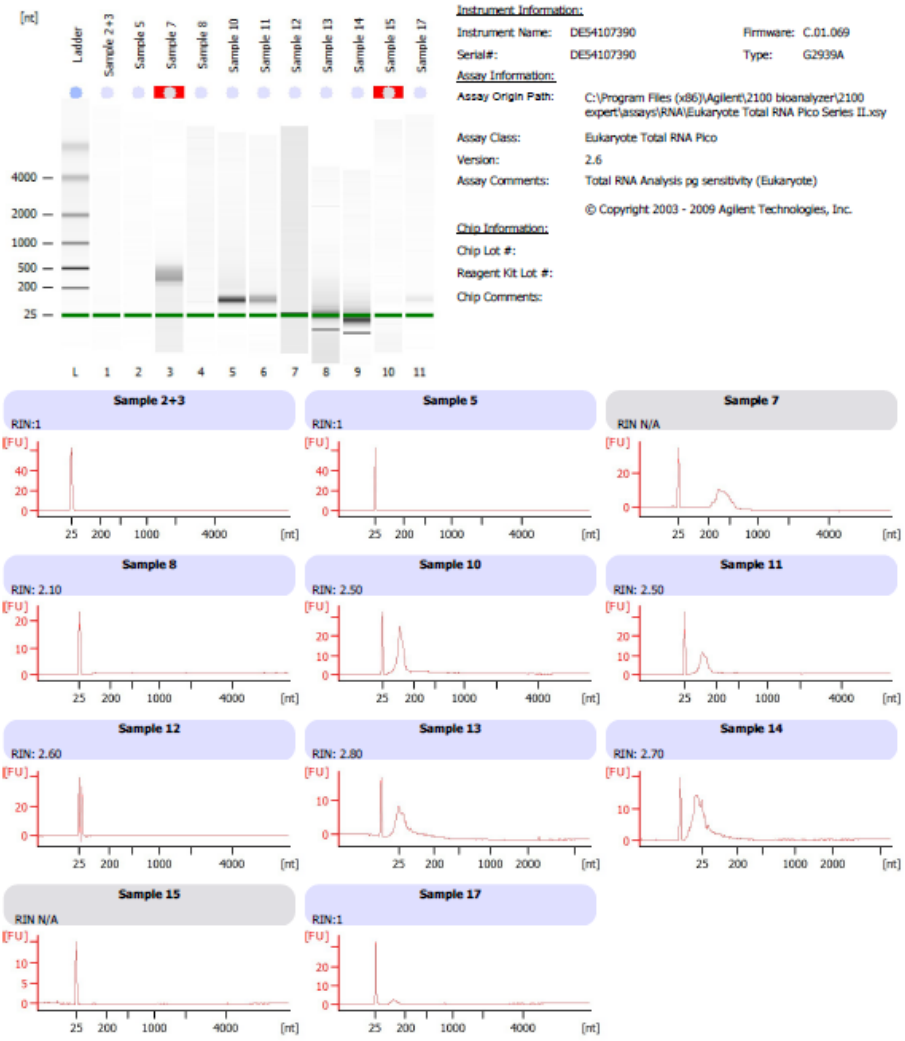

Fig. 36 Analysis of RNA integrity. Data were obtained with 2100 Bioanalyzer Instrument at Hasselt University. All the samples showed very low RIN, indicating a high level of degradation.

To check all the variables of the experimental procedure established for RT-qPCR analysis, some of the new microglia samples arrived from Genoa were immediately analysed for RNA quality at 2100 Bioanalyzer. The two RNA extraction protocols cited above were compared again. RNA was treated or not with DNase and diluted or not to 5 ng/µL. Moreover, RNA isolated from primary culture of astrocytes and microglia were analysed as positive controls. Results (RIN and concentration of RNA) are reported in Table 8.

Sample N°	Genotype	Tissue	DNase treatment	Dilution to 5ng/µL	RNA Extraction	RNA concentration (ng/µL)	RIN
13	SOD1^{G93A}	Brain enriched microglia	–	–	Phenol-chloroform protocol	3.700	2.30
13	SOD1^{G93A}	Brain enriched microglia	–	✔	Phenol-chloroform protocol	1.380	2.40
13	SOD1^{G93A}	Brain enriched microglia	✔	✔	Phenol-chloroform protocol	0.324	2.40
15	SOD1^{G93A}	Brain enriched microglia	✔	✔	RNeasy Mini Kit protocol	0.176	1.70
16	SOD1^{G93A}	Spinal cord enriched microglia	✔	✔	RNeasy Mini Kit protocol	0.058	N/A
14	SOD1^{G93A}	Spinal cord enriched microglia	✔	✔	Phenol-chloroform protocol	0.052	2.10
18	WT	Brain enriched microglia	✔	✔	Phenol-chloroform protocol	0.331	2.60
19	WT	Spinal cord enriched microglia	✔	✔	Phenol-chloroform protocol	0.186	N/A
1	WT	Microglia in culture	✔	✔	Phenol-chloroform protocol	0.177	7.40
2	WT	Astrocytes in culture	✔	✔	Phenol-chloroform protocol	3.450	9.10

Table 8 Analysis of RNA integrity. Data were obtained with 2100 Bioanalyzer Instrument at Hasselt University. All the enriched microglia samples (13, 14, 15, 16, 18 and 19) showed very low RIN, indicating a high level of degradation.

All the enriched microglia samples showed again a very low RIN, in some cases even non detectable (N/A). Conversely, primary astrocytes and microglia cultures showed high RIN, even if the RNA concentration was < 5 ng/µL. These results suggest that the RNA integrity of *enriched* microglia samples is independent from the concentration of the samples.
Taken together these results led to interruption of the qPCR experiments.

4.13 Culture of primary neonatal microglia

Taking advantage from the expertise of the research group of Dr. Vanmierlo at Hasselt University and according to the laboratory in Genoa, a series of experiments were planned to assess the effects of freezing and thawing primary microglia and astrocytes, a procedure

never tried before on primary glial cells, was also implemented to allow future transfer of cultured cells from the two laboratories and their reutilization in culture.

4.13.1 Culture and staining of primary neonatal microglia

After shaking off from astrocytes, microglia were plated in T75 flasks, reached the confluence in few days, and survived for about one month in culture (Figure 37).

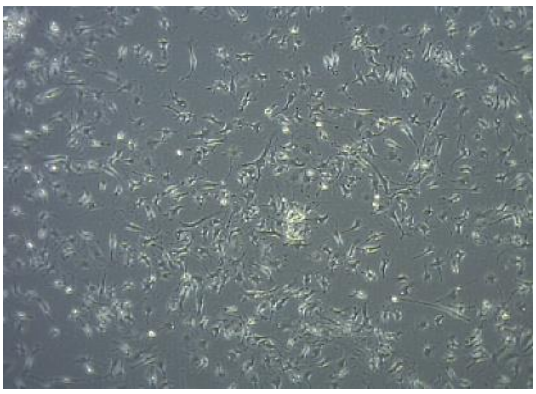

Fig. 37 Spinal cord neonatal primary microglia after shaker. Microglia isolated from the pool of 6 spinal cords of WT P0/P2 mice (about $2x10^6$ cells) were detached from the monolayer of astrocytes, brought in culture, and expanded with LCM-enriched medium for about 1 month. Picture was taken at phase contrast microscope (100x) one day after shaker.

To check the purity of cultured microglia, cells were stained for the microglial marker IBA-1, the astrocyte marker GFAP and the nuclear marker DAPI. The staining confirmed a high purity of the culture (> 90%) (Figure 38A).

Astrocytes were stained with the same markers to check the microglia yield still attached on the astrocytic monolayer after shaking. This staining indicated still a presence of attached microglia together with astrocytes (Figure 38B).

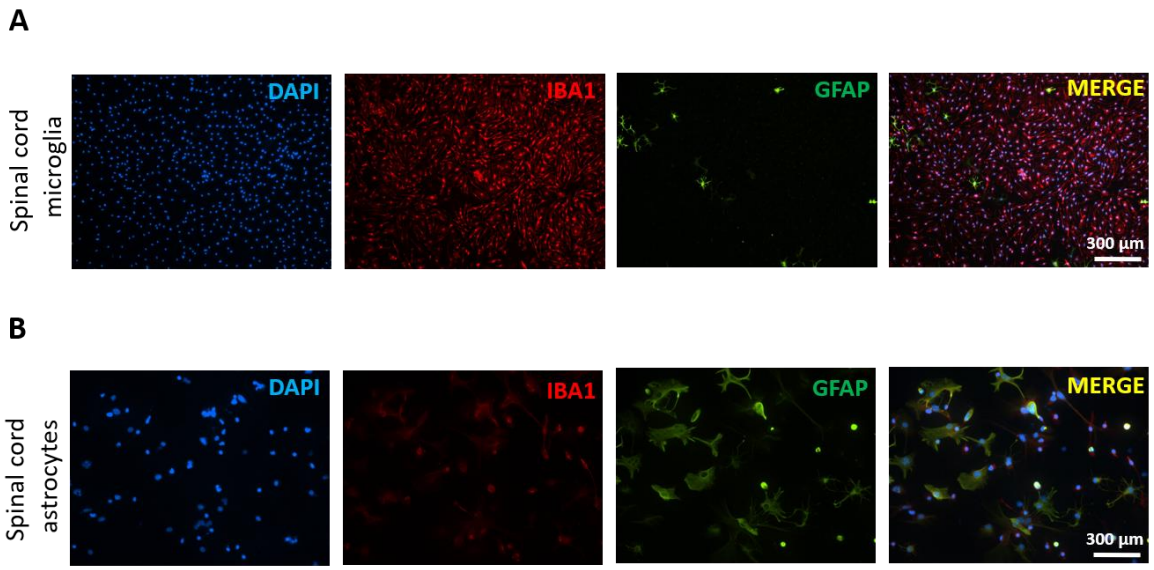

Fig. 38 Staining of glial cells after shaker. (**A**) After shaker from astrocytes, microglia were brought in culture. Five days later, the purity of microglia culture was checked by staining cells with the microglia marker IBA1 (red), the astrocytic marker GFAP (green) and nuclear marker DAPI (blue). (**B**) Astrocytes were also stained with the same markers five days after shaker (objective 20X, scale bar 300 µm).

Primary microglia were then frozen and thawed following the classic procedure used for cell lines (see *Materials and Methods*, chapter 3.19). Microglia from spinal cord (Figure 39A) and brain (Figure 39B) grew in culture after thawing for about 1 month, even after several replating steps.

Astrocytes survival after freezing and thawing in liquid nitrogen was also checked (Figure 39C).

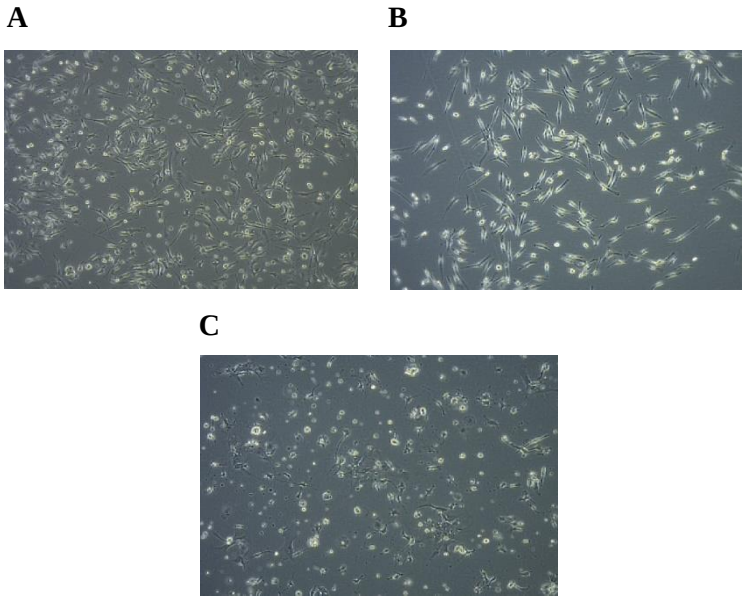

Fig. 39 Culture of primary microglia and astrocytes after thawing from liquid nitrogen. (**A**) Microglia from spinal cord and (**B**) brain were frozen in liquid nitrogen and thawed after about 1 month. (**C**) Astrocytes were also checked for survival after thawing. Pictures were taken at phase contrast microscope (100x) 1 day after thawing.

To confirm the presence of microglia after thawing, cells were stained for the specific microglial marker IBA-1, for the astrocytic marker GFAP and for the nuclear marker DAPI (Figure 40, upper panels). Freshly isolated brain microglia were stained as positive control (Figure 40, panels below). The purity of the microglia cell culture after thawing was about 100%.

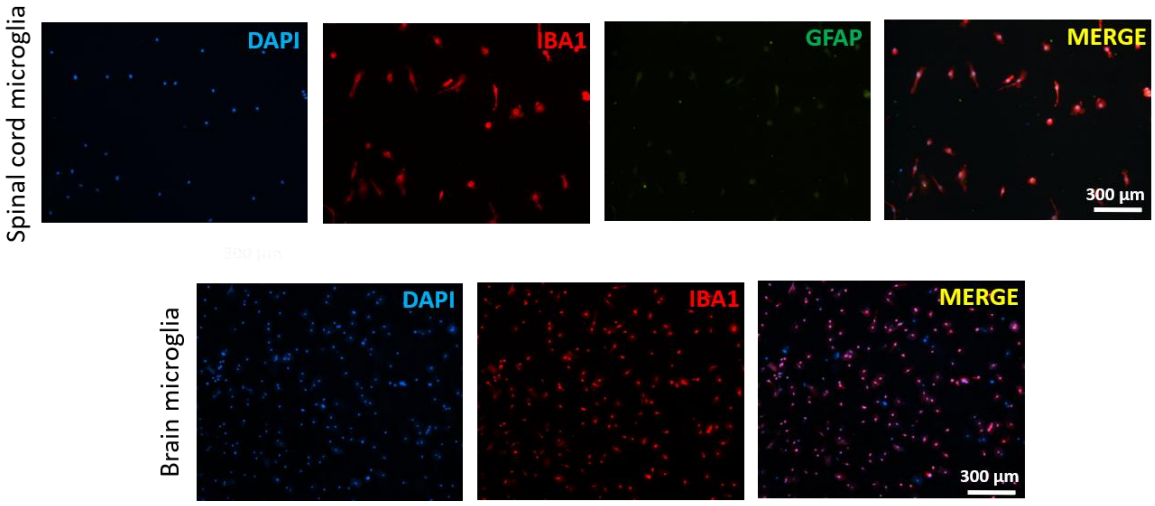

Fig. 40 Staining of spinal cord primary microglia after thawing from liquid nitrogen. (**Upper panels**) Spinal cord microglia were stained few days after thawing with the specific microglial marker IBA1 (red), the astrocytic marker GFAP (green) and the nuclear marker DAPI (blue). (**Panels below**) Freshly isolated brain microglia were stained for IBA1 (red) and DAPI (blue) as positive control (microscope objective 20X, scale bar 300 µm).

5. DISCUSSION

5.1 Studies with astrocytes

The present study highlights the role of mGluR5 in modulating the reactive phenotype of astrocytes isolated from the $SOD1^{G93A}$ mouse model of ALS. Accordingly, it was here demonstrated that the partial ablation of mGluR5 ameliorates the phenotype of $SOD1^{G93A}$ astrocytes by reducing i) the intracellular [Ca^{2+}]; ii) the activation state, as demonstrated by the reduced expression of GFAP and S100β; iii) misfolded SOD1 expression; iv) inflammation state, underlined by the reduced expression of the NPL3 inflammasome complex and of inflammatory cytokine expression and release; v) the uncoupling between oxygen consumption and ATP synthesis and the impairment of mitochondria function. All these events led to the improvement of MN survival, in astrocyte-MN primary co-cultures. Moreover, both the *in-vitro* exposure to an mGluR5 ASO or to the NAM of mGluR5 CTEP also reduced astrogliosis, confirming the results obtained with the genetic knocking down of the receptor.

Group I glutamate metabotropic receptors, mGluR1 and mGluR5, detected at synaptic terminals (Yin and Niswender, 2014), at astrocytes (D'Antoni *et al*., 2008), microglia (Liu *et al*., 2009) and at oligodendrocyte progenitor cells (Luyt *et al*., 2006) are involved in regulation of several cellular processes altered in ALS, playing a key role in the complex scenario of the disease (Nicoletti *et al*., 2011; Aronica *et al*., 2001; Martorana *et al*., 2012; Anneser *et al*., 2004a; Anneser *et al*., 2004b; Rossi *et al*., 2008; Vergouts *et al*., 2018). While low levels of mGluR1 and mGluR5 were usually detected in astrocytes under physiological conditions, higher expression of these receptors has been identified in reactive glial cells in spinal cord of ALS patients (Aronica *et al*., 2001). Overexpression was also detected in striatum, hippocampus, frontal cortex, and spinal cord of $SOD1^{G93A}$ mouse model of ALS, starting from the pre-symptomatic stages and during the progression of the disease (Martorana *et al.*, 2012; Brownell *et al*., 2015; Bonifacino *et al*., 2019b).

The best characterized Group I glutamate metabotropic receptor is mGluR5 which was detected also in astrocytic cultures and contribute to modulate the glial response to changes in local excitatory tone (D'Antoni *et al*., 2008; Verkhratsky and Kirchhoff, 2007). mGluR5 has been suggested to contribute to neuronal growth, regulation of synaptic activity, neuroprotection, and excitotoxicity (Viwatpinyo and Chongthammakun, 2009). Indeed, its activation leads to several effects such as astrocyte proliferation (Kanumili and Roberts, 2006), release of BDNF (Jean *et al.*, 2008) and glio-transmitters, such as ATP and glutamate

(Bezzi and Volterra, 2014; Panatier *et al*., 2011), increased glutamate uptake (Aronica *et al*., 2003; Vermeiren *et al*., 2005) and modulation of inflammatory responses (Shah *et al*., 2012).

This receptor has been found to be involved in several molecular mechanisms causing astroglial damage (Rossi *et al*., 2008). In addition, astrocytes isolated from spinal cord of late symptomatic SOD1^{G93A} mice and from autoptic specimens of sALS patients showed strong immunoreactive for mGluR5 (Aronica *et al.*, 2001).
Similar findings have been reported also in other models of neurological disease, such as HD (Ribeiro *et al*., 2014), AD (Hamilton *et al*., 2016), epilepsy (Ure *et al*., 2016) and fragile X syndrome (Dolen and Bear, 2008), or in cultured astrocytes exposed to metabolic stress (Paquet *et al*., 2013). However, notwithstanding the involvement of mGluR5 in ALS and in other neurological disorders, neither the role of astrocytic mGluR5 nor the alteration of its signalling pathways have been ever deeply investigated.

In our previous studies carried *in-vivo*, both the knocking down (Bonifacino *et al*., 2017) and the complete knock out (Bonifacino *et al*., 2019a) of mGluR5 resulted in an amelioration of the pathological phenotype of SOD1^{G93A} mice and led to a reduced astrogliosis. Similar results were recently obtained after the *in-vivo* treatment of SOD1^{G93A} mice with CTEP, an mGluR5 NAM (Milanese *et al*., under revision).

To obtain the results of this thesis primary astrocyte cultures prepared from spinal cord of 120 days-old SOD1^{G93A} (at the late stage of the disease), age matched WT and SOD1^{G93A}Grm5$^{-/+}$ mice were utilized. This is an important feature of the experiments performed and of the results obtained and the reason why, despite the difficulties to culture and expand astrocytes from adult mice *in-vitro*, we decided to work with these cells, instead of with those isolated from new-born mice, which are almost the sole used worldwide. We believe that astrocyte from late symptomatic mice more correctly recapitulate the cellular and molecular modifications to which astrocytes are subjected *in situ* in the animal model of the disease. Indeed, our astrocytes matured *in-vivo* during the disease progression, spanning from the foetal period to the postnatal pre-symptomatic and symptomatic stages of ALS. Therefore, the activation state evaluated in SOD1^{G93A}-derived astrocytes can be attributed to the chronic exposure to the pathological surrounding milieu, e.g., to the myriad of diverse components that contribute to determine the pathological astrocyte traits. Conversely, the amelioration registered in SOD1^{G93A}Grm5$^{-/+}$ mice can be considered the consequence of

dampening *in-vivo* the contribution of these receptors to the insult-determined cellular damage.

The first obtained results confirmed the efficacy of the genetic partial deletion of mGluR5 in $SOD1^{G93A}Grm5^{-/+}$ astrocytes. My group of research previously demonstrated that the genetic manipulation indeed halved *in-vivo* mGluR5 in $SOD1^{G93A}Grm5^{-/+}$ mice, but no data were available regarding the specific astrocytic expression of mGluR5. With the current experiments we demonstrated that $SOD1^{G93A}$ astrocytes showed high levels of mGluR5 mRNA and overexpressed the protein respect to WT astrocytes, whereas the $SOD1^{G93A}Grm5^{-/+}$ astrocytes produced a significant lower level of mRNA and of the receptor protein. However, western blot investigated the total expression of the receptor in the cell homogenate and further analyses should be carried out to determine the specific membrane expression of mGluR5, which represents the pharmacologically active form of the receptor. In any case, the modulation of the cell status by reducing mGluR5 expression, demonstrated by the experiments discussed below, strongly support that the increase and decrease of mGluR5 total expression likely faces the membrane expression of the receptor.

mGluR5 is coupled with $G_{q/11}$ proteins and the activation of the receptor is linked to the formation of IP3 and the subsequent release of Ca^{2+} from the ER intracellular Ca^{2+} stores. Accordingly, in healthy astrocytes the activation of mGluR5 induces increase of intracellular [Ca^{2+}] (Zur and Deitmer, 2006; Bradley and Challiss, 2011). In ALS, the mGluR5-mediated Ca^{2+} signalling has been shown to be altered (Martorana *et al.*, 2012; Vermeiren *et al*., 2006) representing a very precocious hallmark in experimental models of ALS and patients (Siklos *et al*., 1996; Stifanese *et al*., 2010; Stifanese *et al*., 2014). In light of this evidence, we investigated the intracellular Ca^{2+} oscillations in WT, $SOD1^{G93A}$ and $SOD1^{G93A}Grm5^{-/+}$ astrocytes. $SOD1^{G93A}$ astrocytes showed higher $[Ca^{2+}]_i$ respect to WT cells, both under resting conditions and after stimulus with the Group I mGluRs agonist 3,5-DHPG, possibly resembling the higher membrane expression of these receptors measured in ALS mice. Conversely, reducing the mGluR5 expression in double mutant astrocytes significantly reduced the $[Ca^{2+}]_i$. These results suggest that mGluR5 expression can directly modulate the intracellular calcium release, both under basal conditions and after activation of the receptor. However, the reduction of the excessive $[Ca^{2+}]_i$ present in $SOD1^{G93A}$ astrocytes obtained knocking down mGluR5 is not complete. This implies that also other mechanisms are involved in the homeostasis of this ion, such as calbindin and parvalbumin, two buffering

proteins that are known to be reduced in ALS patients (Ferrer *et al*., 1993). Beside the causes already described in chapter 1.3.4, other important actors actively involved in Ca^{2+} regulation are ions exchangers, among which the Na^{+}/Ca^{2+} exchangers (NCXs). NCXs play an important role in controlling the intracellular Na^{+} and Ca^{2+} dynamics under pathophysiological conditions, with important consequences also on several astrocytic processes (Boscia *et al*., 2016). In particular, the expression of the NCX3 isoform has been found to be strongly reduced in the $SOD1^{G93A}$ mouse, thus impacting on the Ca^{2+} homeostasis (Anzilotti *et al*., 2018). Measuring changes of the multiple actors of the intracellular $[Ca^{2+}]$ control could clarify the regulation of this important multifaceted process under reduced mGluR5 activity.

Knocking down of mGluR5 also positively affected the reactive state of $SOD1^{G93A}$ astrocytes. In physiological conditions, astrocyte activation represents the ability of astrocytes to assume a neuroprotective and regenerative defence toward MNs, related to their so-called A2 status. However, in neurodegenerative disease, such as ALS, this mechanism is exacerbated and astrocytes gain A1-related toxic functions (Verkhratsky and Zorec, 2018). Astrogliosis is often characterized by overexpression of GFAP and S100β (Benninger *et al*., 2016). GFAP is a structural component of astrocytes cytoskeleton and constitutes the type III intermediate filaments of these cells (Tardy *et al*., 1990). Its expression is modulated by several factors including cell development and environmental challenges (see review of Li *et al*., 2019). In physiological conditions GFAP plays an important role in cell communication, blood brain barrier formation and astrocytic plasticity (Kamphuis *et al*., 2014). However, an abnormal expression and regulation of the protein causes the activation of astrocytes, characterized by cell proliferation and hypertrophy of the cell body and processes (see review of Li *et al*., 2019). The upregulation and rearrangements of GFAP can also concur to cause many neurological diseases, among which inflammation, ischemic stroke, traumatic brain injury, and neurodegeneration (Hol and Pekny, 2015; Olabarria M and Goldman JE, 2017). S100β is a calcium binding protein selectively expressed by glial cells. It is involved in several homeostatic functions, such as microtubule assembly, axonal proliferation, astrogliosis, calcium concentration, inflammation and is often dysregulated in ALS. Accordingly, S100β expression is increased in the CSF of patients affected by the disease and its levels are directly correlated with the prognosis of the disease and in cerebral cortex and spinal cord astrocytes and motor neurons of post-mortem ALS patient tissue (Serrano *et al*., 2017). In line with literature (Migheli *et al*., 1999; Benninger *et al*., 2016)

and with the previous *in-vivo* results we obtained in SOD1^{G93A} mouse model (Bonifacino *et al*., 2017), the current experiments demonstrate that SOD1^{G93A} cells display an elevated expression of GFAP and S100β respect to WT cells. Conversely, SOD1^{G93A}Grm5$^{-/+}$ astrocytes show a significantly reduced level of both the proteins respect to SOD1^{G93A} astrocytes. Interestingly, the decrease of S100β has been also demonstrated to affect the expression of pro-inflammatory genes. Accordingly, the silencing of S100β in SOD1^{G93A} astrocytes has been reported to downregulate GFAP, TNF-α, C-X-C motif chemokine ligand 10 (CXCL10) and chemokine (C-C motif) ligand 6 (CCL6) expression (Serrano *et al*., 2017). Therefore, our results suggest a possible positive effect exerted by the knocking down of mGluR5 in modulating inflammation (see below) also through the dampening of S100β.

Another protein strictly related to inflammation is NLRP3. Accordingly, its activation leads to the cleavage of pro-IL-1β and pro-IL-18 to the respective active forms and, consequently, to their secretion by the cell (Mangan *et al*., 2018). NLRP3 has been reported to be increased in ALS (Johann *et al*., 2015; Gugliandolo *et al.*, 2017). In accordance, we detected a dramatic increase of NLRP3 in SOD1^{G93A} astrocytes respect to WT control cells. Interestingly, the partial deletion of mGluR5 reduces this protein level in SOD1^{G93A}Grm5$^{-/+}$ astrocytes, probably contributing to the reduction of IL-1β secretion, which we investigated soon later. Since NLPR3 expression has been evaluated only with western blot, to confirm this result we also planned some immunocytochemical experiments which are currently ongoing.

In the present study the astrocytic morphology was not directly investigated. SOD1^{G93A} and SOD1^{G93A}Grm5$^{-/+}$ astrocytes grow faster and more efficiently than WT cells *in-vitro*. Moreover, the phase contrast microscope observations suggest a more pronounced stellate-like morphology of ALS astrocytes. These data are in accordance with the overexpression of GFAP in SOD1^{G93A} and SOD1^{G93A}Grm5$^{-/+}$ respect to WT cells. However, this marker cannot be the only responsible the cellular morphology (Zhou *et al*., 2019). In-vitro studies analyzing the growth of rodent neonatal astrocytes allowed to distinguish between different cellular morphologies (Burnard Rodnight and Gottfried, 2013). In general, these astrocytes exhibit few processes and show a polygonal fibroblast-like shape. After stimulation, depending on the stimulus nature, process formation can take place, either by *stellation* (a mechanism not involving growth of new membrane) or by *process growth* (requiring protein synthesis because of the extension of long processes over the original boundaries) (Burnard Rodnight and Gottfried, 2013). Although the mechanisms inducing changes of astrocyte morphology are not completely clarified, some of the involved candidates are already known

and may include the gap junction protein connexin 30 (Zhou *et al*., 2019) and the pathways regulated by some GTPase, such as RhoA, Rac1 and Cdc42. Indeed, tonic activation of RhoA pathway maintains the polygonal shape of cultured astrocytes, while its inactivation leads to stellation (Burnard Rodnight and Gottfried, 2013). In light of this evidence, more analyses have to be carried to deepen the morphology of $SOD1^{G93A}Grm5^{-/+}$ astrocytes.

The transgenic mice carrying the G93A mutation in human SOD1, utilized in this project, represent the first animal model created (Gurney *et al*., 1994) and still one of the most widely studied models to understand the pathological mechanisms of fALS because of its ability to generate degeneration of MNs and ALS symptoms close to human disease (Pansarasa *et al.*, 2018; Lutz, 2018). More than 100 mutations of SOD1 have been reported in ALS and the most accredited way by which mutated SOD1 exerts its toxic effects is linked to a gain of function mechanism (Gurney, 2000; Bruijn *et al*., 2004), although other pathological pathways causing MNs injury and death linked to this protein are still unresolved and under study. The hypothesis of toxicity caused by aggregation of mutated SOD1 is particularly attractive because protein aggregates are often associated with neurodegenerative diseases and have been also observed in fALS and sALS patients and in the animal models of the disease. Evidence of altered folding properties of mutant SOD1s has been demonstrated by several *in-vitro* studies (Rodriguez *et al*., 2002; Rakhit *et al*., 2002; Stathopulos *et al*., 2003). Accordingly, mutant SOD1 has been shown to form amyloid-like fibrillary structures (Elam *et al*., 2003). Moreover, SOD1 inclusions were found in neurons and MNs of ALS patients (Kato *et al*., 2000; Liu *et al*., 2009), but not in healthy people (Gruzman *et al*., 2007) suggesting that the protein toxicity might be caused by a higher propensity of SOD1 to get a wrong folding or to aggregate. In accordance, a modified 32 kDa SOD1 polypeptide was detected, together with the well-known 16 kDa SOD1, in spinal cord of fALS and sALS patients (Gruzman *et al*., 2007). This longer polypeptide can acquire toxic properties determining the aggregation of SOD1, in particular in the nuclei of spinal cord astrocytes of ALS patients (Ezzi *et al*., 2007; Forsberg *et al*., 2011). Interestingly, the specific expression of mutant SOD1 in glial cells, neurons or MNs, is unable to induce the pathogenic phenotype observed in the ubiquitous mutant SOD1 transgenic animals (see review of Philips and Rothstein, 2016) indicating the need that mutated SOD1 is expressed both in neurons and glial cells to develop ALS. Accordingly, cell death has been prevented in mutant SOD1 MNs surrounded by wild-type glial cells (Clement *et al*., 2003). The mutated SOD1 expression in

microglia, astrocytes, NG2 oligodendrocyte progenitor cells and oligodendrocytes has been demonstrated to contribute to the selective death of MNs (Boillee *et al*., 2006b; Yamanaka *et al*., 2008a; Kang *et al*., 2013). In the experiments of this study, the dramatic overexpression of misfolded SOD1 in $SOD1^{G93A}$ astrocytes, respect to WT cells was confirmed. Conversely, this high level of misfolded protein is reversed in $SOD1^{G93A}Grm5^{-/+}$ astrocytes. It may be hypothesised that the positive modulation exerted by the knocking down of mGluR5 on the reactive phenotype of $SOD1^{G93A}$ astrocytes could either indirectly favour a reduction of SOD1 aggregation or promote the protein degradation improving the protein quality control system.

This last observation led us to investigate the autophagy efficacy in $SOD1^{G93A}Grm5^{-/+}$ astrocytes by analysing the LC3 level. This protein is involved in the autophagosomes formation. In particular, LC3 is processed into two isoforms: LC3-I and LC3-II (Kabeya *et al.*, 2000; Munz, 2006). The second one is linked to the autophagosomes membrane and is used as a marker of autophagy. Autophagy has been reported to reduce the mutant SOD1-mediated toxicity and its induction decreased the levels of the mutated protein (Kabuta *et al*., 2006). Although a deficiency in autophagy is believed to cause neurodegeneration (Berger *et al*., 2006; Iwata *et al*., 2005; Kabuta *et al*., 2006; Ravikumar *et al*., 2004; Ravikumar *et al*., 2006; Webb *et al*., 2003), an increase of LC3-II has been observed both in $SOD1^{G93A}$ mutant mice and in ALS patients, even if the autophagy was impaired (Li *et al*., 2008; Morimoto *et al*., 2007; Zhang *et al*., 2011). Accordingly, in $SOD1^{G93A}$ mice, the mutated SOD1 has been showed to interact with dynein altering its location and inhibiting the normal fusion of autophagosome-lysosome. Moreover, the efficient autophagic clearance of mutant SOD1 delayed the MN loss, suggesting a positive role of autophagy in ALS (Hetz et al., 2009; Crippa et al., 2010). LC3-II tends to increase with age in spinal cord of $SOD1^{G93A}$ mice, reaching higher levels respect to WT mice, suggesting an increase of autophagosome formation in this ALS mouse model (Morimoto *et al*., 2007). As the disease progresses, the accumulation of autophagic factors is detected not only in spinal cord motor neurons, but also in astrocytes and microglia (Tian *et al*., 2011). One explanation to the increased level of autophagosomes formation in ALS may be represented by the fact that autophagy is upregulated in the attempt to clear the mutated proteins. On the other hand, delaying the clearance of autophagosomes could cause increased autophagosome formation (Morimoto *et al*., 2007). Another explanation for the increase of autophagy in ALS could come from the electron microscopy evidence showing that autophagosomes built-up but did

not reach their matured form of autolysosomes (Li *et al*., 2008; Sasaki, 2011), suggesting an impaired progression of autophagy (Tian *et al*., 2011). Accordingly, an equilibrium exists between autophagosomes formation and its clearance by lysosomes (termed autophagic flux) and it is known that terminal stages of autophagosomes degradation require a correct vesicular trafficking, heterotypic organelle fusion and lysosomal function (Kiselyov *et al*., 2007; Tanida *et al.*, 2005).

In this project the LC3 total expression level and the specific LC3-II form were analysed in our ALS cell model. The results we obtained investigating the total amount of LC3 in $SOD1^{G93A}$ astrocytes are in line with those observed in literature. Accordingly, the expression level of this protein is increased in mutated respect to WT astrocytes. Conversely, $SOD1^{G93A}Grm5^{-/+}$ astrocytes displayed a slight but significative decrease of LC3 expression compared to $SOD1^{G93A}$ astrocytes. Therefore, we can hypothesize that $SOD1^{G93A}Grm5^{-/+}$ astrocytes, which show a less reactive phenotype, can also display an amelioration of the autophagic pathway. Of course, more autophagic markers should be investigated to depict a more complete scenario. An example could be given by the analysis of p62 level, a biomarker to monitor the autophagic flux. This protein possesses dual-binding sites for ubiquitin chains and LC3 and serves as an adaptor between LC3-conjugated autophagosomes and ubiquitin-linked protein aggregates (Bjorkoy *et al*., 2005). p62 has been reported to be associated with mutant SOD1 and LC3 and could link mutant SOD1 to the autophagy machinery. Accordingly, a high expression of p62 in spinal cord of late stage $SOD1^{G93A}$ mice suggested that the fusion of autophagosome to the lysosome is insufficient (Tian *et al*., 2011, Zhang *et al*., 2011).

Unfortunately, the results obtained analysing the specific expression level of LC3-II did not confirm the expected results and are not in line with the ones obtained investigating the total LC3 expression. In accordance, $SOD1^{G93A}$ astrocytes showed a decrease of LC3-II compared to WT cells and $SOD1^{G93A}Grm5^{-/+}$ astrocytes behave in the opposite way as before, displaying an increase of the marker. However, these data are not significative, therefore we planned to repeat them and investigate deeper the autophagic pathway. An example could be given by the investigation of some lysosomal enzymes or by measurement of the clearance time of autophagosomes.

Another feature of animal models and ALS patients is represented by the impairment of the energetic metabolism (Tefera and Borges, 2016). The present study confirmed that ALS astrocytes are characterized by altered aerobic metabolism which is caused by a reduction

of OCR and ATP synthesis, and by the uncoupling of these two pathways. Apparently, this metabolic alteration seems to be reverted by the enhancement of the lactate fermentation. However, SOD1^{G93A} astrocytes consume the same amount of glucose in comparison to WT and SOD1^{G93A}Grm5$^{-/+}$ cells, suggesting a very limited increment of anaerobic metabolism in SOD1^{G93A} astrocytes. On the other hand, all the samples showed a high basal fermentative rate, confirming that astrocytes are characterized by the anaerobic metabolism, devoted to the lactate production to sustain the neuronal energy metabolism needs (Bélanger *et al*., 2011; Aubert *et al*., 2005). Interestingly, these metabolic dysfunctions appear to be reverted in the SOD1^{G93A} Grm5$^{-/+}$ astrocytes, supporting the idea that the overexpression of mGluR5 plays a pivotal role in the astrocytic dysregulation of the energy metabolism in ALS. Moreover, while OCR and ATP synthesis are only partially rescued in SOD1^{G93A} Grm5$^{-/+}$ astrocytes, the efficiency of mitochondrial metabolism seems to rise to levels similar to those of the WT mice, thus limiting the production of oxidative stress. Indeed, when OxPhos is strongly uncoupled, as observed in SOD1^{G93A} astrocytes, the system greatly increases electron leakage through the respiratory complexes favouring the production of reactive oxygen species (Cadenas *et al*., 2000; Ravera *et al*., 2018a).

An early event of the neurodegeneration processes found in SOD1^{G93A} mice is inflammation (Hensley *et al.*, 2002). Together with microglia, astrocytes are involved in the regulation of the immune response of the CNS (Farina *et al*., 2007; Rivest, 2009). Indeed, they can release neurotoxic factors, such as glutamate, NO and pro-inflammatory cytokines (Philips *et al*., 2014). A dysregulation of cytokines production and secretion has been observed in ALS and in several other neurodegenerative disorders (Farina *et al*., 2007; Holden, 2007). An example is represented by the increased expression of TNF-α in spinal cord of SOD1 mutant mice (Bendotti and Carrì, 2004). This cytokine is believed to have a major role in ALS. Indeed, it exert pleiotropic effects in the CNS, affecting the level and the function of growth factors, cytokines, glutamate, monoamine neurotransmitters, AMPA receptors and a wide range of second messenger signalling pathways (Nguyen *et al*., 2004). In the present study we demonstrated that both the production and the release of IL-1β, IL-6 and TNF-α are dramatically increased in SOD1^{G93A} astrocytes respect to WT cells. Conversely, the reduced expression of mGluR5 normalizes the expression and release of the three pro-inflammatory cytokines, suggesting that the genetic strategy could led to an amelioration of the external milieu surrounding MNs.

In order to determine whether the reduction of the mGluR5 expression in SOD1^{G93A} mouse-derived astrocyte and the overall amelioration of the astrocyte phenotype discussed above have a neuroprotective effect on ALS motor neurons, we set up mouse primary astrocyte-MN co-cultures. SOD1^{G93A} mouse embryonic MNs were seeded on SOD1^{G93A} or SOD1^{G93A}Grm5$^{-/+}$ astrocytes and the viability of MNs was assessed between 4-14 days of co-culture. One most relevant achievement of this study was assessing that SOD1^{G93A}Grm5$^{-/+}$ astrocytes decreased MN cell death in MN-astrocyte co-cultures. As a matter of facts, at day 4, MN numbers were comparable between SOD1^{G93A} and SOD1^{G93A}Grm5$^{-/+}$ astrocyte co-cultures; however, from day 6 onwards, MNs co-cultured with SOD1^{G93A} astrocytes displayed a rapid and consistent decline in viability. Dampening mGluR5 made SOD1^{G93A}Grm5$^{-/+}$ astrocytes more supportive towards MNs and significantly slowed down neuronal death, survival reaching the levels of SOD1^{G93A} MN-WT astrocyte co-culture. These results suggest that the less reactive phenotype of astrocytes bearing the partial depletion of mGluR5 significantly reduced their toxicity to MNs, possibly ameliorating of the environment surrounding cells.

Lastly, it was verified whether the acute *in-vivo* manipulation of mGluR5 functions in symptomatic SOD1^{G93A} astrocytes could resemble in a way the *in-vivo* constitutive partial depletion of mGluR5. At this purpose, two different *in-vitro* approaches were exploited: SOD1^{G93A} astrocytes were exposed to a kindly supplied (Ionis Pharmaceuticals^{TM}) mGluR5-directed ASO for 48 h and to the pharmacological treatment with the mGluR5 NAM CTEP for 7 day. The oligonucleotide decreases the mRNA level of mGluR5, respect to scramble-treated SOD1^{G93A} astrocytes and showed to exert positive effects on the reactive state of the cells, reducing the expression of GFAP and S100β proteins. The pharmacological treatment with CTEP also showed positive results. Accordingly, the drug reduces astrogliosis in treated SOD1^{G93A} astrocytes, confirming the *in-vivo* positive effects recently obtained by our group (Milanese *et al.*, under revision). These results show that modifying the mGluR5 function in astrocytes obtained from SOD1^{G93}mice after the disease onset also succeeded in inducing a more beneficial astrocyte phenotype, making it more convincing that astrocytes may take part in the *in-vivo* positive effects of the SOD1^{G93A} mouse treatment with CTEP.

CTEP is an experimental molecule only tested in rodent models of various diseases (Lindemann *et al.*, 2011; Abd-Elrahman *et al.*, 2017; Farmer *et al.*, 2020). Interestingly, other mGluR5 NAMs have been synthetized and tested in human clinical trials for the treatment of disorders other than ALS. In this scenario, basimglurant, an analogue of CTEP,

has been already optimized for human studies (Jaeschke *et al*., 2015; Lindemann *et al*., 2015) and tested in phase III clinical trials for the cure of depression and fragile X syndrome, showing valuable safety and efficacy profiles. (Quiroz *et al*., 2016; Youssef *et al*., 2018). Therefore, on the basis of the present results and on our *in-vivo* animal studies with CTEP, a clinical trial for the treatment of ALS with basimglurant could be proposed.

5.2 Studies on microglia

Microglia represent the other non-neuronal cell type most studied for the important role played in ALS.

During disease progression, microglia dramatically change its characteristics from an anti-inflammatory (M2-like) neuroprotective phenotype to a pro-inflammatory (M1-like) neurotoxic phenotype. Accordingly, the occurrence of these two phenotypes has been recently described in $SOD1^{G93A}$ mice, mainly on the basis of cell morphology. Moreover, several drugs have been tested in animal models to modulate the M1/M2 balance (Cherry *et al*., 2014; Hooten *et al*., 2015; Geloso *et al*., 2017), underlining the non-cell autonomous nature of ALS (Ilieva *et al*., 2009).

Again, the several findings by my research group regarding the role of glutamate excitotoxicity in $SOD1^{G93A}$ mice and the involvement of Group I mGluRs in the disease progression suggested a link between these mechanisms and microglia (Milanese *et al.,* 2014; Bonifacino *et al*., 2017; Bonifacino *et al.,* 2019a). Moreover, mGluR1 and mGluR5 have been found to be expressed on these cells, participating in cell migration (Liu *et al*., 2009) and modulating the inflammatory phenotype (Pinteaux-Jones *et al*., 2008).

This evidence led us to investigate the role of mGluR5 in shaping the properties of this cell population. Therefore, we decided to proceed with molecular and cellular analyses to investigate the expression of mGluR5 in the microglia isolated from $SOD1^{G93A}$ mice at different stages of the disease and the impact of dampening this receptor expression and function in the modulation of the M1/M2 microglial phenotype balance.

Part of this study was carried at Maastricht and Hasselt University and aimed at facing the studies carried in Genoa pointing to the flow cytometry analysing of the protein expression of some pro- and anti-inflammatory markers. RT-qPCR was used to get information about the mRNA expression of the targets.

Experiments were performed using the mRNA extracted from microglia cells acutely isolated from the spinal cord of WT, $SOD1^{G93A}$, $Grm5^{-/+}$ and $SOD1^{G93A}Grm5^{-/+}$ mice. Since the four murine phenotypes were bred in the animal house facility in Genoa and mutated SOD1 were not available in Maastricht or Hasselt Universities, acute spinal cord microglia were purified in Genoa, frozen and sent to Hasselt for mRNA extraction and analysis.

Unfortunately, the amount of RNA obtainable from the biological sample received was too low and of poor quality, possibly due to the biological source. Therefore, many difficulties were experienced in obtaining reliable results, as outlined in the *Results* section, and most of the time was spent to set up the best conditions and to control the various experimental steps. At the end of the copious endeavours, these experiments were suspended because of the lack of suitable biological samples. However, the great experience matured during the attempts to solve the arising problems and check the best experimental conditions, has to be considered unvaluable for the prosecution of these studies in Genoa, where they are at present ongoing.

Briefly, the first experiments have been devoted at validating the best protocol for the RNA isolation. The extraction and purity of high-quality nucleic acids is a critical step for accurate and reliable analyses of gene expression (Bustin *et al*., 2009; Toni *et al*., 2018). The extraction efficiency depends on target density, the adequate homogenization/lysis, the type of biological sample, the genetic complexity, and the amount of the processed material (Bustin *et al*., 2009). Typically, RNA isolation is performed using either the extraction with commercially available silica spin columns kits or phenol-chloroform based RNA extraction. After having tested both the procedures, we decided to use the phenol-chloroform RNA isolation protocol of Toni and colleagues with minor modifications to improve the RNA quality and purity and the accuracy of the RNA quantification (Toni *et al*., 2018). It allows to increase the RNA yield 2.4-93 times than silica column protocols (Deng *et al*., 2005; Santiago-Vazquez *et al*., 2006; Xiang *et al*., 2001); however, it can result in significant RNA contaminations by phenol, chloroform, or salts, that can have an impact on the downstream applications and skew data interpretation (Toni *et al*., 2018). As anticipated, the RNA concentration and the 260/230 absorbance ratio which indicates contaminations of organic compounds (among which chaotropic salts, such as guanidine thiocyanate and guanidine hydrochloride), EDTA, peptides, and phenol, obtained at Nanodrop, were very low. In any case, due to the availability of the samples and to the difficulty to obtain new ones in the short time, we decided to perform the same RT-qPCR experiments.

At this point, another problem raised and regarded the stability of the reference genes, the choice of which can affect the normalization of the results (Vandesompele *et al*., 2002). Since it was found that the genes usually used in the host laboratory in microglia experiments resulted unstable in the experimental conditions utilized, we shifted to an innovative strategy based on the use of EREs/EARs. EREs/EARs are 100-500 bp long, derive from the 7SL RNA part of ribosome complex, contain a common restriction site for Alu I enzyme and have an unknown biological function. They are present in multiple copies and tandemly arrayed throughout approximately 10% of mammalian genome. Therefore, the different expression of a number of genes in the target samples should not influence the EREs/EARs abundance in the transcriptome (Renard *et al.*, 2018). The 11 mouse EREs tested in the present project and already selected in the study of Renard and colleagues (2018) showed a high efficiency in our experimental conditions. The stability of ERE expression was analysed using cultured microglia, astrocytes, OPC, spinal cord enriched microglia from the four different genotypes (WT, $SOD1^{G93A}$, $Grm5^{-/+}$ and $SOD1^{G93A}Grm5^{-/+}$) and brain and spinal cord microglia ad-hoc isolated from WT and $SOD1^{G93A}$ mice. Unfortunately, we always obtained unstable results also with this novel strategy.

At this regard, we hypothesized the presence of bad quality RNA in enriched microglia samples which could have affected the stability of these sequences. Accordingly, Pérez-Novo and colleagues, by analysing the influence of RNA degradation on the stability and expression pattern of different internal control genes, demonstrated that these two parameters are affected by the degradation status of the samples. They also showed that the highly stable genes in intact RNA samples resulted as the most unstable genes in degraded samples and *vice versa* (Pérez-Novo *et al*., 2005).

Therefore, we decided to investigate the RNA integrity, another essential parameter recommended by the Minimum Information for publication of Quantitative Real-Time PCR Experiment (MIQE). The importance of RNA integrity was evaluated by Fleige and colleagues who investigated its impact on the data quantization, mainly on cycle threshold (Ct) values than on PCR efficiency (Fleige *et al*., 2006). They also investigated the effect of the amplified product length on PCR efficiency. They concluded their study by recommending RNA integrity number values above five and PCR products length up to 200 bp as a minimal requirement for a reliable qPCR (Fleige *et al*., 2006).

In the first analysis the effects on the two RNA isolation protocols described above (silica spin columns or phenol-chloroform RNA extraction) on the RNA quality were examined.

Microglia samples acutely isolated from spinal cord mice at the end stage of the disease (120 days old) and belonging to the different genotypes (WT, $Grm5^{-/+}$, $SOD1^{G93A}$, $SOD1^{G93A}Grm5^{-/+}$) were compared and very low RIN values for all the samples analysed were obtained. The same discouraging results were achieved also after checking several other variables, such as freshly isolated RNA samples and microglia acutely isolated from brain and spinal cord mouse tissues with two different genotypes (WT and $SOD1^{G93A}$). The controls (primary microglia and astrocytes cell cultures) showed high RIN values even if their concentrations were lower than expected (< 5ng/ µL). This suggested that RNA integrity does not completely depend on the starting amount of material. Conversely, all the microglia samples acutely isolated from mouse spinal cord and brain showed, again, very low or even undetectable RIN and low concentration.
These results may also explain the low stability of the EREs previously tested.

As to the RNA integrity, we hypothesized a damage of the samples during the isolation protocol of microglia. We excluded the involvement of the shipment because cell pellets always were delivered in 24 h, in dry ice, and. reached the laboratory still frozen. Moreover, mRNA extraction was performed soon after the arrival. Speculating on a possible problem of the microglia to protect our mRNA). Moreover, we plan to test another microglia isolation protocol using the *Adult brain dissociation kit, mouse, and rats* (Miltenyi Biotec, *Cat#* 130-107-677) and *CD11 MicroBeads, human and mouse* (Miltenyi Biotec, *Cat#* 130-049-601) which should improve the yield and the purity of cell preparation.

5.3 Freezing and thawing microglia and astrocyte primary cultures

The results obtained after freezing and thawing primary microglia were encouraging. Cell cultures showed a high purity and managed to grow in culture for a long time after thawing as in the case of freshly isolated samples.
In parallel with the studies with microglia, astrocyte cultures were also tested for survival after thawing with results similar to those obtained with microglia. In the first case, we still found lots of microglia attached in the flasks together with astrocytes. However, this result was quite expected because the immunofluorescence staining was performed few days after shaker from microglia. Therefore, another staining of astrocytes should be done after some passages *in-vitro* to lose all the remaining attached microglia. Because the main interest of this part of the study was represented by microglia, the purity of astrocyte cultures after

thawing was not checked at that time. However, cells were tested for survival and showed the same promising results of microglia.

The results obtained in this part of the study will open to the possibility to freeze and transfer primary glial cells from one laboratory to another, being able to thaw and work on "still alive" cells.

For instance, Professor Prickaerts has a great experience in the study of selective phosphodiesterases (PDEs) and on the involvement of these enzymes in neurodegenerative diseases, including multiple sclerosis, AD, and depression (Prickaerts *et al*., 2017; Heckman *et al*., 2018; Schepers *et al*., 2019; Blokland *et al*., 2019). On the other hand, the research group of Professor Bonanno has developed a great experience in ALS, especially focusing the attention on the role of glutamate excitotoxicity in the pathology and on the non-cell autonomous nature of the disease.

Interestingly, searching on literature there are no data available investigating the role of PDEs in ALS, except for a study of 1992 analysing the general PDEs expression in muscle biopsies of ALS patients (Mishra *et al*., 1992), a review of 2017 (Knott *et al*., 2017) and a recent paper (Chen *et al*., 2020) indicating Ibudilast (a non-selective PDE inhibitor targeting multiple PDE families, such as PDE4 and PDE10) as a possible drug to treat ALS. Therefore, it might be of great interest to investigate the role of these enzymes in modulating the inflammatory pathways of microglia and/or astrocytes isolated from our mouse model of ALS ($SOD1^{G93A}$ mice).

6. CONCLUSIONS

The results here obtained are focused on the investigation of the effect of reducing mGluR5 expression in $SOD1^{G93A}$ astrocytes, thus supporting the data previously obtained *in-vivo* in $SOD1^{G93A}Grm5^{-/+}$ mice and emphasizing the role of mGluR5 in ALS progression. Moreover, they underline the importance of ALS as a non-cell autonomous disease and the impact of astrocytes on MN status.

An innovative aspect of this project relies in the fact that all the data have been obtained using primary astrocytes from adult mice (late symptomatic in the case of $SOD1^{G93A}$ and $SOD1^{G93A}Grm5^{-/+}$ mice), which have matured *in-vivo* during the disease progression and should better recapitulate the severe pathological features of ALS, respect to the new-born mouse cultured astrocytes.

The reduced expression of mGluR5 in $SOD1^{G93A}$ astrocytes determined an amelioration of the reactive state, in particular of the inflammatory phenotype of these cells and modulated several downstream pathways typically affected in ALS astrocytes. Accordingly, the partial depletion of mGluR5 was able to: i) normalize the elevated intracellular calcium concentration; ii) reduce the reactive state of astrocytes; iii) reduce the levels of mutated SOD1 aggregates; iv) improve the energy metabolism and v) decrease the expression and release of pro-inflammatory cytokines.

This inclusive amelioration of the astrocytic phenotype led also to an improvement of $SOD1^{G93A}$ MNs viability, reflecting the important role of astrocytes in affecting the condition of surrounding cells and in counteracting the disease.

The results obtained by the *in-vitro* treatment of $SOD1^{G93A}$ astrocytes with the anti-mGluR5 ASO or the mGlur5 NAM CTEP confirmed the importance of mGluR5 as a target to modulate the reactive phenotype of these cells and suggest that mGluR5 blockade can reasonably turn out to be effective in counteracting ALS.

The consequences of the partial ablation of mGluR5 in $SOD1^{G93A}$ mice could not be investigated with the study of the phenotype of microglia acutely isolated from WT, $Grm5^{-/+}$, $SOD1^{G93A}$ and $SOD1^{G93A}Grm5^{-/+}$ mice. The difficulties based on the quality and the amount of RNA obtained by the samples. However, the experience matured attempting to set up the correct procedures to perform efficient RT-qPCR, has to be considered unvaluable for the prosecution of these studies.

Finally, the method that was validated in Maastricht and Hasselt, aimed at culturing primary microglia and astrocytes after having frozen and thawed previously cultured cells, paves the

way to the possibility of preparing cell cultures from animal models present in one laboratory and sending them to another laboratory to be cultured again for collaborative experiments.

Social impact and translatability of this study

Up to date, no effective cure is available for ALS, which remains a severe and fatal disease, causing death of patients in few years. More recently, the non-cell autonomous facet of the disease has been extensively studied because of the reported involvement of glial cells in MNs death. The present work makes an important contribution to this scientific debate, in particular underling the role of astrocytes in ALS and the link between glial cells and mGluR5, a receptor which is actively implicated in the pathology.

The results obtained *in-vivo* and *in-vitro* after knocking down mGluR5 in $SOD1^{G93A}$ mouse model of ALS suggest that this receptor may represent a valuable target, the blockade of which positively modulates the phenotype of astroglia and in turn rescues MNs survival. In-vivo, the pharmacological treatment of $SOD1^{G93A}$ mice with CTEP increase survival and ameliorates disease progression and, at the same time, reduces also astrogliosis (Milanese *et al*., under revision). The experiments carried *in-vitro* with CTEP, which reduces the astrocyte activation state, further support the role of astrocytes in fostering the *in-vivo* effects of the drug.

Of note, the analogue of CTEP, basimglurant, has been already optimized for human studies (Jaeschke *et al*., 2015; Lindemann *et al*., 2015) and tested in clinical trials for the treatment of fragile X syndrome and depression (Quiroz *et al*., 2016; Youssef *et al*., 2018). Therefore, in light of these encouraging results, and due to already available studies of pharmacokinetics and toxicology of basimglurant, it may be of interest to test its efficacy also in ALS patients.

7. BIBLIOGRAPHY

Abd-Elrahman KS, Hamilton A, Hutchinson SR, Liu F, Russell RC,Ferguson SSG, **2017**. *mGluR5 antagonism increases autophagy and prevents disease progression in the zQ175 mouse model of Huntington's disease*. Sci Signal. 10 (510).

Abe K, Itoyama Y, Sobue G, *et al.,* **2014**. *Confirmatory double-blind, parallel-group, placebo-controlled study of efficacy and safety of edaravone (MCI-186) in amyotrophic lateral sclerosis patients*. Amyotroph Lateral Scler Frontotemporal Degener 15: 610-617.

Abe K and The Writing Group on behalf of the Edaravone (MCI-186) ALS 19 Study Group, **2017**. *Safety and efficacy of edaravone in well-defined patients with amyotrophic lateral sclerosis: a randomised, double-blind, placebo-controlled trial.* Lancet Neurol 16: 505-512.

Ahn Jee-Yin and Ye Keqiang, **2005**. *PIKE GTPase signaling and function*. Int J Biol Sci., 1 (2): 44-50.

Aizawa H, Sawada J, Hideyama T, Yamashita T, Katayama T, Hasebe N, Kimura T, Yahara O, Kwak S, 2010. *TDP-43 pathology in sporadic ALS occurs inmotor neurons lacking the RNA editing enzyme ADAR2*. Acta Neuropathol. 120 (1): 75-84.

Al-Chalabi A and Leigh PN, **2000**. *Recent advances in amyotrophic lateral sclerosis*. Curr Opin Neurol 13(4): 397-405.

Al-Chalabi A, Jones A, Troakes C, King A, Al-Sarraj S, van den Berg LH, **2012**. *The genetics and neuropathology of amyotrophic lateral sclerosis*. Acta Neuropathol 124: 339-352.

Alexianu ME, Ho BK, Mohamed AH, La Bella V, Smith RG, Appel SH, **1994**. *The role of calcium-binding proteins in selective motoneuron vulnerability in amyotrophic lateral sclerosis*. Ann Neurol 36: 846-858.

Alfei S and Baig I, **2017**. *An optimized and very detailed, grams scale synthesis of CTEP, through a complete characterization of all the isolated and purified intermediates*. Org. Commun. 10, 2: 114-121.

Allaman I, Bélanger M, Magistretti PJ, **2011.** *Astrocytes-neuron metabolic relationships: for better and for worse***.** Trends in Neurosciences, Vol. 34, No. 2.

Allaoua H, Chaudieu I, Krieger C, Boksa P, Privat A, Quirion R, **1992.** *Alterations in spinal cord excitatory amino acid receptors in amyotrophic lateral sclerosis patients*. Brain Res. 579 (1):169-172.

Allen SP, Hall B, Castelli LM, Francis L, Woof R, Siskos AP, Kouloura E, Gray E, Thompson AG, Talbot K, Higginbottom A, Myszczynska M, Allen CF, Stopford MJ, Hemingway J, Bauer CS, Webster CP, De Vos KJ, Turner MR, Keun HC, Hautbergue GM, Ferraiuolo L, Shaw PJ, **2019**. *Astrocyte adenosine deaminase loss increases motor neuron toxicity in amyotrophic lateral sclerosis*. Brain. 142 (3): 586-605.

Allen S, Heath PR, Kirby J, Wharton SB, Cookson MR, Menzies FM, Banks RE, Shaw PJ, **2003**. *Analysis of the cystolic proteome in a cell culture model of familial amyotrophic lateral sclerosis reveals alterations to the proteosome, antioxidant defenses and nitric oxide synthetic pathways*. J. Biol. Chem. 278: 63716383.

Akira S, Uematsu S, Takeuchi O, **2006**. *Pathogen recognition and innate immunity*. Cell 124: 783-801.

Andersen PM, Forsgren L, Binzer M, Nilsson P, Ala-Hurula V, Keränen ML, *et al*., **1996**. *Autosomal recessive adult-onset amyotrophic lateral sclerosis associated with homozygosity for Asp90Ala CuZn-superoxide dismutase mutation: a clinical and genealogical study of 36 patients*. Brain 119: 1153-1172.

Andersen PM. **2006**. *Amyotrophic lateral sclerosis associated with mutations in the Cu/Zn superoxide dismutase gene*. Curr Neurol Neurosci Rep. 6 (1): 37-46.

Anneser JM, Borasio GD, Berthele A, Zieglgänsberger W, Tölle TR, **1999**. *Differential Expression of Group I Metabotropic Glutamate Receptors in Rat Spinal Cord Somatic and Autonomic Motoneurons: Possible Implications for the Pathogenesis of Amyotrophic Lateral Sclerosis.* Neurobiology of Disease 6: 140-14.

Anneser JM, Ince PG, Shaw PJ, Borasio GD, **2004a**. *Differential expression of mGluR5 in human lumbosacral motoneurons*. Neuroreport. 15 (2): 271-273.

Anneser JM, Chahli C, Ince PG, Borasio, GD, Shaw PJ, **2004b**. *Glial proliferation and metabotropic glutamate receptor expression in amyotrophic lateral sclerosis*. J. Neuropathol. Exp. Neurol. 63: 831-840.

Annoura H, Fukunaga A, Uesugi M, Tatsuoka T, Horikawa Y, **1996**. *A novel class of antagonists for metabotropic glutamate receptors, 7 (hydroxyimino)cyclopropa[b]chromen-1a-carboxylates*. Bioorg. Med. Chem. Lett. 6: 763-766.

Anzilotti S, Brancaccio P, Simeone G, Valsecchi V, Vinciguerra A, Secondo A, Petrozziello T, Guida N, Sirabella R, Cuomo O, Cepparulo P, Herchuelz A, Amoroso S, Di Renzo G, Annunziato L and Giuseppe Pignataro, **2018**. *Preconditioning, induced by sub-toxic dose of the neurotoxin L-BMAA, delays ALS progression in mice and prevents Na+/Ca2+ exchanger 3 downregulation*. Cell Death and Disease 9: 206.Arai T, Hasegawa M, Akiyama H, Ikeda K, Nonaka T, Mori H, Mann D, Tsuchiya K, Yoshida M, Hashizume Y, Oda T, **2006**. *TDP-43 is a component of ubiquitin-positive tau-negative inclusions in frontotemporal lobar degeneration and amyotrophic lateral sclerosis*. Biochem. Biophys. Res. Commun. 351: 602-611.

Archbold HC, Jackson KL, Arora A, Weskamp K, Tank EMH, Li X, Miguez R, Dayton RD, Tamir S, Klein RL & Barmada SJ, **2018.** *TDP43 nuclear export and neurodegeneration in models of amyotrophic lateral sclerosis and frontotemporal dementia*. Sci. Rep. 8: 4606.

Armada-Moreira A, Gomes JI, Pina C, Savchak OK, Gonçalves-Ribeiro J, Rei N, Pinto S, Morais ST, Martins RS, Ribeiro FF, Sebastião AM, Crunelli V and Vaz SH, **2020**. *Going the Extra (Synaptic)Mile: Excitotoxicity as the RoadToward Neurodegenerative Diseases*. Front. Cell. Neurosci. 14:90.

Aronica E, Catania MV, Geurts J, Yankaya B, Troost D, **2001**. *Immunohistochemical localization of group I and II metabotropic glutamate receptors in control and amyotrophic lateral sclerosis human spinal cord: upregulation in reactive astrocytes*. Neuroscience., 105 (2): 509-520.

Aronica E, Gorter JA, Ijlst-Keizers H, Rozemuller AJ, Yankaya B, Leenstra S, Troost D, **2003**. *Expression and functional role of mGluR3 and mGluR5 in human astrocytes and*

glioma cells: opposite regulation of glutamate transporter proteins. Eur. J. Neurosci. 17: 2106-2118.

Arriza JL, Eliasof S, MP Kavanaugh MP, Amara SG, **1997**. *Excitatory amino acid transporter 5, a retinal glutamate transporter coupled to a chloride conductance*. Proc Natl Acad Sci USA 94: 4155-4160.

Arsova A, Møller TC, Vedel L, Hansen JL, Foster SR, Gregory KJ and Bräuner-Osborne H, **2020**. *Detailed in-vitro Pharmacological Characterization of Clinically Tested Negative Allosteric Modulators of the Metabotropic Glutamate Receptor 5 (mGlu5).* Mol Pharmacol. 98 (1): 49-60.

Ash PEA, Bieniek KF, Gendron TF, Caulfield T, Lin WL, Dejesus-Hernandez M, van Blitterswijk MM, Jansen-West K, Paul JW, Rademakers R, Boylan KB, Dickson DW, Petrucelli L, **2013.** *Unconventional translation of C9ORF72 GGGGCC expansion generates insoluble polypeptides specific to c9FTD/ALS*. Neuron 77, 639-646.

Aubert A, Costalat R, Magistretti PJ, Pellerin L, **2005**. *Brain lactate kinetics: Modeling evidence for neuronal lactate uptake upon activation*. Proc Natl Acad Sci U S A. 102: 16448-16453.

Ayala YM, Zago P, D'Ambrogio A, Xu YF, Petrucelli L, Buratti L, Baralle FE, **2008**. *Structural determinants of the cellular localization and shuttling of TDP-43*. J. Cell Sci. 121, 3778-3785.

Balázs R, Miller S, Chun Y, O'Toole TJ, Cotman CW, **1998**. *Metabotropic glutamate receptor agonists potentiate cyclic AMP formation induced by forskolin or beta-adrenergic receptor activation in cerebral cortical astrocytes in culture*. J Neurochem., 70 (6): 2446-2458.

Ban J, Sámano C, Mladinic M, Munitic I, **2019**. *Glia in amyotrophic lateral sclerosis and spinal cord injury: common therapeutic targets*. Croat. Med. J. 60: 109-120.

Bano D, Young KW, Guerin CJ, Lefeuvre R, Rothwell NJ, Naldini L, *et al*., **2005**. *Cleavage of the plasma membrane NaC/Ca2C exchanger in excitotoxicity*. Cell 120: 275-285.

Bar PR, **2000**. *Motor neuron disease in-vitro: the use of cultured motor neurons to study amyotrophic lateral sclerosis*. Eur. J. Pharmacol. 405, 285-95.

Barger SW and Van Eldik LJ, **1992**. *S100β stimulates calcium fluxes in glial and neuronal cells*. The journal of biological chemistry, 267 (14): 9689-9694.

Barres BA, **2008**. *The mystery and magic of Glia: a perspective on their roles in health and disease*. Neuron Perspective 60.

Bartzokis G, **2004**. *Age-related myelin breakdown: a developmental model of cognitive decline and Alzheimer's disease*. Neurobiol. Aging 25 (1): 5-18.

Battaglia G and Bruno V, **2018**. *Metabotropic glutamate receptor involvement in the pathophysiology of amyotrophic lateral sclerosis: new potential drug targets for therapeutic applications*. Current Opinion in Pharmacology 38: 65-71.

Becker LA, Huang B, Bieri G, Ma R, Knowles DA, Jafar-Nejad P, Messing J, Kim HJ, Soriano A, Auburger G, Pulst SM, Taylor JP, Rigo F, Gitler AD, **2017**. *Therapeutic*

reduction of ataxin-2 extends lifespan and reduces pathology in TDP-43 mice. Nature 544:367.

Beers DR, Henkel JS, Xiao Q, Zhao W, Wang J, Yen AA, Siklos L, McKercher SR, Appel SH, **2006**. *Wild-type microglia extend survival in PU.1 knockout mice with familial amyotrophic lateral sclerosis*. Proc. Natl. Acad. Sci USA 103: 16021-16026.

Beers DR, Henkel JS, Zhao W, Wang J, Huang A, Wen S, Liao B, Appel SH, **2011a**. *Endogenous regulatory T lymphocytes ameliorate amyotrophic lateral sclerosis in mice and correlate with disease progression in patients with amyotrophic lateral sclerosis*. Brain 134: 1293-1314.

Beers DR, Zhao W, Liao B, Kano O, Wang J, Huang A, Appel SH, Henkel JS, **2011b**. *Neuroinflammation modulates distinct regional and temporal clinical responses in ALS mice*. Behav. Immun. 25: 1025-1035.

Beers DR, Zhao W, Wang J, Zhang X, Wen S, Neal D, Thonhoff JR, Alsuliman AS, Shpall EJ, Rezvani K, Appel SH, **2017**. *ALS patients' regulatory T lymphocytes are dysfunctional, and correlate with disease progression rate and severity*. JCI Insight 2 (5): e89530.

Bélanger M, Allaman I, Magistretti PJ, 2011. *Brain Energy Metabolism: Focus on Astrocyte-Neuron Metabolic Cooperation*. Cell Metab. Cell Press 14: 724-738.

Bellezza I, Grottelli S, Costanzi E, Scarpelli P, Pigna E, Morozzi G, Mezzasoma L, Peirce MJ, Moresi V, Adamo S, Minelli A, **2018**. *Peroxynitrite Activates the NLRP3 Inflammasome Cascade in SOD1(G93A) Mouse Model of Amyotrophic Lateral Sclerosis*. Mol Neurobiol. 55 (3): 2350-2361.

Bellingham MC, **2011**. *A review of the neural mechanisms of action and clinical efficiency of Riluzole in treating amyotrophic lateral sclerosis: what have we learned in the last decade?* CNS Neurosci Ther 17: 4-31.

Bendotti C, Tortarolo M, Suchak SK, Calvaresi N, Carvelli L, Bastone A, Rizzi M, Rattray M, Mennini T, **2001.** *Transgenic SOD1 G93A mice develop reduced GLT-1 in spinal cord without alterations in cerebrospinal fluid glutamate levels*. J. Neurochem. 79: 737-746.

Bendotti C and Carrì MT, **2004**. *Lessons from models of SOD1-linked familial ALS*. Trends in Molecular Medicine 10 (8), 393-400.

Benninger F, Glat MJ, Offen D, Steiner I, **2016**. *Glial fibrillary acidic protein as a marker of astrocytic activation in the cerebrospinal fluid of patients with amyotrophic lateral sclerosis*. J Clin Neurosci. 26: 75-78.

Bensimon G, Lacomblez L, Meininger V, **1994**. *A controlled trial of riluzole in amyotrophic lateral sclerosis. ALS/Riluzole study group*. N Engl J Med 330: 585-591.

Bentmann E, Neumann M, Tahirovic S, Rodde R, Dormann D, Haass C, **2012**. *Requirements for stress granule recruitment of fused in sarcoma (FUS) and TAR DNA-binding protein of 43 kDa (TDP-43).* J Biol Chem 287: 23079-23094.

Berger Z, Ravikumar B, Menzies FM, Oroz LG, Underwood BR, Pangalos MN, Schmitt I, Wullner U, Evert BO, O'Kane CJ, Rubinsztein DC, **2006.** *Rapamycin alleviates toxicity of different aggregate-prone proteins*. Hum. Mol. Genet. 15: 433-442.

Bernard-Marissal N, Medard JJ, Azzedine H, Chrast R. Dysfunction inendoplasmic reticulum-mitochondria crosstalk underlies SIGMAR1 loss offunction mediated motor neuron degeneration. Brain. 2015 Apr;138 (Pt 4): 875-90.

Bezzi P and Volterra A, **2014**. *Imaging exocytosis and recycling of synaptic-like microvesicles in astrocytes*. Cold Spring Harbor Protocols, 2014.

Bianchi G, Martella R, Ravera S, Marini C, Capitanio S, Orengo, A, Emionite L, Lavarello C, Amaro A, Petretto A, Pfeffer U, Sambuceti G, Pistoia V, Raffaghello L, Longo VD**, 2015**. *Fasting induces anti-Warburg effect that increases respiration but reduces ATP-synthesis to promote apoptosis in colon cancer models*. Oncotarget, 6, 11806-11819.

Bigio EH, **2011**. *C9ORF72, the new gene on the block, causes C9FTD/ALS: new insights provided by neuropathology.* Acta Neuropathol 122 (6): 653-655.

Bilsland LG, Sahai E, Kelly G, Golding M, Greensmith L, Schiavo G, **2010**. *Deficits in axonal transport precede ALS symptoms in-vivo*. Proc Natl Acad Sci USA 107 (47): 20523-20528.

Blokhuis AM, Groen EJN, Koppers M, van den Berg LH, Pasterkamp RJ, **2013**. *Protein aggregation in amyotrophic lateral sclerosis*. Acta Neuropathol 125:777-794.

Blokland A, Heckman P, Vanmierlo T, Schreiber R, Paes D, Prickaerts J **2019**. Phosphodiesterase Type 4 Inhibition in CNS Diseases. Trends in Pharmacological Sciences, Vol. 40, No. 12.

Bjorkoy G, Lamark T, Brech A, Outzen H, Perander M, Overvatn A, Stenmark H, Johansen T, **2005**. *p62/SQSTM1 forms protein aggregates degraded by autophagy and has a protective effect on huntingtin-induced cell death*. J Cell Biol 171:603-614.

Boillée S, Vande C, Cleveland DW, **2006a**. *ALS: a disease of motor neurons and their nonneuronal neighbors*. Neuron., 52 (1): 39-59.

Boillée S, Yamanaka K, Lobsiger CS, Copeland NG, Jenkins NA, Kassiotis G, Kollias G, Cleveland DW, **2006b**. Onset and Progression in Inherited ALS Determined by Motor Neurons and Microglia. Science Vol 312: 1390-1392.

Boltz-Nitulescu G, Wiltschke C, Holzinger C *et al*., 1987. *Differentiation of rat bone marrow cells into macrophages under the influence of mouse L929 cell supernatant*. *Journal of Leukocyte Biology*, 41, 1: 83-91.

Bombeiro AL, Hell RC, Simões GF, de Castro MV, de Oliveira ALR, **2017**. *Importance of major histocompatibility complex of class I (MHC-I) expression for astroglial reactivity and stability of neural circuits in-vitro*. Neurosci. Lett. 647: 97-103.

Bonifacino T, Musazzi L, Milanese M, Seguini M, Marte A, Gallia E, Cattaneo L, Onofri F, Popoli M, Bonanno G, **2016**. *Altered mechanisms underlying the abnormal glutamate release in amyotrophic lateral sclerosis at a pre-symptomatic stage of the disease*. Neurobiol Dis. 95, 122-133.

Bonifacino T, Cattaneo L, Gallia E, Puliti A, Melone M, Provenzano F, Bossi S, Musante I, Usai C, Conti F, Bonanno G, Milanese M, **2017**. *In-vivo effects of knocking down metabotropic glutamate receptor 5 in the SOD1G93A mouse model of amyotrophic lateral sclerosis*. Neuropharmacology 123: 433-445.

Bonifacino T, Provenzano F, Gallia E, Ravera S, Torazza C, Bossi S, Ferrando S, Puliti A, Van Den Bosch L, Bonanno G, Milanese M, **2019a**. *In-vivo genetic ablation of metabotropic glutamate receptor type 5 slows down disease progression in the SOD1G93A mouse model of amyotrophic lateral sclerosis*. Neurobiology of Disease 129: 79-92.

Bonifacino T, Rebosio C, Provenzano F, Torazza C, Balbi M, Milanese M, Raiteri L, Usai C, Fedele E, Bonanno G, **2019b**. *Enhanced Function and Overexpression of Metabotropic Glutamate Receptors 1 and 5 in the Spinal Cord of the SOD1G93A Mouse Model of Amyotrophic Lateral Sclerosis during Disease Progression.* Int. J. Mol. Sci., 20, 4552.

Boscia F, Begum G, Pignataro G, Sirabella R, Cuomo O, Casamassa A, Sun D and Annunziato L, **2016**. *Glial Na+-dependent Ion Transporters in Pathophysiological Conditions*. Glia 64 (10): 1677-1697.

Bradford MM, **1976**. *A rapid and sensitive method for the quantitation of microgram quantities of protein utilizing the principle of protein-dye binding.* Anal Biochem. 72: 248-254.

Bradley SJ, Watson JM, Challiss RA, **2009**. *Effects of positive allosteric modulators on single-cell oscillatory Ca2+ signaling initiated by the type 5 metabotropic glutamate receptor*. Molecular Pharmacology, 76: 1302-1313.

Brand MD, **2010**. *The sites and topology of mitochondrial superoxide production.* Experimental Gerontology 45 (7- 8): 466-472.

Brown HA and Murphy RC, **2009**. *Working towards an exegesis for lipids in biology*. Nat Chem Biol. 5 (9) :602-606.

Brownell A, Kuruppu D, Kil KE, Jokivarsi K, Poutiainen P, Zhu A, Maxwell M, **2015**. *PET imaging studies show enhanced expression of mGluR5 and inflammatory response during progressive degeneration in ALS mouse model expressing SOD1-G93A gene*. J Neuroinflam, 12:217.

Bruijn LI, Becher MW, Lee MK, Anderson KL, Jenkins NA, Copeland NG, Sisodia SS, Rothstein JD, Borchelt DR, Price DL, Cleveland DW, **1997**. *ALS-linked SOD1 mutant G85R mediates damage to astrocytes and promotes rapidly progressive disease with SOD1-containing inclusions*. Neuron 18, 327-338.

Bsibsi M, Ravid R, Gveric D, van Noort JM, **2002**. *Broad expression of toll-like receptors in the human central nervous system*. J. Neuropathol. Exp. Neurol. 61: 1013-1021.

Bsibsi M, Persoon-Deen C, Verwer RW, Meeuwsen, S, Ravid R, Van Noort JM, **2006.** Toll-like receptor 3 on adult human astrocytes triggers production of neuroprotective mediators. Glia 53, 688-695.

Buratti E and Baralle FE, **2010**. *The multiple roles of TDP-43 in pre-mRNA processing and gene expression regulation*. RNA Biol. 7, 420-429.

Burk K and Pasterkamp RJ, **2019**. *Disrupted neuronal trafficking in amyotrophic lateral sclerosis*. Acta Neuropathologica 137: 859-877.

Bush TG, Puvanachandra N, Horner CH, Polito A, Ostenfeld T, Svendsen CN, Mucke L, Johnson MH, Sofroniew MV, **1999**. *Leukocyte infiltration, neuronal degeneration, and*

neurite outgrowth after ablation of scar-forming, reactive astrocytes in adult transgenic mice. Neuron 23, 297-308.

Bustin SA, Benes V, Garson JA, Hellemans J, Huggett J, Kubista M, Mueller R, Nolan T, Pfaffl MW, Shipley GL, Vandesompele J, Wittwer CT, **2009**. *The MIQE Guidelines: Minimum Information for Publication of Quantitative Real-Time PCR Experiments*. Clinical Chemistry 55, 4: 611-622.

Cadenas E and Davies KJA, **2000**. *Mitochondrial free radical generation, oxidative stress, and aging.* Free Radic Biol Med. 29: 222-230.

Cahoy JD, Emery B, Kaushal A, Foo LC, Zamanian JL, Christopherson KS, Xing Y, Lubischer JL, Krieg PA, Krupenko SA, Thompson WJ, Barres BA, **2008**. *A transcriptome database for astrocytes, neurons, and oligodendrocytes: a new resource for understanding brain development and function.* J. Neurosci. 28, 264-278.

Caraci F, Battaglia G, Sortino MA, Spampinato S, Molinaro G, Copani A, Nicoletti F, Bruno V, **2012**. *Metabotropic glutamate receptors in neurodegeneration/neuroprotection: still a hot topic?* Neurochem. Int., 61 (4): 559-65.

Carrì MT, Ferri A, Battistoni A, Famhy L, Gabbianelli R, Poccia F, Rotilio G, **1997**. *Expression of a Cu,Zn superoxide dismutase typical of familial amyotrophic lateral sclerosis induces mitochondrial alteration and increase of cytosolic Ca2+ concentration in transfected neuroblastoma SH-SY5Y cells*. FEBS Lett.,414 (2): 365-368.

Cartmell J and Schoepp DD, **2000**. *Regulation of neurotransmitter release by metabotropic glutamate receptors*. J Neurochem., 75 (3): 889-907.

Cassina P, Cassina A, Pehar M, Castellanos R, Gandelman M, de León A, Robinson KM, Mason RP, Beckman JS, Barbeito L and Radi R, **2008**. *Mitochondrial dysfunction in SOD1G93A-bearing astrocytes promotes motor neuron degeneration: prevention by mitochondrial-targeted antioxidants*. J. Neurosci. 28, 4115-4122.

Cauli O, Llansola M, Rodrigo R, El Mlili N, Errami M, Felipo V, **2005**. *Altered modulation of motor activity by group I metabotropic glutamate receptors in the nucleus accumbens in hyperammonemic rats*. Metab Brain Dis 20 (4): 347-358.

Cereda C, Leoni E, Milani P, Pansarasa O, Mazzini G, Guareschi S, Alvisi E, Ghiroldi A, Diamanti L, Bernuzzi S, Ceroni M, Cova E, **2013**. *Altered intracellular localization of SOD1 in leukocytes from patients with sporadic amyotrophic lateral sclerosis*. PLoS One. 8 (10): e75916.

Charcot JM and Joffroy A, **1869**. *Deux cas d'atrophie musculaire progressive avec lésions de la substance grise et des faisceaux antéraux de la moelle épinière*. Arch Physiol Neurol Pathol. 2:744-754.

Cherry JD., Olschowka JA., O'Banion MK., **2014**. *Neuroinflammation and M2 microglia:the good, the bad and the inflamed.* J Neuroinflammation 11:98.

Chiò A, Battistini S, Calvo A, Caponnetto C, Conforti FL, Corbo M, Giannini F, Mandrioli J, Mora G, Sabatelli M, ITALSGEN Consortium, Ajmone C, Mastro E, Pain D, Mandich P, Penco S, Restagno G, Zollino M, Surbone A, **2014**. *Genetic counselling in ALS: Facts, uncertainties and clinical suggestions*. J. Neurol. Neurosurg. Psychiatry 85, 478-485.

Chiò A, Mazzini L, Mora G, **2020**. *Disease-modifying therapies in amyotrophic lateral sclerosis*. Neuropharmacology 167: 107986.

Chiry O, Pellerin L, Monnet-Tschudi F, Fishbein WN, Merezhinskaya N, Magistretti PJ, Clarke S, **2011.** *Expression of monocarboxylate transporter MCT1 in the adult human brain cortex*. Brain Res. 1070 (1): 65-70.

Chiu IM, Morimoto ETA, Goodarzi H, Liao JT, O'Keeffe S, Phatnani HP, Muratet M, Carroll MC, Levy S, Tavazoie S, Myers RM, Maniatis T, **2013**. *A neurodegeneration-specific-gene-espression signature of acutely isolated microglia from an amyotrophic lateral sclerosis mouse model*. Cell Rep. 4: 385-401.

Chomczynski P and Sacchi N, 1987. *Single-step method of RNA isolation by acid guanidinium thiocyanate–phenol–chloroform extraction*. Anal. Biochem. 162: 156-159.

Chomczynski P and Sacchi N, 2006. *The single-step method of RNA isolation by acid guanidinium thiocyanate–phenol–chloroform extraction: twenty-something years on*. Nat. Protoc. 1: 581-585.

Ciechanover A, **2006**, *The ubiquitin proteolytic system: from a vague idea, through basic mechanisms, and onto human diseases and drug targeting*. Neurology 66: 7-19.

Cirulli E, Lasseigne BN, Petrovski S, Sapp PC, Dion PA, Leblond CS, Couthouis J, Lu YF, Wang Q, Krueger BJ, Ren Z, Keebler J, Han Y, Levy SE, Boone BE, Wimbish JR, Waite LL, Jones AL, Carulli JP, Day-Williams AG, Staropoli JF, Xin WW, Chesi A, Raphael AL, McKenna-Yasek D, Cady J, Vianney de Jong JMB, Kenna KP, Smith BN, Topp S, Miller J, Gkazi A, FALS Sequencing Consortium, Al-Chalabi A, Van den Berg LH, Veldink J, Silani V, Ticozzi N, Shaw CE, Baloh RH, Appel S, Simpson E, Lagier-Tourenne C, Pulst SM, Gibson S, Trojanowski JQ, Elman L, McCluskey L, Grossman M, Shneider NA, Chung WK, Ravits JM, Glass JD, Sims KB, Van Deerlin VM, Maniatis T, Hayes SD, Ordureau A, Swarup S, Landers J, Baas J, Allen AS, Bedlack RS, Harper JW, Gitler AD, Rouleau GA, Brown R, Harms MB, Cooper GM, Harris T, Myers RM, Goldstein DB, 2015. *Exome sequencing in amyotrophic lateral sclerosis identifies risk genes and pathways*. Science 347: 1436-1441.

Clark BP, Baker R, Goldsworthy J, Harris JR, Kingston AE, **1997**. *(+)-2-methyl-4-carboxyphenylglycine (LY367385) selectively Antagonises metabotropic glutamate mglur1 receptors.* Bioorganic & Medicinal Chemistry Letters, 7 (21): 2777-2780.

Clement AM, Nguyen MD, Roberts EA, Garcia ML, Boillée S, Rule M, McMahon AP, Doucette W, Siwek D, Ferrante RJ, Brown Jr RH, Julien JP, Goldstein LSB, Cleveland DW, **2003**. *Wildtype nonneuronal cells extend survival of SOD1 mutant motor neurons in ALS mice*. Science. 302: 113-117.

Cleveland DW and Rothstein JD, **2001**. *From Charcot to Lou Gehrig: deciphering selective motor neuron death in ALS*. Nat. Rev. Neurosci. 2: 806-819.

Cluskey S and Ramsden DB, **2001**. *Mechanisms of neurodegeneration in amyotrophic lateral sclerosis.* Journal of Clinical Pathology Molecular Pathology 54, 386-392.

Cohen TJ, Hwang, AW, Unger T, Trojanowski, JQ, Lee VMY, **2012**. *Redox signalling directly regulates TDP-43 via cysteine oxidation and disulphide cross-linking*. EMBO J. 31: 1241-1252.

Cohen TJ, **2015**. *An acetylation switch controls TDP-43 function and aggregationpropensity*. Nat Commun. 6:5845. doi: 10.1038/ncomms6845.

Conn PJ and Pin JP, **1997**. *Pharmacology and functions of metabotropic glutamate receptors*. Annual Review of Pharmacology and Toxicology, 37, 205-237.

Cosford NDP, Tehrani L, Roppe J, Schweiger E, Smith ND, Anderson J, Bristow L, Brodkin LJ, Jiang X, McDonald I, Rao S, Washburn M, Varney MA, **2012**. *3-[(2-Methyl-1,3-thiazol-4-yl) ethynyl]-pyridine: a potent and highly selective metabotropic glutamate subtype 5 receptor antagonist with anxiolytic activity*. J. Med. Chem 46 (2): 204-206.

Coussee E, De Smet P, Bogaertbc E, Elensa I, Van Damme P, Willems P, Koopmand W, Van Den Bosch L, Callewaert G, **2010**. *G37R SOD1 mutant alters mitochondrial complex activity, Ca2+ uptake and ATP production*. Cell Calcium 49: 217-225.

Cozzolino M, Pesaresi MG, Gerbino V, Grosskreutz J, Carrì MT, **2012**. *Amyotrophic lateral sclerosis: new insights into underlying molecular mechanisms and opportunities for therapeutic intervention*. Antioxid Redox Signal.,17(9):1277-1330.

Crippa V, Sau D, Rusmini P, Boncoraglio A, Onesto E, Bolzoni E, Galbiati M, Fontana E, Marino M, Carra S, Bendotti C, De Biasi S, Poletti A, **2010**. *The small heat shock protein B8 (HspB8) promotes autophagic removal of misfolded proteins involved in amyotrophic lateral sclerosis (ALS)*. Hum Mol Genet.; 19: 3440-3456.

Cudkowicz ME, Titus S, Kearney M, Yu H, Sherman A, Schoenfeld D, Hayden D, Shui A, Brooks B, Conwit R, Felsenstein D, Greenblatt DJ, Keroack M, Kissel JT, Miller R, Rosenfeld J, Rothstein JD, Simpson E, Tolkoff-Rubin N, Zinman L, Shefner JM, Ceftriaxone Study Investigators., **2014**. *Safety and efficacy of ceftriaxone for amyotrophic lateral sclerosis: a multi-stage, randomised, double-blind, placebo controlled trial.* Lancet Neurol 13: 1083-1091.

D'Antoni S, Berretta A, Bonaccorso CM, Bruno V, Aronica E, Nicoletti F, Catania MV, **2008**. *Metabotropic glutamate receptors in glial cells*. Neurochemistry Research, 33: 2436-2443.

D'Antoni S, Berretta A, Seminara G, Patrizia P, Giuffrida-Stella A, Battaglia G, Sortino MA, Nicoletti F, Catania MV, **2011**. *A prolonged pharmacological blockade of type-5 metabotropic glutamate receptors protects cultured spinal cord motor neurons against excitotoxic death*. Neurobiology of Disease 42: 252-264.

Dal Canto MC and Gurney ME, **1995**. *Neuropathological changes in two lines of mice carrying a transgene mutant human Cu, Zn SOD, and in mice overexpressing wild type human SOD: a model of familial amyotrophic lateral sclerosis (FALS).* Brain Research 676: 25-40.

Damiano M, Starkov AA, Petri S, Kipiani K, Kiaei M, Mattiazzi M, Beal MF, Manfredi G, **2006**. *Neural mitochondrial Ca2+ capacity impairment precedes the onset of motor symptoms in G93A Cu/Zn-superoxide dismutase mutant mice*. J Neurochem., 96 (5): 1349-1361.

Danbolt NC, Storm-Mathisen J, Kanner BI, **1992**. *An [Na+ + K+] coupled L-glutamate transporter purified from rat brain is located in glial cell processes*. Neuroscience. 51:295-310.

Danbolt NC, **1994**. *The high affinity uptake system for excitatory amino acids in the brain.* Prog. Neurobiol. 44: 377-396.

Danbolt NC, Storm-Mathisen J, Ottersen OP, **1994**. *Sodium/potassium-coupled glutamate transporters, a "new" family of eukaryotic proteins: do they have "new" physiological roles and could they be new targets for pharmacological intervention?* Prog. Brain Res. 100: 53-60.

Danbolt NC, **2001**. *Glutamate uptake.* Prog Neurobiol. 65: 1-105.

De Blasi A, Conn PJ, Pin J, Nicoletti F, **2001**. *Molecular determinants of metabotropic glutamate receptor signalin*g. Trends Pharmacol Sci., 22 (3): 114-120.

De Carvalho M, Pinto S, Costa J, Evangelista T, Ohana B, Pinto A, **2010**. *A randomized, placebo-controlled trial of memantine for functional disability in amyotrophic lateral sclerosis*. Amyotroph. Lateral Scler. Off. Publ. World Fed. Neurol. Res. Group Mot. Neuron Dis. 11: 456-460.

De Haas AH, Boddeke HWGM, Biber K, **2008**. *Region-Specific Expression of Immunoregulatory Proteins on Microglia in the Healthy CNS.* GLIA 56:888-894.

De Vos KJ and Hafezparast M, **2017**. *Neurobiology of axonal transport defects in motor neuron diseases: Opportunities for translational research?* Neurobiology of Disease 105: 283–299.

DeJesus-Hernandez M, Mackenzie IR, Boeve BF, Boxer AL, Baker M, Rutherford NJ, Nicholson AM, Finch NA, Gilmer HF, Adamson J, Kouri N, Wojtas A, Sengdy P, Hsiung GYR, Karydas A, Seeley WW, Josephs KA, Coppola G, Geschwind DH, Wszolek ZK, Feldman H, Knopman D, Petersen R, Miller BL, Dickson D, Boylan K, Graff-Radford N, Rademakers R, **2011**. *Expanded GGGGCC hexanucleotide repeat in noncoding region of C9ORF72 causes chromosome 9p-linked FTD and ALS*. Neuron 72, 245-25.

Delisle MB and Carpenter S, **1984**. *Neurofibrillary axonal swellings and amyotrophic lateral sclerosis*. J Neurol Sci., 63 (2): 241-250.

Deng HX, Hentati A, Tainer JA, Iqbal Z, Cayabyab A, Hung WY, Getzoff ED, Hu P, Herzfeldt B, Roos RP, *et al*., **1993**. *Amyotrophic Lateral Sclerosis and Structural Defects in Cu,Zn Superoxide Dismutase*. Science, New Series, Vol. 261, No. 5124, pp. 1047-1051.

Deng J, Yang M, Chen Y, Chen X, Liu J, Sun S, Cheng H, Li Y, Bigio EH, Mesulam M, Xu Q, Du S, Fushimi K, Zhu L, Wu JY, **2015**. *FUS interacts with HSP60 to promote mitochondrial damage*. PLoS Genet. 11 (9): e1005357. doi: 10.1371/journal.pgen.1005357.

Deng MY, Wang H, Ward GB, Beckham TR, McKenna TS, **2005**. *Comparison of six RNA extraction methods for the detection of classical swine fever virus by real-time and conventional reverse transcription–PCR*. J. Vet. Diagn. Invest. 17: 574-578.

Devarajan G, Chen M, Muckersie E, Xu H, **2014**. *Culture and Characterization of Microglia from the Adult Murine Retina.* The Scientific World Journal Volume 2014, Article ID 894368.

Dhami GK and Ferguson SSG, 2006. *Regulation of metabotropic glutamate receptor signaling, desensitization and endocytosis*. Pharmacology & Therapeutics 111: 260-271.

Díaz-Amarilla P, Olivera-Bravo S, Trias E, Cragnolini A, Martínez-Palma L, Cassina P, Beckman J, Barbeito L, **2011**. *Phenotypically aberrant astrocytes that promote motorneuron damage in a model of inherited amyotrophic lateral sclerosis*. Proc. Natl. Acad. Sci 108, 18126-18131.

Ding H, Schwarz DS, Keene A, Affar EIB, Fenton L, Xia X, Shi Y, Zamore PD, Xu Z, **2003**. *Selective silencing by RNAi of a dominant allele that causes amyotrophic lateral sclerosis*. Aging Cell 2: 209-217.

Doble A, **1996**. *The pharmacology and mechanism of action of riluzole.* Neurology 47: S233-241.

Doble A, **1999**. *The Role of Excitotoxicity in Neurodegenerative Disease: Implications for Therapy.* Pharmacol. Ther. Vol. 81, No. 3, pp. 163-221.

Doherty AJ, Palmer MJ, Henley JM, Collingridge GL, Jane DE, **1997**. (*RS)-2-chloro-5-hydroxyphenylglycine (CHPG) activates mGlu5, but no mGlu1, receptors expressed in CHO cells and potentiates NMDA responses in the hippocampus*. Neuropharmacology, 36 (2): 265-267.

Dolen G and Bear MF, **2008**. *Role for metabotropic glutamate receptor 5 (mGluR5) in the pathogenesis of fragile X syndrome*. Journal of Physiology, 586: 1503-1508.

Donnelly CJ, Zhang PW, Pham JT, Haeusler AR, Mistry NA, Vidensky S, Daley EL, Poth EM, Hoover B, Fines DM, Maragakis N, Tienari PJ, Petrucelli L, Traynor BJ, Wang J, Rigo F, Bennett CF, Blackshaw S, Sattler R, Rothstein JD, **2013**. *RNA toxicity from the ALS/FTD C9ORF72 expansion is mitigated by antisense intervention*. Neuron. 80 (2): 415-428.

Doumazane E, Scholler P, Zwier JM, Trinquet E, Rondard P, Pin JP, **2011**. *A new approach to analyze cell surface protein complexes reveals specific hetero-dimeric metabotropic glutamate receptors*. FASEB J., 25 (1): 66-77.

Du L, Zhang Y, Chen Y, Zhu J, Yang Y, Zhang HL, **2016**. *Role of microglia in neurological disorders and their potentials as a therapeutic target*. Mol. Neurobiol. 54 (10):7567-7584.

Dubreuil P, Letard S, Ciufolini M, Gros L, Humbert M, Castéran N, Borge L, Hajem B, Lermet A, Sippl W, Voisset E, Arock M, Auclair C, Leventhal PS, Colin D. Mansfield, Alain Moussy, Olivier Hermine, **2009**. *Masitinib (AB1010), a potent and selective tyrosine kinase inhibitor targeting KIT*. PloS One 4: 7258.

Eisen A, **2009**. *Amyotrophic lateral sclerosis: A 40-year personal perspective*. J Clin Neurosci. 16:505-512.

Elam JS, Taylor AB, Strange R, Antonyuk S, Doucette PA, Rodriguez JA, Hasnain SS, Hayward LJ, Valentine JS, Yeates TO, Hart PJ, **2003**. *Amyloid-like filaments and water-filled nanotubes formed by SOD1 mutant proteins linked to familial ALS*. Nat. Struct. Biol. 10: 461-467.

Ezzi SA, Urushitani M, Julien JP, **2007**. *Wild-type superoxide dismutase acquires binding and toxic properties of ALS-linked mutant forms through oxidation*. J Neurochem. 102 (1): 170-178.

Faas GC, Adwanikar H, Gereau IV RW and Saggau P, **2002**. *Modulation of Presynaptic Calcium Transients by Metabotropic Glutamate Receptor Activation: A Differential Role in Acute Depression of Synaptic Transmission and Long-Term Depression*. The Journal of Neuroscience, *22* (16): 6885-6890.

Fairman WA, Vandenberg RJ, Arriza JL, Kavanaught MP, Amara SG, **1995**. *An excitatory amino-acid transporter with properties of a ligand-gated chloride channel*. Nature 375: 599-603.

Farina C, Aloisi F, Meinl E, **2007**. *Astrocytes are active players in cerebral innate immunity*. Trends Immunol. 28 (3): 138-45.

Farina C, Krumbholz M, Giese T, Hartmann G, Aloisi F, Meinl E, **2005**. *Preferential expression and function of Toll-like receptor 3 in human astrocytes*. J. Neuroimmunol. 159: 12-19.

Farmer K, Abd-Elrahman KS, Derksen A, Rowe EM, Thompson AM, Rudyk CA, Prowse NA, Dwyer Z, Bureau SC, Fortin T, Ferguson SSG, Hayley S, **2020**. *mGluR5 Allosteric Modulation Promotes Neurorecovery in a 6-OHDA-Toxicant Model of Parkinson's Disease*. Mol Neurobiol., 57 (3): 1418-1431.

Fazal A, Parker F, Palmer AM, Croucher MJ, **2003**. *Characterisation of the actions of group I metabotropic glutamate receptor subtype selective ligands on excitatory amino acid release and sodium-dependent re-uptake in rat cerebrocortical minislices*. J Neurochem., 86 (6): 1346-1358.

Ferber EC, Peck B, Delpuech O, Bell GP, East P, Schulze A, **2012**. *FOXO3a regulates reactive oxygen metabolism by inhibiting mitochondrial gene expression*. Cell Death Differ. 19 (6): 968-979. doi: 10.1038/cdd.2011.179.

Ferraguti F, Baldini-Guerra B, Corsi M, Nakanishi S, Corti C, **1999.** *Activation of the extracellular signal-regulated kinase 2 by metabotropic glutamate receptors*. Eur. J. Neurosci. 11: 2073-2082.

Ferraiuolo L, Higginbottom A, Heath PR, Barber S, Greenald D, Kirby J, Shaw PJ. **2011**. *Dysregulation of astrocyte–motoneuron cross-talk in mutant superoxide dismutase 1-related amyotrophic lateral sclerosis*. Brain 134; 2627-2641.

Ferraiuolo L, **2014**. *The non-cell-autonomous component of ALS: new in-vitro models and future challenges.* Biochem. Soc. Trans. 42: 1270-1274.

Ferrer I, Tuñón T, Serrano MT, Casas R, Alcántara S, Zujar MJ and Rivera RM, **1993.** *Calbindin D-28k and parvalbumin immunoreactivity in the frontal cortex in patients with frontal lobe dementia of non-Alzheimer type associated with amyotrophic lateral sclerosis*. J. Neurol. Neurosurg. Psychiatry 56: 257-261.

Ferrucci M, Fulceri F, Toti L, Soldani P, Siciliano G, Paparelli A, Fornai F, **2011**. *Protein clearing pathways in ALS*. Archives Italiennes de Biologie 149: 121-49.

Fiala M, Mizwicki MT, Weitzman R, Magpantay L, Nishimoto N, **2013**. *Tocilizumab infusion therapy normalizes inflammation in sporadic ALS patients*. Am. J. Neurodegener. Dis. 2: 129-139.

Finelli MJ, Liu KX, Wu Y, Oliver PL, Davies KE, **2015**. *Oxr1 improves pathogeniccellular features of ALS-associated FUS and TDP-43 mutations*. Hum Mol Genet. 24 (12): 3529-3544. doi: 10.1093/hmg/ddv104.

Fire A, Xu S, Montgomery MK, Kostas SA, Driver SE, Mello CC, **1998**. *Potent and specific genetic interference by double-stranded RNA in Caenorhabditis elegans*. Nature 391: 806-811.

Fiszman ML, Ricart KC, Latini A, Rodríguez G, Sica REP, **2010**. *In-vitro neurotoxic properties and excitatory aminoacids concentration in the cerebrospinal fluid of amyotrophic lateral sclerosis patients. Relationship with the degree of certainty of disease diagnoses*. Acta Neurol. Scand. 121: 120-126.

Fleige S, Walf V, Huch S, Prgomet C, Sehm J, Pfaffl MW, **2006**. *Comparison of relative mRNA quantification models and the impact of RNA integrity in quantitative real-time RT-PCR*. Biotechnol Lett 28:1601-1613.

Forostyak S, Jendelova P, Sykova E, **2013**. *The role of mesenchymal stromal cells in spinal cord injury, regenerative medicine and possible clinical applications*. Biochimie 95: 2257-2270.

Forsberg K, Andersen PM, Marklund SL, Brännström T, **2011.** *Glial nuclear aggregates of superoxide dismutase-1 are regularly present in patients with amyotrophic lateral sclerosis*. Acta Neuropathol. 121 (5): 623-634. doi: 10.1007/s00401-011-0805-3.

Frakes AE, Braun L, Ferraiuolo L, Guttridge DC, Kaspar BK, **2017**. *Additive amelioration of ALS by co-targeting independent pathogenic mechanisms.* Ann. Clin. Neurol. 4: 76-86.

Fridovich I, **1986**. *Superoxide dismutases*. Adv. Enzymol. 58, 61-97.

Gabellini N *et al*., **1993**. *Carboxyl domain of glutamate receptor directs its coupling to metabolic pathways*. NeuroReport 4: 531-534.

Gegelashvili G, Danbolt NC, Schousboe A, **1997**. *Neuronal soluble factors differentially regulate the expression of the GLT1 and GLAST glutamate transporters in cultured astroglia*. J Neurochem. 1997 Dec;69(6):2612-2615.

Geloso M, Corvino V, Marchese E, Serrano A, Michetti F, D'Ambrosi N, **2017**. *The dual role of microglia in ALS: mechanisms and therapeutic approaches*. Front. Aging Neurosci. 9: 242.

Gendro TF, Bienie KFK, Zhang Y, Jansen-West K, Ash PEA, Caulfield T, Daughrity L, Dunmore JH, Castanedes-Casey M, Jeannie Chew J, Cosio DM, van Blitterswijk M, Lee WC, Rademakers R, Boylan KB, Dickson DW, Petrucelli L, **2013**. *Antisense transcripts of the expanded C9ORF72 hexanucleotide repeat form nuclear RNA foci and undergo repeat-associated non-ATG translation in c9FTD/ALS*. Acta Neuropathol. 126, 829-844.

Ghiasi P, Saman Hosseinkhani S, Noori A, Nafissi S, Khajeh K, **2012**. *Mitochondrial complex I deficiency and ATP/ADP ratio in lymphocytes of amyotrophic lateral sclerosis patients*. Neurological Research, 34:3, 297-303.

Giribaldi F, Milanese M, Bonifacino T, Rossi PIA, Di Prisco S, Pittaluga A, Tacchetti C, Puliti A, Usai C, Bonanno G, **2013**. *Group I metabotropic glutamate autoreceptors induce abnormal glutamate exocytosis in a mouse model of amyotrophic lateral sclerosis*. Neuropharmacology 66, 253-263.

Giunti D, Marini C, Parodi B, Usai C, Milanese M, Bonanno G, Kerlero de Rosbo N, Uccelli A, **accepted in 2020**. *Exosome-shuttled miRNAs contribute to the modulation of the neuroinflammatory microglia phenotype by mesenchymal stem cells. Implication for amyotrophic lateral sclerosis.* Journal of Neuroinflammation.

Goldman RD, Khuon S, Chou YH, Opal P, Steinert PM, **1996**. *The function of intermediate filaments in cell shape and cytoskeletal integrity*. J Cell Biol. 134 (4): 971-983.

Gravel M, Béland LC, Soucy G, Abdelhamid E, Rahimian R, Gravel C, Kriz J, **2016**. *IL-10 controls early microglial phenotypes and disease onset in ALS caused by misfolded superoxide dismutase 1*. J. Neurosci. 36: 1031-1048.

Greger IH, Watson JF, Cull-Candy SG, **2017**. *Structural and Functional Architecture of AMPA-Type Glutamate Receptors and Their Auxiliary Proteins.* Neuron 94 (4):7 13-730.

Gruzman A, Wood WL, Alpert E, Prasad MD, Miller RG, Rothstein JD, Bowser R, Hamilton R, Wood TD, Cleveland DW, Lingappa VR, Liu J, **2007**. *Common molecular signature in SOD1 for both sporadic and familial amyotrophic lateral sclerosis*. Proc Natl Acad Sci U S A. 104 (30): 12524-12529.

Grynkiewicz G, Poenie M, Tsien RY, **1985**. *A new generation of Ca2+ indicators with greatly improved fluorescence properties*. J. Biol. Chem. 260: 3440-3450.

Guatteo E, Carunchio I, Pieri M, Albo F, Canu N, Mercuri NB, Zona C, **2007**. *Altered calcium homeostasis in motor neurons following AMPA receptor but not voltage-dependent calcium channels' activation in a genetic model of amyotrophic lateral sclerosis*. Neurobiol. Dis. 28 (1), 90-100.

Gugliandolo A, Giacoppo S, Bramanti P, Mazzon E, **2018**. N*LRP3 Inflammasome Activation in a Transgenic Amyotrophic Lateral Sclerosis*. Model. Inflammation. 41 (1): 93-103.

Gurney ME, Pu H, Chiu AY, Dal Canto MC, Polchow CY, Alexander DD, Caliendo J, Hentati A, Kwon YW, Deng HX, *et al*., **1994**. *Motor neuron degeneration in mice that express a human Cu,Zn superoxide dismutase mutation*. Science, 264 (5166): 1772-1775.

Gurney ME, **1997**. The use of transgenic mouse models of amyotrophic lateral sclerosis in preclinical drug studies. J Neurol Sci 152(Suppl 1): S67-S73.

Gurney ME, **2000**. *What transgenic mice tell us about neurodegenerative disease*. Bioassays 22, 297-304.

Guttenplan KA, Weigel MK, Adler DI, Couthouis J, Liddelow SA, Aaron D, Gitler AD, Ben A. Barres BA, **2020**. *Knockout of reactive astrocytes activating factors slows disease progression in an ALS mouse model*. Nature Communications 11: 3753.

Haidet-Phillips AM, Hester ME, Miranda CJ, Meyer K, Braun L, Frakes A, Song S, Likhite S, Murtha MJ, Foust KD, Rao M, Eagle A, Kammesheidt A, Christensen A, Mendell JR, Burghes AHM, Kaspar BJ, **2011**. *Astrocytes from familial and sporadic ALS patients are toxic to motor neurons*. Nat Biotechnol. 29: 824-828.

Halliwell B, **2006**. *Reactive Species and Antioxidants. Redox Biology Is a Fundamental Theme of Aerobic Life*. Plant Physiol. 141: 312-322.

Halliwell B and Gutteridge JMC, **1994**. *Oxygen toxicity, oxygen radicals, transition metals and disease*. Biochem J. 219 (1) :1-14.

Hamby ME and Sofroniew MV, **2010**. *Reactive astrocytes as therapeutic targets for CNS disorders*. Neurotherapeutics, 7: 494-506.

Hamida MB, Hentati F, Hamida CB, **1990**. *Hereditary motor system diseases (chronic juvenile amyotrophic lateral sclerosis): conditions combining a bilateral pyramidal syndrome with limb and bulbar atrophy*. Brain 113: 347-363.

Heckman PRA, Blokland A, Bollen EPP, Prickaerts J, **2018**. *Phosphodiesterase inhibition and modulation of corticostriatal and hippocampal circuits: Clinical overview and translational considerations*. Neuroscience and Biobehavioral Reviews 87: 233-254.

Heidinger V, Manzerra P, Wang XQ, Strasser U, Yu SP, Choi DW, Behrens MM, **2002**. *Metabotropic glutamate receptor 1-induced upregulation of NMDA receptor current: mediation through the Pyk2/Src-family kinase pathway in cortical neurons.* J Neurosci 1; 22 (13): 5452-5461.

Hamilton A, Vasefi M, Vander TC, McQuaid, RJ, Anisman H, Ferguson SS, **2016**. Chronic pharmacological mGluR5 inhibition prevents cognitive impairment and reduces pathogenesis in an Alzheimer disease mouse model. Cell Reports, 15:1859-1865.

Hensley K, Floyd RA, Gordon B, Mou S, Pye QN, Stewart C, West M, Williamson K, **2002**. *Temporal patterns of cytokine and apoptosisrelated gene expression in spinal cords of the G93A-SOD1 mouse model of amyotrophic lateral sclerosis*. J. Neurochem. 82: 365-374.

Hermans E and Challiss RA, **2001**. *Structural, signalling and regulatory properties of the group I metabotropic glutamate receptors: prototypic family C G-protein-coupled receptors*. Biochem J. 1; 359 (Pt 3): 465-84.

Herrero I, Miras-Portugal MT, Sánchez-Prieto J, **1992**. *Positive feedback of glutamate exocytosis by metabotropic presynaptic receptor stimulation*. Nature, 360 (6400): 163-166.

Herrero I, Miras-Portugal MT, Sánchez-Prieto J, **1998**. *Functional switch from facilitation to inhibition in the control of glutamate release by metabotropic glutamate receptors*. J. Biol. Chem. 27: 1951-1958.

Hetz C, Thielen P, Matus S, Nassif M, Court F, Kiffin R, Martinez G, Cuervo AM, Brown RH, Glimcher LH, **2009**. *XBP-1 deficiency in the nervous system protects against amyotrophic lateral sclerosis by increasing autophagy*. Genes Dev.; 23: 2294-3000.

Hinkle PC, **2005**. *P/O ratios of mitochondrial oxidative phosphorylation*. Biochim. Biophys. Acta. 1706 (1-2): 1-11.

Holden C, **2007**. *Astrocytes secrete substance that kills motor neurons in ALS*. Science 316 (5823): 353.

Hollmann M and Heinemann S, **1994**. *Cloned glutamate receptors*. A. Rev. Neurosci. 17: 31-108.

Hong-Fu L and Zhi-Ying W, **2016**. *Genotype-phenotype correlations of amyotrophic lateral sclerosis*. Transl. Neurodegener. 5:3. doi: 10.1186/s40035-016-0050-8.

Hooten KG, Beers DR, Zhao W, Appel SH, **2015.** *Protective and Toxic Neuroinflammation in Amyotrophic Lateral Sclerosis*. Neurotherapeutics 12 (2): 364-375.

Houades V, Rouach N, Ezan P, Kirchhoff F, Koulakoff A, Giaume C, **2006**. *Shapes of astrocytes networks in the juvenile brain*. Neuron Glia Biol. 2: 3-14.

Houamed KM, Kuijper JL, Gilbert TL, Haldeman BA, O'Hara PJ, Mulvihill ER, Almers W and Hagen FS, **1991**. *Cloning, expression, and gene structure of a G-protein-coupled glutamate receptor from rat brain*. Science 252: 1318-1321.

Howland DS, Liu J, She YJ, *et al*., **2002**. *Focal loss of the glutamate transporter EAAT2 in a transgenic rat model of SOD1 mutantmediated amyotrophic lateral sclerosis (ALS).* Proc. Natl Acad. Sci. USA 99: 1604-1609.

Hubert GW, Paquet M, Smith Y, **2001**. *Differential subcellular localization of mGluR1a and mGluR5 in the rat and monkey Substantia nigra.* J Neurosci 15; 21 (6): 1838-47.

Husi H, Ward MA, Choudhary JS, Blackstock WP, S G Grant SG, **2000**. *Proteomic analysis of NMDA receptor-adhesion protein signaling complexes*. Nat Neurosci., 3 (7): 661-669.

Huynh W, Ahmed R, Mahoney C, Nguyen C, Tu S, Caga J, Loh P, Lin CSY, Kiernan MC, **2020**. *The impact of cognitive and behavioral impairment in amyotrophic lateral sclerosis*. Expert Review of Neurotherapeutics, 20 (3): 281-293.

Ilieva H, Polymenidou M, Cleveland DW, **2009**. *Non-cell autonomous toxicity neurodegenerative disorders: ALS and beyond*. J Cell Biol 187: 761-772.

Iwata A, Christianson JC, Bucci M, Ellerby LM, Nukina N, Forno LS, Kopito RR, **2005**. *Increased susceptibility of cytoplasmic over nuclear polyglutamine aggregates to autophagic degradation*. Proc. Natl. Acad. Sci. U. S. A. 102: 13135-13140.

Jaarsma D, Rognoni F, van Duijn W, Verspaget HW, Haasdijk ED, Holstege JC, **2001**. *CuZn superoxide dismutase (SOD1) accumulates in vacuolated mitochondria in transgenic mice expressing amyotrophic lateral sclerosis-linked SOD1 mutations*. Acta Neuropathol: 102 :293-305.

Jaeschke G, Kolczewski S, Spooren W, Vieira E, Bitter-Stoll N, Boissin P, Borroni E, Büttelmann B, Ceccarelli S, Clemann N, David B, Funk C, Guba W, Harrison A, Hartung T, Honer M, Huwyler J, Kuratli M, Niederhauser U, Pähler A, Peters JU, Petersen A, Prinssen E, Ricci A, Rueher D, Rueher M, Schneider M, Spurr P, Stoll T, Tännler D, Wichmann J, Porter RH, Wettstein JG, Lindemann L, **2015**. *Metabotropic glutamate receptor 5 negative allosteric modulators: discovery of 2- chloro-4-[1-(4-fluorophenyl)-2,5-dimethyl-1H-imidazol-4-ylethynyl]pyridine (basimglurant, RO4917523), a promising novel medicine for psychiatric diseases*. J Med Chem. 58 (3): 1358-1371.

Janssensa J, Cransbc RAJ, Van Craenenbroeck K, Vandesompele J, Stove CP, Van Dama D, De Deyna PP, **2019**. *Evaluating the applicability of mouse SINEs as an alternative normalization approach for RT-qPCR in brain tissue of the APP23 model for Alzheimer's disease.* Journal of Neuroscience Methods 320: 128-137.

Jean YY, Lercher LD, Dreyfus, CF, **2008**. *Glutamate elicits release of BDNF from basal forebrain astrocytes in a process dependent on metabotropic receptors and the PLC pathway*. Neuron Glia Biology, 4: 35-42.

Johann S, Heitzer M, Kanagaratnam M, Goswami A, Rizo T, Weis J, Troost D, Beyer C, **2015**. *NLRP3 inflammasome is expressed by astrocytes in the SOD1 mouse model of ALS and in human sporadic ALS patients*. Glia 63 (12): 2260-2273.

Joly C, Gomeza J, Brabet I, Curry K, Bockaert J, Pin JP, **1995**. *Molecular, Functional, and Pharmacological Characterization of the Metabotropic Glutamate Receptor Type 5 Splice Variants: Comparison with mGluR1*. The Journal of Neuroscience 75 (5): 3970-3981.

Juneja T, Pericak-Vance MA, Laing NG, Dave S and Siddique T, **1997**. *Prognosis in familial amyotrophic lateral sclerosis: progression and survival in patients with glu100gly and ala4val mutations in Cu,Zn superoxide dismutase*. Neurology 48, 55-57.

Kabuta T, Suzuki Y, Wada K, **2006**. *Degradation of amyotrophic lateral sclerosis-linked mutant Cu,Zn-superoxide dismutase proteins by macroautophagy and the proteasome*. J Biol Chem. 281: 30524-30533.

Kallur T, Darsalia V, Lindvall O, Kokaia Z, **2006**. *Human fetal cortical and striatal neural stem cells generate region-specific neurons in-vitro and differentiate extensively to neurons after Intrastriatal transplantation in neonatal rats*. J Neurosci Res 84: 1630-1644.

Kanai K, Kuwabara S, Misawa S, Tamura N, Ogawara K, Nakata M, Sawai S, Hattori T, Bostock H, **2006**. *Altered axonal excitability properties in amyotrophic lateral sclerosis: impaired potassium channel function related to disease stage*. Brain 129: 953-962.

Kang SH, Li Y, Fukaya M, Lorenzini I, Cleveland DW, Ostrow LW, Rothstein JD, Bergles DE, **2013**. *Degeneration and impaired regeneration of gray matter oligodendrocytes in amyotrophic lateral sclerosis*. Nat. Neurosci. 16 (5): 571-579.

Kanumilli S, and Roberts PJ, **2006**. *Mechanisms of glutamate receptor induced proliferation of astrocytes*. Neuroreport, 17: 1877-1881.

Kato S, Takikawa M, Nakashima K., **2000**. New consensus research on neuropathological aspects of familial amyotrophic lateral sclerosis with superoxide dismutase 1 (SOD1) gene mutations: inclusions containing SOD1 in neurons and astrocytes. Amyotroph Lateral Scler Other Motor Neuron Disord 1:163-184.

Kausar S, Wang F, Cui H, **2018**. The role of mitochondria in reactive oxygen species generation and its implications for neurodegenerative diseases. Cells, 7 (12): 274.

Kawai T and Akira S, **2011**. *Toll-like receptors and their crosstalk with other innate receptors in infection and immunity*. Immunity 34: 637-650.

Kettenmann H, Hanisch UK, Noda M, Verkhratsky A, **2011**. *Physiology of microglia*. Physiol Rev 91: 461-553.

Khalil B, Morderer D, Price PL, Liu F, Rossoll W, **2018**. *mRNP assembly, axonal transport, and local translation in neurodegenerative diseases*. Brain Research 1693: 75-91.

Kiernan MC, Vucic S, Cheah BC, Turner MR, Eisen A, Hardiman O, Burrell JR, Zoing MC, **2011**. *Amyotophic lateral sclerosis*. Lancet. 377:942-55.

Kikuchi S, Shinpo K, Ogata A, Tsuji S, Takeuchi M, Makita Z, Tashiro K, **2002**. *Detection of N-epsilon–(carboxymethyl)lysine (CML) and non–CML advanced glycation end–products in the anterior horn of amyotrophic lateral sclerosis spinal cord*. Amyotroph Lateral Scler Other Motor Neuron Disord. 3 (2): 63-68.

Kim H, Kim HY, Choi MR, Hwang S, Nam KH, Kim HC, Han JS, Kim KS, Yoon HS, Kim SH, **2010**. *Dose-dependent efficacy of ALS-human mesenchymal stem cells transplantation into cisterna magna in SOD1-G93A ALS mice*. Neurosci Lett 468: 190-194.

Kim J, Efe JA, Zhu S, Talantova M, Xu Yuan X, Wang S, Lipton SA, Zhang K, Ding S, **2011**. *Direct reprogramming of mouse fibroblasts to neural progenitors*. Proc Natl Acad Sci USA 108 (19): 7838-7843.

Kim JH, Marton J, Ametamey SM, Cumming P, **2020**. *A Review of Molecular Imaging of Glutamate Receptors*. Molecules, 25, 4749.

Kong Q, Chang LC, Takahashi K, Liu Q, Schulte DA, Lai L, Ibabao B, Lin Y, Stou_er, N, Mukhopadhyay CD, *et al.*, 2014. *Small-molecule activator of glutamate transporter EAAT2 translation provides neuroprotection.* J. Clin. Investig. 124: 1255-1267.

King AE, Woodhouse A, Kirkcaldie MTKK, Vickers JC, **2016**. *Excitotoxicity in ALS: Overstimulation, or overreaction?* Experimental Neurology 275: 162-171.

King OD, Gitler AD, Shorter J, **2012**. *The tip of the iceberg: RNA-binding proteins with prion-like domains in neuro-degenerative disease*. Brain Res 1462: 61-80.

Kirk K, Gennings C, Hupf JC, Tadesse S, D'Aurelio M, Kawamata H, Valsecchi F, Mitsumoto H, ALS/PLS COSMOS Study Groups, Manfredi G, **2014**. *Bioenergetic Markers in Skin Fibroblasts of Sporadic Amyotrophic Lateral Sclerosis and Progressive Lateral Sclerosis Patients*. Ann neurol 76: 620-624.

Kirkinezos IG, Bacman SR, Hernandez D, Oca-Cossio J, Arias LJ, Perez-Pinzon MA, Bradley WG, Moraes CT, **2005**. *Cytochrome c association with the inner mitochondrial membrane is impaired in the CNS of G93A-SOD1 mice*. J Neurosci., 25 (1): 164-172.

Kiselyov K, Jennigs JJ Jr, Rbaibi Y, Chu CT, **2007**. *Autophagy, mitochondria. and cell death in lysosomal storage diseases*. Autophagy 3: 259-262.

Knott EP, Assi M, Rao SNR, Ghosh M, Pearse DD, **2017**. *Phosphodiesterase Inhibitors as a Therapeutic Approach to Neuroprotection and Repair*. Int. J. Mol. Sci. 18: 696.

Koga K, Li S, Zhuo M, **2016**. Metabotropic Glutamate Receptor Dependent Cortical Plasticity in Chronic Pain. *Current Neuropharmacology 14:* 427-434.

Kong J and Xu Z, **1998**. *Massive mitochondrial degeneration in motor neurons triggers the onset of amyotrophic lateral sclerosis in mice expressing a mutant SOD1*. J Neurosci.,18 (9) :3241-3250.

Koppers M, Blokhuis AM, Westeneng HJ, Terpstra ML, Zundel CAC, Vieira de Sá R, Schellevis RD, Waite AJ, Blake DJ, Veldink JH, van den Berg LH, Pasterkamp RJ, **2015.** *C9orf72 ablation in mice does not cause motor neuron degeneration or motor deficits*. Ann. Neurol. 78**,** 426-438.

Kraft A, Resch J, Johnson D, Johnson J, **2007**. *Activation of the Nrf2-ARE pathway in muscle and spinal cord during ALS-like pathology in mice expressing mutant SOD1*. Experimental Neurology, 207 (1): 107-117.

Kuner R, Groom AJ, Müller G, Kornau HC, Stefovska V, Bresink I, Hartmann B, Tschauner K, Waibel S, Albert C, Ludolph AC, Chrysanthy Ikonomidou C, Seeburg PH, Turski L, **2005**. *Mechanisms of disease: motor neuron disease aggravated by transgenic expression of a functionally modified AMPA receptor subunit*. Ann. N. Y. Acad. Sci. 1053: 269-286.

Kunst CB, **2004**. *Complex genetics of Amiotrophic Lateral Sclerosis*. Am. J. Hum. Genet. 75, 933-947.

Kwiatkowski Jr TJ, Bosco DA, Leclerc AL, Tamrazian E, Vanderburg CR, Russ C, Davis A, Gilchrist J, Kasarskis EJ, Munsat T, Valdmanis P, Rouleau GA, Hosler BA, Cortelli P, de Jong PJ, Yoshinaga Y, Haines JL, Pericak-Vance MA, Yan J, Ticozzi N, Siddique T, McKenna-Yasek D, Sapp PC, Horvitz HR, Landers JE, Brown Jr RH, **2009**. *Mutations in the FUS/TLS gene on chromosome 16 cause familial amyotrophic lateral sclerosis*. Science 323 1205–1208.

La Spada AR and Taylor JP, **2010**. *Repeat expansion disease: progress and puzzles in disease pathogenesis*. Nature Rev. Genet. 11**,** 247-258.

Ladner MB, Martin GA, J. A.Noble JA *et al.*, 1988. cDNAcloning and expression of murine macrophage colony-stimulating factor from L929 cells. Proceedings of the NationalAcademy of Sciences of the United States of America, 85,18: 6706-6710.

Lagier-Tourenne C, Polymenidou M, Cleveland DW, **2010**. *TDP-43 and FUS/TLS: emerging roles in RNA processing and neurodegeneration*. Hum. Mol. Genet. 19, R46-64.

Lagier-Tourenne C, Baughn M, Rigo F, Sun S, Liu P, Li HR, Jiang J, Watt AT, Chun S, Katz M, Qiu J, Sun Y, Ling SC, Zhu Q, Polymenidou M, Drenner K, Artates JW, McAlonis-Downes M, Markmiller S, Hutt KR, Pizzo DP, Cady J, Harms MB, Baloh RH, Vandenberg SR, Yeo GW, Fu XD, Bennett CF, Cleveland DW, Ravits J, **2013.** *Targeted degradation of sense and antisense C9orf72 RNA foci as therapy for ALS and frontotemporal degeneration*. *Proc. Natl Acad. Sci. USA* 110**:** E4530–E4539.

Lalli G and Schiavo G, **2002**. *Analysis of retrograde transport in motor neurons reveals common endocytic carriers for tetanus toxin and neurotrophin receptor p75NTR*. J Cell Biol.,156 (2): 233-239.

Lasiene J and Yamanaka K, **2011**. *Glial cells in amyotrophic lateral sclerosis*. Neurol. Res. Int., 718-987.

Leal SS, Cardoso I, Valentine JS, Gomes CM, **2013**. *Calcium ions promote superoxide dismutase 1 (SOD1) aggregation into non-fibrillar amyloid: A link to toxic effects of calcium overload in amyotrophic lateral sclerosis (ALS)?* J. Biol. Chem. 288: 25219-25228.

Lee Y, Morrison BM, Li Y, Lengacher S, Farah MH, Hoffman PN, Liu Y, Tsingalia A, Jin L, Zhang PW, Pellerin L, Magistretti PJ, Rothstein JD, **2012.** *Oligodendroglia metabolically support axons and contribute to neurodegeneration*. Nature 487 (7408): 443-448.

Leigh PN and Meldrum BS, **1996**. *Excitotoxicity in ALS*. Neurology 47: S221-S227.

Leigh PN, Whitwell H, Garofalo O, Buller J, Swash M, Martin JE, Gallo JM, Weller RO, Anderton BH, **1991**. *Ubiquitin-immunoreactive intraneuronal inclusions in amyotrophic lateral sclerosis*. Morphology, distribution, and specificity. Brain 114 (Pt 2): 775-788.

Lepore AC, Rauck B, Dejea C, Pardo AC, Rao MS, Rothstein JD, Maragakis NJ, **2008**. *Focal transplantation-based astrocyte replacement is neuroprotective in a model of motor neuron disease*. Nat Neurosci, 11: 1294-1301.

Levanon D, Lieman-Hurwitz J, Dafni N, Wigderson M, Sherman L, Bernstein Y, Laver-Rudich Z, Danciger E, Stein O, Groner Y, **1985**. *Architecture and anatomy of the chromosomal locus in human chromosome 21 encoding the Cu/Zn superoxide dismutase*. EMBO J. 4: 77-84.

Levine JM, Reynolds R, Fawcett JW, **2001**. *The oligodendrocyte precursor cell in health and disease*. Trends Neurosci. 24 (1): 39-47.

Levine TP, Daniels RD, Gatta AT, Wong LH, Hayes MJ, **2013**. *The product of C9orf72, a gene strongly implicated in neurodegeneration, is structurally related to DENN Rab-GEFs*. Bioinformatics 29: 499-503.

Lewis CM and Suzuki M, **2014**. *Therapeutic applications of mesenchymal stem cells for amyotrophic lateral sclerosis*. Stem Cell Res Ther 5: 32.

Li K, Li J, Zheng J, Qin S, **2019**. *Reactive astrocytes in neurodegenerative diseases*. Aging and Disease, Volume 10, Nr 3: 664-675.

Li L, Zhang X, Le W, **2008**. *Altered macroautophagy in the spinal cord of SOD1 mutant mice*. Autophagy 4: 290-293.

Li L, Acioglu C, Heary RF, Elkabes S, **2020**. *Role of astroglial toll-like receptors (TLRs) in central nervous system infections, injury and neurodegenerative diseases.* Brain, Behavior, and Immunity.

Li YR, King OD, Shorter J, Gitler AD, **2013**. *Stress granules as crucibles of ALS pathogenesis*. J Cell Biol. 201 (3): 361-372.

Liao B, Zhao W, Beers DR, Henkel JS, Appel SH, **2012**. *Transformation from a neuroprotective to a neurotoxic microglial phenotype in a mouse model of ALS*. Exp. Neurol 237: 147-152.

Liddelow S and Barres BA, **2015**. *SnapShot: astrocytes in health and disease*. Cell 162 (5): 1170-1170.e1.

Liddelow SA, Guttenplan KA, Clarke LE, Bennett FC, Bohlen CJ, Schirmer L, Bennett ML, Münch AE, Chung WS, Peterson TC, Wilton DK, Frouin A, Napier BA, Panicker N, Kumar M, Buckwalter MS, Rowitch DH, Dawson VL, Dawson TM, Stevens B, Barres BA, **2017**. *Neurotoxic reactive astrocytes are induced by activated microglia*. Nature 541: 481-487.

Lin CL, Bristol LA, Jin L, Dykes-Hoberg M, Crawford T, Clawson L, Rothstein JD, **1998**. *Aberrant RNA processing in a neurodegenerative disease: the cause for absent EAAT2, a glutamate transporter, in amyotrophic lateral sclerosis*. Neuron. 20 (3): 589-602.

Liu HN, Sanelli T, Horne P., Pioro EP, Strong MJ, Rogaeva E, Bilbao J, Zinman L, Robertson J. **2009**. *Lack of evidence of monomer/misfolded superoxide dismutase-1 in sporadic amyotrophic lateral sclerosis*. Ann Neurol 66:75-80.

Livak KJ and Schmittgen TD, **2001**. *Analysis of Relative Gene Expression Data Using Real-Time Quantitative PCR and the 22DDCT Method*. Methods 25**:** 402-408.

Lorenzini I, Moore S, Sattler R, **2018**. *RNA Editing Deficiency in Neurodegeneration*. Adv Neurobiol. 20: 63-83.

Lindemann L, Jaeschke G, Michalon A, Vieira E, Honer M, Spooren W, Porter R, Hartung T, Kolczewski S, Büttelmann B, Flament C, Diener C, Fischer C, Gatti S, Prinssen EP, Parrott N, Hoffmann G, Wettstein JG, **2011**. *CTEP: A Novel, Potent, Long-Acting, and Orally Bioavailable Metabotropic Glutamate Receptor 5 Inhibitor*. J Pharmacol Exp Ther. 339 (2): 474-486.

Lindemann L, Porter RH, Scharf SH, Kuenneckn B, Bruns A, von Kienlin M, Harrison AC, Paehler A, Funk C, Gloge A, Schneide M, Parrott NJ, Polonchuk L, Niederhauser U, Stephen R, Morairty SR, Kilduff TS, Vieira E, Kolczewski S, Wichmann J, Hartung T, Honer M, Borroni E, Moreau JL, Prinssen E, Spooren W, Wettstein JG, Jaeschke G, **2015**. *Pharmacology of basimglurant (RO4917523, RG7090), a unique metabotropic glutamate receptor 5 negative allosteric modulator in clinical development for depression*. J Pharmacol Exp Ther. 353 (1): 213-33.

Litschig S, Gasparini F, Rueegg D, Stoehr N, Flor PJ, Vranesic I, Prézeau L, Pin JP, Thomsen C, Kuhn R, **1999**. *CPCCOEt, a noncompetitive metabotropic glutamate receptor 1 antagonist, inhibits receptor signaling without affecting glutamate binding*. Mol. Pharmacol. 55, 453-461.

Liu GJ, Nagarajah R, Banati RB, Bennett MR, **2009**. *Glutamate induces directed chemotaxis of microglia*. Eur. J. Neurosci. 29: 1108-1118.

Liu J and Wang F, **2017**. *Role of Neuroinflammation in Amyotrophic Lateral Sclerosis: Cellular Mechanisms and Therapeutic Implications*. Front. Immunol. 8: 1005.

Liu-Yesucevitz L, Bilgutay A, Zhang YJ, Vanderweyde T, Allison Citro A, Mehta T, Zaarur N, McKee A, Bowser R, Sherman M, Petrucelli L, Benjamin Wolozin B, **2010**. *Tar DNA binding protein-43 (TDP-43) associates with stress granules: analysis of cultured cells and pathological brain tissue*. PLoS ONE 5: 13250.

Lobsiger CS and Cleveland DW, **2007**. *Glial cells as intrinsic components of non-cell-autonomous neurodegenerative disease*. Nt. Neurosci. 10, 1355-1360.

Lomen-Hoerth C, **2008**. *Amyotrophic lateral sclerosis from bench to bedside*. Semin Neurol. 2008;28 (2): 205-211.

Longinetti E and Fang F, **2019**. *Epidemiology of Amyotrophic Lateral Sclerosis: An Update of Recent Literature*. Curr. Opin. Neurol. 32 (5): 771-776.

Lu YM, Jia Z, Janus C, Jeffrey T. Henderson JT, Gerlai R, J. Wojtowicz JM, Order JC, **1997**. *Mice lacking metabotropic glutamate receptor 5 show impaired learning and reduced CA1 long-term potentiation (LTP) but normal CA3 LTP*. The Journal of Neuroscience. 1; 17 (13): 5196-5205.

Lutz C, **2018**. *Mouse models of ALS: Past, present and future*. Brain Research 1693: 1-10

Luyt K, Va´radi A, Durant CF, Molna´r E, **2006**. Oligodendroglial metabotropic glutamate receptors are developmentally regulated and involved in the prevention of apoptosis. Journal of Neurochemistry, 99: 641-656.

Ly and Miller, **2018**. *Emerging antisense oligonucleotide and viral therapies for ALS*. Curr Opin Neurol. 31(5): 648-654.

Mackenzie IRA, Bigio EH, Ince PG, Geser F, Neumann M, Cairns NJ, Kwong LK, Forman MS, Ravits J, Stewart H, Eisen A, McClusky L, Kretzschmar HA, Monoranu CM, Highley JR, Kirby J, Siddique T, Shaw PJ, Lee VMY, Trojanowski JQ, **2007**. *Pathological TDP-43 distinguishes sporadic amyotrophic lateral sclerosis from amyotrophic lateral sclerosis with SOD1 mutations*. Ann Neurol. 61(5):427-34.

Mackenzie IR, Ansorge O, Strong M, Bilbao J, Zinman L, Ang LC, Baker M, Stewart H, Eisen A, Rademakers R, Neumann M, **2011**. *Pathological heterogeneity in amyotrophic lateral sclerosis with FUS mutations: two distinct patterns correlating with disease severity and mutation*. Acta Neuropathol. 122 (1): 87-98.

Mackenzie IR, Arzberger T, Kremmer E, Troost D, Lorenzl S, Mori K, Weng SM, Haass C, Kretzschmar HA, Edbauer D, Neumann M, **2013**. *Dipeptide repeat protein pathology in C9ORF72 mutation cases: clinico-pathological correlations*. Acta Neuropathol. 126, 859-879.

Macpherson CE and Bassile CC, **2016**. *Pulmonary Physical Therapy Techniques to Enhance Survival in Amyotrophic Lateral Sclerosis: A Systematic Review*. J Neurol Phys Ther. 40: 165-175.

Magistretti PJ, **2006.** *Neuron-glia metabolic coupling and plasticity*. J. Exp. Biol. 209: 2304-2311.

Magrane, J, Cortez, C, Gan, WB, Manfredi, G, **2014**. *Abnormal mitochondrial transport and morphology are common pathological denominators in SOD1 and TDP-43 ALS mouse models*. Hum Mol Genet. 23 (6): 1413-1424.

Malik R and Wiedau M, **2020**. *Therapeutic Approaches Targeting Protein Aggregation in Amyotrophic Lateral Sclerosis*. Front. Mol. Neurosci. 13:98.

Manders EM, Stap J, Brakenhoff GJ, van Driel R, Aten A, **1992**. *Dynamics of three-dimensional replication patterns during the S phase, analysed by double labelling of DNA and confocal microscopy*. J Cell Sci. 103 (Pt 3):857-862.

Manfredi G and Kawamata H, **2016**. Mitochondria and endoplasmic reticulum crosstalk in amyotrophic lateral sclerosis. Neurobiol Dis. 90:35-42.

Mangan MSJ, Olhava EJ, Roush WR, Seidel HM, Glick GD, Latz E, **2018**. *Targeting the NLRP3 inflammasome in inflammatory diseases*. Nat Rev Drug Discov.17 (8): 588-606.

Mark LP, Prost RW, Ulmer JL, Smith MM, Daniels DL, Strottmann JM, *et al*., **2001**. *Pictorial review of glutamate excitotoxicity: fundamental concepts for neuroimaging.* Am. J. Neuroradiol. 22: 1813-1824.

Marchetto MCN, Muotri AR, Mu Y, Smith AM, Cezar GG, Gage FH, **2008**. *Non-cell-autonomous effect of human SOD1 G37R astrocytes on motor neurons derived from human embryonic stem cells*. Cell Stem Cell 3: 637-648.

Marino MJ, Wittmann M, Rossi Bradley S, Hubert GW, Smith Y, Conn PJ, **2001**. *Activation of group I metabotropic glutamate receptors produces a direct excitation and disinhibition of GABAergic projection neurons in the substantia nigra pars reticulata*. J Neurosci., 21 (18): 7001-7012.

Martorana F, Brambilla L, Valori CF, Bergamaschi C, Roncoroni C, Aronica E, Volterra A, Bezzi P, Rossi D, **2012**. *The BH4 domain of Bcl-X(L) rescues astrocyte degeneration in amyotrophic lateral sclerosis by modulating intracellular calcium signals*. Hum. Mol. Genet. 21: 826-840.

Marullo M, Zuccato C, Mariotti C, Lahiri N, Tabrizi SJ, Di Donato S, Cattaneo E, **2010**. *Expressed Alu repeats as a novel, reliable tool for normalization of real-time quantitative RT-PCR data*. Genome Biology 11: R9.

Masu M, Tanabe Y, Tsuchida K, Shigemoto R, and Nakanishi S, **1991**. *Sequence and expression of a metabotropic glutamate receptor*. Nature 349: 760-765.

Mathis S, Goizet C, Soulages A and Vallat JM, **2019**. *Genetics of amyotrophic lateral sclerosis: A review*. Journal of Neurological Sciences 399: 217-226.

Mattiazzi M, D'Aurelio M, Gajewski CD, Martushova K, Kiaei M, Beal MF, Manfredi G, **2002**. *Mutated Human SOD1 Causes Dysfunction of Oxidative Phosphorylation in Mitochondria of Transgenic Mice*. The journal of biological chemistry Vol. 277, No. 33: 29626-29633.

McGown A, McDearmid JR, Panagiotaki N, Tong H, Al Mashhadi S, Redhead N, Lyon AN, Beattie CE, Shaw PJ, Ramesh TM, **2013**. Early interneuron dysfunction in ALS: insights from a mutant sod1 zebrafish model. Ann Neurol. 73(2):246-58.

McKeage K, **2019**. *Ravulizumab: first global approval*. Drugs 79: 347-352.

Mejzini R, Flynn LL, Pitout IL, Fletcher S, Wilton SD, P. Akkari PA, **2019.** *ALS Genetics, Mechanisms, and Therapeutics: Where Are We Now?* Front. Neurosci. 13:1310.

Mendez EF and Sattler R, **2014.** *Biomarker development for C9orf72 repeat expansion in ALS*. Brain Res. 1607: 26-35.

Mendonça DMF, Chimelli L, Martinez AMB, **2005**. *Quantitative evidence for neurofilament heavy subunit aggregation in motor neurons of spinal cords of patients with amyotrophic lateral sclerosis.* Braz J Med Biol Res., 38 (6): 925-933.

Menzies FM, Cookson MR, Taylor RW, Turnbull DM, Chrzanowska-Lightowlers ZMA, Dong L, Figlewicz DA, Shaw PJ, **2002**. *Mitochondrial dysfunction in a cell culture model of familial amyotrophic lateral sclerosis*. Brain,125 (Pt 7): 1522-1533.

Meyer K, Ferraiuolo L, Miranda CJ, Likhite S, McElroy S, Renusch S, Ditsworth D, Lagier-Tourenne C, Smith RA, Ravits J, Burghes AH, Shaw PJ, Cleveland DW, Kolb SJ, Kaspar BK, **2014**. *Direct conversion of patient fibroblasts demonstrates non-cell autonomous toxicity of astrocytes to motor neurons in familial and sporadic ALS*. Proc. Natl. Acad. Sci. U.S.A. 111: 829-832.

Migheli A, Cordera S, Bendotti C, Atzoria C, Piva R, Schiffera D, **1999**. *S-100β protein is upregulated in astrocytes and motor neurons in the spinal cord of patients with amyotrophic lateral sclerosis*. Neuroscience Letters, Vol 261, Issues 1–2, Pages 25-28.

Milanese M, Zappettini S, Onofri F, Musazzi L, Tardito D, Bonifacino T, Mirko Messa M, Racagni G, Usai C, Benfenati F, Popoli M, Bonanno G, **2011**. *Abnormal exocytotic release of glutamate in a mouse model of amyotrophic lateral sclerosis*. J Neurochem.,116 (6): 1028-1042.

Milanese M, Giribaldi F, Melone M, Bonifacino T, Musante I, Carminati E, Rossi P, Vergani L, Voci A, Conti F, Puliti A, Bonanno G, **2014**. *Knocking down metabotropic glutamate receptor 1 improves survival and disease progression in the SOD1G93A mouse model of amyotrophic lateral sclerosis*. Neurobiology of Disease 64: 48-59.

Milanese M, Bonifacino T, Fedele E, Rebosio C, Cattaneo L, Benfenati F, Usai C, Bonanno G, **2015**. *Exocytosis regulates trafficking of GABA and glycine heterotransporters in spinal cord glutamatergic synapses: a mechanism for the excessive heterotransporter-induced release of glutamate in experimental amyotrophic lateral sclerosis*. Neurobiol. Dis. 74, 314-324.

Milanese M, Bonifacino T, Torazza C, Provenzano F, Kumar M, Ravera S, Zerbo RA, Frumento G, Balbi M, Ferrando S, Bonanno G, **under revision**. *Blocking metabotropic glutamate receptor 5 by the negative allosteric modulator CTEP improves disease course of ALS in SOD1G93A mice.* British Journal of Pharmacology.

Miller TM, Pestronk A, David W, Rothstein J, Simpson E, Appel SH, Andres PL, Mahoney KM, Allred P, Alexander K, Ostrow LW, Schoenfeld D, Macklin EA, Norris DA, Manousakis G, Crisp M, Smith R, Bennett CF, Bishop KM Cudkowicz ME, **2013**. *An antisense oligonucleotide against SOD1 delivered intrathecally for patients with SOD1 familial amyotrophic lateral sclerosis: a phase 1, randomised, first-in-man study*. Lancet Neurol 12: 435-442.

Milligan G, **2006**. *G-protein-coupled receptor heterodimers: pharmacology, function and relevance to drug discovery*. Drug Discovery Today, Volume 11, Numbers 11/12.

Milligan G and Smith NJ, **2007**. *Allosteric modulation of heterodimeric G-protein-coupled receptors*. Trends Pharmacol. Sci., 28 (12): 615-620.

Minelli A, Barbaresi P, Reimer RJ, Edwards RH, Conti F, **2001**. *The glial glutamate transporter GLT-1 is localized both in the vicinity of and at distance from axon terminals in the rat cerebral cortex*. Neuroscience 108: 51-59.

Mishra SK, Menon NK, Roman D, Kumar S, **1992.** *Calcium, calmodulin and 3',5'-cyclic nucleotide phosphodiesterase activity in human muscular disorders*. Journal of the Neurological Sciences; 109: 215-218.

Mitchell J, Paul P, Chen HJ, Morris A, Payling M, Falchi M, Habgood J, Panoutsou S, Winkler S, Tisato V, Hajitou A, Smith B, Vance C, Shaw C, Mazarakis ND, de Bellerochea J, **2010**. *Familial amyotrophic lateral sclerosis is associated with a mutation in D-amino acid oxidase*. Proc Natl. Acad. Sci., 107: 7556-7561.

Mizuno T, Kurotani T, Komatsu Y, Kawanokuchi J, Kato H, Mitsuma N, Suzumura A, **2004**.*Neuroprotective role of phosphodiesterase inhibitor ibudilast on neuronal cell death induced by activated microglia*. Neuropharmacology 46: 404-411.

Mizushima N, **2004**. *Methods for monitoring autophagy*. Int. J. Biochem. Cell Biol. 36: 2491-2502.

Monaghan DT, Bridges RJ, Cotman CW, **1989**. *The excitatory amino acid receptors: their classes, pharmacology and distinct properties in the function of the central nervous system*. A. Rev. Pharmac. Toxic. 29: 365402**.**

Mori K, Weng SM, Arzberger T, May S, Rentzsch K, Kremmer E, Schmid B, Kretzschmar HA, Cruts M, Van Broeckhoven C, Haass C, Edbauer D, **2013**. *The C9orf72 GGGGCC repeat is translated into aggregating dipeptide-repeat proteins in FTLD/ALS*. Science 339**,** 1335-1338.

Morimoto N, Nagai M, Ohta Y, Miyazaki K, Kurata T, Morimoto M, Murakami T, Takehisa Y, Ikeda Y, Kamiya T, Abe K, **2007**. *Increased autophagy in transgenic mice with a G93A mutant SOD1 gene*. Brain Res.; 1167: 112-117.

Moroni F, Cozzi A, Lombardi G, Sourtcheva S, Leonardi P, Carfì M, Pellicciari R, **1998**. *Presynaptic mGlu1 type receptors potentiate transmitter output in the rat cortex*. Eur J Pharmacol., 347 (2-3): 189-195.

Mórotz GM, De Vos KJ, Vagnoni A, Ackerley S, Shaw CE, Miller CC, **2012**. *Amyotrophic lateral sclerosis-associated mutant VAPBP56s perturbscalcium homeostasis to disrupt axonal transport of mitochondria*. Hum Mol Genet. 21 (9): 1979-1988.

Morrison BM, Lee Y, Rothstein JD, **2013.** *Oligodendroglia: metabolic supporters of axons*. Trends Cell. Biol. 23 (12): 644-651.

Moser JM, Bigini P, Schmitt-John T, **2013**. *The wobbler mouse, an ALS animal model.* Mol Genet Genomics. 288 (5-6): 207-229.

Muly EC, Maddox M, Smith Y, **2003**. *Distribution of mGluR1alpha and mGluR5 immunolabeling in primate prefrontal cortex*. J Comp Neurol., 467 (4): 521-535.

Munz C, **2006**. *Autophagy and antigen presentation*. Cell Microbiol. 8: 891-898.

Musante V, Neri E, Feligioni M, Puliti A, Pedrazzi M, Conti V, Usai C, Diaspro A, Ravazzolo R, Henley JM, Battaglia G, Pittaluga A, **2008**. *Presynaptic mGlu1 and mGlu5 autoreceptors facilitate glutamate exocytosis from mouse cortical nerve endings*. Neuropharmacology, 55 (4): 474-482.

Musante V, Summa M, Neri E, Puliti A, Godowicz TT, Severi P, Battaglia G, Raiteri M, Pittaluga A, **2010**. *The HIV-1 viral protein Tat increases glutamate and decreases GABA exocytosis from human and mouse neocortical nerve endings*. Cereb Cortex., 20 (8): 1974-1984.

Myszczynska M and Ferraiuolo L, **2016**. *New n Vitro Models to Study Amyotrophic Lateral Sclerosis*. Brain Pathology 26: 258-265.

Nagy A, Rossant J, Nagy R, Abramow-Newerly W, Order JC, **1993**. *Derivation of completely cell culture-derived mice from early-passage embryonic stem cells*. Proc Natl Acad Sci U S A. 90 (18): 8424-8428.

Nave KA and Trapp BD, **2008.** *Axon-glial signalling and glial support of axon function*. Annu. Rev. Neurosci. 31: 535-561.

Nave KA, **2010a**. *Myelination and the trophic support of long axons*. Nat.Rev. Neurosci. 11(4): 275-283.

Nave KA, **2010b**. *Myelination and support of axonal integrity by glia*. Nature 468 (7321): 244-252.

Neumann M, Sampathu DM, Kwong LK, Truax AC, Micsenyi MC, Chou TT, Bruce J, Schuck T, Grossman M, Clark CM, McCluskey LF, Miller BL, Masliah E, Mackenzie IR, Feldman H, Feiden W, Kretzschmar HA, Trojanowski JQ, Lee VMY, **2006**. *Ubiquitinated TDP-43 in frontotemporal lombar degeneration and amyotrophic Lateral Sclerosis*. Science 314, 130-133.

Neymotin A, Calingasan NY, Wille E, Naseri N, Petri S, Damiano M, Liby KT, Risingsong R, Sporn M, Beal MF, Kiaei M, **2011**. *Neuroprotective effect of Nrf2/ARE activators, CDDO ethylamide and CDDO trifluoroethylamide, in a mouse model of amyotrophic lateral sclerosis*. Free Radic Biol Med. 51 (1): 88-96. doi: 10.1016/j.freeradbiomed.2011.03.027.

Nguyen MD, D'Aigle T, Gowing G, Julien JP, Rivest S, **2004**. *Exacerbation of motor neuron disease by chronic stimulation of innate immunity in a mouse model of amyotrophic lateral sclerosis*. J. Neurosci. 24: 1340-1349.

Niedzielska E, Smaga I, Gawlik M, Moniczewski A, Stankowicz P, Pera J, Filip M, **2016**. *Oxidative Stress in Neurodegenerative Diseases*. Molecular Neurobiology, 53 (6): 4094-4125.

Nicoletti F, Bockaert J, Collingridge GL, Conn PJ, Ferraguti F, Schoepp DD, Wroblewski JT, Pin JP, **2011**. *Metabotropic glutamate receptors: from the workbench to the bedside*. Neuropharmacology, 60 (7-8): 1017-1041.

Nishimura AL, Shum C, Scotter EL, Abdelgany A, Sardone V, Wright J, Lee YB, Chen HJ, Bilican B, Carrasco M, Maniatis T, Chandran S, Rogelj B, Gallo JM, Shaw CE, **2014**. *Allele-specific knockdown of ALS-associated mutant TDP-43 in neural stem cells derived from induced pluripotent stem cells*. PLoS One 9: 91269.

Nishiyama A, Komitova M, Suzuki R, Zhu X, **2009**. *Polydendrocytes (NG2 cells): multifunctional cells with lineage plasticity*. Nat. Rev. Neurosci. 10 (1): 9-22.

Niswender CM and Conn PJ, **2010**. *Metabotropic Glutamate Receptors: Physiology, Pharmacology, and Disease*. Annu Rev Pharmacol Toxicol. 50: 295-322.

Nizzardo M, Simone C, Rizzo F, Ulzi G, Ramirez A, Rizzuti M, Bordoni A, Bucchia M, Gatti S, Bresolin N, Comi GP, Corti S, **2016**. *Morpholino-mediated SOD1 reduction ameliorates an amyotrophic lateral sclerosis disease phenotype*. Sci Rep 6: 21301.

Nonneman A, Robberecht W, Van Den Bosch L, **2014**. *The role of oligodendroglial dysfunction in amyotrophic lateral sclerosis*. Neurodegen. Dis. Manage. 4 (3): 223-239.

Norden DM, Fenn AM, Dugan A, Godbout JP, **2014**. *TGFβ produced by IL-10 re-directed Astrocytes Attenuates Microglial Activation.* Glia 62 (6): 881-895.

Oliveira TC, Montezinho L, Mendes C,Firuzi O, Saso L, Oliveira PJ , Silva FSG, **2020**. *Oxidative Stress in Amyotrophic Lateral Sclerosis: Pathophysiology and Opportunities for Pharmacological Intervention*. Oxidative Medicine and Cellular Longevity, Article ID 5021694, 29 pages doi.org/10.1155/2020/5021694.

Olney JW, **1969**. *Brain lesions, obesity, and other disturbances in mice treated with monosodium glutamate*. Science 164, 719-721.

O'Rourke JG, Bogdanik L, Muhammad AKMG, Gendron TF, Kim KJ, Austin A, Cady J, Liu EY, Zarrow J, Grant S, Ho R, Bell S, Carmona S, Simpkinson M, Lall D, Wu K, Daughrity L, Dickson DW, Harms MB, Petrucelli L, Lee EB, Lutz CM, Baloh RH, **2015**, *C9orf72 BAC transgenic mice display typical pathologic features of ALS/FTD*. Neuron. 88, 892-901.

Osborn MJ, Starker CG, McElroy AN, Webber BR, Riddle MJ, Xia L, DeFeo AP, Gabriel R, Schmidt M, von Kalle C, Carlson DF, Maeder ML, Joung JK, Wagner JE, Voytas DF, Blazar BR, Tolar J, **2013**. *TALEN-based gene correction for epidermolysis bullosa*. Mol Ther 21:1151-1159.

Ousterout DG, Kabadi AM, Thakore PI, William H Majoros WH, Reddy TE, Gersbach CA **2015**. *Multiplex CRISPR/Cas9-based genome editing for correction of dystrophin mutations that cause Duchenne muscular dystrophy.* Nat Commun. 18; 6: 6244.

Pajarillo E, Rizo A, Lee J, Aschner M, Lee E, **2019**. *The role of astrocytic glutamate transporters GLT-1 and GLAST in neurological disorders: Potential targets for neurotherapeutics*. Neuropharmacology 161: 107559.

Panatier A, Vallee J, Haber M, Murai KK, Lacaille JC, Robitaille R, **2011.** *Astrocytes are endogenous regulators of basal transmission at central synapses*. Cell, 146: 785-798.

Pandya NJ, Klaassen RV, van der Schors RC, Slotman JA, Houtsmuller A, Smit AB, Li KW, **2016**. *Group I metabotropic glutamate receptors 1 and 5form a protein complex in mouse hippocampus and cortex*. Proteomics 16 (20): 2698-2705.

Pansarasa O, Bordoni M, Diamanti L, Sproviero D, Gagliardi S, Cereda C, **2018**. *SOD1 in Amyotrophic Lateral Sclerosis: "Ambivalent" Behaviour Connected to the Disease*. Int J Mol Sci. 19 (5). doi: 10.3390/ijms19051345.

Papadeas ST, Kraig SE, O'Banion C, Lepore AC, Maragakis NJ, **2011**. *Astrocytes carrying the superoxide dismutase 1 (SOD1G93A) mutation induce wild-type motor neuron degeneration in-vivo*. Proc. Natl. Acad. Sci 108: 17803-17808.

Paquet M, Ribeiro FM, Guadagno J, Esseltine JL, Ferguson SS, Cregan SP, **2013**. *Role of metabotropic glutamate receptor 5 signaling and homer in oxygen glucose deprivation-mediated astrocyte apoptosis*. Molecular Brain, 6: 9.

Pardo AC, Wong V, Benson LM, Dykes M, Tanaka K, Rothstein JD, Maragakis NJ, **2006**. *Loss of the astrocyte glutamate transporter GLT1 modifies disease in SOD1(G93A) mice*. Exp. Neurol, 201: 120-130.

Park CY, Kim J, Kweon J, Son JS, Lee JS, Yoo JE, Cho SR, Kim JH, Kim JS, Kim DW, **2014**. *Targeted inversion and reversion of the blood coagulation factor 8 gene in human iPS cells using TALENs.* Proc Natl Acad Sci USA 111: 9253-9258.

Parker SJ, Meyerowitz J, James JL, Liddell JR, Crouch PJ, Kanninen KM, White AR, **2012.** *Endogenous TDP-43 localized to stress granules can subsequently form protein aggregates*. Neurochem Int.; 60 (4): 415-424. doi: 10.1016/j.neuint.2012.01.019.

Pascuzzi RM, Shefner J, Chappell AS, Bjerke JS, Tamura R, Chaudhry V, Clawson L, Haas L, Rothstein JD **2010**. *A phase II trial of talampanel in subjects with amyotrophic lateral sclerosis*. Amyotrophic. Lateral Sclerosis. 11: 266-271.

Pasinelli P and Brown RH, **2006**. *Molecular biology of amyotrophic lateral sclerosis: insights from genetics*. Nat. Rev. Neurosci. 7: 710-723.

Peavy RD and Conn PJ, **1998**. *Phosphorylation of mitogenactivated protein kinase in cultured rat corticol glia by stimulation of metabotropic glutamate receptors*. J. Neurochem. 71: 603-612.

Pellerin L, Bouzier-Sore AK, Aubert A, Serres S, Merle M, Costalat R, Magistretti PJ **2007**. *Activity-dependent regulation of energy metabolism by astrocytes: an update*. Glia 55: 1251-1262.

Perry TL, Krieger C, Hansen S, Eisen A, **1990.** *Amyotrophic lateral sclerosis: amino acid levels in plasma and cerebrospinal fluid*. Ann. Neurol. 28: 12-17.

Petri S, Krampfl K, Hashemi F, Grothe C, Hori A, Dengler R, Bufler J, **2003**. *Distribution of GABAA receptor mRNA in the motor cortex of ALS patients*. J. Neuropathol. Exp. Neurol. 62: 1041-1051.

Petri S, Körner S, Kiaei M, **2012**. *Nrf2/ARE Signaling Pathway: Key Mediator in Oxidative Stress and Potential Therapeutic Target in ALS*. Neurol Res Int. 2012: 878030.

Petrozziello T, Secondo A, Tedeschi V, Esposito A, Sisalli M, Scorziello A, Di Renzo G, Annunziato L, **2017**. *SOD1 lacking dismutase activity neuroprotects motor neurons exposed to beta-methylamino-L-alanine through the Ca2+/Akt/ERK1/2 prosurvival pathway*. Cell Death Di_er, 24: 511-522.

Phatnani H and Maniatis T, **2015**. *Astrocytes in neurodegenerative disease*. Cold Spring Harb Perspect Biol, 7.

Phillips EC, Croft CL, Kurbatskaya K, O'Neill MJ, Hutton ML, Hanger DP, Garwood CJ, Noble W, **2014**. *Astrocytes and neuroinflammation in Alzheimer's disease*. Biochem Soc Trans, 42: 1321-1325.

Philips T, Bento-Abreu A, Nonneman A, Haeck W, Staats K, Geelen V, Hersmus N, Küsters B, Van Den Bosch L, Van Damme P, Richardson WD, Robberecht W, **2013**. *Oligodendrocyte dysfunction in the pathogenesis of amyotrophic lateral sclerosis*. Brain 136 (Pt 2): 471-482.

Philips T and Rothstein JD, **2016**. *Rodent Models of Amyotrophic Lateral Sclerosis.* Curr Protoc Pharmacol. 69: 5.67.1-5.67.21.

Picher-Martel V, Valdmanis PN, Gould PV, Julien JP, Dupré N, **2016**. *From animal models to human disease: a genetic approach for personalized medicine in ALS.* Acta Neuropathologica Communications 4:70.

Pieri M, Carunchio I, Curcio L, Mercuri NB, Zona C, **2009**. *Increased persistent sodium current determines cortical hyperexcitability in a genetic model of amyotrophic lateral sclerosis*. Exp Neurol. 215 (2): 368-379.

Pierre K and Pellerin L, **2005.** *Monocarboxylate transporters in the central nervous system: distribution, regulation and function*. J. Neurochem. 94 (1): 1-14.

Pierre K, Pellerin L, Debernardi R, Riederer BM, Magistretti PJ, **2000.** *Cell-specific localization of monocarboxylate transporters, MCT1 and MCT2, in the adult mouse brain revealed by double immunohistochemical labelling and confocal microscopy*. Neuroscience 100 (3): 617-627.

Pereira V and Goudet C, **2018**. *Emerging Trends in Pain Modulation by Metabotropic Glutamate Receptors*. Front Mol Neurosci.11: 464.

Pin JP and Duvoisin R, **1995**. *The metabotropic glutamate receptors: structure and functions.* Neuropharmacology Vol. 34, No. I, pp. l-26.

Pin JP, Galvez T, Prézeau L, **2003**. *Evolution, structure, and activation mechanism of family 3/C G protein-coupled receptors*. Pharmacology and Ther., 98 (3): 325-354.

Pinteaux-Jones F, Sevastou IG, Fry VA, Heales S, Baker D, Pocock JM, **2008**. *Myelin-induced microglial neurotoxicity can be controlled by microglial metabotropic glutamate receptors*. J. Neurochem. 106: 442-454.

Pizzino G, Irrera N, Cucinotta C, Pallio G, Mannino F, Arcoraci V, Squadrito F, Altavilla D, Bitto A, **2017.** *Oxidative stress: harms and benefits for human health*. Oxidative Medicine and Cellular Longevity, Article ID 8416763, 13 pages.

Planas-Fontánez TM, Dreyfus CF, Saitta KS, **2020**. *Reactive Astrocytes as Therapeutic Targets for Brain Degenerative Diseases: Roles Played by Metabotropic Glutamate Receptors.* Neurochemical Research 45: 541-550.

Poliak S and Peles E**, 2003.** *The local differentiation of myelinated axons at nodes of Ranvier*. Nat. Rev. Neurosci. 4 (12): 968-980.

Pollari E, Goldsteins G, Bart G, Koistinaho J, Giniatullin R, **2014**. *The role of oxidative stress in degeneration of the neuromuscular junction in amyotrophic lateral sclerosis*. Front. Cell. Neurosci. 8: 131.

Polymenidou M and Cleveland DW, **2011**. *The seeds of neurodegeneration: prion-like spreading in ALS*. Cell 147: 498-508.

PorteR RHP, Jaeschke G, Spooren W, Ballard TM, Büttelmann B, Kolczewski S, Peters JU, Prinssen E, Wichmann J, Vieira E, Mühlemann A, Gatti S, Mutel V, Malherbe P, **2005.** *Fenobam: a clinically validated nonbenzodiazepine anxiolytic is a potent, selective, and noncompetitive mGlu5 receptor antagonist with inverse agonist activity*. J Pharmacol Exp Ther., 315 (2): 711-721.

Pratt AJ, Getzoff ED, Perry JP, **2012**. *Amyotrophic lateral sclerosis: update and new developments*. Degener. Neurol. Neuromuscul. Dis., (2):1-14.

Prézeau L, Gomeza J, Ahern S, Mary S, Galvez T, Bockaert J, Pin JP, **1996**. *Changes in the carboxyl-terminal domain of metabotropic glutamate receptor 1 by alternative splicing generate receptors with differing agonist-independent activity*. Mol Pharmacol., 49 (3): 422-429.

Prickaerts J, Heckman PRA, Blokland A, **2017**. *Investigational phosphodiesterase inhibitors in phase I and phase II clinical trials for Alzheimer's disease*. Expert opinion on investigational drugs, vol. 26, 9: 1033-1048.

Quiroz JA, Tamburri P, Deptula D, Banken L, Beyer U, Rabbia M, Parkar N, Fontoura P, Santarelli L, **2016**. *Efficacy and Safety of Basimglurant as Adjunctive Therapy for Major Depression: A Randomized Clinical Trial*. JAMA Psychiatry. 73 (7): 675-684.

Rakhit R, Cunningham P, Furtos-Matei A, Dahan S, Qi XF, Crow JP, Cashman NR, Kondejewski LH, Chakrabartty A, **2002**. *Oxidation-induced misfolding and aggregation of superoxide dismutase and its implications for amyotrophic lateral sclerosis.* J. Biol. Chem. 277: 47551-47556.

Raiteri L, Paolucci E, Prisco S, Raiteri M, Bonanno G, **2003**. *Activation of a glycine transporter on spinal cord neurons causes enhanced glutamate release in a mouse model of amyotrophic lateral sclerosis*. Br. J. Pharmacol. 138: 1021-1025.

Raiteri L, Stigliani S, Zappettini S, Mercuri NB, Raiteri M, Bonanno G, **2004**. *Excessive and precocious glutamate release in a mouse model of amyotrophic lateral sclerosis*. Neuropharmacology 46: 782-792.

Raiteri, M, **2008**. Presynaptic metabotropic glutamate and GABAB receptors. Handb. Exp. Pharmacol. 184: 373-407.

Ralph GS, Radcliffe PA, Day DM, Carthy JM, Leroux MA, Lee DCP, Wong LF, Bilsland LG, Greensmith L, Kingsman SM, Mitrophanous KA, Mazarakis ND, Azzouz M, **2005**. *Silencing mutant SOD1 using RNAi protects against neurodegeneration and extends survival in an ALS mode*l. Nat Med 11: 429-433.

Rao SD, Yin HZ, Weiss JH, **2003.** *Disruption of glial glutamate transport by reactive oxygen species produced in motor neurons*. J Neurosci.23 (7): 2627-2633.

Ratti A and Buratti E, **2016**. *Physiological functions and pathobiology of TDP-43 and FUS/TLS proteins.* J. Neurochem. 138: 95-111.

Ravera S, Bonifacino T, Bartolucci M, Milanese M, Gallia E, Provenzano F, Cortese K, Panfoli I, Bonanno G, **2018a**. *Characterization of the Mitochondrial Aerobic Metabolism in the Pre- and Perisynaptic Districts of the SOD1G93A Mouse Model of Amyotrophic Lateral Sclerosis*. Molecular Neurobiology 55: 9220-9233.

Ravera S, Cossu V, Tappino B, Nicchia E, Dufour C, Cavani S, Sciutto A, Bolognesi C, Columbaro M, Degan P, Cappelli E, **2018b**. *Concentration-dependent metabolic effects of metformin in healthy and Fanconi anemia lymphoblast cells*. J. Cell. Physiol. 233 (2): 1736-1751.

Ravera S, Torazza C, Bonifacino T, Provenzano F, Rebosio C, Milanese M, Usai C, Panfoli I, Bonanno G, **2019**, *Altered glucose catabolism in the pre-synaptic and per-synaptic compartments of SOD1G93A mouse spinal cord and motor cortex indicates that mitochondria are the site of bioenergetic imbalance in ALS*. J Neurochem 151 (3): 336-350.

Ravikumar B, Vacher C, Berger Z, Davies JE, Luo S, Oroz LG, Scaravilli F, Easton DF, Duden R, O'Kane CJ, Rubinsztein DC, **2004**. *Inhibition of mTOR induces autophagy and reduces toxicity of polyglutamine expansions in fly and mouse models of Huntington disease*. Nat. Genet. 36: 585-595.

Ravikumar B, Berger Z, Vacher C, O'Kane CJ, Rubinsztein DC, **2006**. *Rapamycin pre-treatment protects against apoptosis*. Hum. Mol. Genet. 15: 1209-1216.

Reaume AJ, Elliott JL, Hoffman EK, Kowall NW, Ferrante RJ, Siwek DR, Wilcox HM, Flood DJ, Beal MF, Brown Jr RH, Scott RW, Snider WD, **1996**. *Motor neurons in Cu/Zn superoxide dismutase deficient mice develop normally but exhibit enhanced cell death after axonal injury*. Nat Genet 13: 43-47.

Récasens M, Guiramand J, Aimar R, Abdulkarim A, Barbanel G, **2007**. *Metabotropic Glutamate Receptors as Drug Targets Current Drug Targets*. 8: 651-681.

Redza-Dutordoir M and Averill-Bates DA, **2016**. *Activation of apoptosis signalling pathways by reactive oxygen species*. Biochim Biophys Acta.1863 (12): 2977-2992.

Reid ME, Toms NJ, Bedingfield JS, Roberts PJ, **1999**. *Group I mGlu receptors potentiate synaptosomal [3H] glutamate release independently of exogenously applied arachidonic acid*. Neuropharmacology, 38 (4): 477-485.

Reilmann R, Rouzade-Dominguez ML, Saft C, Süssmuth SD, Priller J, Rosser A, Rickards H, Schöls L, Pezous N, Gasparini F, Johns D, Landwehrmeye GBr, Gomez-Mancilla B, **2015.** *A randomized, placebo-controlled trial of AFQ056 for the treatment of chorea in Huntington's disease*. Mov Disord., 30 (3): 427-431.

Renard M, Vanhauwaert S, Vanhomwegen M, Rihani A, Vandamme N, Goossens S, Berx G, Van Vlierberghe P, Haigh JJ, Decaesteker B, Van Laere J, Lambertz I, Speleman F, Vandesompele J, Willaert A, **2018**. *Expressed repetitive elements are broadly applicable reference targets for normalization of reverse transcription-qPCR data in mice*. Scientific Reports 8:7642.

Renton AE, Majounie E, Waite A, Simón-Sánchez J, Rollinson S, Gibbs JR, Schymick JC…Traynor BJ, **2011**. *A hexanucleotide repeat expansion in C9ORF72 is the cause of chromosome 9p21-linked ALS-FTD*. Neuron. 72 (2): 257-268.

Renton AE, Chiò A, Traynor BJ, **2014**. *State of play in amyotrophic lateral sclerosis genetics*. Nat. Neurosci. 17: 17-23.

Ribeiro FM, Hamilton A, Doria JG, Guimaraes IM, Cregan SP, Ferguson SS, **2014**. *Metabotropic glutamate receptor 5 as a potential therapeutic target in Huntington's disease*. Expert Opinion on Therapeutic Targets, 18: 1293-1304.

Ribeiro FM, Vieira LB, Pires RGW, Olmo RP, Ferguson SSG, **2017**. *Metabotropic glutamate receptors and neurodegenerative diseases*. Pharmacological Research 115: 179-191.

Rihani A, Van Maerken T, Pattyn F, Van Peer G, Beckers A, De Brouwer S, Kumps C, Mets E, Van der Meulen J, Rondou P, Leonelli C, Mestdagh P, Speleman F, Vandesompele J, **2013**. *Effective Alu Repeat Based RT-Qpcr Normalization in Cancer Cell Perturbation Experiments*. PLOS ONE 8 (8): e71776.

Rinholm JE, Hamilton NB, Kessaris N, Richardson WD, Bergersen LH, Attwell D, **2011.** *Regulation of oligodendrocytes development and myelination by glucose and lactate*. J.Neurosci. 31 (2): 538-548.

Rivest S, **2009**. *Regulation of innate immune responses in the brain*. Nat. Rev. Immunol. 9: 429-439.

Rodriguez JA, Valentine JS, Eggers DK, Roe JA, Tiwari A, Brown Jr RH, Hayward LJ, **2002**. *Familial ALS-associated mutations decrease the thermal stability of distinctly metallated species of human copper-zinc superoxide dismutase*. J. Biol. Chem. 277: 15932-15937.

Rosen DR, Siddique T, Patterson D, Figlewicz DA, Sapp P, Hentati A, Donaldson D, Goto J, O'Regan JP, Deng HX, *et al*., **1993**. *Mutations in Cu/Zn superoxide dismutase gene are associated with familial amyotrophic lateral sclerosis*. Nature 362: 59-62.

Rossi D and Volterra A, **2009**. *Astrocytic dysfunction: insights on the role in neurodegeneration*. Brain Res Bull, 80: 224-232.

Rossi D, Brambilla L, Valori CF, Roncoroni C, Crugnola A, Yokota T, Bredesen DE, Volterra A, **2008**. *Focal degeneration of astrocytes in amyotrophic lateral sclerosis*. Cell Death Differ., 15 (11): 1691-1700.

Rothstein JD, Tsai G, Kuncl RW, Clawson L, Cornblath DR, Drachman DB, Pestronk A, Stauch BL, Coyle JT, **1990**. *Abnormal excitatory amino acid metabolism in amyotrophic lateral sclerosis*. Ann Neurol., 28 (1): 18-25.

Rothstein JD, Martin LJ, Kuncl RW, **1992**. *Decreased glutamate transport by the brain and spinal cord in amyotrophic lateral sclerosis*. N. Engl. J. Med. 326: 1464-1468.

Rothstein JD, Martin L, Levey AI, Dykes-Hoberg M, Jin L, Wu D, Nash N, Kuncl RW, **1994.** *Localization of neuronal and glial glutamate transporters*. Neuron 13: 713-725.

Rothstein JD, Van Kammen M, Levey AI, Martin LJ, Kuncl RW, **1995**. *Selective loss of glial glutamate transporter GLT-1 in amyotrophic lateral sclerosis*. Ann Neurol., 38 (1): 73-84.

Rothstein JD, Dykes-Hoberg M, Pardo CA, Bristol LA, Jin L, Kuncl RW, Kanai Y, Hediger MA, Wang Y, Schielke JP, Welty DF, **1996**. *Knockout of glutamate transporters reveals a major role for astroglial transport in excitotoxicity and clearance of glutamate*. Neuron. 16 (3): 675-686.

Rothstein JD, Patel S, Regan MR, Haenggeli C, Huang YH, Bergles DE, Jin L, Dykes Hoberg M, Vidensky S, Chung DS, *et al.,* **2005**. *Lactam antibiotics offer neuroprotection by increasing glutamate transporter expression*. Nature 433: 73-77.

Rothstein JD, **2009**. *Current hypothesis for the underlying biology of amyotrophic lateral sclerosis*. Ann. Neurol 65 (Suppl. 1) S3-S9.

Rubinsztein DC, Difiglia M, Heintz N, Nixon RA, Qin ZH, Ravikumar B, Stefanis L, Tolkovsky A, **2005**. *Autophagy and its possible roles in nervous system diseases, damage, and repair*. Autophagy 1: 11-22.

Rubio MD, Drummond JB, Meador-Woodruff JH, **2012**. *Glutamate Receptor Abnormalities in Schizophrenia: Implications for Innovative Treatments*. Biomol Ther 20 (1): 1-18

Saccon RA, Bunton-Stasyshyn RKA, Fisher EMC, Fratta P, **2013**. *Is SOD1 loss of function involved in amyotrophic lateral sclerosis?* Brain 136 (Pt 8): 2342–2358.

Santiago A, Soares LM, Schepers M, Milani H, Vanmierlo T, Prickaerts J, Weffort de Oliveira RM, **2018**. *Roflumilast promotes memory recovery and attenuates white matter injury in aged rats subjected to chronic cerebral hypoperfusion*; Neuropharmacology 138: 360-370.

Santiago-Vazquez LZ, Ranzer LK, Kerr RG, **2006**. *Comparison of two total RNA extraction protocols using the marine gorgonian coral pseudopterogorgia elisabethae and its symbiont Symbiodinium* sp. Electron. J. Biotechnol. 9.

Sasabe J, Miyoshi Y, Suzuki M, Mita M, Konno R, Matsuoka M, Hamase K, Aiso S, **2012**. *D-amino acid oxidase controls motor neuron degeneration through D-serine*. Proc. Natl. Acad. Sci. 109: 627-632.

Sasaki S and Iwata M, **1996**. *Impairment of fast axonal transport in the proximal axons of anterior horn neurons in amyotrophic lateral sclerosis.* Neurology., 47 (2): 535-450.

Sasaki S, Warita H, Murakami T, Shibata N, Komori T, Abe K, Kobayashi M, Iwata M, **2005**. *Ultrastructural study of aggregates in the spinal cord of transgenic mice with a G93A mutant SOD1 gene*. Acta Neuropathol., 109 (3): 247-255.

Sasaki S, Iwata M, **2007**. *Mitochondrial Alterations in the Spinal Cord of Patients with Sporadic Amyotrophic Lateral Sclerosis*. J Neuropathol Exp Neurol Vol. 66, No. 1: 10-16.

Sasaki S, **2011**. *Autophagy in spinal cord motor neurons in sporadic amyotrophic lateral sclerosis*. J. Neuropathol. Exp. Neurol. 70: 349-359.

Sau D, De Biasi S, Vitellaro-Zuccarello L, Riso P, Guarnieri S, Porrini M, Simeoni S, Crippa V, Onesto E, Palazzolo I, Rusmini P, Bolzoni E, Bendotti C, Poletti A, **2007**. *Mutation of SOD1 in ALS: a gain of a loss of function*. Hum Mol Genet. 16 (13): 1604-1618.

Sawada M, Suzumura A, Yamamoto H, Marunouchi T, **1977**. *Activation and proliferation of the isolated microglia by colony stimulating factor-1 and possible involvement of protein kinase C*. Brain Research, 509: 119-124.

Schepers M, Tiane A, Paes D, Sanchez S, Rombaut B, Piccart E, Rutten BPF, Brône B, Hellings N, Prickaerts J, Vanmierlo T, **2019**. *Targeting Phosphodiesterases-Towards a Tailor-Made Approach in Multiple Sclerosis Treatment*. Front. Immunol. 10: 1727.

Schiffer D, **1996**. *Reactive astrogliosis of the spinal cord in amyotrophic lateral sclerosis*. J Neurol Sci. 139 Suppl: 27-33.

Schinkmann KA, Kim TA, Avraham S, **2000**. *Glutamate stimulated activation of DNA synthesis via mitogen-activated protein kinase in primary astrocytes: involvement of pr tein kinase*. International Society for Neurochemistry, Journal of Neurochemistry, 83: 1139-1153.

Schoepp DD, **2001**. *Unveiling the functions of presynaptic metabotropic glutamate receptors in the central nervous system*. J Pharmacol Exp Ther., 299 (1): 12-20.

Schwank G, Koo BK, Sasselli V, Dekkers JF, Heo I, Demircan T, Sasaki N, Boymans S, Cuppen E, van der Ent CK, Nieuwenhuis EES, Beekman JM, Clevers H, **2013**. *Functional repair of CFTR b CRISPR/Cas9 in intestinal stem cell organoids of cystic fibrosis patients*. Cell Stem Cell 13: 653-658.

Sea K, Sohn SH, Durazo A, Sheng Y, Shaw BF, Cao X, Taylor AB, Whitson LJ, Holloway SP, Hart PJ, Cabelli DE, Gralla EB, Valentine JS, **2015**. *Insights into the Role of the Unusual Disulfide Bond in Copper-Zinc Superoxide Dismutase*. JBC Papers in Press, November 28.

Serrano A, Donno C, Giannetti S, Perić M, Andjus P, D'Ambrosi N, Michetti F, **2017**. *The Astrocytic S100B Protein with Its Receptor RAGE Is Aberrantly Expressed in SOD1G93A Models, and Its Inhibition Decreases the Expression of Proinflammatory Genes*. Mediators Inflamm. 2017: 1626204.

Sellier C, Campanari ML, Corbier CJ, Gaucherot A, Kolb-Cheynel I, Oulad-Abdelghani M, Ruffenach F, Page A, Ciura S, Kabashi E, Charlet-Berguerand N, **2016**. Loss of C9ORF72 impairs autophagy and synergizes with polyQ Ataxin-2 to induce motor neuron dysfunction and cell death. *EMBO J.* 35**:** 1276-1297.

Shaw PJ and Eggett CJ, **2000**. *Molecular factors underlying selective vulnerability of motor neurons to neurodegeneration in amyotrophic lateral sclerosis*. J. Neurol. 247: 17-27.

Shah A, Silverstein PS, Singh DP, Kumar A, **2012.** *Involvement of metabotropic glutamate receptor 5, AKT/PI3K signaling and NFkappaB pathway in methamphetamine-mediated increase in IL-6 and IL-8 expression in astrocytes*. Journal of Neuroinflammation, 9: 52.

Shaw PJ, Forrest V, Ince PG, Richardson JP, Wastell HJ, **1995**. *CSF and plasma amino acid levels in motor neuron disease: elevation of CSF glutamate in a subset of patients*. Neurodegeneration 4: 209-216.Shibuya K, Misawa S, Arai K, Nakata M, Kanai K, Yoshiyama Y, Ito K, Isose S, Noto Y, Nasu S, Sekiguchi Y, Fujimaki Y, Ohmori S, Kitamura H, Sato Y, Kuwabara S, **2011**. *Markedly reduced axonal potassium channel expression in human sporadic amyotrophic lateral sclerosis: an immunohistochemical study*. Exp Neurol. 232 (2): 149-53.

Shuvaev AN, Hosoi N, Sato Y, Yanagihara D, Hirai H, **2017**. *Progressive impairment of cerebellar mGluR signalling and its therapeutic potential for cerebellar ataxia in spinocerebellar ataxia type 1 model mice*. J Physiol. 595 (1): 141-164.

Siklos L, Engelhardt J, Harati Y, Smith RG, Joo F, Appel SH, **1996**. *Ultrastructural evidence for altered calcium in motor nerve terminals in amyotropic lateral sclerosis*. Ann. Neurol. 39 (2): 203-216.

Simons M and Lyons DA, **2013.** *Axonal selection and myelin sheat generation in the central nervous system*. Curr. Opin. Cell. Biol 25 (4): 512-519.Sistiaga A, Herrero I, Conquet F, Sánchez-Prieto J, **1998**. *The metabotropic glutamate receptor 1 is not involved in the facilitation of glutamate release in cerebrocortical nerve terminals*. Neuropharmacology., 37 (12): 1485-1492.

Smith EF, Shaw PJ, De Vos KJ, **2019**. *The role of mitochondria in amyotrophic lateral sclerosis.* Neuroscience Letters 710: 132933.

Sofroniew MV and Vinters, HV, **2010.** *Astrocytes: Biology and pathology*. Acta Neuropathology, 119: 7-35.

Song C, Guo J, Liu Y, Tang B, **2012**. *Autophagy and Its Comprehensive Impact on ALS*. International Journal of Neuroscience 122: 695-703.

Soo KY, Halloran M, Sundaramoorthy V, Parakh S, Toth RP, Southam KA, McLean CA, Lock P, King A, Farg MA, Atkin JD, **2015**. *Rab1-dependent ER-Golgi transport dysfunction is a common pathogenic mechanism in SOD1, TDP-43 and FUS-associated ALS*. Acta Neuropathol. 1-19.

Spampinato SF, Copani A, Nicoletti F, Sortino MA, Caraci F, **2018**. *Metabotropic Glutamate Receptors in Glial Cells: A New Potential Target for Neuroprotection?* Front. Mol. Neurosci. 11: 414.

Spreux-Varoquaux O, Bensimon G, Lacomblez L, Salachas F, Pradat PF, Le Forestier N, Marouan A, Dib M, Meininger V, **2002**. *Glutamate levels in cerebrospinal fluid in amyotrophic lateral sclerosis: a reappraisal using a new HPLC method with coulometric detection in a large cohort of patients*. J. Neurol. Sci. 193: 73-78.

Stansley BS and Conn PJ, 2019. *Neuropharmacological Insight from Allosteric Modulation of mGlu Receptors*. Trends in Pharmacological Sciences, Vol. 40, No. 4.

Stathopulos PB, Rumfeldt JAO, Scholz GA, Irani RA, Frey HE, Hallewell RA, Lepock JR, Meiering EM, **2003**. *Cu/Zn superoxide dismutase mutants associated with amyotrophic lateral sclerosis show enhanced formation of aggregates in-vitro*. Proc. Natl. Acad. Sci. U. S. A. 100: 7021-7026.

Stern RM and Connell NT, **2019**. *Ravulizumab: a novel C5 inhibitor for the treatment of paroxysmal nocturnal hemoglobinuria*. Ther. Adv. Hematol. 10.

Stieber A, GonataS JO, Gonatas NK, **2000**. *Aggregates of mutant protein appear progressively in dendrites, in periaxonal processes of oligodendrocytes, and in neuronal and astrocytic perikarya of mice expressing the SOD1(G93A) mutation of familial amyotrophic lateral sclerosis*. J. Neurol. Sci. 177 (2): 114-123.

Stifanese R, Averna M, De Tullio R, Pedrazzi M, Beccaria F, Salamino F, Milanese M, Bonanno G, Pontremoli S, Melloni E. **2010**. *Adaptive modifications in the calpain/calpastatin system in brain cells after persistent alteration in Ca2þ homeostasis*. J. Biol. Chem. 285: 631-643.

Stifanese R, Averna M, De Tullio R, Pedrazzi M, Milanese M, Bonifacino T, Bonanno G, Salamino F, Pontremoli S, Melloni E, **2014**. *Role of calpain-1 in the early phase of experimental ALS*. Arch. Biochem. Biophys. 562: 1-8.

Stoica R, De Vos KJ, Paillusson S, Mueller S, Sancho RM, Lau KF, Vizcay-Barrena G, Lin WL, Xu YF, Lewis J, Dickson DW, Petrucelli L, Mitchell JC, Shaw CE, Miller CC, **2014**. *ER-mitochondria associations are regulated by the VAPB-PTPIP51 interaction and are disrupted by ALS/FTD-associated TDP-43*. Nat Commun. 5: 3996.

Stoica R, Paillusson S, Gomez-Suaga P, Mitchell JC, Lau DH, Gray EH, Sancho RM, Vizcay-Barrena G, De Vos KJ, Shaw CE, Hanger DP, Noble W, Miller CC, **2016**. *ALS/FTD-associated FUS activates GSK-3beta to disruptthe VAPB-PTPIP51 interaction and ER-mitochondria associations.* EMBO Rep. 17 (9): 1326-1342.

Stopford MJ, Allen SP, Ferraiuolo L, **2019**. *A High-throughput and Pathophysiologically Relevant Astrocyte-motor Neuron Co-culture Assay for Amyotrophic Lateral Sclerosis Therapeutic Discovery*. Bio Protoc. 9 (17).

Suzumura A, Ito A, Yoshikawa M, Sawada M, **1999**. *Ibudilast suppresses TNFa production by glial cells functioning mainly as type III phosphodiesterase inhibitor in the CNS*. Brain Res. 837: 203-212.

Sykova E and Chavatal A, **1993.** *Extracellular ionic and volume changes: the role in glia-neuron interaction*. J. Chem Neuroanat, 6: 247-260.

Takagi N, Besshoh S, Marunouchi T, Takeo S, Tanonaka K, **2012**. *Metabotropic glutamate receptor 5 activation enhances tyrosine phosphorylation of the N-methyl-D-aspartate (NMDA) receptor and NMDA-induced cell death in hippocampal cultured neurons*. Biol Pharm Bull., 35 (12): 2224-2229.

Takahashi K, Tanabe K, Ohnuki M, Narita M, Ichisaka T, Tomoda K, Yamanaka S, **2007**. *Induction of pluripotent stem cells from adult human fibroblasts by defined factors*. Cell 131: 861-872.

Takuma H, Kwak S, Yoshizawa T, Kanazawa I, **1999**. *Reduction of GluR2 RNA editing, a molecular change that increases calcium influx through AMPA receptors, selective in the spinal ventral gray of patients with amyotrophic lateral sclerosis*. Ann Neurol.,46 (6): 806-815.

Tan JMM, Wong ESP, Kirkpatrick DS, Pletnikova O, Ko HS, Tay SP, Ho MWL, Troncoso J, Gygi SP, Lee MK, Dawson VL, Dawson TM, Lim KL, **2008**. *Lysine 63-linked ubiquitination promotes the formation and autophagic clearance of protein inclusions associated with neurodegenerative diseases*. Hum Mol Genet.;17: 431-9.

Tanida I, Minematsu-Ikeguchi N, Ueno T, Kominami E, **2005**. *Lysosomal turnover, but not a cellular level of endogenous LC3 is a marker for autophagy*. Autophagy 1:84-91.

Tardy M, Fages C, Le Prince G, Rolland B, Nunez J, **1990**. *Regulation of the glial fibrillary acidic protein (GFAP) and of its encoding mRNA in the developing brain and in cultured astrocytes*. Adv Exp Med Biol. 265: 41-52.

Taylor JP, Brown Jr RH, Cleveland DW, **2016**. *Decoding ALS from genes to mechanism*. Nature 539: 197-206.

Tedeschi V, Petrozziello T, Secondo A, **2019**. *Calcium Dyshomeostasis and Lysosomal Ca2+ Dysfunction in Amyotrophic Lateral Sclerosis*. Cells 8, 1216.

Tefera TW and Borges K, **2016**. *Metabolic Dysfunctions in Amyotrophic Lateral Sclerosis Pathogenesis and Potential Metabolic Treatments*. Front Neurosci. Frontiers Media SA 10: 611.

Teng YD, Benn, SC, Kalkanis SN, Shefner JM, Onario RC, Cheng B, Lachyankar MB, Marconi M, Li J, Yu D, Han I, Maragakis NJ, Llado, Erkmen K, Redmond DE, Sidman RL, Przedborski S, Rothstein JD, Brown RH, Snyder EY, **2012**. *Multimodal actions of neural stem cells in a mouse model of ALS: a metaanalysis*. Sci. Transl. Med. 4https://doi.org/10.1126/scitranslmed.3004579.165ra164.

Thandi S, Blank JL, Challiss RAJ, **2002**. *Group-I metabotropic glutamate receptors, mGlu1a and mGlu5a, couple to extracellular signal-regulated kinase (ERK) activation via distinct, but overlapping, signaling pathways*. J Neurochem., 83 (5): 1139-1153.

Tollervey JR, Curk T, Rogelj B, Briese M, Cereda M, Kayikci M, König J, Hortobágyi T, NishimurALa, Zupunski V, Patani R, Chandran S, Rot G, Zupan B, Shaw CE, Ule J, **2011**. *Characterising the RNA targets and position-dependent splicing regulation by TDP-43; implications for neurodegenerative diseases*. Nat. Neurosci. 14: 452-458.

Tolosa L, Caraballo-Miralles V, Olmos G, Lladó J, **2011**. *TNF-α potentiates glutamate-induced spinal cord motoneuron death via NF-κB*. Mol Cell Neurosci. 46 (1): 176-86.

Tomiyama M, Kimura T, Maeda T, Tanaka H, Furusawa K, Kurahashi K, Matsunaga M, **2001**. *Expression of metabotropic glutamate receptor mRNAs in the human spinal cord: implications for selective vulnerability of spinal motor neurons in amyotrophic lateral sclerosis*. J Neurol Sci, 189: 65-69.

Toni LS, Garcia AM, Jeffrey DA, Jiang X, Stauffer BL, Miyamoto SD, Sucharov CC, **2018**. *Optimization of phenol-chloroform RNA extraction*. MethodsX 5: 599-608.

Tortarolo M, Grignaschi G, Calvaresi N, Zennaro E, Spaltro G, Colovic M, Fracasso C, Guiso G, Elger B, Schneider H, Seilheimer B, Caccia S, Bendotti C, **2006**. *Glutamate AMPA receptors change in motor neurons of SOD1G93A transgenic mice and their inhibition by a non-competitive antagonist ameliorates the progression of amyotrophic lateral sclerosis-like disease*. J. Neurosci. Res. 83: 134-146.

Tradewell ML and Durham HD, **2010**. *Calpastatin reduces toxicity of SOD1G93A in a culture model of amyotrophic lateral sclerosis*. Neuroreport., 21 (15): 976-979.

Trenkwalder C, Stocchi F, Poewe W, Dronamraju N, Kenney C, Shah A, von Raison F, Graf A, **2016**. *Mavoglurant in Parkinson's patients with l-Dopa-induced dyskinesias: Two randomized phase 2 studies*. Mov Disord. 31 (7): 1054-1058.

Trotter J, Karram K, Nishiyama A, **2010**. *NG2 cells: properties, progeny and origin*. Brain Res. Rev 63 (1-2): 72-82.

Trotti D, Volterra A, Lehre KP, Rossi D, Gjesdal O, Racagni G. Danbolt NC, **1995**. *Arachidonic acid inhibits a purified and reconstituted glutamate transporter directly from the water phase and not via the phospholipid membrane*. J Biol Chem. 270 (17): 9890-9895.

Tsacopoulus M and Magistretti PJ, **1996**. *Metabolic coupling between glia and neurons*. J. Neurosci. 16: 877-885.

Uccelli A, Milanese M, Principato MC, Morando S, Bonifacino T, Vergani L, Giunti D, Voci A, Carminati E, Giribaldi F, Caponnetto C, Bonanno G, **2012**. *Intravenous mesenchymal stem cells improve survival and motor function in experimental amyotrophic lateral sclerosis*. Mol. Med. 18: 794-804.

Uday B, Dipak D, Ranajit BK, **1990**. *Reactive oxygen species: Oxidative damage and pathogenesis*. Curr. Sci. 77: 658-666.

Ure J, Baudry M, Perassolo M, **2006**. *Metabotropic glutamate receptors and epilepsy*. Journal of Neurological Sciences, 247: 1-9.

Ustyantseva EI, Medvedev SP, Zakian SM, **2020**. *Studying ALS: Current Approaches, Effect on Potential Treatment Strategy.* Springer Nature Switzerland AG 195 D. O.

Valadi N, **2015**. *Evaluation and management of amyotrophic lateral sclerosis*. Prim Care. 42: 1771-1787.

Valenti O, Conn PJ, Marino MJ, **2002**. *Distinct Physiological Roles of the Gq-Coupled Metabotropic Glutamate Receptors Co-Expressed in the Same Neuronal Populations.* Journal of cellular physiology 191:125-137.

Van Damme P, Dewil M, Robberecht W, Van Den Bosch L, **2005**. *Excitotoxicity and amyotrophic lateral sclerosis*. Neurodegener Dis. 2 (3-4): 147-159.

Van Damme P, Robberecht W and Van Den Bosch, **2017**. *Modelling amyotrophic lateral sclerosis: progress and possibilities.* Disease Models & Mechanisms 10: 537-549.Van Den Bosch L, Vandenberghe W, Klaassen H, Van Houtte E, Robberecht W, **2000**. *Ca2+-permeable AMPA receptors and selective vulnerability of motor neurons*. Journal of the Neurological Sciences 180: 29-34.

Van Den Bosch L, Van Damme P, Bogaert E, Robberecht W, **2006**. *The role of excitotoxicity in the pathogenesis of amyotrophic lateral sclerosis*. Biochimica et Biophysica Acta 1762: 1068-1082.

Vance C, Rogelj B, Hortobágyi T, De Vos KJ, Nishimura AL, Sreedharan J, Hu X, Smith B, Ruddy D, Wright P, Ganesalingam J, Williams KL, Tripathi V, Al-Saraj S, Al-Chalabi A, Leigh PN, Blair IP, Nicholson G, de Belleroche J, Gallo JM, Miller CC, Shaw CE, **2009**. *Mutations in FUS, an RNA processing protein, cause familial amyotrophic lateral sclerosis type 6*. Science. 323 (5918): 1208-11.

Vandenberghe W, Van Den Bosch L, Robberecht W, **1998**. *Glial cells potentiate kainate-induced neuronal death in a motoneuron-enriched spinal coculture system*. Brain Res. 807 (1-2): 1-10.

Vandesompele JK, De Preter F, Pattyn B, Poppe N, Van Roy A, De Paepe, Speleman F, **2002**. *Accurate normalization of real-time quantitative RT-PCR data by geometric averaging of multiple internal control genes*. Genome Biol. 3: Research0034.1-Research0034.11.

Vanhauwaert S, Van Peer G, Rihani A, Janssens E, Rondou P, Lefever S, De Paepe A, Coucke PJ, Speleman F, Vandesompele J, Willaert A, **2014**. *Expressed repeat elements improve RT-qPCR normalization across a wide range of zebrafish gene expression studies*. PloS one 9: 1090-1091.

Varcianna A, Myszczynska MA, Castelli LM, O'Neill B, Kim Y, Talbot J, Nyberg S, Nyamali I, Heath PR, Stopford MJ, Hautbergue GM, Ferraiuolo L, **2019**. *Micro-RNAs secreted through astrocyte-derived extracellular vesicles cause neuronal network degeneration in C9orf72 ALS*. EBioMedicine 40: 626-635.

Varney MA, Cosford ND, Jachec C, Rao SP, Sacaan A, Lin FF, Bleicher L, Santori EM, Flor PJ, Allgeier H, Gasparini F, Kuhn R, Hess SD, Veliçelebi G, Johnson, EC **1999**. *SIB-1757 and SIB-1893: selective, noncompetitive antagonists of metabotropic glutamate receptor type 5*. J. Pharmacol. Exp. Ther. 290, 170-181.

Vergouts M, Doyen PJ, Peeters M, Opsomer R, Hermans E, **2018**. *Constitutive downregulation protein kinase C epsilon in hSOD1G93A astrocytes influences mGluR5 signaling and the regulation of glutamate uptake*. Glia 66: 749-761.

Verkhratsky A and Kirchhoff F, **2007**. *Glutamate-mediated neuronal glial transmission*. Journal of Anatomy, 210: 651-660.

Verkhratsky A and Zorec R, **2018**. *Astroglial signalling in health and disease*. Neurosci 689:1-4.

Vermeiren C, Najimi M, Vanhoutte N, Tilleux S, De Hemptinne I, Maloteaux JM, Hermans E, **2005**. *Acute up-regulation of glutamate uptake mediated by mGluR5a in reactive astrocytes*. Journal of Neurochemistry 94: 405-416.

Vermeiren C, de Hemptinne I, Vanhoutte N, Tilleux S, Maloteaux JM, Hermans E, **2006**. *Loss of metabotropic glutamate receptor-mediated regulation of glutamate transport in chemically activated astrocytes in a rat model of amyotrophic lateral sclerosis*. Journal of Neurochemistry 96: 719-731.

Verney C, Monier C, Fallet-Bianco C, Gressens P, **2020**. *Early microglial colonization of the human forebrain and possible involvement in periventricular white-matter injury of preterm infants*. Journal of Anatomy 217: 436-451.

Vielhaber S, Kunz D, Winkler K, Wiedemann FR, Kirches E, Feistner H, Heinze HJ, Elger CE, Schubert W, Kunz WS, **2000**. *Mitochondrial DNA abnormalities in skeletal muscle of patients with sporadic amyotrophic lateral sclerosis*. Brain, 123 (Pt 7): 1339-1348.

Viwatpinyo K and Chongthammakun S, **2009**. *Activation of group I metabotropic glutamate receptors leads to brain-derived neurotrophic factor expression in rat C6 cells*. Neuroscience Letters, 467: 127-130.

Volkening K, Leystra-Lantz C, Yang W, Jaffee H, Strong MJ, **2009**. *Tar DNA binding protein of 43 kDa (TDP-43), 14–3-3 proteins and copper/zinc superoxide dismutase (SOD1) interact to modulate NFL mRNA stability. Implications for altered RNA processing in amyotrophic lateral sclerosis (ALS).* Brain Res 1305: 168–182.

Volterra A and Maldolesi J, **2005**. *Astrocytes, from brain glue to communication elements: the revolution continues*. Nat Rev Neurosci, 6: 626-640.

Von Braunmuhl A, **1932**. *Picksche Krankheit und amyotrophische Lateralsklerose*. Allg Z Psychiat Psychischgerichtliche Med 96: 364-66.

Vucic S and Kiernan MC, **2006**. *Novel threshold tracking techniques suggest that cortical hyperexcitability is an early feature of motor neuron disease*. Brain 129: 2436-2446.

Wagle-Shukla A, Ni Z, Gunraj CA, Bahl N, Chen R, **2009**. *Effects of short interval intracortical inhibition and intracortical facilitation on short interval intracortical facilitation in human primary motor cortex*. J Physiol 587: 5665-5678.

Waibel S, Reuter A, Malessa S, Blaugrund E, Ludolph AC, **2004**. *Rasagiline alone and in combination with riluzole prolongs survival in an ALS mouse model*. J. Neurol. 251: 1080-1084.

Wake H, Moorhouse AJ, Jinno S, Kohsaka S, Nabekura J, **2009**. *Resting microglia directly monitor the functional state of synapses in-vivo and determine the fate of ischemic terminals*. Journal of Neuroscience 29: 3974-3980

Wang L, Sharma K, Grisotti G, Roos RP, **2009**. *The effect of mutant SOD1 dismutase activity on non-cell autonomous degeneration in familial amyotrophic lateral sclerosis*. Neurobiol Dis. 35 (2): 234-240.

Wang P, Wander CM, Yuan CX, Bereman MS, Cohen TJ, **2017**. *Acetylation-induced TDP-43 pathology is suppressed by an HSF1-dependent chaperone program*. Nat Commun. 8 (1): 82.

Wang SJ and Sihra TS, **2004**. *Noncompetitive metabotropic glutamate5 receptor antagonist (E)-2-methyl-6-styryl-pyridine (SIB1893) depresses glutamate release through inhibition of voltage-dependent Ca2+ entry in rat cerebrocortical nerve terminals (synaptosomes).* J Pharmacol Exp Ther., 309 (3): 951-958.

Wang W, Li L, Lin WL, Dickson DW, Petrucelli L, Zhang T, Wang X, **2013**. *The ALS disease-associated mutant TDP-43 impairs mitochondrial dynamics and function in motor neurons*. Hum Mol Genet. 22 (23): 4706-4719.

Webb JL, Ravikumar B, Atkins J, Skepper JN, Rubinsztein DC, **2003**. *Alpha-Synuclein is degraded by both autophagy and the proteasome*. J. Biol. Chem. 278: 25009-25013.

Weiduschat N, Mao X, Hupf J, Armstrong N, Kang G, Lange DJ, Mitsumoto H, Shungu DC**, 2014**. *Motor cortex glutathione deficit in ALS measured in-vivo with the J-editing technique*. Neurosci. Lett. 570: 102-107.

Weydt P, Yuen EC, Ransom BR, Moller T, **2004**. *Increased Cytotoxic Potential of Microglia From ALS-Transgenic Mice*. GLIA 48:179-182.

White R and Kramer-Alberts EM, **2014.** *Axon-glia interaction and membrane traffic in myelin formation*. Front. Cell. Neurosci. 7, 284.

Wiese S, Herrmann T, Drepper C, Jablonka S, Funk N, Klausmeyer A, Rogers ML, Rush R, Sendtner M, **2010**. *Isolation and enrichment of embryonic mouse motoneurons from the lumbar spinal cord of individual mouse embryos*. Nat Protoc. 5 (1): 31-38.

Williams TL, Day NC, Ince PG, Kamboj RK, Shaw PJ, **1997**. *Calcium-permeable alpha-amino-3-hydroxy-5-methyl-4-isoxazole propionic acid receptors: A molecular determinant of selective vulnerability in amyotrophic lateral sclerosis*. Ann. Neurol. 42: 200-207.

Wilkerson JR, Albanesi JP, Huber KM, **2017**. *Roles for Arc in metabotropic glutamate receptor-dependent LTD and synapse elimination: Implications in health and disease*. Semin Cell Dev Biol. 77: 51-62.

Winer L, Srinivasan D, Chun S, Lacomis D, Jaffa M, Fagan A, Holtzman DM, Wancewicz E, Bennett CF, Bowser R, Cudkowicz Merit, Miller TM, **2013**. *SOD1 in cerebral spinal fluid as a pharmacodynamic marker for antisense oligonucleotide therapy*. JAMA Neurol 70: 201.

Wright GSA, Antonyuk SV, Hasnain SS, **2019**. *The biophysics of superoxide dismutase-1 and amyotrophic lateral sclerosis*. Quarterly Reviews of Biophysics 52, e12, 1-39.

Wollmuth LP, **2018**. *Ion permeation in ionotropic glutamate receptors: Still dynamic after all these years.* Curr Opin Physiol. 2: 36-41.

Xiang X, Qiu D, Hegele RD, Tan WC, **2001**. *Comparison of different methods of total RNA extraction for viral detection in sputum*. J. Virol. Methods 94: 129-135.

Xu L, Yan J, Chen D, Welsh AM, Hazel T, Johe K, Hatfield G, Koliatsos VE, **2006.** *Human neural stem cell grafts ameliorate motor neuron disease in SOD1 transgenic rats*. Transplantation 82: 865-875.

Yamanaka K and Komine O, **2018**. *The multi-dimensional roles of astrocytes in ALS*. Neuroscience Research 126: 31-38.

Yamanaka K, Boillee S, Roberts EA, Garcia ML, McAlonis-Downes M, Mikse OR, Cleveland DW, Goldstein LSB, **2008a**. *Mutant SOD1 in cell types other than motor neurons and oligodendrocytes accelerates onset of disease in ALS mice*. Proc. Natl. Acad. Sci. USA. 105: 7594-7599.

Yin S and Niswender CM, **2014.** *Progress toward advanced understanding of metabotropic glutamate receptors: Structure, signaling and therapeutic indications*. Cell Signal, 26: 2284-2297.

Yoshino H and Kimura A, **2006**. *Investigation of the therapeuticeffects of edaravone, a free radical scavenger,on amyotrophic lateral sclerosis (phase II study)*.Amyotroph Lateral Scler 7: 247-251.

Young KM, Psachoulia K, Tripathi RB, Dunn SJ, Cossell L, Attwell D, Tohyama K, Richardson WD, **2013**. *Oligodendrocyte dynamics in the healthy adult CNS. Evidence for myelin remodeling*. Neuron 77 (5): 873-885.

Youssef EA, Berry-Kravis E, Czech C, Hagerman RJ, Hessl D, Wong CY, Rabbia M, Deptula D, John A, Kinch R, Drewitt P, Lindemann L, Marcinowski M, Langland R, Horn C, Fontoura P, Santarelli L, Quiroz JA, FragX is Study Group, **2018**. *Effect of the mGluR5-NAM Basimglurant on Behavior in Adolescents and Adults with Fragile X Syndrome in a Randomized, Double-Blind, Placebo- Controlled Trial: FragXis Phase 2 Results. FragXis Study Group*. Neuropsychopharmacology, 43 (3): 503-512.

Yu YC, Kuo CL, Cheng WL, Liu CS, Hsieh M, **2009**. *Decreased antioxidant enzyme activity and increate mitochondrial DNA damage in cellular models of Machado Joseph disease*. J Neurosci Res. 87 (8): 1884-1891.

Zhang F, Ström AL, Fukada K, Lee K, Hayward LJ, Zhu H, **2007**. *Interaction between familial amyotrophic lateral sclerosis (ALS)- linked SOD1 mutants and the dynein complex*. J Biol Chem.; 282: 16691-16699.

Zhang B, Tu P, Abtahian F, Trojanowski JQ, Lee VM, **1997**. *Neurofilaments and orthograde transport are reduced in ventral root of transgenic mice that express human SOD1 with a G93A mutation*. J Cell Biol., 139 (5): 1307-1315.

Zhang T, Baldie G, Periz G, Wang J, **2014**. *RNA-processing protein TDP-43 regulates FOXO-dependent protein quality control in stress response*. PLoS Genet. 10 (10): e1004693.

Zhang X, Li L, Chen S, Yang D, Wang Y, Zhang X, Wang Z, Le W, **2011**. *Rapamycin treatment augments motor neuron degeneration in SOD1G93A mouse model of amyotrophic lateral sclerosis.* Autophagy 7: 412-25.

Zongbing H, Rui W, Haigang R, Guanghui W, **2020**. *Role of the C9ORF72 Gene in the Pathogenesis of Amyotrophic Lateral Sclerosis and Frontotemporal Dementia*. Neurosci. Bull. 36 (9): 1057-1070.

Zu T, Gibbens B, Doty NS, Gomes-Pereira M, Huguet A, Stone MD, Margolis J, Peterson M, Markowski TW, Ingram MAC, Nan Z, Forster C, Low WC, Schoser B, Somia NV, Clark HB, Schmechel S, Bitterman PB, Gourdon G, Swanson MS, Moseley M, Ranum LPW, **2011.** *Non-ATG-initiated translation directed by microsatellite expansions*. *Proc.* Natl Acad. Sci. USA 108**:** 260-265.

Zu T, Liu Y, Bañez-Coronel M, Reid T, Pletnikova O, Lewis J, Miller TM, Harms MB, Falchook AE, Subramony SH, Ostrow LW, Rothstein JD, Troncoso JC, Ranum LPW, **2013**. *RAN proteins and RNA foci from antisense transcripts in C9ORF72 ALS and frontotemporal dementia*. Proc. Natl Acad. Sci. USA 110**:** E4968-E4977.

Zur NR and Deitmer JW, **2006**. *The role of metabotropic glutamate receptors for the generation of calcium oscillations in rat hippocampal astrocytes in situ*. Cerebral Cortex, 16: 676-687.

PUBLICATIONS

The data described in this thesis represent the work done for my PhD project and are the matter of a manuscript in preparation. During my doctorate course I collaborated to other research of the group on ALS producing the following five papers:

Milanese M, Bonifacino T, **Torazza C**, Provenzano F, Kumar M, Ravera S, Zerbo RA, Frumento G, Balbi M, Ferrando S, Bonanno G. *Blocking metabotrobic glutamate receptor 5 by the negative allosteric modulator CTEP improves disease course of ALS in SOD1G93A mice.* British Journal of Pharmachology, under revision.

Marini C, Cossu V, Bonifacino T, Bauckneht M, **Torazza C**, Bruno S, Castellani P, Ravera S, Milanese M, Venturi C, Carlone S, Piccioli P, Emionite L, Morbelli S, Orengo A, Donegani MI, Miceli M, Raffa S, Marra S, Cortese K, Grillo F, Fiocca R, Bonanno G, Sambuceti G. *Mechanisms underlying the predictive power of high skeletal muscle uptake of FDG in Amyotrophic Lateral Sclerosis.* EJNMMI Research 2020, 10:76.

Bonifacino T, Provenzano F, Gallia E, Ravera S, **Torazza C**, Bossi S, Ferrando S, Puliti A, Van Den Bosch L, Bonanno G, Milanese M. *In-vivo genetic ablation of metabotropic glutamate receptor type 5 slows down disease progression in the SOD1G93A mouse model of amyotrophic lateral sclerosis*. Neurobiology of Disease 2019 (129): 79-92.

Bonifacino T, Rebosio C, Provenzano F, **Torazza C**, Balbi M, Milanese M, Raiteri L, Usai C, Fedele E, Bonanno G. *Enhanced Function and Overexpression of Metabotropic Glutamate Receptors 1 and 5 in the Spinal Cord of the SOD1G93A Mouse Model of Amyotrophic Lateral Sclerosis during Disease Progression*. International Journal of Molecular Sciences 2019 (20), 4552.

Ravera S, **Torazza C**, Bonifacino T, Provenzano F, Rebosio C, Milanese M, Usai C, Panfoli I, Bonanno G. *Altered glucose catabolism in the presynaptic and perisynaptic compartments of SOD1G93A mouse spinal cord and motor cortex indicates that mitochondria are the site of bioenergetic imbalance in ALS*. Journal of neurochemistry 2019 (151): 336-350.

Current position: post doc at the Department of Pharmacy (DIFAR), Pharmacology and Toxicology Section, University of Genoa (Italy); Disciplinary Sector: BIO/14 PHARMACOLOGY.

ACKNOWLEDGEMENTS

Throughout this project I have received a great deal of support and assistance.
I would like first to thank my promotors, Professor Giambattista Bonanno and Professor Jos Prickaerts.
Prof. Bonanno (also known as GB in our group of research) has known me for more than three years and encouraged me, since the beginning, to develop new ideas and projects. He is always available for discussion and ready to teach, as a good Professor should do. He trusts me and has always supported me, step by step, during my PhD project and in writing this thesis. He also gave me the possibility to continue working in his group of research, as a post doc, to start an amazing project that involves my favourite cells…astrocytes!
He is a great Professor, but also a good man, two characteristics, which, in my opinion, are both fundamental at work and in human life.
When I chose to join the competition for this PhD position, I was very attracted by the international collaboration with Prof. Prickaerts, at Maastricht University. In particular, I was fascinated by his professional profile and his research (of past and present). When I met him for the first time, he confirmed my positive feelings. Indeed, he was always ready to give me a hand and every kind of suggestion, both for my personal and scientific life before my arrival and during the months in Maastricht and Hasselt. He is a very enthusiastic scientist. Everything seems possible in his group of research. When I asked suggestion or permission to proceed with some experiments for my project, he always answered me: “Do whatever you want but enjoy it!”.

If I think about Jos, I cannot help thinking about my co-promotor, Dr. Tim Vanmierlo. Indeed, during my period abroad I almost spent every day in Tim’s laboratory with his group of research, composed by excellent PhD students who work both with Jos at Maastricht and with Tim at Hasselt University, forming a unique and great research group. Since the first day I met and talked with Tim I realised he was a great scientist and a good man. I had the possibility to discuss with him whenever I needed it. He helped me developing my project, day after day. He introduced me to several great Professors and scientists who helped me with their experience. He taught me to write and then put and “close” the unnecessary complains in a real carton box on his desk and to go on. Not only he introduced me to new experimental techniques, but he also showed me a new way to approach to science issues. He is also one of the most patient and happy persons I ever met and, together with Jos, he

has the great merit of having created a marvellous group of researchers, with a big knowledge, amazing scientific projects and full of energy and enthusiasm.

Even if they are not personally or officially involved in my project, I would really like to thank Professor Ernesto Fedele of University of Genoa and Professor Bert Brone of Hasselt University.
Prof. Fedele has supported me many times during my PhD, often "behind the scenes" (especially for bureaucracy issues) and has valued me both as a person and young scientist since I was only a student at Biotechnology.
Prof. Brone accepted me in his "microglia group" since the beginning of my experience in Hasselt, making me feel at home and helping me to study this kind of cells, which are not always very easy to work with. He has created a great group of research too, composed by excellent PhD students who were always ready to help me with my project. Especially, I would like to thank Sofie Kessels, a very sweet girl and a great scientist.

A big acknowledge goes to Associate Professor Marco Milanese, who helped me a lot realising this PhD thesis, giving me precious scientific suggestion and Assistant Professor Tiziana Bonifacino, always ready to give me a hand. They both are like parents in our group of research. They have always supported and helped me, exerting a big patience (even when they are full of things to do…mostly always!). They are great scientists and sweet people and represent my future. Indeed, together with Professor Bonanno they proposed me the position of post doc to continue working in their group of research to develop new projects. They trust me and give me always the possibility to express my own ideas and suggestion. We are becoming a real big family…the already called *Ghianda* Group!

I also desire to thank Professor Cesare Usai, Professor Aldamaria Puliti, Assistant Professor Silvia Ravera and Dr. Simone Bossi. Without their support several experiments shown in this project could not have been developed. Thanks to Silvia I learned a lot, especially most of the secrets to perform a good western blot. She was always ready to help me, giving me any kind of suggestion every day of the week, including weekend!
Professor Usai, represents, I think for all the students who met him, both a sweet man and a great scientist, always available for doubts and clarifications.

Dr. Simone Bossi besides being a young and great scientist is a friend. We shared funny moments working together in the animal house and we still get in touch for scientific suggestion.

I want also to thank all the Professors, researchers and members of Pharmacology and Toxicology Section at the Department of Pharmacy (University of Genoa) I have not mentioned above for supporting me over these years and for dedicating their time reading my PhD thesis, giving me useful suggestion.

A precious thanks goes also to the *Fondazione Bellandi-Bernardoni* for their important donation which was extremely useful for developing the cell culture experiments of this project: the cell incubator.

Moreover, I would like to thank in advance all the referees who will spend their time analysing my PhD project and giving me any kind of suggestion, opinions, or constructive criticism to conclude it in the best way.

Now, I would like to dedicate a big acknowledge to my Italian, Dutch and Belgian colleagues.
Starting from the Italian group, I would like to thank all the PhD students and post doc of *Ghianda* Group. As written above we quickly became a big family. Everybody of us is characterized by a particular "phenotype", scientifically speaking, and this allows us to enjoy and work well together.
Mandeep Kumar and Nhung Nguyen, foreign PhD students, are showing us their different cultures and are helping us practice English daily!
I want to thank Matilde Balbi because her irony and sense of humour bright our days in the laboratory. Moreover, she represents the "microglial" counterpart of our group of research, together with Tiziana. Therefore, it is always fun to discuss with her. We often create a sort of competition: microglia vs. astrocytes.
Giulia Frumento and Roberta Arianna Zerbo are a sort of perfect couple, like Sandra and Raimondo, a famous Italian couple who worked together on television. They are completely opposite, but they compensate each other. Together with them we depict ourselves like the penguins of *Madagascar* cartoon: every day is an adventure in the laboratory, characterized by a lot of fun. We also represent the "astrocytic" counterpart of the *Ghianda* Group.

Astrocytes are like our "babies" and we take care of them daily (also speaking with them!). Another big thank goes to Francesca Provenzano, a great, young, and enthusiastic scientist who is now working abroad as a post doc. She was also part of the "astrocytic" team and I shared with her two years of my PhD, helping each other with our projects. She is always ready to give me a hand also now from distance.

A big acknowledge is also dedicated to the PhD students of the other groups of the Pharmacology and Toxicology Section, especially to Francesca Cisani and Simone Pelassa. We started together our PhD, sharing the joys and the sorrows of this work, including the time to write our PhD theses. I will miss them a lot!

Luckily, Assistant Professor Guendalina Olivero and the PhD students Alessandra Roggeri and Giulia Vallarino, the so called *Apine* (members of Professor Anna Pittaluga's group of research) are still in the laboratory and are very sweet girls. We often try to help each other and have fun together.

Let us move to the Netherlands now.

I first want to thank Ellis Nelissen and Dean Paes, two PhD students of Prof. Prickaerts's group. Even if I could not spend a lot of time with them, we shared funny moments together. They are very nice people, always ready to help me. They fascinated me because they are already great scientists…more than simple PhD students!

I also want to thank Manon van den Berg, another PhD student of the same group. I had the possibility to know her better during a workshop in Crete, which I will never forget! Moreover, she spent some months with us at University of Genoa. In few days she became more Italian than several other "truly" Italian people. Everybody enjoyed her presence in the laboratory.

And now it is the turn of Belgium.

I have no words to describe my love for *Tim Team,* composed by brilliant PhD students: Melissa, Assia, Ben, Jan, and Sam (Sam is not officially part of this team, but for me and the other guys he is!).

Melissa Schepers and Assia Tiane are an amazing "couple", I love them! They were the first people who welcomed me at Hasselt University. They showed me all the laboratories and supported me day by day, helping with my experiments and friendly teaching me several new techniques. They never said "no" to me, even if they were always full of things to do. Indeed, they work hard for their projects but are always ready to give a hand to anybody who

asks for it. In addition, they are sweet and funny girls! We did not spend a day without laughing in the laboratory! This merit goes also to Ben Rombaut, characterized by his typical "Heee-Hooo" and his inimitable neck movement! Every morning started with a coffee, a song, and a laugh, often with Tim too. Everything proceeded in a very "informal way" at Hasselt and this helped me to feel like at home, notwithstanding the lack of my family. We also shared great time together at lunch and during parties organized by the University. As I said at the beginning, it is hard to me to find all the words to describe this amazing experience with them, especially in English! Luckily, we still manage to see each other during the video call of Wednesday, the lab-meeting day, and we often texted. Assia, in particular, helped me a lot for my PhD thesis and was the first of the group to know the news about my baby Antonio (the new entry of my life).

Sam Vanherle was my desk mate for a long time. He seemed shy at the beginning, but he showed me his sensibility and sweetness very soon. Also, he was always ready to help me, especially with PCR experiments. We shared the good and the bad days in the laboratory. Together with Melissa they are probably the strongest PhD students I ever met (and the ones who spend more time in the laboratory…you can find them there every day at every hour!).

Finally, Jan Spaas, the last, but not least for importance! At the beginning I thought he hated me, but it was only shyness! We managed to spend great moments together, especially, and may be unfortunately, during my last days in Hasselt. He is a great person, with a big heart and a great young scientist, even if he does not want to admit it. Moreover, he could have a great future as touristic guide (everything started one day during our visit in Leuven!).

Honestly, I could never have imagined meeting such special people. They are the best PhD students I ever met, and I am sure they will become great and famous scientists soon! They taught me a lot and we will never lose each other… "We are never apart maybe in distance but never in heart!"

I would also like to add a big thank to all the people I met at Hasselt University. I cannot mention one by one but, among all, I thank Professor Niels Hellings, the Director of the Biomedical Research Institute (Hasselt University), Evelien Houben, Paulien Baeten, Leen Timmermans, Katrien Wauterickx, Kristina Laginestra, and Melissa Lo Monaco.

I also thank the group of Italians of Hasselt. We had nice free time and lunches together, supporting each other and the Italian culture abroad!

To conclude, few words to my family.

Starting from my “new” family I would like to thank my husband Marco and my son Antonio.
Marco has supported me since the first time we met at the University, telling me, almost every day, I am the best woman and scientist he has ever met. I would like to tell him too many things, but he already knows them because we are a perfect couple, and our love is unique. In this occasion I would like to thank him for having supported me day by day, especially during the period abroad and writing this PhD thesis. He helped me many times by sharing his scientific knowledge, even after a hard workday and had the patience to stand against my typical anxiety. He told me the right words at right time or simply hugged to make me feel safe. I could never have chosen a better man for my life!
Then, a big thank goes to Antonio, our son. I am writing these words meanwhile he is still in my belly, moving as much as he can, trying to make me stand up and stop working. He is still not in this world, or, at least, we cannot see his face yet, but he already shares every days and moments with me. His presence helped me a lot during these months making me fall in love with him. I hope he will not be so anxious like his mother!

A big acknowledge goes also to my grandparents Ninì and Giorgio. Even if we could not meet very often because of the pandemic they supported me with their special food (in particular my grandmother), phone calls and scientific suggestion (especially given by my grandfather, full Professor of Physical Chemistry, now retired).

Finally, my mother, Francesca, and my father, Paolo. They are the best parents I could ever had. They have supported me since the beginning of my life (and now I can appreciate better with Antonio). They know me as nobody else and they always know how to help me (with a word, a kiss, a hug, a present, or some chocolate!). They supported me during the months abroad, making thousands of sacrifices (and kilometres!) to stay with me even only for few hours. I will never forget any of those moments! During these years I got older, becoming their favourite scientist, a wife, and a mother and they learned how to “change” their presence in my life. However, I know and feel that I will be their *Treccina* forever and this is the most important thing for me!